

**Gating of small RNA mobility
in plant stem cell niches**

Dissertation

der Mathematisch-Naturwissenschaftlichen Fakultät

der Eberhard Karls Universität Tübingen

zur Erlangung des Grades eines

Doktors der Naturwissenschaften

(Dr. rer. nat.)

vorgelegt von

Simon Christoph Klesen

aus Lebach

Tübingen

2020

Gedruckt mit Genehmigung der Mathematisch-Naturwissenschaftlichen Fakultät der Eberhard Karls Universität Tübingen.

Tag der mündlichen Prüfung: 17.12.2020

Stellvertretender Dekan: Prof. Dr. József Fortágh

1. Berichterstatter: Prof. Dr. Marja Timmermans

2. Berichterstatter: Prof. Dr. Gerd Jürgens

Contents

Abbreviations.....	- 1 -
Publications.....	- 4 -
Zusammenfassung.....	- 5 -
Summary.....	- 7 -
Introduction.....	- 8 -
Small RNA discovery.....	- 8 -
Small RNAs behave non-cell autonomous	- 10 -
Two opposing gradients of small RNA define leaf polarity	- 12 -
A miR166 mobility gradient specifies cell fates within the root.....	- 14 -
Mobile miR394 regulates proper shoot apical meristem establishment in the embryo	- 15 -
Small RNAs as developmental signals.....	- 16 -
How do small RNAs move; our knowledge so far.....	- 17 -
Objectives and expected output of the thesis	- 20 -
Chapter one: Small RNAs as plant morphogens.....	- 22 -
Abstract	- 22 -
Contributions:.....	- 22 -
Chapter two: Gating of miRNA movement at defined cell-cell interfaces governs their impact as positional signals	- 23 -
Abstract	- 23 -
Contributions:.....	- 23 -
Chapter three: Regulation of miRNA mobility by receptor-like kinases localised at plasmodesmata.....	- 24 -
Abstract	- 24 -
Contributions.....	- 24 -

Introduction	- 25 -
Results	- 27 -
Selection of potential facilitators of miRNA mobility	- 27 -
Efficient, parallel induction of heritable, biallelic CRISPR/Cas9 mutations in a single generation	- 29 -
Amplicon sequencing for fast detection of CRISPR/Cas9 induced mutations	- 32 -
The BAM1 and BAM2 receptor kinases facilitate miRNA mobility	- 33 -
Discussion	- 37 -
BAM1 and BAM2 are general facilitators of miRNA mobility in the root	- 37 -
Positive, negative, or missing regulation of miRNA mobility?	- 39 -
Alternative screening designs	- 40 -
Preliminary data quality and alternatives to the PD proteome data	- 41 -
Perspective	- 42 -
Chapter four: A high-throughput forward genetic screen for gatekeepers limiting miRNA mobility	- 43 -
Abstract	- 43 -
Contributions	- 43 -
Introduction	- 44 -
Results	- 45 -
A phenotypic forward genetic screen targeting miRNA mobility factors	- 45 -
amiRSCRs efficiently bind and downregulate target transcript	- 46 -
amiRSCR3 consistently induces the <i>scr</i> phenotype in T1 plants	- 47 -
Single-cell RNA sequencing data highlight tissue-specific promoters for amiRSCR3 expression	- 48 -
Restrictive miRNA mobility in the stele and phloem as a basis for a potential screening line	- 50 -

Discussion	- 52 -
Perspective.....	- 52 -
miRNA mobility is differentially regulated within distinct root tissues	- 54 -
Combination of the reverse and forward genetic screens optimises candidate identification.....	- 54 -
Chapter five: Spatiotemporal Developmental Trajectories in the <i>Arabidopsis</i> Root Revealed Using High-Throughput Single-Cell RNA Sequencing	
Summary	- 56 -
Contributions:.....	- 56 -
General conclusions and discussion.....	- 57 -
Methods.....	- 60 -
Plant materials and growth conditions.....	- 60 -
Design of sgRNAs.....	- 60 -
Generation of constructs and transgenic plants	- 60 -
Creation of amplicon libraries	- 61 -
Confocal microscopy.....	- 61 -
Transient protoplast assay to access small RNA-target regulation in single protoplast cells.....	- 62 -
References.....	- 63 -
Appendix I	- 77 -
Appendix II.....	- 104 -
Appendix III.....	- 129 -
Appendix IV.....	- 131 -
Curriculum vitae	- 159 -
Acknowledgement	- 161 -

Abbreviations

AGO	ARGONAUTE
amiRNA	artificial miRNA
APS	ATP sulfurylase
ARF	AUXIN RESPONSE FACTOR
BAK1	BRI1-ASSOCIATED RECEPTOR KINASE
BAM	BARELY ANY MERISTEM
BR11	BRASSINOSTEROID INSENSITIVE 1
Cas9	CASCADE9
CHS	CHALCONE SYNTHASE
CLV3	CLAVATA 3
CRISPR	clustered regularly interspaced short palindromic repeats
CZ	central zone
DCL	DICER-LIKE
GFP	Green fluorescent protein
GO	gene ontology
HD-ZIPIII	class III HOMEODOMAIN-LEUCIN ZIPPER
InDel	insertion/deletion
KRAB	Krüppel-associated box
LCR	LEAF CURLING RESPONSIVENESS
LRR	leucine-rich repeat
mRNA	messenger RNA

miRGFP	artificial miRNA targeting the <i>GFP</i> transcript
miRNA	micro RNA
miRSCR	artificial miRNA targeting the <i>SCR</i> transcript
MS	mass spectrometry
OC	organising centre
OLE	OLEOSIN
PD	plasmodesmata
PDLP	PLASMODESMATA-LOCATED PROTEIN
PHO2	PHOSPHATE 2
Pol II	RNA polymerase II
PTGS	post-transcriptional gene silencing
QC	quiescent centre
RLK	receptor-like kinase
RDR6	RNA-DEPENDENT RNA POLYMERASE 6
RNAi	RNA interference
SAM	shoot apical meristem
SCR	SCARECROW
scRNA-seq	single-cell RNA sequencing
SDN	SMALL RNA DEGRADING NUCLEASES
SEL	size exclusion limit
sgRNA	single guide RNA
SGS3	SUPPRESSOR OF GENE SILENCING 3
SHR	SHORT ROOT

siRNA	short interfering RNA
SRDX	EAR repression domain
sRNA	small RNA
tasiARF	<i>TAS3</i> -derived trans-acting short interfering RNAs targeting AUXIN RESPONSE FACTORs
TF	transcription factor
TML	TOO MUCH LOVE
turboID	highly active biotin ligase variants
WUS	WUSCHEL

Publications

Published papers (in order of appearance):

Klesen S., Hill K., Timmermans M. C. P. (2020) Small RNAs as plant morphogens. *Current Topics in Developmental Biology*, 137, 455-480.

Skopelitis D.S., Hill K., **Klesen S.**, Marco C.F., von Born P., Chitwood D.H., Timmermans M.C.P. (2018) Gating of miRNA movement at defined cell-cell interfaces governs their impact as positional signals. *Nature Communications*, 9, 3107.

Denyer T., Ma X., **Klesen S.**, Scacchi E., Nieselt K., Timmermans M.C.P. (2019) Spatiotemporal Developmental Trajectories in the *Arabidopsis* Root Revealed Using High-Throughput Single-Cell RNA Sequencing. *Developmental Cell*, 48, 840-852.

Manuscripts:

Klesen S., Symeonidi E., Bayer M., Timmermans M.C.P. (2020) Regulation of miRNA mobility by receptor-like kinases localised at plasmodesmata.

Klesen S., Amorim M., Timmermans M.C.P. (2020) A high-throughput forward genetic screen for gatekeepers limiting miRNA mobility.

Zusammenfassung

Die Signalgebung in Pflanzen ist entscheidend für die richtige räumlich-zeitliche Koordination der Entwicklung. Zusätzlich zu den klassischen Signalmolekülen wie Phytohormone, Peptide und kleine mobile Proteine haben sich kleine RNAs (sRNAs) als potente Signale herauskristallisiert, die Positionsinformationen über eine Distanz vermitteln können. Mobile sRNAs spielen eine wichtige Rolle bei der Differenzierung von Pflanzengeweben. Im Blatt erzeugen entgegengesetzte Gradienten von tasiARF und miRNA166 eine scharfe Differenzierungsschwelle der ad- und abaxialen Zellidentität. In der Wurzel wandert miR166 von der Endodermis in die zentrale Vaskulatur, wo sie die HD-ZIPIII-Expression reguliert, was zur Differenzierung von Proto- und Metaxylem führt. Darüber hinaus ist im sich entwickelnden Embryo die nicht-zellautonome miR394 an der Initiierung des zukünftigen apikalen Sprossmeristems beteiligt.

Trotz ihrer Bedeutung ist sehr wenig über die Mobilität der sRNAs bekannt. Mit Hilfe eines hochempfindlichen GFP-basierten synthetischen miRNA-Sensorsystems konnten wir zeigen, dass die miRNA-Mobilität einen fein regulierten Mechanismus beinhaltet, der auf „Gatekeepern“ beruht, die an ausgewählten Zell-Zell-Verbindungen polarisiert sind und eine Direktionalität zwischen benachbarten Zellen erzeugen. In Stammzellnischen zeigten wir, dass die sRNA-Mobilität restriktiv ist, obwohl Plasmodesmata (PD), die für die sRNA-Mobilität entscheidenden Zell-Zell-Verbindungen, reichlich vorhanden sind. Das restriktive Mobilitätsverhalten in Stammzellnischen ist exklusiv für sRNAs und unabhängig von der Proteinbewegung, sei es durch passive Diffusion oder aktiven Transport.

Die Idee eines unabhängigen Mechanismus, der die sRNA-Mobilität kontrolliert, ist denkbar, doch die Identifizierung eines solchen Mechanismus ist eine Herkulesaufgabe. Wir entwarfen einen Ansatz für einen revers genetischen Hochdurchsatz-CRISPR/Cas9 basierten „Screen“ welcher darauf abzielt, positive Regulatoren der miRNA-Mobilität aufzudecken. Wir induzierten Mutationen in mehr als 50 Kandidatengenomen und identifizierten die PD-lokalisierten rezeptorähnlichen Kinasen BARELY ANY MERISTEM 1 und BARELY ANY MERISTEM 2 als positive Regulatoren der miRNA-Mobilität in der Wurzel. Um Komponenten des negativen Regulationsmechanismus auf der Grundlage von „Gatekeepern“ an spezifischen Zell-Zell-Verbindungen zu identifizieren, entwarfen wir einen vorwärts genetischen „Screen“ welcher auf

einem morphologischen Phänotyp basiert. Dazu nutzten wir Einzelzell-RNA Sequenzierungsdaten, um eine „Screening“-Plattform für die schnelle und zuverlässige Identifizierung von mutmaßlichen Mutanten, die am „Gatekeeping“-Mechanismus beteiligt sind, einzurichten.

In dieser Studie gaben wir wichtige Einblicke in die Regulation der sRNA-Mobilität in Stammzellnischen und richteten genetische „Screens“ ein, die zur Identifizierung von sRNA-Mobilitätsmechanismen beitragen werden.

Summary

Signalling in plants is crucial for the proper spatio-temporal coordination of development. Small RNAs (sRNAs), in addition to classical signalling molecules like phytohormones, peptides and small mobile proteins, have emerged as potent signals that can convey positional information over space. Mobile sRNAs play important roles in differentiation of plant tissues. In the leaf, an opposing gradient of *tasiARF* and *miR166* creates a sharp on-off switch of ad- and abaxial cell identity. In the root, *miR166* has been shown to migrate from the endodermis into the central stele regulating *HD-ZIPIII* expression resulting in the differentiation of proto- and metaxylem. Moreover, in the developing embryo, the non-cell autonomous *miR394* is involved in the initiation of the future shoot apical meristem.

Despite its importance, very little is known about the mobility of sRNAs. Using a highly sensitive GFP-based synthetic miRNA sensor system, we showed that miRNA mobility involves a finely regulated mechanism based on gatekeepers polarised at select cell-cell interfaces creating directionality between neighbouring cells. In stem cell niches, we showed that sRNA mobility is highly restrictive although plasmodesmata (PD), cell-cell connections crucial for sRNA mobility, are abundant. The restrictive behaviour of mobility in stem cell niches is exclusive for sRNAs and independent from protein movement whether via passive diffusion or active transport.

The idea of an independent mechanism controlling sRNA mobility is conceivable, however, identifying such a mechanism is a herculean task. We designed a reverse genetic candidate approach based on a high-throughput CRISPR/Cas9 system aiming to uncover facilitators of miRNA mobility. We introduced mutations in more than 50 candidate genes and identified the PD-localised receptor-like kinases *BARELY ANY MERISTEM 1* and *BARELY ANY MERISTEM 2* as facilitators of miRNA mobility in the root. To identify components of the negative regulation mechanism based on gatekeepers at specific cell-cell interfaces, we designed a forward genetic morphology-based screen. For this we utilised single-cell RNA sequencing data to setup a screening platform for quick and reliable identification of putative mutants involved in the gatekeeping mechanism.

In this study we provided major insight into the regulation of sRNA mobility in stem cell niches and setup genetic screens that will contribute to the identification of sRNA mobility mechanisms.

Introduction

Small RNA discovery

In 1990, several researchers made the striking discovery that overexpression of *CHALCONE SYNTHASE (CHS)*, a gene that produces a deep purple petal colour, counterintuitively leads to white flowers (Napoli et al., 1990; Smith et al., 1990; Van der Krol et al., 1990). The phenomenon referred to as co-suppression, or later as post-transcriptional gene silencing (PTGS), was quickly reproduced in other plant systems, and proved a convenient tool to study gene function. Moreover, Palauqui et al., reproducing this effect in tobacco, showed that transgene-induced silencing can move unidirectional in grafting experiments from a silenced stock to a non-silenced scion. The transmission of PTGS showed sequence specificity and was therefore proposed to be due to an unknown diffusible messenger molecule (Palauqui et al., 1997; Voinnet and Baulcombe, 1997). The nature of the mobile molecule would remain elusive for years to come. As first insights, Fire et al. demonstrated that infection with long double-stranded RNAs triggers a PTGS-like silencing phenomenon, termed RNA interference (RNAi), in the nematode *C. elegans* (Fire et al., 1998; Montgomery et al., 1998; Elbashir et al., 2002). In addition, Hamilton & Baulcombe detected transgene and viral induced sRNAs and identified them as the responsible molecules for the sequence-specific PTGS in plants (Hamilton and Baulcombe, 1999). This led to a framework for PTGS/RNAi in which double-stranded RNAs are processed into sRNAs that in a homology-dependent manner trigger the silencing of further RNAs in the cell.

Interestingly, the first sRNA was described in 1993 in the model organism *C. elegans*, where Lee et al. showed that the *LIN-4* gene encodes a 22nt sRNA that targets the *LIN-14* transcript to downregulate its expression (Lee et al., 1993). This sRNA belongs to a now major group, termed microRNAs (miRNAs). The term miRNA was first established in 2001 after several hundred of “tiny RNAs” in various organisms had been identified (Ruvkun, 2001). The first miRNAs in plants were found one year later using the direct cloning technology (Llave et al., 2002; Park et al., 2002; Reinhart et al., 2002). The majority of these molecules consist out of 21-24 nucleotides, which implies specificity to their complementary target mRNA strands. miRNAs form a particularly interesting class of sRNAs which are generated from endogenous genes and also regulate expression of endogenous target genes (Bartel, 2004). The primary miRNA transcript (pri-

miRNA) features a stem-loop structure, which is processed into the precursor miRNA (pre-miRNA) by DICER-LIKE 1 (DCL1), an RNase III enzyme (Figure 1 a). DCL1, aided by further proteins, processes the pre-miRNA into the miRNA duplex, from which the mature miRNA strand is loaded into ARGONAUTE (AGO) proteins (Figure 1 a) (Borges and Martienssen, 2015). The miRNA-AGO complex in a highly specific manner targets mRNAs within the cell and triggers their site-specific cleaved and/or translational repression (Figure 1 a) (Rhoades et al., 2002; Bartel, 2004; Willmann and Poethig, 2007; Yu et al., 2017).

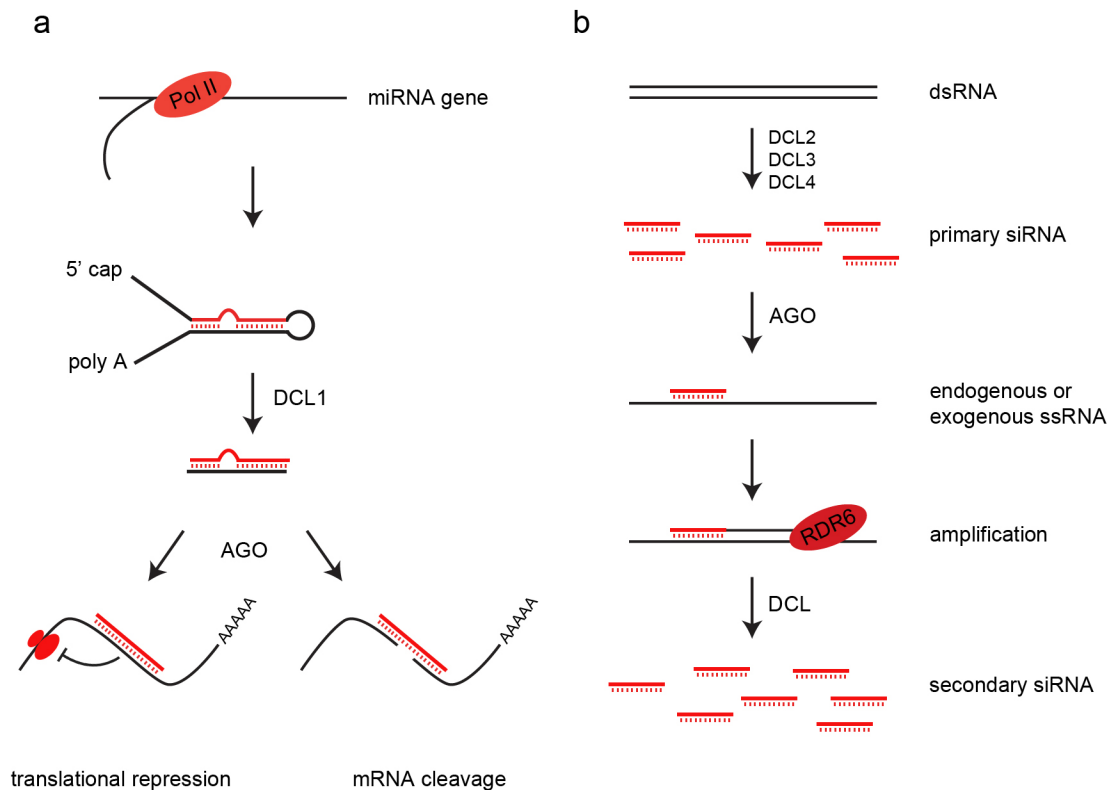


Figure 1: Pathways for the biogenesis of miRNAs and the transitivity mechanism in plants.

(a) miRNA precursors transcribed by RNA polymerase II (Pol II) adopt a hairpin-like structure that is processed by DCL1 into a miRNA duplex typically 21bp in length. The mature miRNA is loaded into an AGO effector complex that in a homology-dependent manner guides the post-transcriptional repression of target mRNAs. Plant miRNAs, unlike their animal counterparts, show near perfect complementarity to target transcripts and direct their cleavage as well as translational repression. (b) Endogenous or exogenous dsRNA precursors are processed by DCL2, DCL3 and DCL4 into primary siRNAs. In a next step, predominantly exogenous transcripts e.g. from transgenes and viral RNA are targeted and amplified by RDR6. Most endogenous sequences are resistant to the RDR6 routing (Vaistij et al., 2002; Himber et al., 2003; Kościńska et al., 2005; Miki et al., 2005; Petersen and Albrechtsen, 2005; Bleys et al., 2006; Aregger et al., 2012). After

priming and amplification by RDR6 the dsRNA is again processed by DCLs resulting in secondary siRNAs.

Another major class of sRNAs are short interfering RNAs (siRNAs). These sRNAs are derived from long double stranded transcripts of repetitive sequences and transposons within the genome, or from exogenous sources such as viral RNAs and transgenes (Figure 1 b). Contrary to miRNAs, siRNAs thus serve in the recognition of self versus non-self. These transcripts are again primed by complementary siRNA, which leads to a secondary amplification step. After the annealing, the siRNA acts similar to an oligonucleotide and the RNA is amplified into a double strand by RNA-DEPENDENT RNA POLYMERASE 6 (RDR6) assisted by SUPPRESSOR OF GENE SILENCING 3 (SGS3) (Figure 1 b). The amplified RNA is then processed into 21nt and 22nt siRNAs by DICER-LIKE 4 (DCL4), DICER-LIKE 2 (DCL2) and DICER-LIKE 3 (DCL3) (Figure 1 b). This mechanism of secondary amplification is called transitivity. Transitivity e.g. triggered by viral RNA enables siRNAs to extend the immunising silencing from a single leaf systemically throughout the plant, thereby forming an important component of siRNA-based plant immunity (Borges and Martienssen, 2015).

Both, miRNA and siRNA, have the potential to act, in their own way, as signalling molecules. With the ancestral directive of siRNA being immune response, miRNAs seem to have adapted this mode of action to regulate endogenous transcription. We now know that both miRNA and siRNA are involved in a multitude of processes in plants, with many of them relying on mobility.

Small RNAs behave non-cell autonomous

The idea that sRNAs might act non-cell autonomously was hypothesised over twenty years ago. Grafting experiments showed that transgene-induced gene silencing in tobacco produces a sequence-specific silencing signal that can spread from a silenced rootstock into a non-silenced shoot scion via the phloem (Palauqui et al., 1997). Additionally, a sequence-specific silencing signal can spread short-range from cell-to-cell, as shown by the transient and local induction of GFP-derived siRNAs that progressively trigger the silencing of a ubiquitously expressed GFP transgene in tobacco (Voinnet et al., 1998). Although sRNAs quickly emerged as candidates for

this signal, experimental evidence was difficult to be attained (Chitwood and Timmermans, 2010). We now know that siRNAs move from cell-to-cell via plasmodesmata (PD, microchannels that connect adjacent plant cells), and systemically through the vasculature (Yoo et al., 2004; Buhtz et al., 2008; Pant et al., 2008; Buhtz et al., 2010; Molnar et al., 2010; Vatén et al., 2011). Particularly, the ability of siRNAs to trigger transitivity enables siRNAs to propagate the spread of silencing from a single leaf systemically throughout the plant (Figure 1 b) (Borges and Martienssen, 2015).

In contrast to siRNAs, plant miRNAs were initially reported to behave cell autonomously (Parizotto et al., 2004; Alvarez et al., 2006). Indeed, with few exceptions, miRNAs do not trigger transitivity (Allen et al., 2005; Montgomery et al., 2008; Manavella et al., 2012). However, miRNAs have been identified in phloem sap and are known to spread systemically via the vascular phloem to coordinate physiological responses between the shoot and root (Lin et al., 2008; Pant et al., 2008; Buhtz et al., 2010; Tsikou et al., 2018). miR395, miR398 and miR399, which coordinate the response to sulphate, copper, and phosphate starvation, respectively, are expressed exclusively in the phloem of the shoot (Fujii et al., 2005; Buhtz et al., 2008; Matthewman et al., 2012). From there miR399 can translocate through the phloem of an *Arabidopsis* scion into a crafted rootstock to regulate its target mRNA *PHOSPHATE 2 (PHO2)*, which in turn mediates the phosphate starvation response. Likewise, miR395 is mobile through the phloem and is translocated from the shoot to root where it targets the *ATP SULFURYLASE (APS)* transcripts, involved in the sulphate assimilation pathway of *Arabidopsis* (Buhtz et al., 2010).

Another example for long-range mobility of miRNAs came recently from the legume model plant *Lotus japonicus*. Legumes have the unique ability to form symbiosis with rhizobia. These bacteria can fix atmospheric nitrogen and process it into ammonium, which can be used by the plant for the biosynthesis of nitrogenous amino acids. Rhizobia are hosted in so called root nodules, which are initially induced by rhizobial signalling molecules and systemically regulated by the host plant (Ferguson et al., 2019). Nodule emergence is suppressed by a root-active kelch-repeat F-box protein, TOO MUCH LOVE (TML) (Takahara et al., 2013). Under nitrogen-deficient conditions, expression of miR2111, which specifically targets TML transcripts, is induced in leaf veins. From there, miR2111 moves into the root where TML translation gets downregulated and therefore susceptibility to rhizobial infection and nodule emergence is observed. This is an impressive example of long-range movement of a miRNA, since miR2111 is exclusively present in the shoot

(Tsikou et al., 2018). Interestingly, miR2111 does not possess the properties to trigger transitivity (Moissiard et al., 2007; de Felippes and Waterhouse, 2020), meaning the movement and offloading through the phloem is highly efficient, considering the effective downregulation of TML in the root (Tsikou et al., 2018).

Besides moving long distance through the phloem, miRNAs can move from cell-to-cell acting as short-range positional signals in development. For instance, several observations hint to mobile sRNAs being important factors in the reproductive development of *Arabidopsis*, contributing to regulation of genome dosage, megasporogenesis and epigenetic reprogramming in the male and female germ cells (Slotkin et al., 2009; Olmedo-Monfil et al., 2010; Tucker et al., 2012; Su et al., 2017; Borges et al., 2018; Su et al., 2020). In addition, the examples described in the paragraphs below provide conclusive evidence that sRNAs act as mobile instructive signals in various developmental contexts.

Two opposing gradients of small RNA define leaf polarity

One of these examples is the development of a flat leaf structure where short-range mobile sRNAs play a crucial role as spatio-temporal signals. The flat leaf with distinct cell types on the adaxial (top) and abaxial (bottom) sides is an important innovation in the evolution of land plants that serves to maximize photosynthesis while minimizing water loss to the environment. The development of flat leaf architecture also poses a mechanistically challenging problem; namely, how to create a stable adaxial-abaxial boundary within the plane of a long and wide, but shallow, structure. The acquisition and maintenance of adaxial-abaxial polarity involves an intricate gene regulatory network with several highly conserved transcription factors that promote either adaxial or abaxial fate at its core (Kuhlemeier and Timmermans, 2016). These transcription factors are expressed in complementary domains delineating the top and bottom side of the developing primordium, respectively (Husbands et al., 2015; Caggiano et al., 2017). The positional information that is needed to define these domains is provided in part by sRNAs.

One sRNA important to the establishment and maintenance of the polarised leaf is miR166. This miRNA contributes to organ polarity by restricting the accumulation of class III HOMEODOMAIN-LEUCIN ZIPPER (HD-ZIPIII) transcription factors, key determinants of

adaxial cell fate (Figure 2 a) (McConnell et al., 2001; Emery et al., 2003; Juarez et al., 2004; Mallory et al., 2004). Plants in which this regulatory interaction is perturbed develop a strong radial adaxialised leaf phenotype, reflecting an early role for miR166 in setting up adaxial-abaxial polarity. miR166 is generated specifically in the abaxial epidermis of leaf primordia, but was shown to move from the epidermis across the leaf to form a concentration gradient that dissipates towards the adaxial side (Juarez et al., 2004; Nogueira et al., 2007; Yao et al., 2009). Interestingly this gradient is interpreted into a binary readout and creates a sharply delineated domain of HD-ZIPIII expression that is limited to the two uppermost layers of developing leaf primordia (Skopelitis et al., 2017).

Maintenance of adaxial-abaxial polarity relies on an additional sRNA gradient formed by tasiARF (Nagasaki et al., 2007; Nogueira et al., 2007; Chitwood et al., 2009; Yifhar et al., 2012; Petsch et al., 2015). Biogenesis of this sRNA occurs through the specialized *TAS3* trans-acting siRNA pathway, which in leaf primordia is active exclusively on the upper surface (Figure 2 a) (Allen et al., 2005; Montgomery et al., 2008; Chitwood et al., 2009). Similar to miR166, movement of tasiARF from its defined source of biogenesis creates a concentration gradient across the leaf that results in discrete expression domains of its targets, the abaxial determinants AUXIN RESPONSE FACTOR 3 (ARF3) and AUXIN RESPONSE FACTOR 4 (ARF4), on the bottom side (Figure 2 a) (Chitwood et al., 2009; Skopelitis et al., 2017). The division of leaf primordia into distinct adaxial and abaxial domains thus relies on a novel developmental patterning mechanism in which tasiARF and miR166 form inverse mobility gradients that are read out into on-off expression boundaries of their targets, the *ARF3/4* and *HD-ZIPIII* genes, respectively (Figure 2 a). Considerations for how this morphogen-like patterning mechanism might work are outlined in chapter one (Klesen et al., 2020).

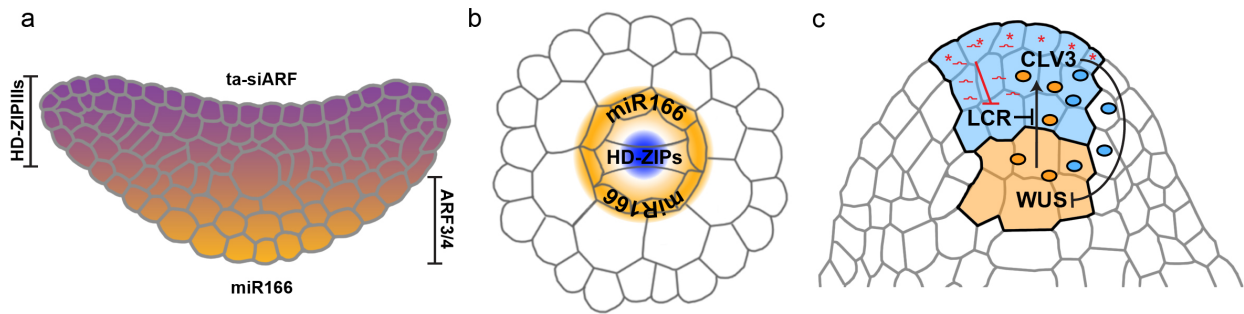


Figure 2: Mobile small RNA gradients play important roles in plant development. (a) In the developing leaf, tasiARF (purple) and miR166 (orange) form opposing concentration gradients through movement from a source in the top and bottom epidermis, respectively. These gradients generate a morphogen-like, threshold-based readout that limits expression of the respective HD-ZIPIII and ARF3/4 targets (transcribed throughout the developing primordium) to sharply defined domains on the top and bottom side of the developing leaf, respectively. (b) Proper patterning of the root vasculature requires that miR166 (orange) moves from its source in the endodermis to generate a concentration gradient across the central stele that is readout into an inverse gradient of HD-ZIPIII activity (blue) to specify proto- and metaxylem cell fate. (c) Stem cell activity in the SAM is maintained via a negative feedback loop in which the WUS transcription factor moves from the OC (orange) to induce CLV3 expression in the CZ (blue). This secreted peptide in turn signals a down-regulation of WUS expression, restricting its activity. miR394 (red squiggle) produced in the CZ epidermis (red asterisks) moves into the subjacent two cell layers where it downregulates its F-box target, LCR, enabling these cells to respond to WUS activity.

A miR166 mobility gradient specifies cell fates within the root

miR166 also serves as a short-range positional signal in patterning of the root, which consists of a central vascular stele surrounded by concentric layers of pericycle, endodermis, cortex, and epidermis (Carlsbecker et al., 2010; Miyashima et al., 2011). Within the vasculature, the water conducting xylem tissue comprises two cell types, the outer protoxylem and the inner metaxylem. These cell fates are defined by the level of HD-ZIPIII activity that is determined by the dose-dependent readout of a miR166 mobility gradient originating in the endodermis (Figure 2 b) (Carlsbecker et al., 2010; Miyashima et al., 2011). The basis for the endodermal-specific production of miR166 lies in the reciprocal movement of the transcription factor SHORT ROOT (SHR) from the central stele into the adjacent endodermis (Nakajima et al., 2001; Gallagher et al., 2004; Cui et al., 2007). Here, it captures its interaction partner SCARECROW (SCR), and together

activates miR166 expression. Movement of miR166 out of the endodermis also affects the development of cortex and pericycle (Miyashima et al., 2011). Thus, as for adaxial-abaxial patterning of the leaf, acquisition of discrete cell fates along the radial axis of the root is in part driven by the dose-dependent readout of a sRNA gradient. Although the miR166 and tasiARF gradients in the leaf generate an on-off switch in target gene expression, the miR166 gradient in the root sets up an inverse gradient of its HD-ZIPIII targets, which then drives the acquisition of discrete cell fates (Carlsbecker et al., 2010).

Mobile miR394 regulates proper shoot apical meristem establishment in the embryo

A third example in which cell fate decisions are governed by mobility of a miRNA is found in the regulation of stem cell activity within the embryonic *Arabidopsis* shoot meristem. Plant meristems are specialized niches that orchestrate the balance between stem cell proliferation and organ initiation essential for post-embryonic growth (Greb and Lohmann, 2016). Stem cells within the shoot apical niche are located within the central zone (CZ) positioned at the meristem tip. This spatial organisation is stably maintained, despite ongoing cell divisions. Two opposing signalling centres provide relevant positional cues to maintain stem cell number and position within the growing niche. The organising centre (OC), positioned directly below the stem cells, expresses the homeodomain transcription factor WUSCHEL (WUS), which moves into the CZ where it promotes stem cell identity and activates CLAVATA3 (CLV3) expression (Figure 2 c) (Yadav et al., 2011; Daum et al., 2014). This secreted peptide in turn signals a downregulation in WUS expression, thus establishing a negative feedback loop that maintains WUS levels and thereby stem cell number (Soyars et al., 2016).

In addition to this regulatory loop, classical surgical experiments predicted the need for an epidermal-derived signal in maintaining stem cell activity (Steeves and Sussex, 1989; Reinhardt et al., 2005). This signal, we now know, involves miR394 (Knauer et al., 2013). miR394 is generated in the surface layer, or protoderm, of the developing embryo, but moves into the subtending two cell layers where it represses expression of the F-box protein, LEAF CURLING RESPONSIVENESS (LCR) (Figure 2 c) (Knauer et al., 2013). As a result, these cells become competent to respond to the stem cell promoting activity of WUS. The limited mobility of miR394

thus defines a zone of stem cell activity and given that the protoderm is propagated by stereotypic anticlinal cell divisions, in addition, stably anchors this zone to the growing shoot tip.

The above examples illustrate the potential mobile sRNAs can have in development. However, not all sRNAs are allowed to move. For example, miR166 in the *Arabidopsis* embryo is expressed in the developing vasculature from where its movement is blocked to safeguard HD-ZIPIII transcription factor expression and stem cell maintenance in the shoot apical meristem (SAM) (Zhu et al., 2011; Zhang and Zhang, 2012). Due to a distinctive mismatch in the miR166 duplex, miR166 is preferentially incorporated into AGO10, rather than AGO1 (Zhu et al., 2011). AGO10 then specifically restrains miR166 from moving into the SAM above. AGO10's function against miR166 is exclusively "mechanical" since it is catalytically dead, which means that the purpose here is to fish out any mobile miR166 and keep them within the cells that express AGO10 (Liu et al., 2009; Zhu et al., 2011). However, AGO10 is involved in the quick onset of degradation of bound miRNAs by SMALL RNA DEGRADING NUCLEASES (SDN) 1 and 2 (Yu et al., 2017) suggesting a more active role of AGO10, sequestering miR166 in these cells by a "search and destroy" mechanism.

Small RNAs as developmental signals

But why use sRNAs as mobile signalling molecules? sRNAs have properties that make them particularly well suited to drive developmental change. Regulation by sRNAs confers sensitivity and robustness onto gene regulatory networks, in part by dampening intrinsic noise resulting from inherent variability in gene expression (Schmiedel et al., 2015; Plavskin et al., 2016). Both features promote the faithful transfer of information through a signalling network and, consistent with the prevalence of evolutionarily conserved sRNA-target modules in plants as well as animals (Yu et al., 2017; Gramzow and Theißen, 2019), mechanisms underlying these network properties provide a selective advantage during evolution (Frankel et al., 2010; Metzger et al., 2015). Plant sRNAs in addition provide an unprecedented degree of signal specificity, often showing near perfect complementarity to target transcripts, and have a direct mode of action that allows for rapid cell fate transitions (Rhoades et al., 2002; Bartel, 2004). In addition, the ability of sRNAs to form gradients that convey developmental signals to cells in a gradient field allows them to shape a

tissue in a morphogen like manner (Figure 2 a, see chapter one). A further conceivable advantage of employing sRNAs as mobile signals in development may be that they represent another class of molecules. Patterning processes often occur in close spatial and temporal vicinity, requiring careful coordination between events. Within plant stem cell niches, cells perceive inputs from a multitude of secreted peptides, hormones, mobile transcription factors, as well as mobile sRNAs (Greb and Lohmann, 2016; Soyars et al., 2016). Thus, perhaps, an additional advantage of employing mobile sRNAs in development is that they broaden the spectrum of available signalling pathways needed to mitigate a “signalling gridlock”.

How do small RNAs move - our knowledge so far

Despite the central importance of sRNA mobility with respect to development, as well as the coordination of biotic and abiotic stress responses across the plant (Lin et al., 2008; Pant et al., 2008; Buhtz et al., 2010; Borges and Martienssen, 2015; Tsikou et al., 2018), remarkably little is known about how the cell-to-cell movement of sRNAs is mediated, except that PD are required (Vatén et al., 2011). These microchannels connect adjacent plant cells. They contain a desmotubule, an endoplasmic reticulum (ER) derived membrane structure, surrounded by a layer of cytoplasm, and thus enable molecules to move within a field of cells either via the cytosolic or ER route (Burch-Smith and Zambryski, 2012; Reagan et al., 2018). PD have a dynamically regulated aperture that controls the size exclusion limit (SEL) and thereby the passive diffusion of water, nutrients, hormones, peptides, and small proteins between adjoining cells, whereas bigger proteins are actively transported (Wu and Gallagher, 2012; Daum et al., 2014; Tilsner et al., 2016). The PD aperture changes while tissues develop, e.g., younger leaves tend to have a higher SEL than more mature leaves (Oparka et al., 1999; Kim et al., 2005; Tilsner et al., 2016). In addition, the SEL is modified in response to stress, both biotic and abiotic (Crawford and Zambryski, 2001; Burch-Smith and Zambryski, 2012). Changes in the SEL limit are realised by callose deposition around the PD which reduces the aperture (Sagi et al., 2005; Levy et al., 2007). Experiments manipulating the callose system to close PD revealed their critical role in plant development; plants with permanently closed PD are barely viable (Zavaliev et al., 2009). By inducing callose synthesis at PD in the endodermis of the *Arabidopsis* root, Vatén et al. provided direct evidence that miRNAs

move from cell-to-cell through PD (Vatén et al., 2011). However, major questions regarding miRNA mobility remain with the nature and possible chaperoning of the primary mobile RNAi signal utilising PD as a gateway still being vague.

Determining this primary signal that moves from cell-to-cell is an important step in unravelling the mobility mechanism. This signal has been under lots of speculation, be it long single-stranded, double stranded, free or protein bound RNA (Brosnan and Voinnet, 2011; Pyott and Molnar, 2015; Liu and Chen, 2018; Zhang et al., 2019). Devers et al. recently showed that for siRNA-induced RNAi, AGO-free primary siRNA duplexes are the mobile signal in short- and long-distance movement (Devers et al., 2020). There is selectivity between the mobility of siRNA and miRNA. This selectivity can be seen by the siRNA exclusive mobility from the pollen into the sperm cells (Martinez et al., 2018; Wang et al., 2018), as well as the overall greater range of mobility that siRNAs typically show (Felippes et al., 2010). With these differences, it will be interesting if the primary signal for miRNA and siRNA mobility turns out to be the same or if mobility of the primary miRNA signal is realised in another way, e.g. protein bound. Additionally, specific processing of sRNAs in form of interaction or modification within the cell might be a crucial part of mobility to ensure sRNAs reach PD, the starting point of cell-to-cell mobility.

In addition to uncertainties about the nature of the mobile component, major questions remain as to whether sRNA mobility is a regulated process, and if so, where, when, and how mobility is regulated. sRNAs that move short range from cell-to-cell will form an accumulation gradient that has its maximum at the source tissue and decreases with cellular distance (Skopelitis et al., 2017). Accordingly, the effective range of mobility is correlated to the abundance of the sRNA at the source (Felippes et al., 2010; Skopelitis et al., 2017). The shape of miRNA gradients generated by movement from an epidermal source in the leaf is consistent with the passive diffusion of sRNAs between cells, establishing passive diffusion as an important variable in mobility (Chitwood et al., 2009; Skopelitis et al., 2017). Nonetheless, there is clear evidence that sRNA mobility occurs via an actively regulated process, in some developmental contexts. In the SAM of *Arabidopsis*, sRNA mobility is more restrictive. This is perhaps best illustrated by the activity of miR394, which through the repression of LCR promotes stem cell identity (Figure 2 c). The movement of miR394 is restricted after the L3 layer, which prevents a shift from organising to stem cell identity in the OC, thus providing a mechanism to maintain stem cell number (Knauer et al., 2013). Likewise,

movement of miR166, while essential for the specification of adaxial-abaxial polarity in the incipient primordium, cannot extend into the CZ where its HD-ZIPIII targets are required for stem cell activity (Liu et al., 2009; Zhu et al., 2011; Zhang et al., 2017; Skopelitis et al., 2018). To resolve this regulation in the SAM and if this regulation is a general feature of plant stem cell niches is one major question that we will address in this thesis.

It is evident that the sRNA mobility in the stem cell niche is tightly regulated, however further experiments are needed to resolve the molecular underpinnings and to unravel the complex interactions that create this selectivity in sRNA mobility. We are addressing this major mechanistic question in this thesis by presenting different genetic approaches. These molecular components have proven difficult to identify. Forward genetic screens designed to pinpoint such factors have led to the discovery of numerous sRNA biogenesis components, but failed to uncover genes directly affecting mobility (Brosnan and Voinnet, 2011; Melnyk et al., 2011; Taochy et al., 2017). The first insights, which support the idea that the movement of sRNAs is regulated at the PD, came from a recent biochemical study into the antiviral immune response (Rosas-Diaz et al., 2018). The systemic spread of virus-derived siRNAs is one of the plant's main antiviral defence mechanisms (Burgyán and Havelda, 2011; Melnyk et al., 2011). To combat this defence strategy, viruses evolved various suppressor strategies, one of which targets the PD-associated RLKs, BARELY ANY MERISTEM 1 (BAM1) and BARELY ANY MERISTEM 2 (BAM2), to block the movement of siRNA from the vasculature (Rosas-Diaz et al., 2018). Whether these RLKs regulate mobility of miRNA to the same extent as siRNA is one of the major questions in this thesis.

Parts of this introduction appeared in the publication: Klesen S., Hill K., Timmermans M. C. P. (2020). Small RNAs as plant morphogens. *Current Topics in Developmental Biology*, 137, 455-480.

For details see chapter one.

Objectives and expected output of the thesis

This work focused specifically on miRNA mobility in meristematic tissues, like the SAM, root meristem and vasculature, where tight regulation of gene expression is crucial to coordinate the many cell fate decisions occurring in close spatial proximity. It was known that sRNAs move locally via PD, but how sRNAs move and how their mobility is regulated across development remained key unanswered questions. Previous studies focussed on the propagation of RNA silencing through the vasculature as well as the transitive spread of siRNAs on a whole organism level. In Chapter two *Gating of miRNA movement at defined cell-cell interfaces governs their impact as positional signals*, we used a synthetic fluorescence-based miRNA sensor system to understand the scope of sRNA mobility across developmental contexts. We show that miRNAs in stem cell niches generally behave domain autonomously, meaning that mobility between functional domains is restricted. This restriction is independent from facilitated transport of proteins and is not explained by simple diffusion of miRNAs. We proposed a model where unknown factors polarised at specific cell-cell interfaces regulate sRNA mobility at the PD.

Considering this model, it is interesting to note that many proteins, including many RLKs, are preferentially located at PD (Fernandez-Calvino et al., 2011; Stahl and Faulkner, 2016), thus providing lots of scope to regulate the movement of sRNAs. In Chapter three *Regulation of miRNA mobility by receptor-like kinases localised at plasmodesmata*, we developed a reverse genetic approach that takes advantage of the previously published PD proteome to arrive at possible facilitators of sRNA mobility (Fernandez-Calvino et al., 2011). Over 50 PD-associated RLKs and RNA-binding proteins along with their close paralogs were mutated using a high-throughput CRISPR/Cas9-based approach. Mutations were introduced in lines carrying the synthetic fluorescence-based miRNA sensor system to allow efficient screening for miRNA mobility phenotypes in the root. While the screening process is still ongoing, this candidate-focused approach has shown the BAM receptors to facilitate miRNA mobility in the root, thus validating this strategy. In addition, this work has created a vast library of RLK mutants which will greatly benefit the research community and will further provide insight on phylogenetic relation and developmental functions of so far uncharacterised RLKs.

In addition to the reverse genetic approach, chapter four *A high-throughput forward genetic screen for gatekeepers limiting miRNA mobility* outlines an unbiased forward genetic screen to identify the mechanism underlying the restrictive mobility of sRNAs in the root stem cell niche. Here, we generated a highly efficient artificial miRNA targeting *SCR* transcripts (miRSCR) that upon movement into the niche results in an easy-to-score short root phenotype. Chapter five, *Spatiotemporal Developmental Trajectories in the Arabidopsis Root Revealed Using High-Throughput Single-Cell RNA Sequencing* describes a high-resolution single-cell RNA sequencing (scRNA-seq) expression atlas from the root where we identified all major cell type clusters by a combination of a biased and unbiased approach. From this atlas, we identified cell type specific promoters needed to express miRSCR in cells adjacent to the niche. We have thus generated the genetic tools for a successful screening platform which can reliably identify mutants of the putative mobility gatekeepers in the root stem cell niche.

Chapter one: Small RNAs as plant morphogens

Simon Klesen, Kristine Hill, & Marja C. P. Timmermans

Abstract

The coordination of cell fate decisions within complex multicellular structures rests on intercellular communication. To generate ordered patterns, cells need to know their relative positions within the growing structure. This is commonly achieved via the production and perception of mobile signalling molecules. In animal systems, such positional signals often act as morphogens and subdivide a field of cells into domains of discrete cell identities using a threshold-based readout of their mobility gradient. Reflecting the independent origin of multicellularity, plants evolved distinct signalling mechanisms to drive cell fate decisions. Many of the basic principles underlying developmental patterning are, however, shared between animals and plants, including the use of signalling gradients to provide positional information. In plant development, small RNAs can act as mobile instructive signals, and similar to classical morphogens in animals, employ a threshold-based readout of their mobility gradient to generate precisely defined cell fate boundaries. Given the distinctive nature of peptide morphogens and small RNAs, how might mechanisms underlying the function of traditionally morphogens be adapted to create morphogen-like behavior using small RNAs? In this review, we highlight the contributions of mobile small RNAs to pattern formation in plants and summarize recent studies that have advanced our understanding regarding the formation, stability, and interpretation of small RNA gradients.

Contributions:

Prime author writing and editing the manuscript.

For details, see appendix I.

Chapter two: Gating of miRNA movement at defined cell-cell interfaces governs their impact as positional signals

Damianos S. Skopelitis*, Kristine Hill*, Simon Klesen, Cristina F. Marco, Patrick von Born, Daniel H. Chitwood & Marja C. P. Timmermans

Abstract

Mobile small RNAs serve as local positional signals in development and coordinate stress responses across the plant. Despite its central importance, an understanding of how the cell-to-cell movement of small RNAs is governed is lacking. Here, we show that miRNA mobility is precisely regulated through a gating mechanism polarised at defined cell–cell interfaces. This generates directional movement between neighbouring cells that limits long-distance shoot-to-root trafficking, and underpins domain-autonomous behaviours of small RNAs within stem cell niches. We further show that the gating of miRNA mobility occurs independent of mechanisms controlling protein movement, identifying the small RNA as the mobile unit. These findings reveal gatekeepers of cell-to-cell small RNA mobility generate selectivity in long-distance signalling, and help safeguard functional domains within dynamic stem cell niches while mitigating a ‘signalling gridlock’ in contexts where developmental patterning events occur in close spatial and temporal vicinity.

Contributions:

Analysis of miRNA mobility in the root. Generation and analysis of all quantitative data. Design, assembly and editing of figures; help with writing and editing the paper.

*These authors contributed equally.

For details, see appendix II.

Chapter three: Regulation of miRNA mobility by receptor-like kinases localised at plasmodesmata

Simon Klesen, Efthymia Symeonidi, Martin Bayer and Marja C. P. Timmermans

Abstract

Mobile small RNAs (sRNA) have emerged as potent signals with morphogen-like capabilities that control key developmental processes. MicroRNA (miRNA) mobility is a precisely regulated process involving polarised gatekeepers at defined cell-cell interfaces, controlling mobility independently from other mobile molecules. This gating mechanism can generate directional movement at cell-cell interfaces, creating selectivity in long distance sRNA mobility by regulating entry into the phloem. In addition, selective regulation of sRNA mobility in stem cell niches restricts them to functional domains. Although regulation of sRNA mobility is crucial to plant development, the underlying mechanism is not yet understood. To investigate this mechanism, we took advantage of a synthetic GFP sensor system in a reverse genetic screen based on receptor-like kinases and RNA-binding proteins extracted from a previously published dataset of the plasmodesmata (PD) proteome. We created a mutant library containing more than 50 lines and more than 130 mutant alleles with individual segregation. From this, we identified the plasmodesmata-associated leucine-rich repeat (LRR) receptor-like protein kinases (RLKs) BARELY ANY MERISTEM 1 (BAM1) and BARELY ANY MERISTEM 2 (BAM2) as facilitators of miRNA mobility in the root. The ongoing analysis of this library will identify additional putative mobility facilitators, advancing the discovery of the sRNA mobility mechanism

Contributions

All work outlined in this chapter was done by me except for the setup and analysis of the amplicon sequencing, which was done together with Efthymia Symeonidi. Martin Bayer helped me with phylogenetic analysis.

Introduction

sRNAs can act as mobile signalling molecules and move from one cell to another through PD (Vatén et al., 2011). They are involved in the regulation of biotic and abiotic stress responses and can move systemically either via the phloem or through the iterative production of secondary siRNAs (Buhtz et al., 2008; Lin et al., 2008; Ruiz-Ferrer and Voinnet, 2009; Molnar et al., 2010; Zhang et al., 2014; Lewsey et al., 2016). In recent years, sRNAs have also emerged as potent signals with morphogen-like capabilities in the control of key developmental processes (D'Ario et al., 2017). The specification of adaxial-abaxial polarity in the developing leaf, for example, relies on two opposing sRNA gradients of tasiARF and miR166, originating from the ad- and abaxial epidermis, respectively (Juarez et al., 2004; Mallory et al., 2004; Nagasaki et al., 2007; Nogueira et al., 2007; Chitwood et al., 2009; Husbands et al., 2015; Petsch et al., 2015; Caggiano et al., 2017). These gradients result in a sharp on-off gene expression boundary of their respective targets, the adaxial determinants class III HOMEODOMAIN-LEUCINE ZIPPER (HD-ZIPIII) transcription factors (TFs) and the abaxial determinants AUXIN RESPONSE FACTOR 3 and 4 (ARF3 and 4) (McConnell et al., 2001; Emery et al., 2003; Yifhar et al., 2012; Skopelitis et al., 2017). Another developmentally relevant, mobile sRNA, miR394, mitigates stem cell initiation in the embryo of *Arabidopsis*. Expressed only in the L1 (outer-most) layer of the *Arabidopsis* embryo, miR394 moves into the underlying tissue, silencing its target LEAF CURLING RESPONSIVENESS (LCR), thus allowing WUSCHEL (WUS) to determine the future shoot apical meristem (SAM) (Knauer et al., 2013). More recently, another mobile miRNA has been identified as involved in a regulatory network in the SAM. The L1 derived miR171 moves from the epidermis, two cell layers into the SAM where it regulates expression of its target HAIRY MERISTEM (HAM), resulting in a gradual downregulation (Han et al., 2020). Further, mobility of miR166 within the root coordinates the differentiation of discrete cell fates in the stele. Originating from the endodermis, miR166 forms a gradient into the central stele, establishing an inverse gradient of HD-ZIPIII expression. In turn, this gradient regulates development of the pericycle and results in the differentiation of the outer protoxylem and the inner metaxylem (Carlsbecker et al., 2010; Miyashima et al., 2011).

Although these mobile miRNAs play a crucial role in development and patterning of tissues, we know little about the mobility mechanisms and key players involved. However, we do know that

the movement of miRNAs is a precisely regulated process (Skopelitis et al., 2018). After entry into the phloem, sRNAs are able to move systemically through the plant, establishing the ground tissue/phloem border as an important checkpoint to pass for long-range mobility (Buhtz et al., 2010; Ham and Lucas, 2017). Indeed, a highly selective directional barrier for miRNA mobility is present at this interface, so far that miRNAs expressed in the ground tissue are unable to enter the phloem, whereas miRNAs present in the phloem are able to move out into adjacent cells (Skopelitis et al., 2018). Expression in the phloem thus is a prerequisite for sRNAs that act as long-distance signals (Yoo et al., 2004; Fujii et al., 2005; Lin et al., 2008; Pant et al., 2008; Matthewman et al., 2012; Skopelitis et al., 2018; Tsikou et al., 2018).

In plant stem cell niches, miRNA mobility is precisely coordinated. In the SAM, miRNA mobility is restricted to functional domains, such as the organising centre (OC) and the central zone (CZ) (Skopelitis et al., 2018). Similarly, in the root meristem, movement in and out of the quiescent centre (QC) and central stele is restrained, resulting in a bidirectional restriction of mobility between the QC and the surrounding stem cells (Skopelitis et al., 2018). This mobility is regulated independently from the facilitated transport of proteins such as WUS in the shoot, and WUSCHEL RELATED HOMEODOMAIN 5 (WOX5) in the root, and cannot be explained by PD connectivity or permeability, as diffusion of small proteins in and out of these niche contexts has been observed (Yadav et al., 2011; Daum et al., 2014; Pi et al., 2015; Skopelitis et al., 2018).

The selectivity in miRNA mobility is controlled by an unknown mechanism that is polarised at specific cell-cell interfaces (Skopelitis et al., 2018). This mechanism, likely found at the PD, can through positive or negative regulation, create tissue domains of restricted sRNA mobility. Many proteins specifically involved in signalling are preferentially located at PD, creating lots of scope for possible PD-associated sRNA regulators (Fernandez-Calvino et al., 2011; Stahl and Faulkner, 2016). Indeed, the PD-associated receptor-like protein kinases BAM1 and BAM2 have been shown to positively regulate siRNA mobility in the leaf (Rosas-Diaz et al., 2018).

Here, we designed a reverse genetic screen to uncover regulators of miRNA mobility. From the published PD proteome, we identified 38 receptor-like kinases as prime candidates regulating miRNA mobility. We show that a multitude of candidates can be obtained by clustered regularly interspaced short palindromic repeats (CRISPR) – CASCADE9- (Cas9) (CRISPR/Cas9) induced mutations in a short amount of time. Among these candidates, the receptor-like protein kinases

BAM1 and BAM2 were found to facilitate miRNA mobility. With the involvement of BAM1 and BAM2 in siRNA and miRNA mobility, we showed that both are affected by the same mobility mechanism. The identification of BAM1 and BAM2 as positive regulators of miRNA mobility gave us the first insights into how a mobility mechanism might act, although further work is needed to resolve specificity, redundancy, and to identify additional candidate genes involved.

Results

Selection of potential facilitators of miRNA mobility

Taking into consideration the recent understanding in the sRNA mobility field, pointing to PD as a major site of regulation, we decided to analyse a previously published PD proteome dataset for putative candidates of miRNA mobility regulation. The proteome was created from purified PD, by analysing isolated and digested cell wall extract with nano-liquid chromatography and mass spectrometry (MS) for enrichment in membrane proteins. In contrast to cell wall proteomes, the PD-proteome is depleted of wall proteins but enriched for membrane proteins. In total, 1341 proteins were identified as PD-associated. However, the high number of cytoplasmic contaminants (35% of isolated proteins) illustrates the limitations of this dataset (Fernandez-Calvino et al., 2011).

For undertaking a reverse genetic screen, an informative selection of promising candidates is key to success. To confidently identify candidates, we established a bioinformatics workflow. We first filtered proteins in the PD proteome by the gene ontology (GO) terms “kinase activity”, “DNA-” or “RNA-binding”, “nucleotide/ATP binding”, “nucleic acid binding”, and “receptor-binding” or “-activity”. This reduced the number of candidates in the proteome from 856 to 212 proteins. Given the likelihood that highly expressed proteins may contaminate the PD proteome, we used the data from Van Leene et al., which provides a hierarchical list of common contaminants in plant immunoprecipitations, to exclude such non-specific contaminants (Van Leene et al., 2015). With this, 53 contaminants were removed, most of them ribosomal proteins, leaving 159 candidates to screen. This list was refined through a functional filtration step whereby 31 additional proteins, including mitochondrial- and chloroplast-localised proteins were removed. Further, proteins with

a predicted embryo lethal mutant phenotype were deprioritised. Although these may well have a role in sRNA mobility, such genes require an alternate screen design (see discussion). Due to missing peptide data in the PD proteome, we decided to remove candidates for which no information could be retrieved from the proteome, excluding RLKs, leaving us with a final catalogue of 54 candidate genes (see Appendix III).

This list of candidates includes 38 RLKs, which, given their scope in regulating miRNA mobility, were prioritized in the screen. In addition, a recent LRR-kinase interaction study proposes that small LRR-receptor kinases, such as the common cofactor BRI1-ASSOCIATED RECEPTOR KINASE (BAK1), act as regulatory scaffolds organising their larger counterparts into signalling networks (Smakowska-Luzan et al., 2018). With the idea in mind that such scaffolds can uncover the function of several LRR-receptor kinases at once, we added common co-receptors to the list of proteins to screen. Accordingly, the well-described LRR-kinase co-receptors BAK1 and BRASSINOSTEROID INSENSITIVE 1 (BRI1), as well as the newly identified APEX (AT5G63710), were added to the screen (Smakowska-Luzan et al., 2018).

The RLK family in plants is extensive, including over 900 genes in *Arabidopsis*. Within this large gene family, subsets of RLKs form closely related sub-families, often resulting in functional redundancy (Zulawski et al., 2014; Man et al., 2020). To overcome this, we performed a phylogenetic analysis of candidate RLK mobility factors based on protein sequence homology (PhyloGenes browser www.phylogenies.org), and on kinase domain homology (Zulawski et al., 2014). Phylogenies of candidate genes that are not a member of the RLK family were evaluated based on protein sequence homology (www.phylogenies.org) (Figure 1 e). Given the technical characteristics of the CRISPR-Cas9 system, we are limited to mutagenesis of three genes maximum in one line. The two closest related genes have been included in the list as homologous candidates, given that co-expression is a prerequisite for homologues to act redundantly. We therefore used a single-cell RNA sequencing (scRNA-seq) root atlas to check for co-expression (Denyer et al., 2019, for details see chapter five) (Figure 1 a-d). Since any mobility phenotype will be detected by screening of artificial miRNAs (amiRNAs) targeting a GFP sensor (miRGFP) in the root, homologues not expressed in the root, or not co-expressed with their respective candidates, were excluded.

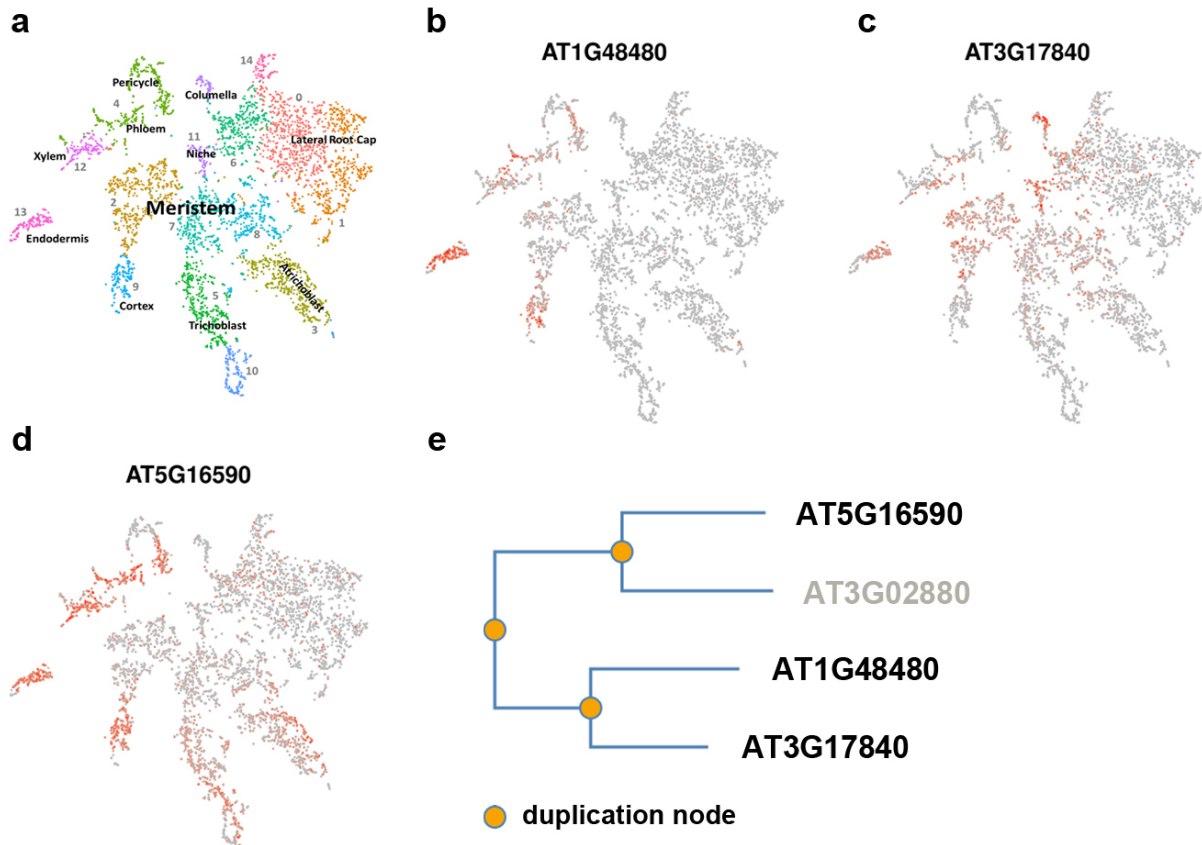


Figure 1: Selection of redundancy candidates based on expression and phylogenetic data. (a) Cluster legend for interpretation of expression data (Denyer et al., 2019). (b-d) Homologues of the candidate AT1G48480 (b) are chosen based on co-expression in root tissue. Homologues are co-expressed in the vasculature, endodermis and cortex. (e) In addition to co-expression, phylogenetic relation is a prerequisite to be included as a homologue. AT3G02880, which is least related to the candidate gene AT1G48480, was not included due to technical characteristics of the CRISPR/Cas9 system. The phylogeny is based on whole protein sequences taken from the PhyloGenes browser (www.phylogen.es.org) and is consistent with RLK specific kinase-based phylogeny (Zulawski et al., 2014).

Efficient, parallel induction of heritable, biallelic CRISPR/Cas9 mutations in a single generation

Mutations in the genes of interest were generated using the CRISPR/Cas9 system, which induces mutations that can generate premature stop codons or other deleterious effects. We designed two single guide RNAs (sgRNAs) per candidate gene, and for each of that gene’s close homologues. Although a single sgRNA per target allele is sufficient, we used two to maximize the opportunity

for generating small insertion/deletion (InDel) mutations, and potential larger deletions (Chen et al., 2014). For sgRNA design, we followed commonly used guidelines for on-target and off-target scores (Hsu et al., 2013; Doench et al., 2016). To facilitate mutant detection in T1 plants, the two sgRNAs were designed to fall within a maximum window of 300bp. Events within this range can be detected through high-throughput amplicon sequencing (for details see below).

In order to ensure efficient introduction of heritable mutations, we avoided mosaic plants. For this, we designed a binary vector in which Cas9 expression is driven by a combination of egg cell promoters 1.1 and 1.2 (EC1.1, EC1.2) (Sprunck et al., 2012; Wang et al., 2015). Due to the high stability of *Cas9* mRNA and Cas9 protein, expression in the egg cell ensures activity also in the one-cell embryo (Wang et al., 2015). CRISPR/Cas9 events occurring there are inherited, avoiding problematic chimeras. Additionally, this vector carries a red fluorescence marker driven by the *OLEOSIN (OLE)* promoter, active in the seed coat. This allows for quick and convenient selection of transformants (Figure 2 b).

To target multiple potentially redundant genes simultaneously, we modified an already-established cloning system from Decaestecker et al. (Decaestecker et al., 2019). This allows us to combine six sgRNAs with the binary vector pEC:Cas9, in a single step. We created an intermediate vector containing both GreenGate- and Gateway-compatible cloning sites (Figure 2 a). This serves as a donor for the Gateway compatible pEC:Cas9 binary vector (Figure 2 b). The resulting system allows efficient targeting of up to three genes using a single construct, and creates (depending on sgRNA efficiency) high numbers of mutants in a single generation.

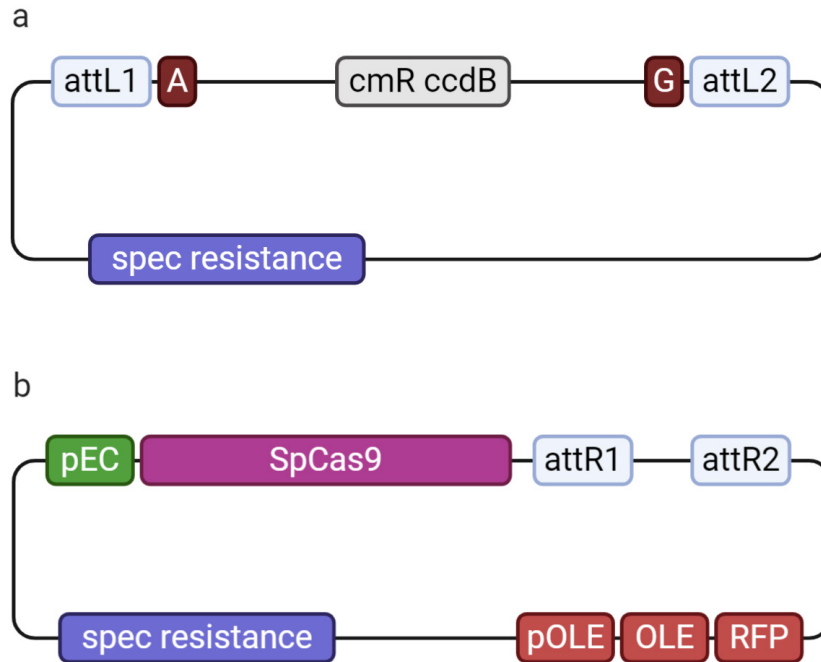


Figure 2: Maps of the intermediate vector and the binary expression vector for efficient cloning of up to six sgRNAs. (a) The intermediate vector combines the Golden Gate system for introducing a cassette of six sgRNAs (Decaestecker et al., 2019), with the Gateway compatible pEC:Cas9 binary expression vector (b).

Using this system, we cloned sgRNA pairs for all 54 selected candidates and their near homologues. These constructs were transformed into a line expressing the miRGFP sensor (for details see chapter two) from the *SCARECROW* (*SCR*) promoter (*pSCR:miRGFP*) in an ubiquitous, nuclear localised GFP background (Skopelitis et al., 2018). The SCR promoter is active specifically in the endodermis, and the QC, in the *Arabidopsis* root (Chapter two, Supplementary Figure 2 c). Expression of the sensor under this promoter leads to an extensive silencing in the root meristem (Figure 5 b). The miRGFP can move from the endodermis and QC into the stele, mimicking the endogenous mobility of miR166, as well as the cortex, epidermis, and columella (Figure 5 b). The extensive silencing shown by *pSCR*-driven miRGFP allows us to utilise this line to screen for facilitators of mobility. A phenotype caused by a putative facilitator will show limited mobility, resulting in a reoccurrence of GFP signal in the root meristem, a phenotype which can be screened for by confocal microscopy.

Amplicon sequencing for fast detection of CRISPR/Cas9 induced mutations

In order to evaluate inherited CRISPR/Cas9 events, we carried out amplicon sequencing (Figure 3). For the preparation of small amplicon libraries, we followed the protocol from Symeonidi et al. (Symeonidi et al., 2020).

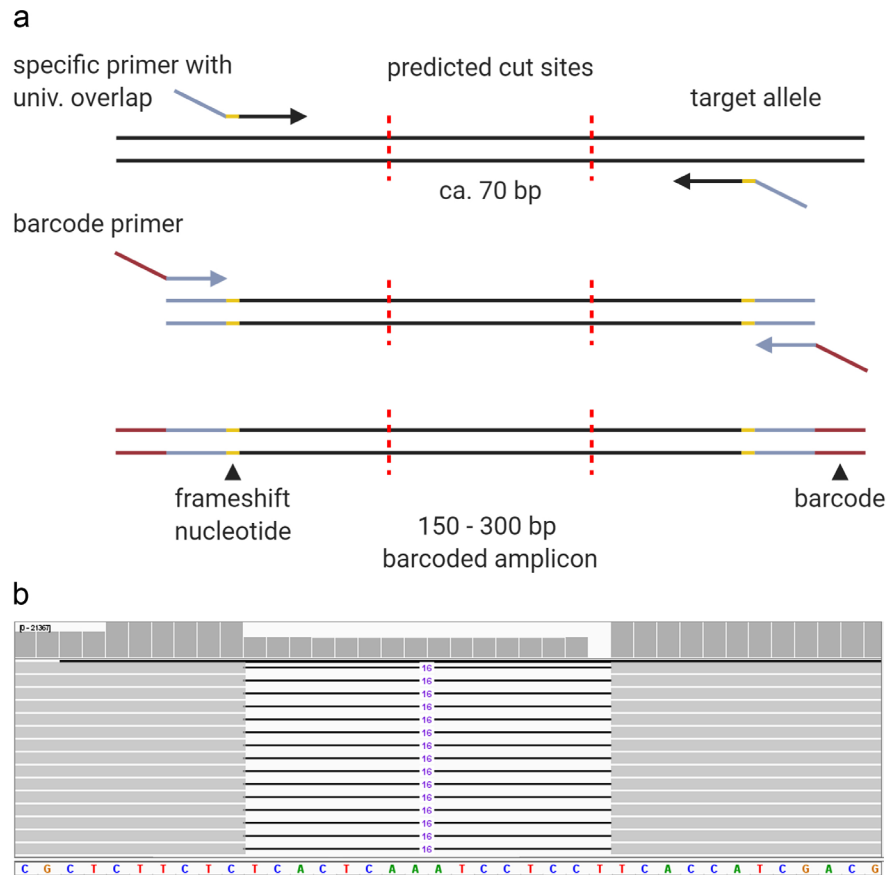


Figure 3: Amplicon sequencing for fast and efficient identification of CRISPR/Cas9 events. (a) For first amplification of an amplicon loci, specific primers are created that contain universal 5' overhangs. In a second step of amplification, 96 uniquely barcoded primers that bind to these overhangs are used to tag individuals. If more than 96 individuals of the same locus are processed, frameshifting nucleotides are introduced in the locus specific primers used to identify individuals in the same wells on different 96-well plates. (b) After sequencing the pooled amplicon library, reads are demultiplexed first based on the barcodes introduced and, if applicable, a second time to distinguish individuals per plate for the frameshifting nucleotides. Different loci can be distinguished using the beginning of the locus-specific read as a barcode. Shown is a typical result of a sequenced, individual where a homozygous 16bp deletion was detected.

The number of T1 plants needed for successful identification of mutants correlates with the number of target genes. For single targets, homozygous or bi-allelic mutations are recovered with an estimated efficiency of up to 30%. The efficiency drops to ~13% when targeting two genes, and to ~8% when targeting three genes (Wang et al., 2015). Considering these data, we evaluated 40 T1 individuals per single target, 80 individuals for those with double-targets, and 120 individuals for triple knockout lines. Using this high-throughput pipeline, we identified mutations in the first five candidate lines, all of them with single targets. In contrast to the mutation frequencies mentioned above, we could detect five individuals carrying biallelic (~3%), and 14 individuals carrying monoallelic (~8%) mutations. These lower numbers might reflect variation in plant health, sgRNA performance, allele accessibility, and general variability using CRISPR/Cas9 (Doench et al., 2016; Chen et al., 2017; Labuhn et al., 2018; LeBlanc et al., 2018; Verkuijl and Rots, 2019).

The BAM1 and BAM2 receptor kinases facilitate miRNA mobility

Using the pipeline described above, we identified mutations in the closely related BAM1 and BAM2 RLKs, previously described as positive regulators of siRNA mobility in the leaf (Rosas-Diaz et al., 2018). However, within the realm of sRNA mobility, there is still selectivity between subspecies of sRNA. This selectivity can be seen by the exclusive mobility of siRNAs from the vegetative cell of pollen into the sperm cells (Slotkin et al., 2009; Martínez et al., 2016; Wang et al., 2018), as well as from the selectivity in the class of siRNAs that move, and the greater range of mobility that siRNAs typically show (Felippes et al., 2010; Molnar et al., 2010; Lewsey et al., 2016). Therefore, it will be interesting to investigate if BAM1 and BAM2 play a similar role in miRNA mobility in the root, or if this is an exclusive mechanism for siRNA mobility. Here, scRNA-seq data shows that BAM1 is expressed broadly in the root tip, though predominantly in the niche (Figure 4 b, d). Conversely, BAM2 is highly expressed in the endodermis (Figure 4 c, e) (Denyer et al., 2019).

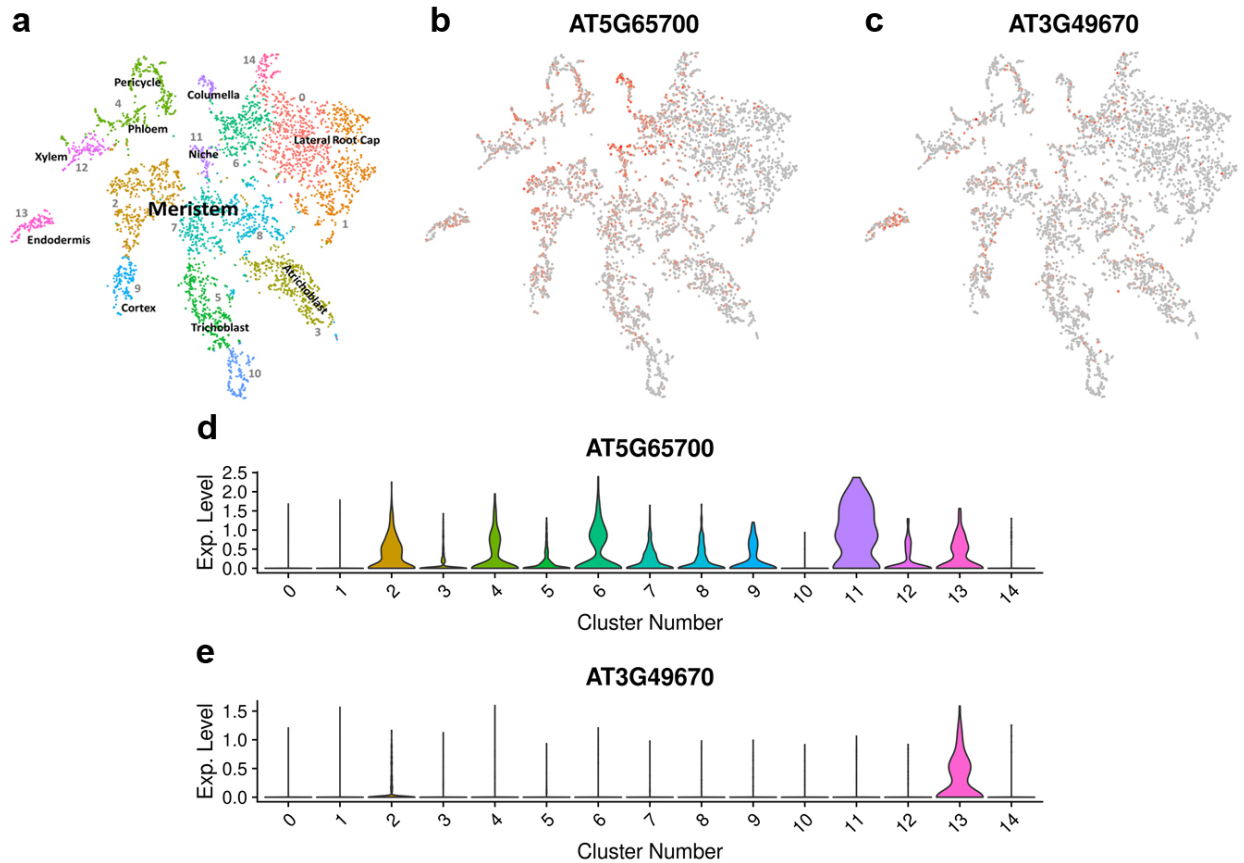


Figure 4: Expression of BAM1 and BAM2 in the root of *Arabidopsis*. (a) Cluster legend for interpretation of expression data (Denyer et al., 2019). (b-c) BAM1 and BAM2 show a broad expression in the tissues of the root tip with BAM1 expression predominant in the niche (d) (cluster 11), and BAM2 in the endodermis (e) (cluster 13).

To study the effect of BAM1 and BAM2 on miRNA mobility, we introduced CRISPR/Cas9 induced mutations in the *pSCR:miRGFP* reporter line, in which a positive regulation of mobility can be detected in the root tip by expanded presence of the miRGFP sensor (see chapter two). In the *pSCR:miRGFP* reporter line we could identify a total of 21 deleterious CRISPR/Cas9 events out of 136 T1 individuals; only one of them in the *bam1* allele. The discrepancy in event frequency between alleles is reflected in the predicted target scores of both sgRNAs: BAM1 with 48.26/100 and BAM2 with 60.87/100 (Doench et al., 2016). The predominant event in these lines were single thymine insertions, accounting for 78% of total events, with the rest being small InDels. In general, the performance of these sgRNAs was very poor, as demonstrated by the overall very low event frequency of ~15%. However, these sgRNAs were chosen since they have previously been used

successfully (Rosas-Diaz et al., 2018). Despite the low event frequency, we were able to identify a segregating double mutant in the *pSCR:miRGFP* reporter line for further analysis.

The *bam1 bam2* mutant reveals a visible phenotype. Seven-day-old seedlings show a severely affected root, and are only about 50% as long as wild type roots (Figure 5 a). Not only is root length impaired, also the apical dominance of the primary root; resulting in multiple synchronously-growing crown-like roots (Figure 5 a). On a cellular level, cells in the root meristem are disorganised, complicating identification of the radial-symmetric, distinct cell files (Figure 5 c, e). In addition to the root phenotype, leaf development also appears slightly impaired, resulting in a steeper angle of petioles and leaves (Figure 5 a).

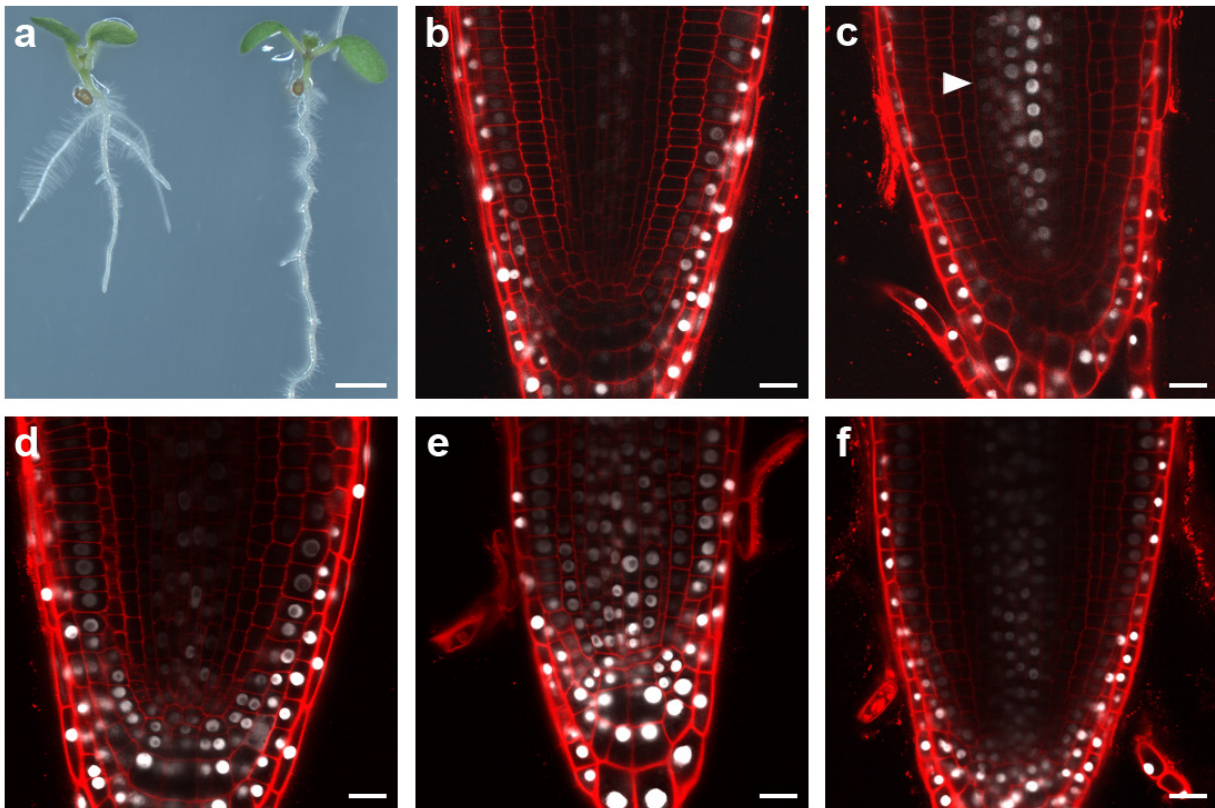


Figure 5: *bam1 bam2* results in a short root phenotype. (a) The double mutant (left) shows a heavily impaired root growth compared to WT (right). (b) Extensive silencing spreads from the endodermis throughout the meristem in wild type roots of the *pSCR:miRGFP* reporter line. (c) Mobility of miRGFP towards the central stele is impaired in the *bam1 bam2* mutant, where GFP signal is visible up to the pericycle cell file (arrowhead). (d) Silencing pattern in the wild type root of the *pmiR166a:miRGFP* reporter line. (e) The mobility of miRGFP is dramatically reduced in the *bam1 bam2* mutant of the *pmiR166a:miRGFP* reporter line. (f) The *bam1 bam2* mutant in the *pmiR166a:miRGFP* reporter line recovers the organisational and mobility phenotype after 14 days. Scale bars: (a) 2cm, (b-f) 20µm.

In six days old root meristems of the *bam1 bam2* mutant, the range of mobility of miRGFP in the *pSCR:miRGFP* reporter line is reduced. This is indicated by the GFP signal seen in the stele (Figure 5 b-c). GFP signal is visible up to the pericycle layer, with an increasing intensity towards the central stele (Figure 5 c). This gradual reduction of miRNA mobility towards the central stele reflects the endogenous miR166 gradient originating in the endodermis, suggesting that while miRNA mobility is not completely abolished, BAM1 and BAM2 lower the general mobility of miRNAs into the stele. Mobility from the endodermis outward into the cortex and epidermis seems to be maintained, suggesting that BAM1 and BAM2 specifically promote the mobility of miRNA towards the centre of the root vasculature (Figure 5 c). In the wild type root, the *SCR* promoter leads to an extensive spread of silencing (Figure 5 b). Higher quantities of miRGFP increase its range of mobility (Skopelitis et al., 2017), possibly obscuring subtle effects on mobility. To overcome this, we introduced mutations in *bam1 bam2*, in the *pmiR166a:miRGFP* reporter line, whereby the miRGFP sensor is expressed exclusively in the endodermis, but at lower levels compared to the *pSCR:miRGFP* reporter line. This revealed that mobility is impaired in both radial directions, as GFP signal in the mutant root meristems is detected within almost all cell files (Figure 5 d-e).

In the *bam1 bam2* mutants, the cells in the root meristem are disorganised compared to wild type (Figure 5 b-e). This organisational phenotype might reflect defects in cell file identity establishment. This presents the possibility that expression of miRGFP in the endodermis is affected, thus indirectly mimicking a mobility phenotype. To verify the integrity of the endodermis, we introduced mutations in *BAM1* and *BAM2* in a reporter line expressing free GFP in the QC and endodermis, driven by the *SCR* promoter. Going forward, this will address two questions. Firstly, whether the endodermis and QC are intact and whether specific expression there is maintained in the mutant. And secondly, whether diffusion of GFP through PD is affected by-, or independent from- the miRNA mobility phenotype in the *bam1 bam2* mutant.

If grown longer, the mobility phenotype can be recovered in mutant root meristems. After 14 days, mutant root meristems recover their mobility phenotype and show wild type-like organisation of cell files (Figure 5 f). This suggests that the mobility phenotype might relate to the cell file organisation phenotype and indicates an additional mechanism that can restore both.

Discussion

sRNAs can move throughout the plant organism and are crucial for proper developmental patterning. Insights into molecular mobility mechanisms, however, are very much limited. We used a reverse genetic high-throughput approach in order to identify genetic components of this mechanism and identified the PD-associated RLKs BAM1 and BAM2 as general facilitators of sRNA mobility in the root meristem of *Arabidopsis*.

BAM1 and BAM2 are general facilitators of miRNA mobility in the root

As mentioned above, the BAM RLKs were described as positive regulators for siRNA mobility out of the phloem companion cells into the leaf mesophyll. In a set of experiments, Rosas-Diaz et al. showed that a viral effector protein targets BAM1 and BAM2 to suppress the spread of RNA interference (RNAi) and promote infection (Rosas-Diaz et al., 2018). We elaborate on this work by showing that BAM1 and BAM2 also play an important role for miRNA mobility within the root, and thereby contribute to normal root development. The gradual increase in GFP signal intensity in the central stele of *bam1 bam2* mutants mimics the endogenous gradient of miR166a originating in the endodermis (Figure 5 c), meaning that mobility is lowered but not abolished. This identifies BAM1 and BAM2 as general facilitators of miRNA mobility in the root but also hints at additional regulation being present maintaining mobility. Identifying these additional regulators is a main focus of this project. The reduced mobility of miRGFP towards the centre of the central stele also suggests that BAM1 and BAM2 might facilitate miRNA mobility in a directional way. This is conceivable since a similar directionality is active at the phloem border where entry from the adjacent cells is limited (Skopelitis et al., 2018). This directional channelling of miRNA towards the central stele could be realised by a polar localisation of BAM1, and specifically the endodermis-exclusive BAM2 (Figure 4 c, e). Given the structural characteristic of the endodermis as the main barrier tissue in the root, it would make sense to limit sRNAs derived from outer tissues and the environment and only allow endogenous sRNA produced within the endodermis to move into the stele. However, if mobility from the epidermis and cortex towards the stele is possible is unclear. The mobility of miRGFP in the *pSCR:miRGFP* reporter line is not as dramatically reduced as in *pmiR166:miRGFP*. The range of sRNA mobility directly correlates

with sRNA levels produced in the source tissue (Skopelitis et al., 2017). The more than four times stronger expression driven by *pSCR* explains the differences in the mutant individuals of both reporter lines (Denyer et al., 2019).

A developed endodermis is a prerequisite for miRGFP to be expressed. The loss of the distinct endodermal cell file results in a short root phenotype (Helariutta et al., 2000). The developmental phenotype of the *bam1 bam2* mutant mimics these short root phenotypes, suggesting that the endodermis is not properly formed. Missing expression in the endodermis in turn would mimic a mobility phenotype in the root. However, also misregulation of HD-ZIPIII TFs within the stele leads to a short root phenotype, coinciding with the decreased mobility of endogenous miR166 (Prigge et al., 2005; Carlsbecker et al., 2010). In any case, the results suggest that the endodermis is intact since extensive mobility could be detected in the *pSCR:miRGFP* reporter line; active in the endodermis (Figure 5 b). Our data further suggests that although the overall structure and organisation of the root is impaired, the endodermis cell layer is physically present.

In addition to the mobility phenotype, a secondary developmental phenotype, namely a disorganisation of the root cell files and defect in root length occurs. This might in part be due to the limited movement of miR166, resulting in miss-regulation of HD-ZIPIII in the central stele (Prigge et al., 2005; Carlsbecker et al., 2010; Miyashima et al., 2019). However, given the broad functions of BAM1 and BAM2 in development, the disorganised cell phenotype might be a consequence of both the limited movement, as well as the missing developmental regulation in the meristem (Hord et al., 2006; Shimizu et al., 2015; Soyars et al., 2016). The disorganisation as well as the miRNA mobility phenotype in the *bam1 bam2* mutant can be recovered after 14 days. Additionally, the *bam1 bam2* mutant shows a rather subtle phenotype in the leaves. This is surprising given the importance of sRNAs in leaf development (Juarez et al., 2004; Chitwood et al., 2009; Yang et al., 2018). Together these results suggest that additional mechanisms are in place that can restore miRNA mobility. This could involve sets of related RLKs that have not been identified yet.

Positive, negative, or missing regulation of miRNA mobility?

While the BAM1 and BAM2 RLKs hint at a positive regulation of mobility in the root, other modes of regulation are plausible. For example, it seems unlikely that the positive regulation of RLKs explains the restricted mobility of sRNAs seen in the context of the stem cell niches. In the SAM, no movement of sRNAs is seen between the CZ and OC (Skopelitis et al., 2018). Preliminary scRNA-seq data points at a rather ubiquitous expression of BAM1 and BAM2 in the SAM (unpublished data), suggesting an additional layer of regulation that would counteract the positive regulation there. Similarly, BAM1 is broadly expressed in the root meristem and predominantly in the QC and stem cells where mobility is restricted (Skopelitis et al., 2018). In the case of the domain autonomous behaviour of sRNAs in the SAM and root meristem, the existence of a polarised, PD-localised restriction mechanism is conceivable. Such a negative regulation could overwrite the positive regulation of mobility, creating isolated domains in the meristems. With the presented reverse genetic screen, we could identify such a mechanism by identifying a more extensive spread of silencing in an alternative screening line e.g. *pmiR166a:miRGFP* or *pWOX5:miRGFP*. However, whether this would be a general mechanism, also present and functional to the same extent in the SAM, is ambiguous.

Entry of sRNA into the phloem of the hypocotyl is selective, allowing only sRNAs expressed in the phloem but not the mesophyll to travel long range (Skopelitis et al., 2018). Intuitively, the regulation in this case seems to be negative, restricting mobility at the mesophyll-phloem border. A prerequisite for this would be a high degree of organisation and positional “sense” of cells, since multiple individual vascular cells adjacent to the phloem companion cell would have to recruit polarised inhibitors to the specific cell interface. Indeed, it is conceivable that this could be established through a mobile feedback regulation, originating from the phloem, similar to the known examples of mobile TFs, SHORT ROOT and WOX5 (Helariutta et al., 2000; Pi et al., 2015; Di Ruocco et al., 2018). However, another theory is that mobility is not restricted, but rather that positive regulators of mobility are missing, in this case within the phloem companion cell. Speaking against this is expression data of the root, leaf and SAM, suggesting a high presence of BAMs in the meristems and phloem of the leaf (Denyer et al., 2019, unpublished data). If the expression of BAM1 and BAM2 is consistent in the hypocotyl, let alone if the positive regulation of miRNA mobility by the BAMs remains the same in the SAM, leaf and hypocotyl is unclear.

Alternative screening designs

The reverse genetic candidate screen depends on pre-existing knowledge. This opens it up to potential biases. We focussed on candidates filtered from the PD proteome (Fernandez-Calvino et al., 2011). However, this relies on the idea that sRNA mobility is regulated at the PD. Multiple sources point to a likelihood of PD-based regulation. Firstly, we know that mobility relies on the presence of PD, meaning that the channels must be passed by sRNAs (Vatén et al., 2011). Secondly, the gating mechanism described in chapter two is realised by polarisation of gate-keepers at specific cell-cell interfaces. Thirdly, the first two sRNA regulating candidates are indeed PD-located LRR RLKs (Rosas-Diaz et al., 2018). The biases of a reverse genetic screen can be circumvented by employing an unbiased forward genetic screen. Here, the caveat is to detect mobility phenotypes in a fast and convenient way. Further disadvantages of a forward genetic screen are those of lethality and redundancy. Strong mutant alleles of essential genes are not recovered in forward screens, and redundancy either in individual components or between multiple mobility mechanisms greatly lowers the possibility of observing a scorable phenotype. Thus, relying on the existence of single master regulators of mobility that are non-essential during early stages of development.

Additional strategies include, for example, amiRNA- and repression/induction domain-based screens such as Krüppel-associated box (KRAB), the plant EAR repression domain (SRDX) or the CRISPRa system (Margolin et al., 1994; Hiratsu et al., 2003; Schwab et al., 2006; Ossowski et al., 2008; Gilbert et al., 2013; Konermann et al., 2015; Lowder et al., 2018). In employing an amiRNA-based screen, an advantage is that redundancy can be efficiently eliminated by targeting conserved domains within a candidate pool. Indeed, this might be a viable alternative to the CRISPR/Cas9 based screen although extensive downregulation of multiple RLKs, by high mRNA sequence homology within the family, might cause severe phenotypes where cause and effect of a mobility phenotype would be hard to determine. A repressor or activator domain in combination with the CRISPR/Cas9 system, or fused to a candidate itself, can be a powerful tool to alter protein activity without knocking out the respective locus. Indeed, this system is also able to intervene with protein-protein interaction of candidates, revealing phenotypes that might contribute to a greater network of interactions (Hiratsu et al., 2003). This might be a worthy addition to the presented CRISPR/Cas9 screen as it would also address the question of specificity in the mobility

mechanism. However, the individual workload per candidate would be quite extensive. This is why we propose to use these systems only as a follow up for identified putative candidate genes. These strategies might be worthwhile additions to the reverse genetic screen, however they will also share the biases from the candidate selection. To overcome these, we present the design of a forward genetic screen for gatekeepers of miRNA mobility in chapter four.

Preliminary data quality and alternatives to the PD proteome data

We used the previously published PD proteome dataset for candidate identification (Fernandez-Calvino et al., 2011). Despite being a great resource for PD-associated proteins, this dataset lacks quality in some aspects. The method of purifying the PD and subsequent MS identification could bias towards more abundant and against low abundant proteins (Van Leene et al., 2015). This is indicated by the high number of proteins that appear not PD-associated; such as ribosomal-mitochondrial- or chloroplast-located proteins. The purification of PD from cell culture could have further biased the PD-proteome since expression often dramatically changes in tissue culture (Birnbaum et al., 2003; Brady et al., 2007; Denyer et al., 2019). However, after several steps of data filtration, we created a promising candidate list from the PD proteome with which we had confidence.

Thanks to the advancement of affinity purification of proteins, we propose to use the recently published turboID method to create a new, refined PD proteome (Mair et al., 2019). The advantage of this method is not only the specificity in affinity purification, but also the fact that different linkers and bait proteins provide flexibility in the physical range at which associated proteins can be tagged. In other words, also proteins indirectly associated with PD can be recovered. This new high-resolution proteome could be based on the PLASMODESMATA-LOCATED PROTEIN (PDLP) family, and will greatly advance the proceedings of the PD and mobility field as a useful resource (Amari et al., 2010).

Perspective

With the presented reverse genetic high-throughput screen utilising the CRISPR/Cas9 system, we successfully created more than 50 mutant lines and more than 130 mutant alleles in receptor-like and RNA-binding proteins associated with PD. Further, phenotypic and molecular analysis of this mutant library will likely identify candidate genes involved in the sRNA mobility mechanisms. Additionally, we will gain insights on developmental phenotypes as well as the phylogenetic relationship between so far uncharacterised RLKs. Lastly, the mutant library created throughout the course of this work will greatly benefit the research community focussing on RLKs in plants.

Chapter four: A high-throughput forward genetic screen for gatekeepers limiting miRNA mobility

Simon Klesen, Marcella Amorim and Marja C. P. Timmermans

Abstract

Precise regulation of small RNA (sRNA) mobility in plants is evident. However, the molecular basis of the mobility mechanism is still unclear. Even with the identification of BARELY ANY MERISTEM 1 (BAM1) and BARELY ANY MERISTEM 2 (BAM2) as facilitators of sRNA mobility in the root the precise mechanism is lacking explanation. Results of restrictive mobility in stem cell niches further hints at the presence of additional layers of sRNA regulation in form of gatekeepers. Here we present the design of a forward genetic screen aiming at the identification of such a negative regulation. Potential restrictor mutants are identified through a short root phenotype, induced by increased mobility of an artificial microRNA (amiRNA) targeting the SCARECROW (SCR) transcription factor (TF) required for quiescent centre (QC) activity. This screening platform builds a solid foundation for reliable identification of putative mobility gatekeepers and adds to the discovery of additional mobility mechanisms.

Contributions

All work outlined in this chapter was done by me except for testing of amiRs in the transient protoplast assay, which was performed by Marcella Amorim.

Introduction

The reverse genetic candidate approach presented in chapter three identified BAM1 and BAM2 as facilitators of miRNA mobility, located at the plasmodesmata (PD). Positive regulation of sRNAs seems to be the intuitive explanation for the majority of sRNA mobility in most tissues. However, it is unlikely to be the unique mechanism controlling this. As discussed in chapters two and three, mobility in the shoot apical meristem (SAM) is restricted to within the central zone (CZ) and the organising centre (OC) (Skopelitis et al., 2018). Similarly, miRNA mobility in the root meristem is restricted within the procambium and between the stem cells and QC (Chapter two, Figure 5 d-f). This conflicts with the ubiquitous expression of BAM1 and BAM2 in the SAM and root meristem, which should facilitate sRNA mobility in these tissues (Denyer et al., 2019, and unpublished data). These results suggest the presence of an additional regulatory mechanism, which overwrites the action of mobility facilitators. This mechanism is realised by polarised gatekeepers restricting sRNA mobility at specific cell-cell interfaces (Skopelitis et al., 2018). The combination of a positive and a negative regulation can thus create the observed selectivity in sRNA mobility in different developmental tissues (Martínez et al., 2016; Skopelitis et al., 2018; Wang et al., 2018). To identify this restricting sRNA mobility mechanism, we setup a forward genetic screen.

The reverse genetic candidate approach described in chapter three relies on the previously-published PD proteome (Fernandez-Calvino et al., 2011). One disadvantage of this approach is that we rely on the quality of the dataset itself, from candidate to candidate. The chance that a crucial player in miRNA mobility might be missed is high (see discussion chapter three). In contrast, a forward genetic screen delivers us an almost saturated study of genes in *Arabidopsis* that may play a role in mobility but is confounded by redundancy and potential lethality (Gaillochet et al., 2020). To overcome biases, we performed a forward genetic candidate screen to complement the reverse genetic approach. In combining both screens, we give ourselves the best possible chance of identifying putative mobility mutants.

Initially, screens were designed based on the amiRNA targeting the *GFP* transcript (miRGFP) reporter lines described in chapter two, to detect changes in GFP levels as a readout of altered miRNA mobility. This system works well for characterisation of miRNA mobility in different tissues, where the number of generations is minimal. However, transcriptional gene silencing of

the GFP sensor over multiple generations was too variable and we ultimately had to abandon GFP-based forward genetic screens. Because of this setback, we decided to design the forward genetic screen based on a visible phenotype in lines carrying a single simple transgene construct.

Here we developed a morphology-based forward genetic screen that exploits the critical role of SCR in the QC, and the restricted mobility of miRNAs into these cells. With this intelligent design we are able to quickly identify suitable screening lines and already gathered new information on miRNA mobility in the root. This system will allow us in the near future to perform a high throughput forward genetic screen for gatekeepers of miRNA mobility.

Results

A phenotypic forward genetic screen targeting miRNA mobility factors

A benefit of moving to a morphology-based forward genetic screen is that seedlings can be screened in a time-efficient way since microscopic visualisation of a fluorophore is no longer necessary. The setup of the initial screening line is crucial and must be thorough to ensure consistency through multiple generations. In the root, miRNA mobility is restricted within the procambium and between the stem cells and QC (Chapter two, Figure 5 d-f). We took advantage of this restriction and designed a forward genetic screen for negative regulators acting in these tissues. We generated stable *Arabidopsis* lines where a mutation in such a restrictor will result in a short root phenotype. For this we designed an amiRNA targeting the *SCR* transcript (amiRSCR). SCR is a TF expressed in the endodermis and QC of the *Arabidopsis* root and is involved in the regulation of radial root development (Chapter two, Supplementary Figure 2 c) (Di Laurenzio et al., 1996; Wysocka-Diller et al., 2000; Sabatini et al., 2003). Depletion of SCR results in a short root phenotype (Figure 3 a). To induce this phenotype in a putative miRNA mobility mutant, we express amiRSCR in tissues surrounding the endodermis and QC. While in a wild type situation the amiRSCR will be prevented from moving into the QC, in a putative restrictor mutant the amiRSCR will be able to enter the QC, resulting in a short root phenotype. For reliable phenotyping of mutants, the *SCR* transcript must be repressed efficiently enough in the QC. Two points are

relevant for this, the efficiency of the miRNA, and its level of expression relative to that of SCR itself (see chapter one).

amiRSCRs efficiently bind and downregulate target transcript

To identify an efficient amiRNA, we designed eleven distinct amiRSCRs using the Web MicroRNA Designer (Schwab et al., 2006; Ossowski et al., 2008), and criteria used in the design of the highly efficient miRGFP (Skopelitis et al., 2017). Their efficiencies were tested in a high-throughput transient protoplast assay. For this, we designed a construct with two fluorescent reporters that allows us to track gene expression in individual cells with the presence and absence of sRNA regulation. While one of the fluorophores is targeted by the amiRSCR, the other one is used as a normalisation control. With this, we can correlate both and visualise the efficiency of amiRSCRs in the assay. Two of the designed amiRSCRs showed great efficiency, comparable to the previously described miRGFP (Figure 1 c) (Skopelitis et al., 2017). With repression of GFP fluorescence close to that observed for miRGFP, we can confidently proceed with amiRSCR3 and amiRSCR7 for further experiments (Figure 1 a-b).

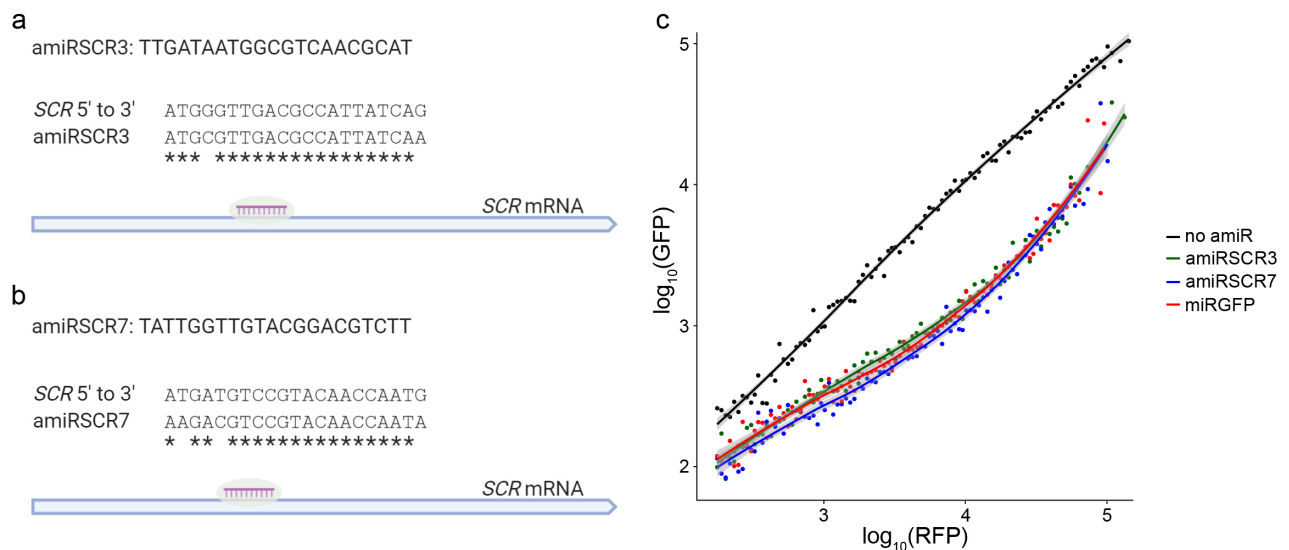


Figure 1: amiRSCR design and transient protoplast assay to assess amiRSCR efficiency. (a) amiRSCR3 and (b) amiRSCR7 target a single site in the first half of the SCR mRNA. Complementarity between target site and amiRNA is indicated by asterisks. (c) amiRSCR3 and amiRSCR7 efficiently downregulate GFP transcript containing amiRSCR binding sites. The

efficiency of both in the transient protoplast assay is comparable to that of the previously described miRGFP (Skopelitis et al., 2017). Note, while *SCR* target sites are shown (a-b), the assay was performed by amiRSCRs targeting a fluorophore containing binding sites identical to the ones shown (a-b).

amiRSCR3 consistently induces the *scr* phenotype in T1 plants

Testing the amiRSCRs in the transient protoplast assay is a convenient first tool to assay target downregulation. However, efficiency might alter when targeting the endogenous *SCR* transcript in plants. To test efficiency and functionality of amiRSCR3 and amiRSCR7 *in planta*, we designed a Gateway-based vector where both, the amiRSCR and promoter driving it, can be easily exchanged (Figure 2). Combining this with a seed coat expressing RFP cassette, we can assess the downregulation of *SCR* transcript by amiRSCRs driven from several promoters in the T1 generation. This enables an informed decision about promoter selection for a potential downstream mutant screening line.

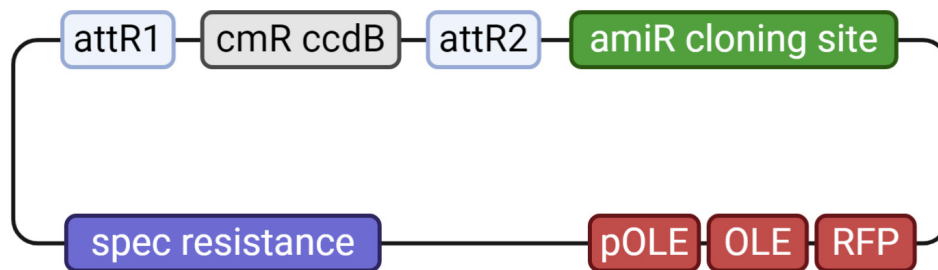


Figure 2: Binary vector for customised expression of amiRNAs. The desired promoter can be inserted using the Gateway technology (attR1 and attR2 sites), and the respective amiRNA can be cloned using the amiRNA cloning site, containing unique restriction sites.

Expression of amiRSCR3 and amiRSCR7 under the control of the *SCR* promoter (positive control) shows that both are potent enough to downregulate *SCR* to a critical level, resulting in a *scr-3*-like phenotype (Figure 3). However, amiRSCR3 induces a more severe and uniform *scr* phenotype, suggesting a higher degree of *SCR* downregulation. For this reason, we decided to use it for further experiments (Figure 3 b).

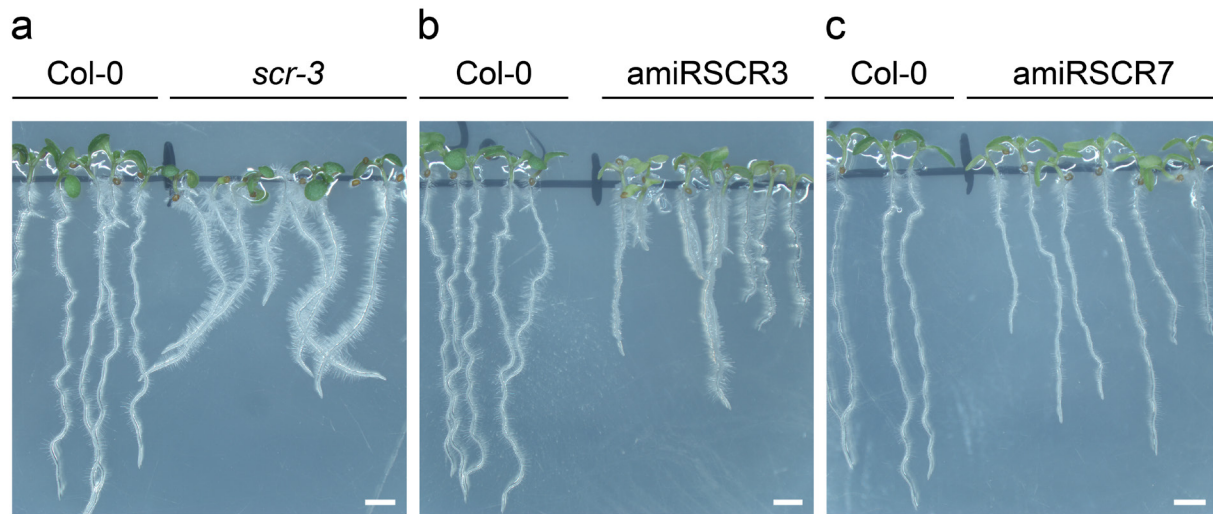


Figure 3: amiRSCR3 and amiRSCR7 induce a short root phenotype in T1 seedlings. (a) *scr-3* T-DNA mutant seedlings have shorter roots and an increased number of root hairs. (b) *pSCR:amiRSCR3* transgenic seedlings resemble the *scr-3* phenotype. The severity of the phenotype varies between T1 individuals. (c) *pSCR:amiRSCR7* induces an intermediate phenotype that results in a shorter, but not as severely affected root. Note: *scr-3* showing a milder phenotype than *amiRSCR3* might be due to truncated protein being present in the *scr-3* line (Fukaki et al., 1998). Scale bars = 2mm.

Single-cell RNA sequencing data highlight tissue-specific promoters for amiRSCR3 expression

We used expression data from the single-cell RNA sequencing (scRNA-seq) atlas of the root to identify promoters that can drive tissue-specific expression of *amiRSCR3* for the generation of a potential screening line (Denyer et al., 2019). Cluster identification is a challenge in analysing scRNA-seq data. To this end, we combined an informed cluster identification based on pre-existing data with an unbiased approach (for details see Chapter five). Here we identified differentially expressed genes in distinct clusters and subclusters and validated the spatiotemporal patterns of expression using transcriptional *promoter:3xVenus-NLS* reporter lines (Chapter five, Figure 3).

After successful cluster identification, we chose additional promoters from the dataset by two criteria. Firstly, expression must be specific to the tissues surrounding the endodermis and QC, such as in the stele, pericycle, and the surrounding cortex. Secondly, expression levels of promoters should be in a comparable range to the *SCR* promoter to produce sufficient *amiRSCR*.

With these guidelines, we predicted the expression patterns of the following promoters to be differential within the distinct tissues of the root (for details on prediction of highly differential genes in the root, see chapter five): *pAT2G16850* (pericycle), *pAT2G26700* (stele), *pAT5G50090* (xylem), *pAT1G62510* (cortex), *pAT1G62500* (meristematic cortex) and *pAT3G15680* (phloem). To verify expression *in vivo*, we created transcriptional *promoter:3xVenus-NLS* and *promoter:3xNLS-GFP* reporter constructs of candidate promoters (Figure 4, Denyer et al., 2019). Indeed, we validated the scRNA-seq predicted tissue-specific expression for all promoters in the root of *Arabidopsis* (Figure 4 a-f). Moving forward, we used the candidate promoters to drive tissue-specific expression of amiRSCR3 for analysis of silencing effects in the T1 generation.

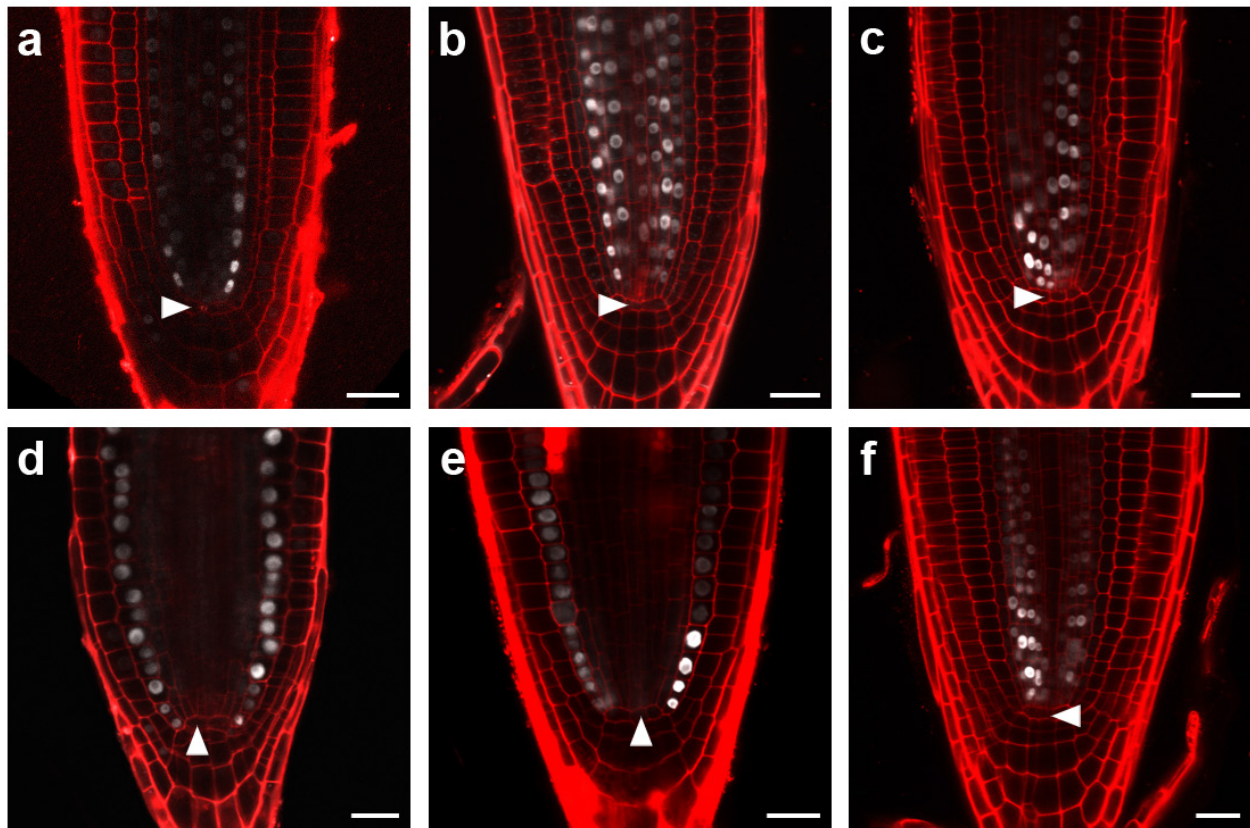


Figure 4: Promoter fusions verify predicted tissue-specific expression. (a) *pAT2G16850* in the pericycle (b) *pAT2G26700* in the stele (c) *pAT5G50090* in the xylem (d) *pAT1G62510* in the cortex (e) *pAT1G62500* in the meristematic cortex and (f) *pAT3G15680* in the phloem poles. Arrowheads indicate the position of the QC.

Restrictive miRNA mobility in the stele and phloem as a basis for a potential screening line

The analysis of T1 individuals driving amiRSCR3 from the selected promoters shows that in general, miRNA mobility originating in distinct root tissues is differential. Only the xylem-specific expression of amiRSCR3 results in an intermediate short root phenotype, while stele- and phloem-specific expression reproduces wild type-like roots. The wild type-like phenotypes from the stele and phloem specific expression confirm the previously reported, restrictive behaviour of miRNA in these tissues (Chapter two Figure 5 e, Supplementary Figure 6 g-k) (Skopelitis et al., 2018). Taken together, the results from the phenotypic screen of T1 individuals suggest that expression of amiRSCR3 in the phloem and the stele is suitable to screen for factors restricting entry into the endodermis or the QC. Xylem-specific expression of amiRSCR3 is ruled out as a potential screening line since restrictors of miRNA mobility seem to be absent in this tissue. The coming T1 plants expressing amiRSCR3 in the cortex and pericycle (Figure 4 a, d-e) will additionally give insights on mobility regulation from these cell files towards the endodermis and QC.

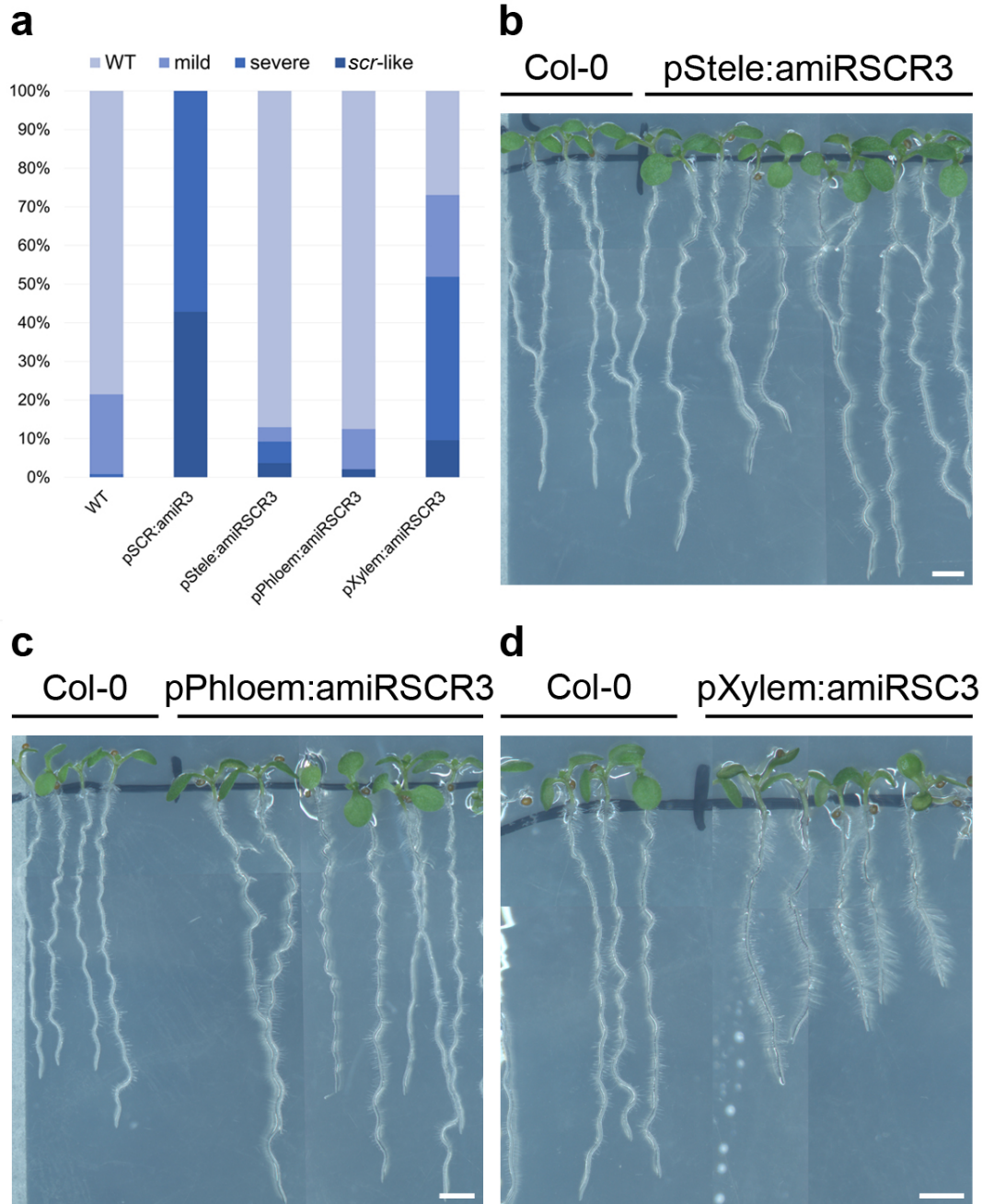


Figure 5: Tissue-specific expression of amiRSCR3 results in different phenotypes. (a) Distribution of T1 short root phenotypes ($n \geq 28$). Root length was categorised in *scr*-like < 0.5 cm, severe < 1 cm, mild < 1.75 cm and wild type-like > 1.75 cm. (b) amiRSCR3 expressed in the stele does not result in a short root phenotype, with most T1 plants showing wild type-like root lengths. (c) amiRSCR3 expressed in the phloem, similarly to (b), does not show a short root phenotype. (d) amiRSCR3 expressed in the xylem results in an intermediate phenotype with shorter roots, and increased number and length of root hairs. Images are composites. All T1 individuals within a single panel were grown on the same plate. Compare figure 3 b for the *pSCR:amiRSCR3* line phenotype. Scale bars = 2mm.

Discussion

Perspective

We identified lines that express amiRSCR3 in a phloem- and stele-specific manner, as being most promising for use in a forward genetic morphology-based screen. We are now propagating T1 individuals with a range of phenotypic variability. In the following T2 generation, we will test individual lines for homozygosity, consistency of the phenotype, and will look to quantify the generated amount of amiRSCR3. The quantification of amiRSCR3 is essential, since the ratio between target and miRNA is an important variable for effective downregulation of target mRNA (Skopelitis et al., 2017). High amount of amiRSCR3 in a line that shows a consistent wild type-like phenotype is desirable for an effective screening later. This guarantees the consistent downregulation of *SCR* transcript in a family that carries a mutagenised restrictor, and therefore eases the detection of the short root phenotype. Homozygous T2 lines will also be crossed to a previously generated *Arabidopsis* line containing ubiquitously expressed GFP with an amiRSCR3 target site. We will use the F1 offspring of this cross to visualise and confirm the activity of amiRSCR3 in plant roots. While analysing the amiRSCR3 lines for consistency, T2 lines will be propagated to obtain large amounts of T3 seed which will undergo ethyl methanesulfonate (EMS) treatment for mutagenesis to induce small nucleotide polymorphisms (SNPs) (Kim et al., 2006; Weigel and Glazebrook, 2006). Given that defects other than in miRNA gating might result in a short root phenotype (Benfey et al., 1993; Scheres et al., 1995), we generated a translational fusion construct *pSCR:SCR-GFP* in the Landsberg-*erecta* (Ler) ecotype to exclude false positive candidates from the screen. We will cross families showing a short root phenotype to this line to visualise and confirm that mobility of amiRSCR3 is increased, and *SCR* transcript depleted, in the endodermis and QC. Additionally, the offspring of this cross can later be used for whole genome sequencing to detect a putative causative allele by SNP enrichment.

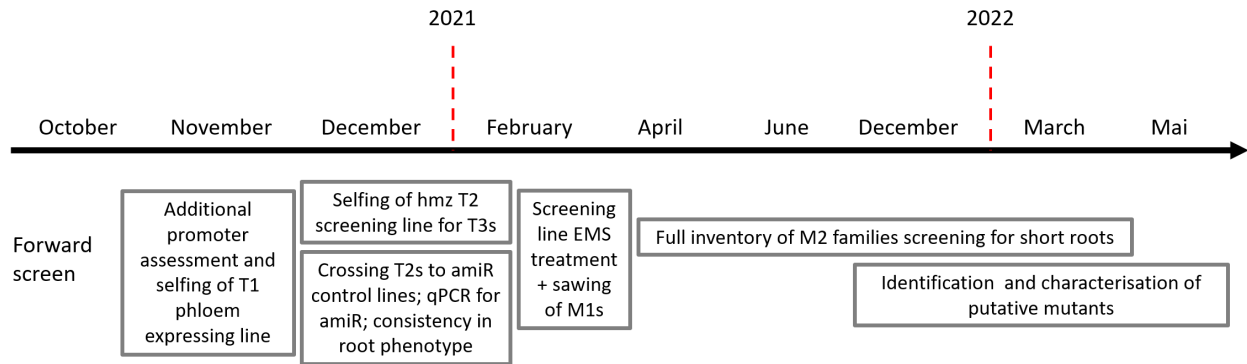


Figure 6: Expected timeline for the forward genetic screen.

Characterisation of an identified restrictor mutant will be a major task while screening and also after the screen. We previously showed that sRNA mobility is independently regulated from small protein diffusion (Skopelitis et al., 2018). Verifying the independence of both mechanisms in a mutant will give insights whether PD integrity is affected. In this regard it will also be interesting to compare the putative sRNA mobility with the active transport of proteins. This can be realised by comparing miRGFP mobility to mobility of an actively transported protein like WUSCHEL RELATED HOMEBOX 5 (WOX5) in the root meristem or WUSCHEL (WUS) in the SAM (Yadav et al., 2011; Daum et al., 2014; Pi et al., 2015). A developmental phenotype in a putative restrictor mutant hints at an endogenous mobile sRNAs being affected. We can identify these through e.g. transcriptomic analysis of target genes and determine the affected developmental processes. Putative restrictor candidates may be PD-localised and belong to the receptor-like kinase family (RLK). In any case it will be very exciting to identify interaction partners of these candidates, test whether these are involved in the mobility mechanism as well and to clarify the molecular framework.

Although the identification of mutants disrupting the gated movement of miRNAs will take more time (Figure 6), we have built the foundation for a successful screening platform. Moving forward with experiments confirming consistency in the eventual screening line, the later screen can quickly identify mutant families that show a phenotype due to increased miRNA mobility. The putative mutants obtained from this screen will be an insightful addition to the facilitators of mobility and will advance the discovery of the final sRNA mobility apparatus.

miRNA mobility is differentially regulated within distinct root tissues

The observed phenotypes in lines expressing amiRSCR3 in distinct cell files of the root supports the previously reported differential regulation of miRNA mobility in meristems (see chapter two). amiRSCR3 expressed in the stele and phloem is not able to move into the QC, making it impossible for amiRSCR3 to act on the *SCR* transcript. This results in a wild type-like phenotype. The restrictive mobility of amiRSCR in the phloem confirms the data obtained in chapter two where we showed that miRGFP present in the phloem is not offloaded into the root tip, however small molecules like free GFP are (Chapter two, Supplementary Figure 6 g-k). In contrast, amiRSCR3 expressed in the xylem tissue is mobile, leading to an intermediate *scr*-like phenotype. This intermediate phenotype may be due to amiRSCR3 partially deleting *SCR* transcript in the endodermis, but not in the QC. Another point could be that mobile amiSCR3 is able to downregulate *SCR* transcript to some degree but fails to completely eliminate its functionality. This is conceivable since scRNA-Seq expression data shows that the xylem-specific *AT5G50090* produces about ten times less transcripts as *SCR* (Denyer et al., 2019). These results highlight that expression levels are an important variable to keep in mind when screening for miRNA mobility. However, we can also be confident that a much weaker promoter coupled to amiRSCR3 is still able to produce a root phenotype that can be easily screened. This is beneficial for the future screen.

Combination of the reverse and forward genetic screens optimises candidate identification

As discussed in chapter three, a forward genetic screen struggles to identify mechanisms that rely on multiple, redundantly functioning proteins. Indeed, the first evidence for positive miRNA mobility regulators identified the BAM1 and BAM2 RLKs which act redundantly. This is problematic for a forward genetic screen since the probability of simultaneously mutagenising two closely related genes is extremely low. However, the forward genetic screen is still of use. Firstly, we are aiming to identify gatekeepers of mobility rather than facilitators, which might very well be an independent mechanism. Secondly, with the biases inherent in the reverse genetic screen, there is the need for an unbiased, easy-to-score morphology-based screen, which can reliably discover novel miRNA mobility regulators (see discussion of chapter three). An additional advantage of the forward genetic screen is that it does not rely on the phenotype of the GFP sensor

readout, but rather uses a morphology-based readout of mobility. With the combination of both, the candidate screen described in chapter three, and the forward genetic screen in this chapter, we optimise the probability of identifying miRNA mobility regulators.

Chapter five: Spatiotemporal Developmental Trajectories in the *Arabidopsis* Root Revealed Using High-Throughput Single-Cell RNA Sequencing

Tom Denyer*, Xiaoli Ma*, Simon Klesen, Emanuele Scacchi, Kay Nieselt, Marja C. P. Timmermans

Summary

High-throughput single-cell RNA sequencing (scRNA-seq) is becoming a cornerstone of developmental research, providing unprecedented power in understanding dynamic processes. Here, we present a high-resolution scRNA-seq expression atlas of the *Arabidopsis* root composed of thousands of independently profiled cells. This atlas provides detailed spatiotemporal information, identifying defining expression features for all major cell types, including the scarce cells of the quiescent center. These reveal key developmental regulators and downstream genes that translate cell fate into distinctive cell shapes and functions. Developmental trajectories derived from pseudotime analysis depict a finely resolved cascade of cell progressions from the niche through differentiation that are supported by mirroring expression waves of highly interconnected transcription factors. This study demonstrates the power of applying scRNA-seq to plants and provides an unparalleled spatiotemporal perspective of root cell differentiation.

Contributions:

Verification of *Arabidopsis* root single-cell clusters and pseudotime analysis through a set of unbiased reporter lines. Design, assembly and editing of figures.

*These authors contributed equally.

For details, see appendix IV.

General conclusions and discussion

sRNAs are mobile signalling molecules with regulatory functions in development. In this work we contributed to the understanding of how the mobility, a prerequisite for sRNA to act as a signalling molecule, might be realised on a molecular level. The experiments described in chapter two were focussed on regulation of mobility in different developmental contexts. Initial observations of mobile sRNAs hinted at passive diffusion being the mechanism of mobility represented by developmental sRNA gradients in the leaf and the root (Juarez et al., 2004; Chitwood et al., 2009; Carlsbecker et al., 2010). However, we showed that sRNA mobility is tightly regulated, especially in plant meristems and at the phloem/mesophyll border. This regulation is independent from passive diffusion and active protein transport. In the meristems and the phloem, the regulated sRNA mobility appears to rely on a restrictive mechanism. This negative regulation is realised via a gatekeeping mechanism polarised at specific cell-cell interfaces.

In addition to a negative regulation, recent evidence hints at the presence of a positive mechanism acting as facilitators of sRNA mobility. Indeed, in the examples of the leaf and root, facilitators might play a role in the establishment of sRNA gradients (see chapter one). In chapter three we presented the design of a reverse genetic screen based on the CRISPR/Cas9 system to identify facilitators of sRNA mobility in the root. We verified the workflow for efficient candidate mutagenesis and further identified the PD-localised RLKs BAM1 and BAM2 as facilitators of miRNA mobility. Among the upcoming candidates we might well identify additional genes involved in the regulation of sRNA mobility. For sure, the changes in mobility observed in this chapter hinted at additional mobility mechanisms being present that can recover and also may counteract the positive regulation of BAM1 and BAM2.

The negative regulation of sRNA mobility in stem cell niches described in chapter two suggests the presence of gatekeepers able to polarise at specific cell-cell interfaces. The combination of a positive and negative regulation might give the mobility mechanism unprecedented modulation possibilities. This could be imagined by a positive regulation being active in a tissue ubiquitously while the negative regulation could overwrite it to create distinct regions or borders of limited sRNA mobility. In chapter four of this work we presented the design for a forward genetic screen to identify these gatekeepers. This screen is based on an amiRNA targeting the *SCR* transcript. To

express this miRNA in distinct tissues, we identified tissue-specific promoters using the scRNA-seq atlas of the root, described in chapter five of this work. In this screen design, we can identify mutations in putative gatekeepers of sRNA mobility by a short root phenotype. The combination of both screens and their results will greatly advance our understanding of the sRNA mobility mechanism in plants.

The results obtained in this thesis hint at multiple, probably independent sRNA mobility mechanism being present in plants. Given the importance of sRNA in development, redundancy in the mobility mechanism is expected. While the results of chapter three hint at the same mode of mobility for both, miRNA and siRNA, it is unclear if this will be the case for additional positive or negative regulation mechanisms. It will also be interesting to determine how specificity is conveyed, either through sequence or interactions of proteins bound to the sRNA. Recently, Devers et al. showed that for siRNA-induced gene silencing, AGO-free primary siRNA duplexes are the mobile signal in short- and long-distance movement (Devers et al., 2020). If this is the case for mobile miRNAs as well, must be ascertained. However, it is still unclear how sRNAs are chaperoned towards the PD and what additional RNA binding proteins might play a role there. A sRNA could be captured by an RNA binding protein which then interacts with a PD-localised partner, for example an RLK. If this function could be carried out by AGO proteins remains an open question.

It is likely that any mode of regulation might happen at the PD. They are crucial for mobile signalling in general and the sRNA facilitators BAM1 and BAM2 are acting there. According to the idea that plasma membrane proteins organise in dynamic scaffolds it might be possible that BAM1 and BAM2 are partially involved in the maintenance of such a structure rather than being direct facilitators (Smakowska-Luzan et al., 2018). This fits the results obtained in chapter three where mobility is still possible but to a lower extent. There seems to be a need of such a scaffolding to concentrate proteins involved in the mobility mechanism given the amount and distribution of sRNA a cell might face (Huang et al., 2020). Concentrating this to PD might be an efficient way to centralise regulation of signalling and act as checkpoint for mobile sRNAs at the cell-cell interface.

With BAM1 and BAM2 being identified as the first facilitators of sRNA mobility it will be also interesting to determine further components involved and if these components are additional

members of the RLK family in *Arabidopsis* or might belong into other gene families. Additional regulators might well be identified as a result of the screens described in chapter three and four. siRNA mobility can be modified by a viral repressor protein binding to the kinase domains of BAM1 and BAM2. In the future it will be an interesting question to identify additional proteins, endogenous or exogenous, which might modulate sRNA mobility regulators, and how specificity is conveyed through these interactions.

Although the exact mechanism of sRNA mobility remains unknown, this study provided major insights into where sRNAs move and how mobility is regulated. As a result, major achievements into the mechanisms regulating mobility are within grasp, and it will be in the next years that sRNA mobility is ultimately resolved.

Methods

Plant materials and growth conditions

All analyses were performed in the Col-0 ecotype, either wild type, *bam1 bam2* or *rdr6-15* (SAIL_617). Plants were grown at 23 °C under long-day conditions in soil or on 0.7% agar plates containing 0.5x Murashige and Skoog (MS) medium (Duchefa) supplemented with 1% sucrose and appropriate antibiotics. Analyses on roots were performed 6-8 days after germination. *Arabidopsis* plants were transformed using the floral dip method as described by Clough & Bent, 1998 (Clough and Bent, 1998).

Design of sgRNAs

All sgRNAs in this study were designed using the benchling.com CRISPR/Cas9 guide tool. This tool is based on on-target and off-target data from recent publications commonly used for prediction (Hsu et al., 2013; Doench et al., 2016). To correspond with the amplicon sequencing approach for detection of CRISPR/Cas9 events we designed two sgRNAs in a range of 150bp as close to the ATG of the respective gene as the quality allowed. In general, only sgRNAs with an on-target value of more than 65 (ranging from 0-100, with 100 being the best) were chosen. All sgRNAs were ordered as oligos from Sigma Aldrich / Merck and cloned according to Decaestecker et al. (Decaestecker et al., 2019).

Generation of constructs and transgenic plants

For generation of CRISPR/Cas9 induced knock out lines we modified an already existing system to fit the pEC:Cas9 expression vector. For this, we added attL1 and attL2 sites into the vector pGGP_A-G to use it as an intermediate vector for Golden Gate assembly of the individual sgRNA entry clones as described by Decaestecker et al. (Decaestecker et al., 2019). This allowed us to first combine sgRNAs with a Golden Gate reaction into the intermediate vector, which then functions as a donor for the LR reaction into the pEC:Cas9 binary vector. The pEC:Cas9 vector was created by combining parts of the backbone of pDe-Cas9 with the EC promoter (Fauser et al., 2014; Wang et al., 2015). pDe-Cas9 was digested using EcoRI. The pEC and the Cas9 fragment

were amplified by PCR and combined with the digested backbone of pDE-Cas9 by In-Fusion cloning (Takara). The new vector was verified by sequencing.

Finished CRISPR/Cas9 expression vectors were verified by sequencing and transformed into the *pSCR:miRGFP* reporter line (Skopelitis et al., 2018). Additionally, every construct was transformed into Col-0 wild type plants to create a mutant seed library.

For creation of the promoter:amiR constructs, a cloning site was introduced by Gibson Assembly (Gibson Assembly® Master Mix, NEB #E2611L) into SK176, carrying a Gateway cassette as well as the OLE selection. By a first cloning step the desired amiR is incorporated into the pFK/390-B/c plasmid and then amplified for classical cloning into the binary vector SK176 (Carbonell et al., 2014). After the insertion of any amiR into SK176, this construct was further used to incorporate any promoter sequence to drive the amiR expression by using the Gateway system.

Creation of amplicon libraries

Genomic DNA was extracted of leaves from two-week-old seedlings using a 96-plate format and the Edwards DNA extraction protocol (Edwards et al., 1991). For each candidate we designed primers spanning the desired amplicon including the predicted CRISPR/Cas9 cutting sites. These first primers contained individual overhangs that served as an annealing site for barcoding primers used in the second PCR. For lines where we analysed more than 96 individuals, we used frameshifting nucleotides within the first primer to later identify individuals of the same line from different plates. Both PCRs were cleaned up with Ampure beads to remove primer and incomplete PCR residues. The final PCR was quantified using Quant-iT™ PicoGreen™ dsDNA Assay-Kit as well as running the pooled library on a Agilent 2100 Bioanalyzer chip (Agilent Technologies). The concentration of the pooled library was evaluated using the QuantiFluor® ONE dsDNA System where the samples were prepared according to the manufacturer's instructions. Libraries were sequenced 150bp paired end by NovaSeq 6000 (Novogene Ltd). Events were analysed by sequence alignment to the respective locus.

Confocal microscopy

Roots were supplied in 10 µg/mL Propidium Iodide (PI) (Sigma-Aldrich) in water on the microscope slide and immediately imaged. Excitation of PI was captured at 561 nm and GFP was

captured at 490–533 nm. Root imaging was performed using a Leica SP8 laser-scanning confocal microscope and a Zeiss LSM 880.

Transient protoplast assay to access small RNA-target regulation in single protoplast cells

amiRNAs for targeting the *SCR* transcript were designed using the Web MicroRNA Designer (Schwab et al., 2006; Ossowski et al., 2008). We designed a construct with two fluorescent reporters; GFP is modified to be targeted by the selected amiR, while RFP is used as a normalisation control. Target sites of individual amiRs were introduced at the 3' end of the *GFP* coding region. Target sites were designed as oligonucleotides and incorporated by classical cloning. Protoplasts were co-transfected with the amiRNA and the respective target. Samples were analysed in BD LSRFortessa with the following voltages: FSC 50V, SSC 210, mCherry 330V and eGFP 270V. mCherry was excited at 561nm and eGFP at 488nm. We used un-transfected and samples only transfected with eGFP and mCherry as controls. The raw data were analysed with FlowJo to gate cells according to their forward (FSC) and side (SSC) scatter profiles. After gating for the positive mCherry, the gated data was exported and analysed in R.

References

- Allen, E., et al. (2005). "microRNA-directed phasing during trans-acting siRNA biogenesis in plants." Cell **121**(2): 207-221.
- Alvarez, J. P., et al. (2006). "Endogenous and synthetic microRNAs stimulate simultaneous, efficient, and localized regulation of multiple targets in diverse species." Plant Cell **18**(5): 1134-1151.
- Amari, K., et al. (2010). "A family of plasmodesmal proteins with receptor-like properties for plant viral movement proteins." PLoS Pathog **6**(9): e1001119.
- Aregger, M., et al. (2012). "Primary and secondary siRNAs in geminivirus-induced gene silencing." PLoS Pathog **8**(9): e1002941.
- Bartel, D. P. (2004). "MicroRNAs: genomics, biogenesis, mechanism, and function." Cell **116**(2): 281-297.
- Benfey, P. N., et al. (1993). "Root development in Arabidopsis: four mutants with dramatically altered root morphogenesis." Development **119**(1): 57-70.
- Birnbaum, K., et al. (2003). "A gene expression map of the Arabidopsis root." Science **302**(5652): 1956-1960.
- Bleys, A., et al. (2006). "The frequency and efficiency of endogene suppression by transitive silencing signals is influenced by the length of sequence homology." Plant physiology **142**(2): 788-796.
- Borges, F. and R. A. Martienssen (2015). "The expanding world of small RNAs in plants." Nature Reviews Molecular Cell Biology **16**(12): 727.
- Borges, F., et al. (2018). "Transposon-derived small RNAs triggered by miR845 mediate genome dosage response in Arabidopsis." Nature genetics **50**(2): 186.
- Brady, S. M., et al. (2007). "A high-resolution root spatiotemporal map reveals dominant expression patterns." Science **318**(5851): 801-806.
- Brosnan, C. A. and O. Voinnet (2011). "Cell-to-cell and long-distance siRNA movement in plants: mechanisms and biological implications." Curr Opin Plant Biol **14**(5): 580-587.

Buhtz, A., et al. (2010). "Phloem small RNAs, nutrient stress responses, and systemic mobility." BMC plant biology **10**(1): 64.

Buhtz, A., et al. (2008). "Identification and characterization of small RNAs from the phloem of *Brassica napus*." The Plant Journal **53**(5): 739-749.

Burch-Smith, T. M. and P. C. Zambryski (2012). "Plasmodesmata paradigm shift: regulation from without versus within." Annual review of plant biology **63**: 239-260.

Burgyán, J. and Z. Havelda (2011). "Viral suppressors of RNA silencing." Trends in Plant Science **16**(5): 265-272.

Caggiano, M. P., et al. (2017). "Cell type boundaries organize plant development." Elife **6**: e27421.

Carbonell, A., et al. (2014). "New generation of artificial microRNA and synthetic trans-acting small interfering RNA vectors for efficient gene silencing in *Arabidopsis*." Plant physiology **165**(1): 15-29.

Carlsbecker, A., et al. (2010). "Cell signalling by microRNA165/6 directs gene dose-dependent root cell fate." Nature **465**(7296): 316.

Chen, L., et al. (2017). "Identify key sequence features to improve CRISPR sgRNA efficacy." IEEE Access **5**: 26582-26590.

Chen, X., et al. (2014). "Dual sgRNA-directed gene knockout using CRISPR/Cas9 technology in *Caenorhabditis elegans*." Scientific reports **4**: 7581.

Chitwood, D. H., et al. (2009). "Pattern formation via small RNA mobility." Genes & development **23**(5): 549-554.

Chitwood, D. H. and M. C. Timmermans (2010). "Small RNAs are on the move." Nature **467**(7314): 415.

Clough, S. J. and A. F. Bent (1998). "Floral dip: a simplified method for *Agrobacterium*-mediated transformation of *Arabidopsis thaliana*." The Plant Journal **16**(6): 735-743.

Crawford, K. M. and P. C. Zambryski (2001). "Non-targeted and targeted protein movement through plasmodesmata in leaves in different developmental and physiological states." Plant physiology **125**(4): 1802-1812.

Cui, H., et al. (2007). "An evolutionarily conserved mechanism delimiting SHR movement defines a single layer of endodermis in plants." Science **316**(5823): 421-425.

D'Ario, M., et al. (2017). "Small RNAs: big impact on plant development." Trends in Plant Science **22**(12): 1056-1068.

Daum, G., et al. (2014). "A mechanistic framework for noncell autonomous stem cell induction in Arabidopsis." Proceedings of the National Academy of Sciences **111**(40): 14619-14624.

de Felippes, F. F. and P. M. Waterhouse (2020). "The whys and wherefores of transitivity in plants." Front Plant Sci **11**: 1340.

Decaestecker, W., et al. (2019). "CRISPR-TSKO: a technique for efficient mutagenesis in specific cell types, tissues, or organs in Arabidopsis." Plant Cell **31**(12): 2868-2887.

Denyer, T., et al. (2019). "Spatiotemporal developmental trajectories in the Arabidopsis root revealed using high-throughput single-cell RNA sequencing." Developmental cell **48**(6): 840-852. e845.

Devers, E. A., et al. (2020). "Movement and differential consumption of short interfering RNA duplexes underlie mobile RNA interference." Nature Plants **6**(7): 789-799.

Di Laurenzio, L., et al. (1996). "The SCARECROW gene regulates an asymmetric cell division that is essential for generating the radial organization of the Arabidopsis root." Cell **86**(3): 423-433.

Di Ruocco, G., et al. (2018). "Building the differences: a case for the ground tissue patterning in plants." Proceedings of the Royal Society B **285**(1890): 20181746.

Doench, J. G., et al. (2016). "Optimized sgRNA design to maximize activity and minimize off-target effects of CRISPR-Cas9." Nature biotechnology **34**(2): 184-191.

Edwards, K., et al. (1991). "A simple and rapid method for the preparation of plant genomic DNA for PCR analysis." Nucleic acids research **19**(6): 1349.

Elbashir, S. M., et al. (2002). "Analysis of gene function in somatic mammalian cells using small interfering RNAs." Methods **26**(2): 199-213.

Emery, J. F., et al. (2003). "Radial patterning of Arabidopsis shoots by class III HD-ZIP and KANADI genes." Current Biology **13**(20): 1768-1774.

Fausser, F., et al. (2014). "Both CRISPR/C as-based nucleases and nickases can be used efficiently for genome engineering in Arabidopsis thaliana." The Plant Journal **79**(2): 348-359.

Felippes, F. F. d., et al. (2010). "Comparative analysis of non-autonomous effects of tasiRNAs and miRNAs in Arabidopsis thaliana." Nucleic acids research **39**(7): 2880-2889.

Ferguson, B. J., et al. (2019). "Legume nodulation: The host controls the party." Plant, cell & environment **42**(1): 41-51.

Fernandez-Calvino, L., et al. (2011). "Arabidopsis plasmodesmal proteome." PloS one **6**(4).

Fire, A., et al. (1998). "Potent and specific genetic interference by double-stranded RNA in *Caenorhabditis elegans*." Nature **391**(6669): 806-811.

Frankel, N., et al. (2010). "Phenotypic robustness conferred by apparently redundant transcriptional enhancers." Nature **466**(7305): 490.

Fujii, H., et al. (2005). "A miRNA involved in phosphate-starvation response in Arabidopsis." Current Biology **15**(22): 2038-2043.

Fukaki, H., et al. (1998). "Genetic evidence that the endodermis is essential for shoot gravitropism in Arabidopsis thaliana." The Plant Journal **14**(4): 425-430.

Gaillochet, C., et al. (2020). "CRISPR Screens in Plants: Approaches, Guidelines, and Future Prospects." Plant Cell.

Gallagher, K. L., et al. (2004). "Mechanisms regulating SHORT-ROOT intercellular movement." Current Biology **14**(20): 1847-1851.

Gilbert, L. A., et al. (2013). "CRISPR-mediated modular RNA-guided regulation of transcription in eukaryotes." Cell **154**(2): 442-451.

Gramzow, L. and G. Theißen (2019). Plant miRNA Conservation and Evolution. Plant MicroRNAs, Springer: 41-50.

Greb, T. and J. U. Lohmann (2016). "Plant stem cells." Current Biology **26**(17): R816-R821.

Ham, B.-K. and W. J. Lucas (2017). "Phloem-mobile RNAs as systemic signaling agents." Annual review of plant biology **68**: 173-195.

Hamilton, A. J. and D. C. Baulcombe (1999). "A species of small antisense RNA in posttranscriptional gene silencing in plants." Science **286**(5441): 950-952.

Han, H., et al. (2020). "A signal cascade originated from epidermis defines apical-basal patterning of Arabidopsis shoot apical meristems." Nature communications **11**(1): 1-17.

Helariutta, Y., et al. (2000). "The SHORT-ROOT gene controls radial patterning of the Arabidopsis root through radial signaling." Cell **101**(5): 555-567.

Himber, C., et al. (2003). "Transitivity-dependent and-independent cell-to-cell movement of RNA silencing." The EMBO journal **22**(17): 4523-4533.

Hiratsu, K., et al. (2003). "Dominant repression of target genes by chimeric repressors that include the EAR motif, a repression domain, in Arabidopsis." The Plant Journal **34**(5): 733-739.

Hord, C. L., et al. (2006). "The BAM1/BAM2 receptor-like kinases are important regulators of Arabidopsis early anther development." Plant Cell **18**(7): 1667-1680.

Hsu, P. D., et al. (2013). "DNA targeting specificity of RNA-guided Cas9 nucleases." Nature biotechnology **31**(9): 827-832.

Huang, K., et al. (2020). "Quantitative, super-resolution localization of small RNAs with sRNA-PAINT." Nucleic acids research **48**(16): e96-e96.

Husbands, A. Y., et al. (2015). "The ASYMMETRIC LEAVES complex employs multiple modes of regulation to affect adaxial-abaxial patterning and leaf complexity." Plant Cell **27**(12): 3321-3335.

Juarez, M. T., et al. (2004). "microRNA-mediated repression of rolled leaf1 specifies maize leaf polarity." Nature **428**(6978): 84.

Kim, I., et al. (2005). "Cell-to-cell movement of GFP during embryogenesis and early seedling development in Arabidopsis." Proceedings of the National Academy of Sciences **102**(6): 2227-2231.

- Kim, Y., et al. (2006). EMS mutagenesis of Arabidopsis. Arabidopsis Protocols, Springer: 101-103.
- Klesen, S., et al. (2020). Small RNAs as plant morphogens. Current Topics in Developmental Biology, Elsevier. **137**: 455-480.
- Knauer, S., et al. (2013). "A protodermal miR394 signal defines a region of stem cell competence in the Arabidopsis shoot meristem." Developmental cell **24**(2): 125-132.
- Konermann, S., et al. (2015). "Genome-scale transcriptional activation by an engineered CRISPR-Cas9 complex." Nature **517**(7536): 583-588.
- Kościańska, E., et al. (2005). "Analysis of RNA silencing in agroinfiltrated leaves of *Nicotiana benthamiana* and *Nicotiana tabacum*." Plant molecular biology **59**(4): 647-661.
- Kuhlemeier, C. and M. C. Timmermans (2016). "The Sussex signal: insights into leaf dorsiventrality." Development **143**(18): 3230-3237.
- Labuhn, M., et al. (2018). "Refined sgRNA efficacy prediction improves large-and small-scale CRISPR-Cas9 applications." Nucleic acids research **46**(3): 1375-1385.
- LeBlanc, C., et al. (2018). "Increased efficiency of targeted mutagenesis by CRISPR/Cas9 in plants using heat stress." The Plant Journal **93**(2): 377-386.
- Lee, R. C., et al. (1993). "The *C. elegans* heterochronic gene *lin-4* encodes small RNAs with antisense complementarity to *lin-14*." Cell **75**(5): 843-854.
- Levy, A., et al. (2007). "A plasmodesmata-associated β -1, 3-glucanase in Arabidopsis." The Plant Journal **49**(4): 669-682.
- Lewsey, M. G., et al. (2016). "Mobile small RNAs regulate genome-wide DNA methylation." Proceedings of the National Academy of Sciences **113**(6): E801-E810.
- Lin, S.-I., et al. (2008). "Regulatory network of microRNA399 and PHO2 by systemic signaling." Plant physiology **147**(2): 732-746.
- Liu, L. and X. Chen (2018). "Intercellular and systemic trafficking of RNAs in plants." Nature Plants **4**(11): 869-878.

Liu, Q., et al. (2009). "The ARGONAUTE10 gene modulates shoot apical meristem maintenance and establishment of leaf polarity by repressing miR165/166 in Arabidopsis." The Plant Journal **58**(1): 27-40.

Llave, C., et al. (2002). "Cleavage of Scarecrow-like mRNA targets directed by a class of Arabidopsis miRNA." Science **297**(5589): 2053-2056.

Lowder, L. G., et al. (2018). "Robust transcriptional activation in plants using multiplexed CRISPR-Act2. 0 and mTALE-Act systems." Molecular plant **11**(2): 245-256.

Mair, A., et al. (2019). "Proximity labeling of protein complexes and cell-type-specific organellar proteomes in Arabidopsis enabled by TurboID." Elife **8**: e47864.

Mallory, A. C., et al. (2004). "MicroRNA control of PHABULOSA in leaf development: importance of pairing to the microRNA 5' region." The EMBO journal **23**(16): 3356-3364.

Man, J., et al. (2020). "Structural evolution drives diversification of the large LRR-RLK gene family." New phytologist **226**(5): 1492-1505.

Manavella, P. A., et al. (2012). "Plant secondary siRNA production determined by microRNA-duplex structure." Proceedings of the National Academy of Sciences **109**(7): 2461-2466.

Margolin, J. F., et al. (1994). "Krüppel-associated boxes are potent transcriptional repression domains." Proceedings of the National Academy of Sciences **91**(10): 4509-4513.

Martínez, G., et al. (2016). "Silencing in sperm cells is directed by RNA movement from the surrounding nurse cell." Nature Plants **2**(4): 1-8.

Martinez, G., et al. (2018). "Paternal easiRNAs regulate parental genome dosage in Arabidopsis." Nature genetics **50**(2): 193-198.

Matthewman, C. A., et al. (2012). "miR395 is a general component of the sulfate assimilation regulatory network in Arabidopsis." FEBS Lett **586**(19): 3242-3248.

McConnell, J. R., et al. (2001). "Role of PHABULOSA and PHAVOLUTA in determining radial patterning in shoots." Nature **411**(6838): 709-713.

Melnyk, C. W., et al. (2011). "Intercellular and systemic movement of RNA silencing signals." The EMBO journal **30**(17): 3553-3563.

Metzger, B. P., et al. (2015). "Selection on noise constrains variation in a eukaryotic promoter." Nature **521**(7552): 344.

Miki, D., et al. (2005). "RNA silencing of single and multiple members in a gene family of rice." Plant physiology **138**(4): 1903-1913.

Miyashima, S., et al. (2011). "Non-cell-autonomous microRNA165 acts in a dose-dependent manner to regulate multiple differentiation status in the Arabidopsis root." Development **138**(11): 2303-2313.

Miyashima, S., et al. (2019). "Mobile PEAR transcription factors integrate positional cues to prime cambial growth." Nature **565**(7740): 490-494.

Moissiard, G., et al. (2007). "Transitivity in Arabidopsis can be primed, requires the redundant action of the antiviral Dicer-like 4 and Dicer-like 2, and is compromised by viral-encoded suppressor proteins." Rna **13**(8): 1268-1278.

Molnar, A., et al. (2010). "Small silencing RNAs in plants are mobile and direct epigenetic modification in recipient cells." Science **328**(5980): 872-875.

Montgomery, M. K., et al. (1998). "RNA as a target of double-stranded RNA-mediated genetic interference in *Caenorhabditis elegans*." Proceedings of the National Academy of Sciences **95**(26): 15502-15507.

Montgomery, T. A., et al. (2008). "Specificity of ARGONAUTE7-miR390 interaction and dual functionality in TAS3 trans-acting siRNA formation." Cell **133**(1): 128-141.

Nagasaki, H., et al. (2007). "The small interfering RNA production pathway is required for shoot meristem initiation in rice." Proceedings of the National Academy of Sciences **104**(37): 14867-14871.

Nakajima, K., et al. (2001). "Intercellular movement of the putative transcription factor SHR in root patterning." Nature **413**(6853): 307.

Napoli, C., et al. (1990). "Introduction of a chimeric chalcone synthase gene into petunia results in reversible co-suppression of homologous genes in trans." Plant Cell **2**(4): 279-289.

Nogueira, F. T., et al. (2007). "Two small regulatory RNAs establish opposing fates of a developmental axis." Genes & development **21**(7): 750-755.

Olmedo-Monfil, V., et al. (2010). "Control of female gamete formation by a small RNA pathway in Arabidopsis." Nature **464**(7288): 628.

Oparka, K. J., et al. (1999). "Simple, but not branched, plasmodesmata allow the nonspecific trafficking of proteins in developing tobacco leaves." Cell **97**(6): 743-754.

Ossowski, S., et al. (2008). "Gene silencing in plants using artificial microRNAs and other small RNAs." The Plant Journal **53**(4): 674-690.

Palauqui, J. C., et al. (1997). "Systemic acquired silencing: transgene-specific post-transcriptional silencing is transmitted by grafting from silenced stocks to non-silenced scions." The EMBO journal **16**(15): 4738-4745.

Pant, B. D., et al. (2008). "MicroRNA399 is a long-distance signal for the regulation of plant phosphate homeostasis." The Plant Journal **53**(5): 731-738.

Parizotto, E. A., et al. (2004). "In vivo investigation of the transcription, processing, endonucleolytic activity, and functional relevance of the spatial distribution of a plant miRNA." Genes & development **18**(18): 2237-2242.

Park, W., et al. (2002). "CARPEL FACTORY, a Dicer homolog, and HEN1, a novel protein, act in microRNA metabolism in Arabidopsis thaliana." Current Biology **12**(17): 1484-1495.

Petersen, B. O. and M. Albrechtsen (2005). "Evidence implying only unprimed RdRP activity during transitive gene silencing in plants." Plant molecular biology **58**(4): 575-583.

Petsch, K., et al. (2015). "Novel DICER-LIKE1 siRNAs bypass the requirement for DICER-LIKE4 in maize development." Plant Cell **27**(8): 2163-2177.

Pi, L., et al. (2015). "Organizer-derived WOX5 signal maintains root columella stem cells through chromatin-mediated repression of CDF4 expression." Developmental cell **33**(5): 576-588.

Plavskin, Y., et al. (2016). "Ancient trans-acting siRNAs confer robustness and sensitivity onto the auxin response." Developmental cell **36**(3): 276-289.

Prigge, M. J., et al. (2005). "Class III homeodomain-leucine zipper gene family members have overlapping, antagonistic, and distinct roles in Arabidopsis development." Plant Cell **17**(1): 61-76.

Pyott, D. E. and A. Molnar (2015). "Going mobile: Non-cell-autonomous small RNAs shape the genetic landscape of plants." Plant Biotechnol J **13**(3): 306-318.

Reagan, B. C., et al. (2018). "RNA on the move: The plasmodesmata perspective." Plant Science **275**: 1-10.

Reinhardt, D., et al. (2005). "Microsurgical and laser ablation analysis of leaf positioning and dorsoventral patterning in tomato." Development **132**(1): 15-26.

Reinhart, B. J., et al. (2002). "MicroRNAs in plants." Genes & development **16**(13): 1616-1626.

Rhoades, M. W., et al. (2002). "Prediction of plant microRNA targets." Cell **110**(4): 513-520.

Rosas-Diaz, T., et al. (2018). "A virus-targeted plant receptor-like kinase promotes cell-to-cell spread of RNAi." Proceedings of the National Academy of Sciences **115**(6): 1388-1393.

Ruiz-Ferrer, V. and O. Voinnet (2009). "Roles of plant small RNAs in biotic stress responses." Annu Rev Plant Biol **60**: 485-510.

Ruvkun, G. (2001). "Glimpses of a tiny RNA world." Science **294**(5543): 797.

Sabatini, S., et al. (2003). "SCARECROW is involved in positioning the stem cell niche in the Arabidopsis root meristem." Genes & development **17**(3): 354-358.

Sagi, G., et al. (2005). "Class 1 reversibly glycosylated polypeptides are plasmodesmal-associated proteins delivered to plasmodesmata via the Golgi apparatus." Plant Cell **17**(6): 1788-1800.

Scheres, B., et al. (1995). "Mutations affecting the radial organisation of the Arabidopsis root display specific defects throughout the embryonic axis." Development **121**(1): 53-62.

Schmiedel, J. M., et al. (2015). "MicroRNA control of protein expression noise." Science **348**(6230): 128-132.

Schwab, R., et al. (2006). "Highly specific gene silencing by artificial microRNAs in Arabidopsis." Plant Cell **18**(5): 1121-1133.

Shimizu, N., et al. (2015). "BAM 1 and RECEPTOR-LIKE PROTEIN KINASE 2 constitute a signaling pathway and modulate CLE peptide-triggered growth inhibition in Arabidopsis root." New phytologist **208**(4): 1104-1113.

Skopelitis, D. S., et al. (2017). "Boundary formation through a direct threshold-based readout of mobile small RNA gradients." Developmental cell **43**(3): 265-273. e266.

Skopelitis, D. S., et al. (2018). "Gating of miRNA movement at defined cell-cell interfaces governs their impact as positional signals." Nature communications **9**(1): 3107.

Slotkin, R. K., et al. (2009). "Epigenetic reprogramming and small RNA silencing of transposable elements in pollen." Cell **136**(3): 461-472.

Smakowska-Luzan, E., et al. (2018). "An extracellular network of Arabidopsis leucine-rich repeat receptor kinases." Nature **553**(7688): 342-346.

Smith, C., et al. (1990). "Expression of a truncated tomato polygalacturonase gene inhibits expression of the endogenous gene in transgenic plants." Molecular and General Genetics MGG **224**(3): 477-481.

Soyars, C. L., et al. (2016). "Ready, aim, shoot: stem cell regulation of the shoot apical meristem." Curr Opin Plant Biol **29**: 163-168.

Sprunck, S., et al. (2012). "Egg cell–secreted EC1 triggers sperm cell activation during double fertilization." Science **338**(6110): 1093-1097.

Stahl, Y. and C. Faulkner (2016). "Receptor complex mediated regulation of symplastic traffic." Trends in Plant Science **21**(5): 450-459.

Steeves, T. A. and I. M. Sussex (1989). Patterns in plant development, Cambridge University Press.

Su, Z., et al. (2020). "Regulation of female germline specification via small RNA mobility in Arabidopsis." Plant Cell **32**(9): 2842-2854.

Su, Z., et al. (2017). "The THO complex non-cell-autonomously represses female germline specification through the TAS3-ARF3 module." Current Biology **27**(11): 1597-1609. e1592.

Symeonidi, E., et al. (2020). "CRISPR-finder: A high throughput and cost effective method for identifying successfully edited *A. thaliana* individuals." bioRxiv.

Takahara, M., et al. (2013). "TOO MUCH LOVE, a novel kelch repeat-containing F-box protein, functions in the long-distance regulation of the legume–Rhizobium symbiosis." Plant and Cell Physiology **54**(4): 433-447.

Taochy, C., et al. (2017). "A genetic screen for impaired systemic RNAi highlights the crucial role of DICER-LIKE 2." Plant physiology **175**(3): 1424-1437.

Tilsner, J., et al. (2016). "Staying tight: plasmodesmal membrane contact sites and the control of cell-to-cell connectivity in plants." Annual review of plant biology **67**.

Tsikou, D., et al. (2018). "Systemic control of legume susceptibility to rhizobial infection by a mobile microRNA." Science **362**(6411): 233-236.

Tucker, M. R., et al. (2012). "Somatic small RNA pathways promote the mitotic events of megagametogenesis during female reproductive development in Arabidopsis." Development **139**(8): 1399-1404.

Vaistij, F. E., et al. (2002). "Spreading of RNA targeting and DNA methylation in RNA silencing requires transcription of the target gene and a putative RNA-dependent RNA polymerase." Plant Cell **14**(4): 857-867.

Van der Krol, A. R., et al. (1990). "Flavonoid genes in petunia: addition of a limited number of gene copies may lead to a suppression of gene expression." Plant Cell **2**(4): 291-299.

Van Leene, J., et al. (2015). "An improved toolbox to unravel the plant cellular machinery by tandem affinity purification of Arabidopsis protein complexes." Nature protocols **10**(1): 169-187.

Vatén, A., et al. (2011). "Callose biosynthesis regulates symplastic trafficking during root development." Developmental cell **21**(6): 1144-1155.

Verkuijl, S. A. and M. G. Rots (2019). "The influence of eukaryotic chromatin state on CRISPR–Cas9 editing efficiencies." Curr Opin Biotechnol **55**: 68-73.

Voinnet, O. and D. C. Baulcombe (1997). "Systemic signalling in gene silencing." Nature **389**(6651): 553.

Voinnet, O., et al. (1998). "Systemic spread of sequence-specific transgene RNA degradation in plants is initiated by localized introduction of ectopic promoterless DNA." Cell **95**(2): 177-187.

Wang, G., et al. (2018). "Sequestration of a transposon-derived siRNA by a target mimic imprinted gene induces postzygotic reproductive isolation in Arabidopsis." Developmental cell **46**(6): 696-705. e694.

Wang, Z.-P., et al. (2015). "Egg cell-specific promoter-controlled CRISPR/Cas9 efficiently generates homozygous mutants for multiple target genes in Arabidopsis in a single generation." Genome Biol **16**(1): 144.

Weigel, D. and J. Glazebrook (2006). "EMS mutagenesis of Arabidopsis seed." Cold Spring Harbor Protocols **2006**(5): pdb. prot4621.

Willmann, M. R. and R. S. Poethig (2007). "Conservation and evolution of miRNA regulatory programs in plant development." Curr Opin Plant Biol **10**(5): 503-511.

Wu, S. and K. L. Gallagher (2012). "Transcription factors on the move." Curr Opin Plant Biol **15**(6): 645-651.

Wysocka-Diller, J. W., et al. (2000). "Molecular analysis of SCARECROW function reveals a radial patterning mechanism common to root and shoot." Development **127**(3): 595-603.

Yadav, R. K., et al. (2011). "WUSCHEL protein movement mediates stem cell homeostasis in the Arabidopsis shoot apex." Genes & development **25**(19): 2025-2030.

Yang, T., et al. (2018). "The making of leaves: how small RNA networks modulate leaf development." Front Plant Sci **9**: 824.

Yao, X., et al. (2009). "Two types of cis-acting elements control the abaxial epidermis-specific transcription of the MIR165a and MIR166a genes." FEBS Lett **583**(22): 3711-3717.

Yifhar, T., et al. (2012). "Failure of the tomato trans-acting short interfering RNA program to regulate AUXIN RESPONSE FACTOR3 and ARF4 underlies the wiry leaf syndrome." Plant Cell **24**(9): 3575-3589.

Yoo, B.-C., et al. (2004). "A systemic small RNA signaling system in plants." Plant Cell **16**(8): 1979-2000.

Yu, Y., et al. (2017). "ARGONAUTE10 promotes the degradation of miR165/6 through the SDN1 and SDN2 exonucleases in Arabidopsis." PLoS biology **15**(2): e2001272.

Yu, Y., et al. (2017). "The 'how' and 'where' of plant micro RNA s." New phytologist **216**(4): 1002-1017.

Zavaliev, R., et al. (2009). "The constitutive expression of Arabidopsis plasmodesmal-associated class 1 reversibly glycosylated polypeptide impairs plant development and virus spread." Journal of Experimental Botany **61**(1): 131-142.

Zhang, W., et al. (2014). "Graft-transmissible movement of inverted-repeat-induced si RNA signals into flowers." The Plant Journal **80**(1): 106-121.

Zhang, X., et al. (2019). "Mini review: Revisiting mobile RNA silencing in plants." Plant Science **278**: 113-117.

Zhang, Z., et al. (2017). "A molecular framework for the embryonic initiation of shoot meristem stem cells." Developmental cell **40**(3): 264-277. e264.

Zhang, Z. and X. Zhang (2012). "Argonautes compete for miR165/166 to regulate shoot apical meristem development." Curr Opin Plant Biol **15**(6): 652-658.

Zhu, H., et al. (2011). "Arabidopsis Argonaute10 specifically sequesters miR166/165 to regulate shoot apical meristem development." Cell **145**(2): 242-256.

Zulawski, M., et al. (2014). "The Arabidopsis Kinome: phylogeny and evolutionary insights into functional diversification." BMC genomics **15**(1): 1-15.

Appendix I



Small RNAs as plant morphogens

Simon Klesen, Kristine Hill, Marja C.P. Timmermans*

Center for Plant Molecular Biology, University of Tübingen, Tübingen, Germany

*Corresponding author: e-mail address: marja.timmermans@zmbp.uni-tuebingen.de

Contents

1. Introduction	456
2. Small RNAs as mobile instructive signals	457
2.1 Opposing gradients of mobile small RNAs establish leaf polarity	458
2.2 A miR166 mobility gradient specifies cell fate within the root	461
2.3 miR394 mobility delineates the embryonic shoot stem cell niche	462
3. Reading out the gradient	463
3.1 Patterning properties of small RNA gradients are developmental-context dependent	463
3.2 Making the switch	464
4. Generating the small RNA gradient	467
4.1 Small RNA turnover	468
4.2 Regulation of small RNA mobility	468
5. Why so complicated?	471
6. Concluding remarks	472
Acknowledgments	473
References	473
Further reading	480

Abstract

The coordination of cell fate decisions within complex multicellular structures rests on intercellular communication. To generate ordered patterns, cells need to know their relative positions within the growing structure. This is commonly achieved via the production and perception of mobile signaling molecules. In animal systems, such positional signals often act as morphogens and subdivide a field of cells into domains of discrete cell identities using a threshold-based readout of their mobility gradient. Reflecting the independent origin of multicellularity, plants evolved distinct signaling mechanisms to drive cell fate decisions. Many of the basic principles underlying developmental patterning are, however, shared between animals and plants, including the use of signaling gradients to provide positional information. In plant development, small RNAs can act as mobile instructive signals, and similar to classical morphogens in animals, employ a threshold-based readout of their mobility gradient to generate precisely defined cell fate boundaries. Given the distinctive nature of peptide morphogens and small RNAs,

how might mechanisms underlying the function of traditionally morphogens be adapted to create morphogen-like behavior using small RNAs? In this review, we highlight the contributions of mobile small RNAs to pattern formation in plants and summarize recent studies that have advanced our understanding regarding the formation, stability, and interpretation of small RNA gradients.



1. Introduction

A fundamental principle of development is the ability to generate complex multicellular structures starting from a single cell. To coordinate the many cell fate decisions that characterize development of multicellular organisms, cells must be able to assess their relative positions within the growing structure. This is achieved through intercellular communication, commonly based on the production and perception of mobile signaling molecules. In animal systems, much of development is dependent upon morphogens, a term first coined by [Turing \(1952\)](#) to describe ‘diffusible form-generating substances.’ To qualify as a morphogen, mobile signals must fulfill the following two criteria: it must trigger discrete cell fate decisions through a dose-dependent, threshold-based readout of its concentration gradient, and act directly on target cells rather than using a relay of intermediary signals. These principles, first described by Lewis Wolpert in his now 50 years old ‘French flag model’ ([Wolpert, 1969](#)), explain how a field of cells can be subdivided into discrete domains of different fates according to the relative position from the morphogen source.

Plants evolved multicellularity independently of animals, and accordingly utilize distinct mobile signals to drive cell fate decisions. Nevertheless, basic principles underlying developmental patterning are often shared between animals and plants, including the use of signaling gradients to provide positional information. A classic example of a gradient-regulated response is the directional growth of a plant shoot toward a source of light ([Darwin & Darwin, 1880](#); [Wiesner, 1878](#)). This response is mediated by the phytohormone auxin, which is actively exported by polarized efflux carriers termed PIN proteins, to form a concentration gradient that is highest on the side furthest from the light (see [Fankhauser & Christie, 2015](#); [Finet & Jaillais, 2012](#)). The gradient-readout is mediated by auxin-response factors that promote growth toward the light source. Graded auxin levels are also instructive in other patterning contexts, e.g., the organization of the growing root tip ([Blilou et al., 2005](#); [Friml, 2003](#);

Grieneisen, Scheres, Hogeweg, & Marée, 2012; Grieneisen, Xu, Marée, Hogeweg, & Scheres, 2007), but the status of auxin as a bona fide morphogen has remained controversial, in part because auxin action is not dictated by its absolute levels, but instead appears to sense a differential (Benková, Ivanchenko, Friml, Shishkova, & Dubrovsky, 2009; Finet & Jaillais, 2012; Smith et al., 2006). In fact, the existence of morphogens in plants in general was a topic of much debate (e.g., Benková et al., 2009; Bhalerao & Bennett, 2003; Friml, 2003; Grieneisen et al., 2012). We now know that small RNAs can act as mobile instructive signals in plant development, and similar to morphogens in animal systems, employ a threshold-based readout of their mobility gradient to generate precisely defined cell fate boundaries. Here, we summarize the contributions of mobile small RNAs to plant development and discuss recent studies that have advanced our understanding of how small RNA gradients could be created, maintained, and interpreted.



2. Small RNAs as mobile instructive signals

The idea that small RNAs might act non-cell autonomously was posited over 20 years ago. Grafting experiments showed that transgene-induced gene silencing in tobacco produces a sequence-specific silencing signal that can spread from a silenced rootstock into a non-silenced shoot scion (Palauqui, Elmayan, Pollien, & Vaucheret, 1997). Although small RNAs quickly emerged as candidates for this signal, formal proof to that effect was less easily attained (see Chitwood & Timmermans, 2010). We now know that short interfering RNAs (siRNAs) move from cell to cell via plasmodesmata (microchannels that connect adjacent plant cells), as well as long distance through the vasculature (Buhtz, Pieritz, Springer, & Kehr, 2010; Buhtz, Springer, Chappell, Baulcombe, & Kehr, 2008; Molnar et al., 2010; Pant, Buhtz, Kehr, & Scheible, 2008; Vatén et al., 2011; Yoo et al., 2004). Particularly, the ability of siRNAs to trigger the production of secondary siRNAs, a process called transitivity that relies on the activities of RNA-dependent RNA polymerase 6 (RDR6) and the DICER proteins DCL4 and DCL2, enables siRNAs to propagate the spread of silencing from a single leaf systemically throughout the plant, thereby forming an important component of siRNA-based plant immunity (see Borges & Martienssen, 2015).

In contrast to siRNAs, plant miRNAs were initially reported to behave cell autonomously (Alvarez et al., 2006; Parizotto, Dunoyer, Rahm,

Himber, & Voinnet, 2004). Indeed, with few exceptions, miRNAs do not trigger transitivity (Allen, Xie, Gustafson, & Carrington, 2005; Manavella, Koenig, & Weigel, 2012; Montgomery et al., 2008). However, not only are miRNAs transported through the vascular phloem to coordinate physiological responses between the shoot and root (Buhtz et al., 2010; Lin et al., 2008; Pant et al., 2008; Tsikou et al., 2018), miRNAs can move from cell to cell and act as short-range positional signals in development. For instance, several observations hint to mobile small RNAs as important factors in the reproductive development of *Arabidopsis*, contributing to regulation of genome dosage, epigenetic reprogramming in the male and female germ cells, and to megasporogenesis (Borges et al., 2018; Olmedo-Monfil et al., 2010; Slotkin et al., 2009; Su et al., 2017; Tucker et al., 2012). In addition, the examples described below provide conclusive evidence that small RNAs act as mobile instructive signals in various developmental contexts. It should in this regard be noted that plant miRNAs, unlike their animal counterparts, show high target specificity, typically regulating transcripts derived from closely-related members of just a single gene family to which they show near perfect complementarity (see Willmann & Poethig, 2007; Yu, Jia, & Chen, 2017). The high complementarity between miRNAs and targets in plants also allows for target repression via both transcript cleavage as well as translational repression (Fig. 1A).

2.1 Opposing gradients of mobile small RNAs establish leaf polarity

Flat leaves with distinct cell types on their dorsal/adaxial (top) and ventral/abaxial (bottom) faces are an important innovation in the evolution of land plants that serves to maximize photosynthesis while minimizing water loss to the environment. Development of flat leaf architecture also poses a mechanically challenging problem; namely, how to create a stable dorsoventral boundary within the plane of a long and wide, but shallow, structure. The acquisition and maintenance of dorsoventral polarity involves an intricate gene regulatory network with several highly conserved transcription factors that promote either dorsal or ventral fate at its core (see Kuhlemeier & Timmermans, 2016). These are expressed in complementary domains delineating the top and bottom side of the developing primordium, respectively (Caggiano et al., 2017; Husbands, Benkovics, Nogueira, Lodha, & Timmermans, 2015). The positional information needed to define these domains is provided in part by small RNAs.

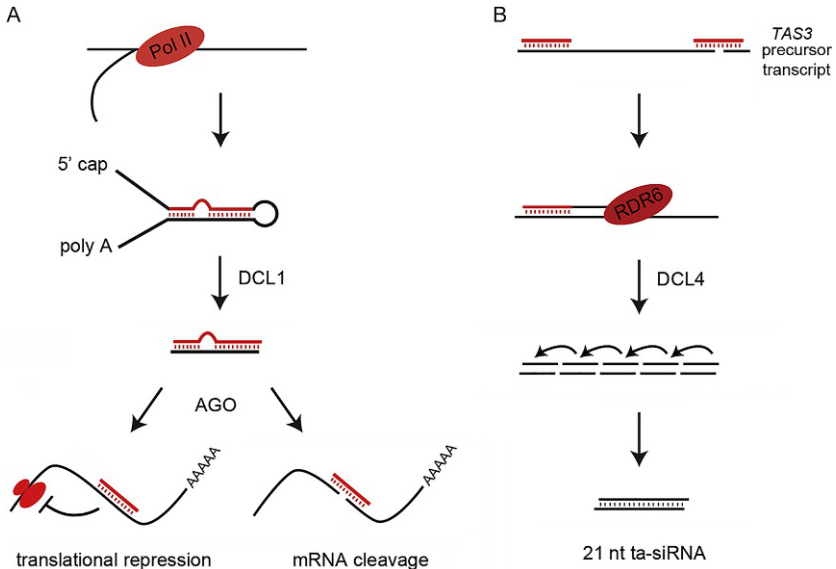


Fig. 1 Pathways for the biogenesis of developmentally-important small RNAs in plants. (A) miRNA precursors transcribed by RNA polymerase II (Pol II) adopt a hairpin-like structure that is processed by DICER-LIKE 1 (DCL1) into a miRNA duplex typically 21 bp in length. The mature miRNA is loaded into an AGO effector complex that in a homology-dependent manner guides the post-transcriptional repression of target mRNAs. Plant miRNAs, unlike their animal counterparts, show near perfect complementarity to target transcripts and direct their cleavage as well as translational repression. (B) A select subset of miRNAs can trigger the production of secondary siRNAs. In the production of *tasiARF*, *TAS3* precursor transcripts are targeted at two sites by miR390-loaded AGO7, triggering cleavage at the 3' site. The 5' cleavage product is subsequently converted into double-stranded RNA by RDR6, and processed into phased 21 nucleotides ta-siRNAs by DCL4. Among the *TAS3*-derived ta-siRNAs, *tasiARF* represses expression of *ARF3/4* in a manner similar to miRNAs. Note: while transitivity is important for *tasiARF* biogenesis, this amplification mechanism is dispensable for the morphogenic activity of small RNAs.

miR166 contributes to organ polarity by restricting the accumulation of class III HOMEODOMAIN-LEUCIN ZIPPER (HD-ZIPIII) transcription factors, key determinants of dorsal cell fate (Fig. 2A) (Emery et al., 2003; Juarez, Kui, Thomas, Heller, & Timmermans, 2004; Mallory et al., 2004; McConnell et al., 2001). Plants in which this regulatory interaction is perturbed develop a strong radial dorsalized leaf phenotype, reflecting an early role for miR166 in setting up dorsoventral polarity. miR166 is generated specifically in the ventral epidermis of leaf primordia, but was shown to move from the epidermis across the leaf to form a concentration gradient

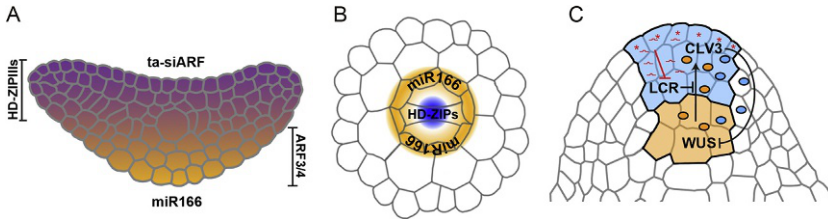


Fig. 2 Mobile small RNA gradients play important roles in plant development. (A) In the developing leaf, *tasiARF* (purple) and *miR166* (orange) form opposing concentration gradients through movement from a source in the top and bottom epidermis, respectively. These gradients generate a morphogen-like, threshold-based readout that limits expression of the respective HD-ZIPIII and ARF3/4 targets (transcribed throughout the developing primordium) to sharply defined domains on the top and bottom side of the developing leaf, respectively. (B) Proper patterning of the root vasculature requires that *miR166* (orange) moves from its source in the endodermis to generate a concentration gradient across the central stele that is readout into an inverse gradient of HD-ZIPIII activity (blue) to specify proto- and metaxylem cell fate. (C) Stem cell activity in the shoot apical meristem is maintained via a negative feedback loop in which the WUS transcription factor moves from the organizing center (orange) to induce CLV3 expression in the central zone (blue). This secreted peptide in turn signals a down-regulation of WUS expression, restricting its activity. *miR394* (red squiggle) produced in the central zone epidermis (red asterisks) moves into the subjacent two cell layers where it down-regulates its F-box target, LCR, enabling these cells to respond to WUS activity. Polarization of factors that block miRNA mobility to defined cell–cell interfaces creates domains with confined miRNA mobility (black outline), safeguarding cell identities within the stem cell niche.

that dissipates toward the dorsal side (Juarez et al., 2004; Nogueira et al., 2009; Yao et al., 2009). Interestingly this gradient is interpreted into a binary readout and creates a sharply delineated domain of HD-ZIPIII expression that is limited to the two uppermost layers of developing leaf primordia (Skopelitis, Benkovics, Husband, & Timmermans, 2017).

Maintenance of dorsoventral polarity relies on an additional small RNA gradient formed by *tasiARF* (Chitwood et al., 2009; Nagasaki et al., 2007; Nogueira, Madi, Chitwood, Juarez, & Timmermans, 2007; Petsch et al., 2015; Yifhar et al., 2012). Biogenesis of this small RNA occurs through the specialized *TAS3* trans-acting siRNA pathway (Fig. 1B), which in leaf primordia is active exclusively on the upper surface (Allen et al., 2005; Chitwood et al., 2009; Montgomery et al., 2008). Similar to *miR166*, movement of *tasiARF* from its defined source of biogenesis creates a concentration gradient across the leaf that is read out into a discrete expression domain of its targets, the ventral determinants ARF3 and ARF4, on the bottom side (Fig. 2A) (Chitwood et al., 2009; Skopelitis et al., 2017).

The division of leaf primordia into distinct dorsal and ventral domains thus relies on a novel developmental patterning mechanism in which *tasiARF* and *miR166* form inverse mobility gradients that are read out as the on-off expression of the direct targets, *ARF3/4* and *HD-ZIPIII* genes, respectively.

Given that flat-leaf architecture requires a correctly positioned dorsoventral boundary, the activities of the *miR166* and *tasiARF* gradients must be coordinated and carefully tuned. How the spatiotemporal patterns of *miR166* and *tasiARF* precursor expression are first established remains to be resolved, but once initiated, the larger polarity network directly reinforces this expression (Husbands et al., 2015; Merelo et al., 2016; Nogueira et al., 2007). Integration of the positional information contained within opposing *tasiARF* and *miR166* gradients underlies specification of a stable, uniformly positioned dorsoventral boundary. Thus, the cell-to-cell movement of small RNAs allows the formation of sharply defined target gene expression boundaries, and together, the integrated readouts of opposing small RNA gradients provide a mechanism to specify a robust developmental boundary (Skopelitis et al., 2017).

2.2 A *miR166* mobility gradient specifies cell fate within the root

miR166 also serves as a short-range positional signal in patterning of the root, which consists of a central vascular stele surrounded by concentric layers of pericycle, endodermis, cortex, and epidermis (Carlsbecker et al., 2010; Miyashima, Koi, Hashimoto, & Nakajima, 2011). Within the vasculature, the water conducting xylem tissue comprises two cell types, the outer protoxylem and inner metaxylem. These cell fates are specified according to the level of *HD-ZIPIII* activity determined by the dose-dependent readout of a *miR166* mobility gradient that has its source at the endodermis (Fig. 2B) (Carlsbecker et al., 2010; Miyashima et al., 2011). The basis for the endodermal-specific production of *miR166* lies in the reciprocal movement of the transcription factor *SHORT ROOT* (*SHR*) from the central stele into the adjacent endodermis (Cui et al., 2007; Gallagher, Paquette, Nakajima, & Benfey, 2004; Nakajima, Sena, Nawy, & Benfey, 2001). Here, it captures its interaction partner *SCARECROW* (*SCR*), and together activates *miR166* expression. Movement of *miR166* out of the endodermis also affects positioning of cortex and pericycle (Miyashima et al., 2011). Thus, as for dorsoventral patterning of the leaf, acquisition of discrete cell fates along the radial axis of the root is in part driven by

the dose-dependent readout of a small RNA gradient. However, whereas the miR166 and tasiARF gradients in the leaf generate an on-off switch in target gene expression, the miR166 gradient in the root sets up an inverse gradient of its HD-ZIPIII targets, which then drives the acquisition of discrete cell fates.

2.3 miR394 mobility delineates the embryonic shoot stem cell niche

A third example in which cell fate decisions are governed by mobility of a miRNA is found in the regulation of stem cell activity within the embryonic *Arabidopsis* shoot meristem. Plant meristems are specialized niches that orchestrate the balance between stem cell proliferation and organ initiation essential for post-embryonic growth (see Greb & Lohmann, 2016). Stem cells within the shoot apical niche are located within the central zone (CZ) positioned at the meristem tip. This spatial organization is stably maintained, despite ongoing cell divisions. Two opposing signaling centers provide relevant positional cues to maintain stem cell number and position within the growing niche. The organizing center (OC), positioned directly below the stem cells, expresses the homeodomain transcription factor WUSCHEL (WUS), which moves into the CZ where it promotes stem cell identity and activates CLV3 expression (Fig. 2C) (Daum, Medzihradzky, Suzaki, & Lohmann, 2014; Yadav et al., 2011). This secreted peptide in turn signals a downregulation in WUS expression, thus establishing a negative feedback loop that maintains WUS levels and thereby stem cell number (see Soyars, James, & Nimchuk, 2016).

In addition to this regulatory loop, classical surgical experiments predicted the need for an epidermal-derived signal in maintaining stem cell activity (see Reinhardt, Frenz, Mandel, & Kuhlemeier, 2005; Steeves & Sussex, 1989). This signal, we now know, involves miR394 (Knauer et al., 2013). miR394 is generated in the surface layer, or protoderm, of the developing embryo, but moves into the subtending two cell layers where it represses expression of the F-box protein, LEAF CURLING RESPONSIVENESS (LCR) (Knauer et al., 2013). As a result, these cells become competent to respond to the stem cell promoting activity of WUS. The limited mobility of miR394 thus defines a zone of stem cell activity and given that the protoderm is propagated by stereotypic anticlinal cell divisions, in addition, stably anchors this zone to the growing shoot tip.



3. Reading out the gradient

3.1 Patterning properties of small RNA gradients are developmental-context dependent

In each of the above examples, the short-range mobility of a small RNA provides positional information essential for the specification of a critical cell fate boundary. The exact manner with which the mobility-derived small RNA gradients pattern their targets, however, appears context dependent. Whereas the movement of miR166 in the root generates an inverse gradient of HD-ZIPIII activity, the opposing *tasiARF* and miR166 gradients in the leaf create a sharp on-off switch in expression of their respective targets (Carlsbecker et al., 2010; Miyashima et al., 2011; Skopelitis et al., 2017). Why the patterning properties of miR166 in the root and shoot are distinct, even though the targets and range of mobility seem the same, is not currently understood. The readout of a small RNA gradient could be tuned by the gene regulatory network into which it is integrated (see Briscoe & Small, 2015; Cotterell & Sharpe, 2010; Rogers & Schier, 2011). Alternatively, parameters affecting small RNA-target interaction may provide inputs to shape the gradient readout and potentially force it from being inversely graded to being binary or vice versa. For example, AGO10, which specifically binds miR166, is thought to act as a decoy that prevents miR166 from being loaded into a catalytically active AGO1 complex (Zhang & Zhang, 2012; Zhu et al., 2011). As AGO10 shows distinctive tissue specific patterns of expression across the plant (Lynn et al., 1999), it is easy to envision how the readout of the miR166 gradient could be tuned across tissues via pre-patterning at the effector level.

While feedback regulation and pre-patterning are common features of developmental patterning, it was recently shown that these regulatory mechanisms are not essential for the conversion of a small RNA gradient into an on-off boundary of target gene expression. Inversion of the *tasiARF* and miR166 gradients, by displacing their source to the opposite side of the leaf, inverts their readout (Skopelitis et al., 2017). Irrespective of gradient orientation, a binary switch in target gene expression was observed. The information needed to convert a small RNA gradient into discrete domains of target gene expression must thus be contained within the gradient itself. Moreover, the patterning behaviors of small RNA gradients could be recapitulated in an *rdr6* mutant background, ruling out a contribution of transitivity, as well as in a fluorescence-based synthetic miRNA

sensor system (Skopelitis et al., 2017). The latter indicates that the readout of a small RNA mobility gradient relies solely on properties captured in the small RNA–target–AGO interaction. Similar to morphogens in animal systems, plant small RNAs thus have the inherent capacity to generate sharp boundaries of target gene expression through a direct threshold-based readout of their mobility gradients.

3.2 Making the switch

The recognition that small RNAs can function as morphogens raises a number of interesting questions, especially given that their nature is distinct from classical morphogens. Most animal morphogens are extracellular peptide ligands, such that cells can discern their position along the gradient based on the number of activated, ligand-bound receptors at their surface (see Ashe & Briscoe, 2006; Lewis, 2008; Rogers & Schier, 2011). This information is translated via a linear signal transduction pathway into the differential activation of target gene expression, often mediated by the cooperative binding of downstream transcription factors, in a manner depending on whether or not a given signaling intensity threshold is surpassed.

But how might a cell assess where along a small RNA gradient it is positioned to yield the appropriate expression response? Cells on either side of the target boundary can show remarkably subtle (~30%) differences in small RNA levels. Accordingly, the position along the gradient at which the switch is triggered is highly sensitive to the level of small RNA at the source (Skopelitis et al., 2017). Within the context of the developing leaf, a two- to threefold change in epidermal small RNA levels was sufficient to shift the position of the threshold one cell layer. Such sensitivity is also seen for animal morphogens (the *hunchback* gene in flies, for instance, can respond in an all or none fashion to a 10% change in Bicoid concentration), and may be fundamental to generating on–off transitions (Briscoe & Small, 2015; Gregor, Tank, Wieschaus, & Bialek, 2007; Rogers & Schier, 2011). On the other hand, target abundance also affects the readout, as is evident from the sensitivity of developmental programs in the leaf and root to variations in ARF3 or HD-ZIPIII levels (e.g., Carlsbecker et al., 2010; Chitwood et al., 2009; Fahlgren et al., 2006; McConnell et al., 2001; Miyashima et al., 2011). This pinpoints the ratio of small RNA-to-target levels as a means by which the graded information captured within a small RNA gradient is read out. At the high end of the gradient, where the small RNA-to-target ratio exceeds a certain threshold, small RNAs completely eliminate target expression

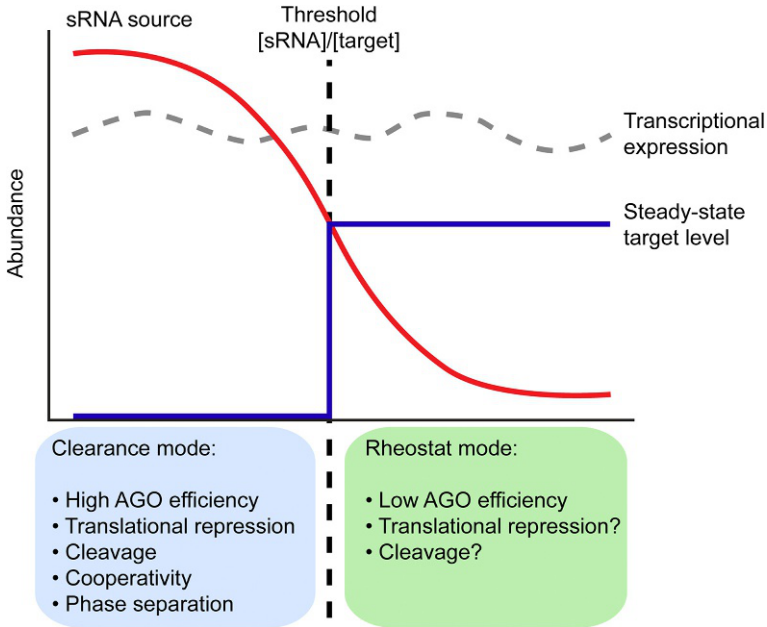


Fig. 3 Small RNA-to-target ratio creates a threshold-based readout of mobility gradients. The cell-to-cell movement of a small RNA from a defined source (left) generates a concentration gradient (red line) across a field of cells. In cells at the high end of the gradient where the small RNA-to-target ratio exceeds a given threshold (black dotted line), small RNAs completely repress target expression (clearance mode). In cells toward the tail end of the gradient where the small RNA-to-target ratio drops below the threshold, small RNAs cause target expression to be reduced and less variable, buffering stochastic fluctuations inherent in gene expression (rheostat mode). Select parameters potentially driving the threshold-based switch in AGO activity are listed. Please see the text for more details.

(Fig. 3). However, once the small RNA-to-target ratio falls below the threshold, the mode of small RNA regulation changes. At the tail end of the gradient, small RNAs no longer clear target expression, but instead cause it to be reduced and considerably less variable (Skopelitis et al., 2017). Two models for the regulation of developmental targets by small RNAs had previously been recognized. In the clearance model, miRNAs clear target transcripts to delineate mutually exclusive domains of accumulation, whereas in the homeostasis model, miRNAs act as rheostats to dampen the noise in target gene expression and refine their domains of activity (Bartel, 2004; Cartolano et al., 2007; Nikovics et al., 2006; Rhoades et al., 2002; Sieber, Wellmer, Gheyselinck, Riechmann, & Meyerowitz,

2007; Vaucheret, Mallory, & Bartel, 2006). The morphogen-like patterning properties of mobile small RNAs thus seem to reflect a highly sensitive switch from a clearance into a rheostat mode of regulation that is dictated by a small RNA-to-target ratio threshold.

A second critical question to be resolved is how the switch in small RNA activity that drives the binary readout and therefore cell fate acquisition might be realized. Switching behavior can follow from strong positive feedback directly coupled to a highly sensitive signaling input. AGO proteins are subject to a number of post-translational modifications that affect the efficacy of AGO complexes via changes in stability, conformation, and composition (see Huberdeau et al., 2017; Jee & Lai, 2014; Lopez-Orozco et al., 2015). For instance, the release of mammalian AGO2 from a miRNA-target mRNA duplex is triggered by its phosphorylation, which in turn is coupled to target loading (Golden et al., 2017). Given that AGO levels are generally limiting in the cell, the phosphorylation and subsequent dephosphorylation of AGO2 provides a timing mechanism to limit the duration of target interaction and thereby tune the overall silencing efficiency. Phosphorylation of AGO2 can also lead to a shift in its mechanism of repression from endonucleolytic cleavage toward translational repression, a point that may be particularly relevant given the properties of AGO proteins mentioned below (Horman et al., 2013). Interestingly, several of these modifications occur in response to specific internal or external cues (Cho, Ryu, Shah, Poulsen, & Yang, 2016; Shen et al., 2013; Von Born, Bernardo-Faura, & Rubio-Somoza, 2018), which could conceivably shape the output of small RNA gradients in a tissue- or state-dependent manner. Knowledge of post-translational regulatory modifications on plant AGO proteins is lacking, but many of the residues modified on animal AGO proteins are conserved also in plants.

Cooperativity provides an alternative, non-mutually exclusive, mechanism via which to create a non-linear, threshold-based response. Like many transcription factors, AGO1, 3 and 4 proteins in animal systems act cooperatively at targets containing multiple small RNA binding sites, allowing for a dose-dependent bimodal silencing response (Broderick, Salomon, Ryder, Aronin, & Zamore, 2011; Denzler et al., 2016; Djuranovic et al., 2010; Klein, Chandradoss, Depken, & Joo, 2017; Mukherji et al., 2011). AGO2, however, does not show this behavior. AGO1, 3, and 4 exert their effects primarily at the translational level, whereas AGO2 also directs the cleavage of perfectly matched small RNA targets. This may hint at a role

for translational repression in generating the cooperativity-driven, non-linear behavior of animal small RNAs. Although plant miRNAs and tasiRNAs show extensive complementarity to their targets, most repress translation in addition to guiding the cleavage of target transcripts (Brodersen et al., 2008; Li et al., 2013). Particularly, both tasiARF and miR166 mediate the translational repression of their respective targets (Chitwood et al., 2009; Fahlgren et al., 2006; Li et al., 2013; Pekker, Alvarez, & Eshed, 2005). ARF3 transcripts also bear two tasiARF binding sites and can further be targeted by secondary siRNAs (Allen et al., 2005; Petsch et al., 2015; Yifhar et al., 2012). Assuming conservation in AGO function, cooperativity resulting from AGO occupancy at multiple binding sites may well contribute to the binary readout of this small RNA gradient. However, given that the HD-ZIPIII transcripts carry just a single miR166 target site (Emery et al., 2003; Juarez et al., 2004; Mallory et al., 2004), this form of cooperativity unlike explains the full morphogenic activity of mobile plant small RNAs. In this regard, the observation that AGO proteins condense into phase-separated droplets upon interaction with GW-scaffolding proteins may be particularly intriguing (Sheu-Gruttadauria & MacRae, 2018). Droplet formation was shown to enhance the silencing efficiency of miRNA-target-AGO complexes by over 10-fold, making it quite apparent how phase separation could drive a switching behavior. The recent finding that phosphorylation of RNA-polymerase II underlies a droplet-based switch from transcription initiation to RNA processing may then provide a valuable paradigm on how a signal input might be integrated into such a switch (Guo et al., 2019). Still, the major challenge in understanding the morphogenic activity of small RNAs would be to resolve how a cell assesses a given small RNA-to-target ratio to trigger droplet formation, or otherwise switch miRNA-target-AGO complex activity.



4. Generating the small RNA gradient

To act as morphogens, small RNAs must establish a stable concentration gradient across a field of cells. Exactly how the parameters of the gradient are established and maintained is so far unknown, but this almost certainly reflects a balance between: (1) the production of the small RNA at its source, (2) its rate of movement from source to sink, and (3) the degree of degradation in cells along the field.

4.1 Small RNA turnover

Two distinct degradation pathways have been recognized in plants (see Yu et al., 2017). Small RNA-degrading exonucleases direct the 3' truncation of small RNAs (Ramachandran & Chen, 2008). In addition, small RNAs can be marked for degradation by 3' poly-uridylation (Ren, Chen, & Yu, 2012; Zhai et al., 2013; Zhao et al., 2012). The occurrence of overlapping and opposing small RNA gradients predicts that small RNA turnover must be regulated at the level of individual small RNAs. The enzymes mediating these degradation reactions show distinct substrate specificities (Yu et al., 2017; Zhai et al., 2013), supporting the possibility that turnover rate varies between small RNAs. More importantly, small RNA-degrading exonucleases as well as 3' uridyl-transferases act on small RNAs bound to AGO1 (Yu et al., 2017; Zhai et al., 2013), and this in a manner that appears coupled to target loading. Although the exact mechanism in plants has yet to be investigated, data from other species predicts that AGO proteins undergo a conformational change upon loading of a highly complementary target, such as is the case in plants, which releases the miRNA 3' end and exposes this for degradation (Ameres et al., 2010; Sheng et al., 2014). Target-induced small RNA decay presents a perfect means by which to differentially regulate the turnover of individual small RNAs. As small RNA turnover would be linked to target levels, it is also easy to envision how such a decay mechanism can be used to tune the effective range and shape of a small RNA gradient across tissues or in response to specific cues. In addition, target-induced small RNA decay is predicted to refine the threshold-based readout of a small RNA gradient (Levine, McHale, & Levine, 2007). The coupling of miRNA activity and turnover may thus serve multiple functions; to shape and stabilize a small RNA gradient and to sharpen the on-off target gene expression boundary this creates.

4.2 Regulation of small RNA mobility

A second criterion critical to the establishment of a gradient is the movement of a small RNA from its source. Despite the central importance of small RNA mobility, also with respect to the coordination of biotic and abiotic stress responses across the plant (Borges & Martienssen, 2015; Buhtz et al., 2010; Lin et al., 2008; Pant et al., 2008; Tsikou et al., 2018), remarkably little is known about how the cell-to-cell movement of small RNAs is mediated, except that plasmodesmata are required (Vatén et al., 2011). The shape of miRNA gradients generated by movement from an epidermal

source in the leaf is consistent with the passive diffusion of small RNAs between cells (Chitwood et al., 2009; Skopelitis et al., 2017). Accordingly, the effective range of mobility is correlated to the abundance of the small RNA at the source (Felippes, Ott, & Weigel, 2010; Skopelitis et al., 2017). Specific properties of cells across the mobility field are, however, likely to influence the range and shape of a small RNA gradient. As mentioned, expression of target transcripts in cells between source and sink is predicted to lower small RNA abundance. Likewise, as AGO proteins act cell-autonomously (Zhu et al., 2011), AGO loading is expected to limit the pool of available mobile small RNAs and reduce the length of the gradient. Given that loading into AGO complexes is a selective process (Mi et al., 2008; Montgomery et al., 2008; Zhu et al., 2011), such an effect on mobility may similarly vary between individual miRNAs. This point is nicely illustrated by AGO10, which shows a unique preference for loading of miR166 and specifically prevents its movement out of the central vasculature to maintain stem cell activity in the embryonic shoot meristem above (Liu et al., 2009; Zhu et al., 2011).

Small RNAs move from cell to cell via plasmodesmata (Vatén et al., 2011), providing a further means via which to govern the formation or shape of a small RNA gradient. Plasmodesmata also permit the movement of water, nutrients, hormones, peptides, and small proteins between adjoining cells, and larger proteins, such as transcription factors, may be transported via active processes controlled by unique domains or motifs inherent to the transported protein (see Wu & Gallagher, 2012). Understandably, transport through these channels is precisely regulated, and plasmodesmatal properties, such as density, architecture and aperture, change substantially during development or in instances of stress (see Burch-Smith & Zambryski, 2012; Tilsner, Nicolas, Rosado, & Bayer, 2016; Zavaliev, Sagi, Gera, & Epel, 2009). Interestingly, mechanisms modulating the symplastic diffusion of small proteins do not necessarily impact miRNA mobility. Nonetheless, not all cells are symplastically connected, and in select developmental contexts, mechanisms are in place to specifically limit the movement of small RNAs (Skopelitis et al., 2018). For instance, small RNAs are able to move out but not into phloem cells of the central vasculature. The observed mobility patterns predict the existence of plasmodesmata-associated 'gatekeepers' that polarize at defined cell–cell interfaces to prevent the passage of small RNAs between select cells (Skopelitis et al., 2018).

Gating of small RNA mobility at the central vasculature creates a movement barrier that ensures some small RNA-mediated signaling responses are

contained, while others are permitted to propagate systemically. Within meristems, the polarized gating mechanism underpins a domain autonomous behavior. Small RNAs are able to move between stem cells in the niche or within the organizing center but cannot move between these functional domains (Fig. 2C). Likewise, small RNAs are unable to move between stem cells and more determined daughter cells (Skopelitis et al., 2018). The limited movement of miRNAs is thought to help safeguard cell identities within the dynamically growing niche. This is perhaps best illustrated by the action of miR394, which through the repression of LCR promotes stem cell identity (Fig. 2C). The restricted movement of miR394 prevents a shift from organizer to stem cell identity, thus providing a mechanism to maintain stem cell number (Knauer et al., 2013). Likewise, movement of miR166, while essential for the specification of dorsoventral polarity in the incipient primordium, cannot extend into the central zone where its HD-ZIPIII targets are required for stem cell activity (Liu et al., 2009; Zhang, Tucker, Hermann, & Laux, 2017; Zhu et al., 2011).

The molecular components underpinning the regulated movement of small RNAs have proven difficult to identify. Forward genetic screens designed to pinpoint such factors have led to the discovery of numerous small RNA biogenesis components, but failed to uncover genes directly affecting mobility (Brosnan & Voinnet, 2011; Melnyk, Molnar, & Baulcombe, 2011; Taochy et al., 2017). The first insights, which support the idea that the movement of small RNAs is regulated at plasmodesmata, came from a recent biochemical study into the antiviral immune response (Rosas-Diaz et al., 2018). The systemic spread of virus-derived siRNAs is one of the plant's main antiviral defense mechanisms (Burguán & Havelda, 2011; Melnyk et al., 2011). To combat this defense strategy, viruses evolved various suppressor strategies, one of which targets the plasmodesmata-associated receptor-like kinases, BAM1 and BAM2, to block the movement of siRNA from the vasculature (Rosas-Diaz et al., 2018). It will be interesting to see whether this paradigm holds for miRNA mobility in other developmental contexts, or what other specialized mechanisms exist to regulate small RNA mobility during development. A wide spectrum of proteins, including various receptors-like kinases, is associated with plasmodesmata (Brault et al., 2019; Fernandez-Calvino et al., 2011; Stahl et al., 2013), providing lots of scope to regulate the movement of small RNAs and thereby shape the gradient.



5. Why so complicated?

Why would patterning mechanisms based on the repression of key developmental regulators by miRNA mobility gradients have evolved? Why not simply regulate expression of the respective developmental targets at the transcriptional level? Morphogen gradients, which instruct cells to adopt distinct identities according to their relative position from a fixed source, allow the pattern of cell fate acquisition to be uncoupled from the pattern of cell division. Accordingly, despite variations in the direction or rate of cell division, morphogen gradients enable formation of precise and reliable cell fate boundaries by ‘respecifying’ the fate of ‘mispositioned’ cells. The morphogenic behavior of mobile small RNAs thus generates robustness at the tissue or organ level (Skopelitis et al., 2017). In addition, signal gradients are tunable, as illustrated by the fact that relatively subtle changes in miRNA levels at the source can be sufficient to shift the position of a target gene expression boundary (Skopelitis et al., 2017). As a result, morphogen gradients are in principle scalable, such that spatial patterns can be proportionally maintained irrespective of organ size (Ashe & Briscoe, 2006; Briscoe & Small, 2015; Lewis, 2008; Rogers & Schier, 2011). The tunability of a morphogen gradient also allows for plasticity, a point that given their sessile nature may be particularly relevant in plants. Indeed, cell fates within the shoot and root apical meristems are dynamically specified (Gaillochet & Lohmann, 2015). Likewise, the dorsoventral boundary in the leaf, while robustly specified, is flexible in its positioning with the number of dorsal and ventral cell layers dependent on a range of environmental cues (e.g., de Carbonnel et al., 2010; Waites & Hudson, 1995). Subtle changes in small RNA levels at their source permit the flexible positioning of a boundary while maintaining it uniform across the developing organ. Finally, a mobile small RNA gradient can be tuned to create stochasticity (Skopelitis et al., 2017). Stochastic cell fate decisions are often favored in scenarios where variability allows a bet-hedging strategy to better cope with unpredictable environments. An explicit example of this in plants is seen in the regulation of stem cell differentiation in the moss *Physcomitrella patens*. Here, a central source of tasiARF generates a stochastic pattern of ARF expression in stem cells at the plant’s edge, creating the variability needed to balance differentiation in response to environmental cues (Plavskin et al., 2016). Thus, the beauty of small RNA gradients, and morphogen gradients in general, is that

they provide a means by which to create robust developmental patterns that nonetheless can be flexibly tuned whether as an aspect of environmentally driven phenotypic plasticity or of programmed developmental change.

But why use small RNAs? Small RNAs have properties that make them particularly well suited to drive developmental change. Regulation by small RNAs confers sensitivity and robustness onto gene regulatory networks, in part by dampening intrinsic noise resulting from inherent variability in gene expression (Plavskin et al., 2016; Schmiedel et al., 2015). Both features promote the faithful transfer of information through a signaling network and, consistent with the prevalence of evolutionarily conserved small RNA-target modules in plants as well as animals (Gramzow & Theißen, 2019; Yu et al., 2017), mechanisms underlying these network properties provide a selective advantage during evolution (Frankel et al., 2010; Metzger et al., 2015). Plant small RNAs in addition provide an unprecedented degree of signal specificity, often showing near perfect complementarity to target transcripts, and have a direct mode of action that allows for rapid cell fate transitions (Bartel, 2004; Rhoades et al., 2002). A further conceivable advantage of employing small RNAs as mobile signals in development may be that they represent yet another class of molecules. Patterning processes often occur in close spatial and temporal vicinity, requiring careful coordination between events. Within plant stem cell niches, cells perceive inputs from a multitude of secreted peptides, hormones, mobile transcription factors, as well as mobile small RNAs (see Greb & Lohmann, 2016; Soyars et al., 2016). Thus, perhaps, an additional advantage of employing mobile small RNAs in development is that they broaden the spectrum of available signaling pathways needed to mitigate a ‘signaling gridlock.’



6. Concluding remarks

The recent discovery that small RNAs in plants function similar to the classical animal morphogens reveals an intriguing new paradigm in developmental patterning. Morphogenic behavior is an inherent property of small RNAs that relies on their ability to establish a mobility gradient and to trigger a switch in AGO activity dictated by the small RNA-to-target ratio. The elegance of the system lies in the fact that it creates robust on-off cell fate boundaries in a manner that allows for plasticity and that, in principle, is scalable to function across tissues and organs of various sizes. However, the mechanism by which the gradient is established and read out leaves many

open questions. How do cells assess a given small RNA-to-target ratio or how is the switch in AGO activity realized? To resolve these questions a deeper understanding of plant AGO complexes is needed. What are their interaction partners and biochemical modifications, and how might these promote cooperative behavior or impact the mode of repression? Similarly, what effects will parameters such as small RNA-target complementarity and sub-cellular compartmentalization have on these processes? Equally important, quantitative insights into the production, turnover, and movement of small RNAs are needed to resolve how stable gradients are formed. It is evident that the movement of small RNAs within the plant stem cell niches is a tightly regulated process, but further experiments are needed to resolve the molecular underpinnings and to unravel the complex interactions that can shape individual small RNA gradients to allow diversity in patterning behaviors. Finally, it remains to be resolved whether animal small RNAs share the capacity to serve as morphogens. The recent observation that layer formation within the neocortex relies on opposing small RNA gradients (Shu et al., 2019), may support this intriguing possibility, especially if we consider that small RNAs in animal systems are sorted into extracellular vesicles and able to move from cell to cell (see Temoche-Diaz et al., 2019). How the distinctive attributes of plant and animal miRNAs will influence the readout of a gradient, only time will tell. For sure, pattern formation by small RNA gradients is a feature common to both kingdoms.

Acknowledgments

The authors thank current and former members of the Timmermans lab for helpful discussions. Work on small RNA regulation and leaf polarity in the Timmermans lab is supported by grants from The Deutsche Forschungsgemeinschaft (SFB 1101 project C06) and an Alexander von Humboldt Professorship. Kristine Hill was supported by a Marie Skłodowska-Curie Individual Fellowship (GAP-709293). We apologize to colleagues for work not cited due to space limitations.

References

- Allen, E., Xie, Z., Gustafson, A. M., & Carrington, J. C. (2005). microRNA-directed phasing during trans-acting siRNA biogenesis in plants. *Cell*, *121*, 207–221.
- Alvarez, J. P., Pekker, I., Goldshmidt, A., Blum, E., Amsellem, Z., & Eshed, Y. (2006). Endogenous and synthetic microRNAs stimulate simultaneous, efficient, and localized regulation of multiple targets in diverse species. *Plant Cell*, *18*, 1134–1151.
- Ameres, S. L., Horwich, M. D., Hung, J.-H., Xu, J., Ghildiyal, M., Weng, Z., et al. (2010). Target RNA-directed trimming and tailing of small silencing RNAs. *Science*, *328*, 1534–1539.
- Ashe, H. L., & Briscoe, J. (2006). The interpretation of morphogen gradients. *Development*, *133*, 385–394.

- Bartel, D. P. (2004). MicroRNAs: Genomics, biogenesis, mechanism, and function. *Cell*, 116, 281–297.
- Benková, E., Ivanchenko, M. G., Friml, J., Shishkova, S., & Dubrovsky, J. G. (2009). A morphogenetic trigger: Is there an emerging concept in plant developmental biology? *Trends in Plant Science*, 14, 189–193.
- Bhalerao, R. P., & Bennett, M. J. (2003). The case for morphogens in plants. *Nature Cell Biology*, 5, 939.
- Blilou, I., Xu, J., Wildwater, M., Willemsen, V., Paponov, I., Friml, J., et al. (2005). The PIN auxin efflux facilitator network controls growth and patterning in Arabidopsis roots. *Nature*, 433, 39.
- Borges, F., & Martienssen, R. A. (2015). The expanding world of small RNAs in plants. *Nature Reviews Molecular Cell Biology*, 16, 727.
- Borges, F., Parent, J.-S., van Ex, F., Wolff, P., Martínez, G., Köhler, C., et al. (2018). Transposon-derived small RNAs triggered by miR845 mediate genome dosage response in Arabidopsis. *Nature Genetics*, 50, 186.
- Brault, M. L., Petit, J. D., Immel, F., Nicolas, W. J., Glavier, M., Brocard, L., et al. (2019). Multiple C2 domains and Transmembrane region proteins (MCTPs) tether membranes at plasmodesmata. *EMBO Reports*, 20.
- Briscoe, J., & Small, S. (2015). Morphogen rules: Design principles of gradient-mediated embryo patterning. *Development*, 142, 3996–4009.
- Broderick, J. A., Salomon, W. E., Ryder, S. P., Aronin, N., & Zamore, P. D. (2011). Argonaute protein identity and pairing geometry determine cooperativity in mammalian RNA silencing. *RNA*, 17, 1858–1869.
- Brodersen, P., Sakvarelidze-Achard, L., Bruun-Rasmussen, M., Dunoyer, P., Yamamoto, Y. Y., Sieburth, L., et al. (2008). Widespread translational inhibition by plant miRNAs and siRNAs. *Science*, 320, 1185–1190.
- Brosnan, C. A., & Voinnet, O. (2011). Cell-to-cell and long-distance siRNA movement in plants: Mechanisms and biological implications. *Current Opinion in Plant Biology*, 14, 580–587.
- Buhtz, A., Pieritz, J., Springer, F., & Kehr, J. (2010). Phloem small RNAs, nutrient stress responses, and systemic mobility. *BMC Plant Biology*, 10, 64.
- Buhtz, A., Springer, F., Chappell, L., Baulcombe, D. C., & Kehr, J. (2008). Identification and characterization of small RNAs from the phloem of *Brassica napus*. *The Plant Journal*, 53, 739–749.
- Burch-Smith, T. M., & Zambryski, P. C. (2012). Plasmodesmata paradigm shift: Regulation from without versus within. *Annual Review of Plant Biology*, 63, 239–260.
- Burgýán, J., & Havelda, Z. (2011). Viral suppressors of RNA silencing. *Trends in Plant Science*, 16, 265–272.
- Caggiano, M. P., Yu, X., Bhatia, N., Larsson, A., Ram, H., Ohno, C. K., et al. (2017). Cell type boundaries organize plant development. *eLife*, 6, e27421.
- Carlsbecker, A., Lee, J.-Y., Roberts, C. J., Dettmer, J., Lehesranta, S., Zhou, J., et al. (2010). Cell signalling by microRNA165/6 directs gene dose-dependent root cell fate. *Nature*, 465, 316–321.
- Cartolano, M., Castillo, R., Efreanova, N., Kuckenberger, M., Zethof, J., Gerats, T., et al. (2007). A conserved microRNA module exerts homeotic control over *Petunia hybrida* and *Antirrhinum majus* floral organ identity. *Nature Genetics*, 39, 901–905.
- Chitwood, D. H., Nogueira, F. T., Howell, M. D., Montgomery, T. A., Carrington, J. C., & Timmermans, M. C. (2009). Pattern formation via small RNA mobility. *Genes & Development*, 23, 549–554.
- Chitwood, D. H., & Timmermans, M. C. (2010). Small RNAs are on the move. *Nature*, 467, 415.

- Cho, S. K., Ryu, M. Y., Shah, P., Poulsen, C. P., & Yang, S. W. (2016). Post-translational regulation of miRNA pathway components, AGO1 and HYL1, in plants. *Molecules and Cells*, *39*, 581.
- Cotterell, J., & Sharpe, J. (2010). An atlas of gene regulatory networks reveals multiple three-gene mechanisms for interpreting morphogen gradients. *Molecular Systems Biology*, *6*.
- Cui, H., Levesque, M. P., Vernoux, T., Jung, J. W., Paquette, A. J., Gallagher, K. L., et al. (2007). An evolutionarily conserved mechanism delimiting SHR movement defines a single layer of endodermis in plants. *Science*, *316*, 421–425.
- Darwin, C., & Darwin, F. (1880). *The power of movement in plants*. John Murray.
- Daum, G., Medzihradsky, A., Suzuki, T., & Lohmann, J. U. (2014). A mechanistic framework for noncell autonomous stem cell induction in Arabidopsis. *Proceedings of the National Academy of Sciences of the United States of America*, *111*, 14619–14624.
- de Carbonnel, M., Davis, P., Roelfsema, M. R. G., Inoue, S.-i., Schepens, I., Lariguet, P., et al. (2010). The Arabidopsis PHYTOCHROME KINASE SUBSTRATE2 protein is a phototropin signaling element that regulates leaf flattening and leaf positioning. *Plant Physiology*, *152*, 1391–1405.
- Denzler, R., McGeary, S. E., Title, A. C., Agarwal, V., Bartel, D. P., & Stoffel, M. (2016). Impact of microRNA levels, target-site complementarity, and cooperativity on competing endogenous RNA-regulated gene expression. *Molecular Cell*, *64*, 565–579.
- Djuranovic, S., Zinchenko, M. K., Hur, J. K., Nahvi, A., Brunelle, J. L., Rogers, E. J., et al. (2010). Allosteric regulation of Argonaute proteins by miRNAs. *Nature Structural & Molecular Biology*, *17*, 144.
- Emery, J. F., Floyd, S. K., Alvarez, J., Eshed, Y., Hawker, N. P., Izhaki, A., et al. (2003). Radial patterning of Arabidopsis shoots by class III HD-ZIP and KANADI genes. *Current Biology*, *13*, 1768–1774.
- Fahlgren, N., Montgomery, T. A., Howell, M. D., Allen, E., Dvorak, S. K., Alexander, A. L., et al. (2006). Regulation of AUXIN RESPONSE FACTOR3 by TAS3 ta-siRNA affects developmental timing and patterning in Arabidopsis. *Current Biology*, *16*, 939–944.
- Fankhauser, C., & Christie, J. M. (2015). Plant phototropic growth. *Current Biology*, *25*, R384–R389.
- Felippes, F. F. d., Ott, F., & Weigel, D. (2010). Comparative analysis of non-autonomous effects of tasiRNAs and miRNAs in Arabidopsis thaliana. *Nucleic Acids Research*, *39*, 2880–2889.
- Fernandez-Calvino, L., Faulkner, C., Walshaw, J., Saalbach, G., Bayer, E., Benitez-Alfonso, Y., et al. (2011). Arabidopsis plasmodesmal proteome. *PLoS One*, *6*, e18880.
- Finet, C., & Jaillais, Y. (2012). Auxology: When auxin meets plant evo-devo. *Developmental Biology*, *369*, 19–31.
- Frankel, N., Davis, G. K., Vargas, D., Wang, S., Payre, F., & Stern, D. L. (2010). Phenotypic robustness conferred by apparently redundant transcriptional enhancers. *Nature*, *466*, 490.
- Friml, J. (2003). Auxin transport—Shaping the plant. *Current Opinion in Plant Biology*, *6*, 7–12.
- Gaillochot, C., & Lohmann, J. U. (2015). The never-ending story: From pluripotency to plant developmental plasticity. *Development*, *142*, 2237–2249.
- Gallagher, K. L., Paquette, A. J., Nakajima, K., & Benfey, P. N. (2004). Mechanisms regulating SHORT-ROOT intercellular movement. *Current Biology*, *14*, 1847–1851.
- Golden, R. J., Chen, B., Li, T., Braun, J., Manjunath, H., Chen, X., et al. (2017). An Argonaute phosphorylation cycle promotes microRNA-mediated silencing. *Nature*, *542*, 197.
- Gramzow, L., & Theißen, G. (2019). Plant miRNA conservation and evolution. In *Plant microRNAs* (pp. 41–50). Springer.

- Greb, T., & Lohmann, J. U. (2016). Plant stem cells. *Current Biology*, *26*, R816–R821.
- Gregor, T., Tank, D. W., Wieschaus, E. F., & Bialek, W. (2007). Probing the limits to positional information. *Cell*, *130*, 153–164.
- Grieneisen, V. A., Scheres, B., Hogeweg, P., & Marée, A. F. (2012). Morphogengineering roots: Comparing mechanisms of morphogen gradient formation. *BMC Systems Biology*, *6*, 37.
- Grieneisen, V. A., Xu, J., Marée, A. F., Hogeweg, P., & Scheres, B. (2007). Auxin transport is sufficient to generate a maximum and gradient guiding root growth. *Nature*, *449*, 1008.
- Guo, Y. E., Manteiga, J. C., Henninger, J. E., Sabari, B. R., Dall'Agnesse, A., Hannett, N. M., et al. (2019). Pol II phosphorylation regulates a switch between transcriptional and splicing condensates. *Nature*, 1–6.
- Horman, S. R., Janas, M. M., Litterst, C., Wang, B., MacRae, I. J., Sever, M. J., et al. (2013). Akt-mediated phosphorylation of argonaute 2 downregulates cleavage and upregulates translational repression of MicroRNA targets. *Molecular Cell*, *50*, 356–367.
- Huberdeau, M. Q., Zeitler, D. M., Hauptmann, J., Bruckmann, A., Fressigné, L., Danner, J., et al. (2017). Phosphorylation of Argonaute proteins affects mRNA binding and is essential for microRNA-guided gene silencing in vivo. *The EMBO Journal*, *36*, 2088–2106.
- Husbands, A. Y., Benkovic, A. H., Nogueira, F. T., Lodha, M., & Timmermans, M. C. (2015). The ASYMMETRIC LEAVES complex employs multiple modes of regulation to affect adaxial-abaxial patterning and leaf complexity. *The Plant Cell*, *27*, 3321–3335.
- Jee, D., & Lai, E. C. (2014). Alteration of miRNA activity via context-specific modifications of Argonaute proteins. *Trends in Cell Biology*, *24*, 546–553.
- Juarez, M. T., Kui, J. S., Thomas, J., Heller, B. A., & Timmermans, M. C. (2004). microRNA-mediated repression of *rolled leaf1* specifies maize leaf polarity. *Nature*, *428*, 84.
- Klein, M., Chandradoss, S. D., Depken, M., & Joo, C. (2017). Why Argonaute is needed to make microRNA target search fast and reliable. In *Seminars in cell & developmental biology* (pp. 20–28): Elsevier.
- Knauer, S., Holt, A. L., Rubio-Somoza, I., Tucker, E. J., Hinze, A., Pisch, M., et al. (2013). A protodermal miR394 signal defines a region of stem cell competence in the Arabidopsis shoot meristem. *Developmental Cell*, *24*, 125–132.
- Kuhlemeier, C., & Timmermans, M. C. (2016). The Sussex signal: Insights into leaf dorso-ventrality. *Development*, *143*, 3230–3237.
- Levine, E., McHale, P., & Levine, H. (2007). Small regulatory RNAs may sharpen spatial expression patterns. *PLoS Computational Biology*, *3*, e233.
- Lewis, J. (2008). From signals to patterns: Space, time, and mathematics in developmental biology. *Science*, *322*, 399–403.
- Li, S., Liu, L., Zhuang, X., Yu, Y., Liu, X., Cui, X., et al. (2013). MicroRNAs inhibit the translation of target mRNAs on the endoplasmic reticulum in Arabidopsis. *Cell*, *153*, 562–574.
- Lin, S.-I., Chiang, S.-F., Lin, W.-Y., Chen, J.-W., Tseng, C.-Y., Wu, P.-C., et al. (2008). Regulatory network of microRNA399 and PHO2 by systemic signaling. *Plant Physiology*, *147*, 732–746.
- Liu, Q., Yao, X., Pi, L., Wang, H., Cui, X., & Huang, H. (2009). The ARGONAUTE10 gene modulates shoot apical meristem maintenance and establishment of leaf polarity by repressing miR165/166 in Arabidopsis. *The Plant Journal*, *58*, 27–40.
- Lopez-Orozco, J., Pare, J. M., Holme, A. L., Chaulk, S. G., Fahlman, R. P., & Hobman, T. C. (2015). Functional analyses of phosphorylation events in human Argonaute 2. *RNA*, *21*, 2030–2038.
- Lynn, K., Fernandez, A., Aida, M., Sedbrook, J., Tasaka, M., Masson, P., et al. (1999). The PINHEAD/ZWILLE gene acts pleiotropically in Arabidopsis development and has overlapping functions with the ARGONAUTE1 gene. *Development*, *126*, 469–481.

- Mallory, A. C., Reinhart, B. J., Jones-Rhoades, M. W., Tang, G., Zamore, P. D., Barton, M. K., et al. (2004). MicroRNA control of PHABULOSA in leaf development: Importance of pairing to the microRNA 5' region. *The EMBO Journal*, *23*, 3356–3364.
- Manavella, P. A., Koenig, D., & Weigel, D. (2012). Plant secondary siRNA production determined by microRNA–duplex structure. *Proceedings of the National Academy of Sciences of the United States of America*, *109*, 2461–2466.
- McConnell, J. R., Emery, J., Eshed, Y., Bao, N., Bowman, J., & Barton, M. K. (2001). Role of PHABULOSA and PHAVOLUTA in determining radial patterning in shoots. *Nature*, *411*, 709–713.
- Melnyk, C. W., Molnar, A., & Baulcombe, D. C. (2011). Intercellular and systemic movement of RNA silencing signals. *The EMBO Journal*, *30*, 3553–3563.
- Metzger, B. P., Yuan, D. C., Gruber, J. D., Duveau, F., & Wittkopp, P. J. (2015). Selection on noise constrains variation in a eukaryotic promoter. *Nature*, *521*, 344.
- Merelo, P., Ram, H., Caggiano, M. P., Ohno, C., Ott, F., Straub, D., et al. (2016). Regulation of MIR165/166 by class II and class III homeodomain leucine zipper proteins establishes leaf polarity. *Proceedings of the National Academy of Sciences of the United States of America*, *113*, 11973–11978.
- Mi, S., Cai, T., Hu, Y., Chen, Y., Hodges, E., Ni, F., et al. (2008). Sorting of small RNAs into Arabidopsis argonaute complexes is directed by the 5' terminal nucleotide. *Cell*, *133*, 116–127.
- Miyashima, S., Koi, S., Hashimoto, T., & Nakajima, K. (2011). Non-cell-autonomous microRNA165 acts in a dose-dependent manner to regulate multiple differentiation status in the Arabidopsis root. *Development*, *138*, 2303–2313.
- Molnar, A., Melnyk, C. W., Bassett, A., Hardcastle, T. J., Dunn, R., & Baulcombe, D. C. (2010). Small silencing RNAs in plants are mobile and direct epigenetic modification in recipient cells. *Science*, *328*, 872–875.
- Montgomery, T. A., Howell, M. D., Cuperus, J. T., Li, D., Hansen, J. E., Alexander, A. L., et al. (2008). Specificity of ARGONAUTE7–miR390 interaction and dual functionality in TAS3 trans-acting siRNA formation. *Cell*, *133*, 128–141.
- Mukherji, S., Ebert, M. S., Zheng, G. X., Tsang, J. S., Sharp, P. A., & van Oudenaarden, A. (2011). MicroRNAs can generate thresholds in target gene expression. *Nature Genetics*, *43*, 854.
- Nagasaki, H., Itoh, J.-i., Hayashi, K., Hibara, K.-i., Satoh-Nagasawa, N., Nosaka, M., et al. (2007). The small interfering RNA production pathway is required for shoot meristem initiation in rice. *Proceedings of the National Academy of Sciences of the United States of America*, *104*, 14867–14871.
- Nakajima, K., Sena, G., Nawy, T., & Benfey, P. N. (2001). Intercellular movement of the putative transcription factor SHR in root patterning. *Nature*, *413*, 307–311.
- Nikovics, K., Blein, T., Peaucelle, A., Ishida, T., Morin, H., Aida, M., et al. (2006). The balance between the MIR164A and CUC2 genes controls leaf margin serration in Arabidopsis. *The Plant Cell*, *18*, 2929–2945.
- Nogueira, F. T., Chitwood, D. H., Madi, S., Ohtsu, K., Schnable, P. S., Scanlon, M. J., et al. (2009). Regulation of small RNA accumulation in the maize shoot apex. *PLoS Genetics*, *5*, e1000320.
- Nogueira, F. T., Madi, S., Chitwood, D. H., Juarez, M. T., & Timmermans, M. C. (2007). Two small regulatory RNAs establish opposing fates of a developmental axis. *Genes & Development*, *21*, 750–755.
- Olmedo-Monfil, V., Durán-Figueroa, N., Arteaga-Vázquez, M., Demesa-Arévalo, E., Autran, D., Grimanelli, D., et al. (2010). Control of female gamete formation by a small RNA pathway in Arabidopsis. *Nature*, *464*, 628.

- Palauqui, J. C., Elmayan, T., Pollien, J. M., & Vaucheret, H. (1997). Systemic acquired silencing: Transgene-specific post-transcriptional silencing is transmitted by grafting from silenced stocks to non-silenced scions. *The EMBO Journal*, *16*, 4738–4745.
- Pant, B. D., Buhtz, A., Kehr, J., & Scheible, W. R. (2008). MicroRNA399 is a long-distance signal for the regulation of plant phosphate homeostasis. *The Plant Journal*, *53*, 731–738.
- Parizotto, E. A., Dunoyer, P., Rahm, N., Himber, C., & Voinnet, O. (2004). In vivo investigation of the transcription, processing, endonucleolytic activity, and functional relevance of the spatial distribution of a plant miRNA. *Genes & Development*, *18*, 2237–2242.
- Pekker, I., Alvarez, J. P., & Eshed, Y. (2005). Auxin response factors mediate Arabidopsis organ asymmetry via modulation of KANADI activity. *The Plant Cell*, *17*, 2899–2910.
- Petsch, K., Manzotti, P. S., Tam, O. H., Meeley, R., Hammell, M., Consonni, G., et al. (2015). Novel DICER-LIKE1 siRNAs bypass the requirement for DICER-LIKE4 in maize development. *The Plant Cell*, *27*, 2163–2177.
- Plavskin, Y., Nagashima, A., Perroud, P.-F., Hasebe, M., Quatrano, R. S., Atwal, G. S., et al. (2016). Ancient trans-acting siRNAs confer robustness and sensitivity onto the auxin response. *Developmental Cell*, *36*, 276–289.
- Ramachandran, V., & Chen, X. (2008). Degradation of microRNAs by a family of exoribonucleases in Arabidopsis. *Science*, *321*, 1490–1492.
- Reinhardt, D., Frenz, M., Mandel, T., & Kuhlemeier, C. (2005). Microsurgical and laser ablation analysis of leaf positioning and dorsoventral patterning in tomato. *Development*, *132*, 15–26.
- Ren, G., Chen, X., & Yu, B. (2012). Uridylation of miRNAs by *hen1 suppressor1* in Arabidopsis. *Current Biology*, *22*, 695–700.
- Rhoades, M. W., Reinhart, B. J., Lim, L. P., Burge, C. B., Bartel, B., & Bartel, D. P. (2002). Prediction of plant microRNA targets. *Cell*, *110*, 513–520.
- Rogers, K. W., & Schier, A. F. (2011). Morphogen gradients: From generation to interpretation. *Annual Review of Cell and Developmental Biology*, *27*, 377–407.
- Rosas-Diaz, T., Zhang, D., Fan, P., Wang, L., Ding, X., Jiang, Y., et al. (2018). A virus-targeted plant receptor-like kinase promotes cell-to-cell spread of RNAi. *Proceedings of the National Academy of Sciences of the United States of America*, *115*, 1388–1393.
- Schmiedel, J. M., Klemm, S. L., Zheng, Y., Sahay, A., Blüthgen, N., Marks, D. S., et al. (2015). MicroRNA control of protein expression noise. *Science*, *348*, 128–132.
- Shen, J., Xia, W., Khotskaya, Y. B., Huo, L., Nakanishi, K., Lim, S.-O., et al. (2013). EGFR modulates microRNA maturation in response to hypoxia through phosphorylation of AGO2. *Nature*, *497*, 383.
- Sheng, G., Zhao, H., Wang, J., Rao, Y., Tian, W., Swarts, D. C., et al. (2014). Structure-based cleavage mechanism of *Thermus thermophilus* Argonaute DNA guide strand-mediated DNA target cleavage. *Proceedings of the National Academy of Sciences of the United States of America*, *111*, 652–657.
- Sheu-Gruttadauria, J., & MacRae, I. J. (2018). Phase transitions in the assembly and function of human miRISC. *Cell*, *173*, 946–957, e916.
- Shu, P., Wu, C., Ruan, X., Liu, W., Hou, L., Fu, H., et al. (2019). Opposing gradients of microRNA expression temporally pattern layer formation in the developing neocortex. *Developmental Cell*, *49*, 764–785, e764.
- Sieber, P., Wellmer, F., Gheyselinck, J., Riechmann, J. L., & Meyerowitz, E. M. (2007). Redundancy and specialization among plant microRNAs: Role of the *MIR164* family in developmental robustness. *Development*, *134*, 1051–1060.
- Skopelitis, D. S., Benkovic, A. H., Husbands, A. Y., & Timmermans, M. C. (2017). Boundary formation through a direct threshold-based readout of mobile small RNA gradients. *Developmental Cell*, *43*, 265–273, e266.

- Skopelitis, D. S., Hill, K., Klesen, S., Marco, C. F., von Born, P., Chitwood, D. H., et al. (2018). Gating of miRNA movement at defined cell-cell interfaces governs their impact as positional signals. *Nature Communications*, *9*, 3107.
- Slotkin, R. K., Vaughn, M., Borges, F., Tanurdžić, M., Becker, J. D., Feijó, J. A., et al. (2009). Epigenetic reprogramming and small RNA silencing of transposable elements in pollen. *Cell*, *136*, 461–472.
- Smith, R. S., Guyomarc'h, S., Mandel, T., Reinhardt, D., Kuhlemeier, C., & Prusinkiewicz, P. (2006). A plausible model of phyllotaxis. *Proceedings of the National Academy of Sciences of the United States of America*, *103*, 1301–1306.
- Soyars, C. L., James, S. R., & Nimchuk, Z. L. (2016). Ready, aim, shoot: Stem cell regulation of the shoot apical meristem. *Current Opinion in Plant Biology*, *29*, 163–168.
- Stahl, Y., Grabowski, S., Bleckmann, A., Kühnemuth, R., Weidtkamp-Peters, S., Pinto, K. G., et al. (2013). Moderation of Arabidopsis root stemness by CLAVATA1 and ARABIDOPSIS CRINKLY4 receptor kinase complexes. *Current Biology*, *23*, 362–371.
- Steeves, T. A., & Sussex, I. M. (1989). *Patterns in plant development*. Cambridge University Press.
- Su, Z., Zhao, L., Zhao, Y., Li, S., Won, S., Cai, H., et al. (2017). The THO complex non-cell-autonomously represses female germline specification through the TAS3-ARF3 module. *Current Biology*, *27*, 1597–1609, e1592.
- Taochy, C., Gursansky, N. R., Cao, J., Fletcher, S. J., Dressel, U., Mitter, N., et al. (2017). A genetic screen for impaired systemic RNAi highlights the crucial role of DICER-LIKE 2. *Plant Physiology*, *175*, 1424–1437.
- Temoche-Diaz, M. M., Shurtleff, M. J., Nottingham, R. M., Yao, J., Fadadu, R. P., Lambowitz, A. M., et al. (2019). Distinct mechanisms of microRNA sorting into cancer cell-derived extracellular vesicle subtypes. *eLife*, *8*, e47544.
- Tilsner, J., Nicolas, W., Rosado, A., & Bayer, E. M. (2016). Staying tight: Plasmodesmal membrane contact sites and the control of cell-to-cell connectivity in plants. *Annual Review of Plant Biology*, *67*, 337–364.
- Tsikou, D., Yan, Z., Holt, D. B., Abel, N. B., Reid, D. E., Madsen, L. H., et al. (2018). Systemic control of legume susceptibility to rhizobial infection by a mobile microRNA. *Science*, *362*, 233–236.
- Tucker, M. R., Okada, T., Hu, Y., Scholefield, A., Taylor, J. M., & Koltunow, A. M. (2012). Somatic small RNA pathways promote the mitotic events of megagametogenesis during female reproductive development in Arabidopsis. *Development*, *139*, 1399–1404.
- Turing, A. M. (1952). The chemical basis of morphogenesis. *Philosophical Transactions of the Royal Society London B*, *237*, 37–72.
- Vatén, A., Dettmer, J., Wu, S., Stierhof, Y.-D., Miyashima, S., Yadav, S. R., et al. (2011). Callose biosynthesis regulates symplastic trafficking during root development. *Developmental Cell*, *21*, 1144–1155.
- Vaucheret, H., Mallory, A. C., & Bartel, D. P. (2006). AGO1 homeostasis entails coexpression of *MIR168* and *AGO1* and preferential stabilization of miR168 by AGO1. *Molecular Cell*, *22*, 129–136.
- Von Born, P., Bernardo-Faura, M., & Rubio-Somoza, I. (2018). An artificial miRNA system reveals that relative contribution of translational inhibition to miRNA-mediated regulation depends on environmental and developmental factors in Arabidopsis thaliana. *PLoS One*, *13*, e0192984.
- Waites, R., & Hudson, A. (1995). *phantastica*: A gene required for dorsoventrality of leaves in *Antirrhinum majus*. *Development*, *121*, 2143–2154.
- Wiesner, J. (1878). *Die heliotropischen Erscheinungen im Pflanzenreich*. Vienna, Austria: Kaiserlich-Königlichen Hof- und Staatsdruckerei.

- Willmann, M. R., & Poethig, R. S. (2007). Conservation and evolution of miRNA regulatory programs in plant development. *Current Opinion in Plant Biology*, *10*, 503–511.
- Wolpert, L. (1969). Positional information and the spatial pattern of cellular differentiation. *Journal of Theoretical Biology*, *25*, 1–47.
- Wu, S., & Gallagher, K. L. (2012). Transcription factors on the move. *Current Opinion in Plant Biology*, *15*, 645–651.
- Yadav, R. K., Perales, M., Gruel, J., Girke, T., Jönsson, H., & Reddy, G. V. (2011). WUSCHEL protein movement mediates stem cell homeostasis in the Arabidopsis shoot apex. *Genes & Development*, *25*, 2025–2030.
- Yao, X., Wang, H., Li, H., Yuan, Z., Li, F., Yang, L., et al. (2009). Two types of cis-acting elements control the abaxial epidermis-specific transcription of the *MIR165a* and *MIR166a* genes. *FEBS Letters*, *583*, 3711–3717.
- Yifhar, T., Pekker, I., Peled, D., Friedlander, G., Pistunov, A., Sabban, M., et al. (2012). Failure of the tomato trans-acting short interfering RNA program to regulate AUXIN RESPONSE FACTOR3 and ARF4 underlies the wiry leaf syndrome. *Plant Cell*, *24*, 3575–3589.
- Yoo, B.-C., Kragler, F., Varkonyi-Gasic, E., Haywood, V., Archer-Evans, S., Lee, Y. M., et al. (2004). A systemic small RNA signaling system in plants. *Plant Cell*, *16*, 1979–2000.
- Yu, Y., Jia, T., & Chen, X. (2017). The ‘how’ and ‘where’ of plant micro RNAs. *New Phytologist*, *216*, 1002–1017.
- Zavaliev, R., Sagi, G., Gera, A., & Epel, B. L. (2009). The constitutive expression of Arabidopsis plasmodesmal-associated class 1 reversibly glycosylated polypeptide impairs plant development and virus spread. *Journal of Experimental Botany*, *61*, 131–142.
- Zhai, J., Zhao, Y., Simon, S. A., Huang, S., Petsch, K., Arikat, S., et al. (2013). Plant microRNAs display differential 3′ truncation and tailing modifications that are ARGONAUTE1 dependent and conserved across species. *Plant Cell*, *25*, 2417–2428.
- Zhang, Z., Tucker, E., Hermann, M., & Laux, T. (2017). A molecular framework for the embryonic initiation of shoot meristem stem cells. *Developmental Cell*, *40*, 264–277, e264.
- Zhang, Z., & Zhang, X. (2012). Argonautes compete for miR165/166 to regulate shoot apical meristem development. *Current Opinion in Plant Biology*, *15*, 652–658.
- Zhao, Y., Yu, Y., Zhai, J., Ramachandran, V., Dinh, T. T., Meyers, B. C., et al. (2012). The Arabidopsis nucleotidyl transferase HESO1 uridylates unmethylated small RNAs to trigger their degradation. *Current Biology*, *22*, 689–694.
- Zhu, H., Hu, F., Wang, R., Zhou, X., Sze, S.-H., Liou, L. W., et al. (2011). Arabidopsis Argonaute10 specifically sequesters miR166/165 to regulate shoot apical meristem development. *Cell*, *145*, 242–256.

Further reading

- Husbands, A. Y., Chitwood, D. H., Plavskin, Y., & Timmermans, M. C. (2009). Signals and prepatterns: New insights into organ polarity in plants. *Genes & Development*, *23*, 1986–1997.
- Liu, Q., Wang, F., & Axtell, M. J. (2014). Analysis of complementarity requirements for plant microRNA targeting using a *Nicotiana benthamiana* quantitative transient assay. *Plant Cell*, *26*, 741–753.
- Martin, H. C., Wani, S., Steptoe, A. L., Krishnan, K., Nones, K., Nourbakhsh, E., et al. (2014). Imperfect centered miRNA binding sites are common and can mediate repression of target mRNAs. *Genome Biology*, *15*, R51.

Appendix II

ARTICLE

DOI: 10.1038/s41467-018-05571-0

OPEN

Gating of miRNA movement at defined cell-cell interfaces governs their impact as positional signals

Damianos S. Skopelitis¹, Kristine Hill², Simon Klesen², Cristina F. Marco¹, Patrick von Born¹, Daniel H. Chitwood^{1,3} & Marja C.P. Timmermans^{1,2}

Mobile small RNAs serve as local positional signals in development and coordinate stress responses across the plant. Despite its central importance, an understanding of how the cell-to-cell movement of small RNAs is governed is lacking. Here, we show that miRNA mobility is precisely regulated through a gating mechanism polarised at defined cell-cell interfaces. This generates directional movement between neighbouring cells that limits long-distance shoot-to-root trafficking, and underpins domain-autonomous behaviours of small RNAs within stem cell niches. We further show that the gating of miRNA mobility occurs independent of mechanisms controlling protein movement, identifying the small RNA as the mobile unit. These findings reveal gate-keepers of cell-to-cell small RNA mobility generate selectivity in long-distance signalling, and help safeguard functional domains within dynamic stem cell niches while mitigating a 'signalling gridlock' in contexts where developmental patterning events occur in close spatial and temporal vicinity.

¹Cold Spring Harbor Laboratory, One Bungtown Road, Cold Spring Harbor, NY 11724, USA. ²Center for Plant Molecular Biology (ZMBP), University of Tübingen, Auf der Morgenstelle 32, 72076 Tübingen, Germany. ³Present address: Department Horticulture and Computational Mathematics, Science & Engineering, Michigan State University, 1066 Bogue Street, East Lansing, MI 48824, USA. These authors contributed equally: Damianos S. Skopelitis, Kristine Hill. Correspondence and requests for materials should be addressed to M.C.P.T. (email: marja.timmermans@zmbp.uni-tuebingen.de)

The movement of small RNAs is fundamental to the growth and survival of plants. Small RNAs move from cell-to-cell via plasmodesmata¹, as well as systemically through the phloem to coordinate abiotic and biotic stress responses across the plant (see refs. 2–7). Particularly, the spread of siRNA-mediated gene silencing is one of the main defence mechanisms against viral attack and the damaging effects of transposons (see refs. 8–10). Similarly, miRNAs induced in response to nutrient stress, such as phosphate, copper, or sulphur deprivation, are transported through the phloem to coordinate physiological responses between the shoot and root^{2,3,11,12}.

More recently, small RNA mobility emerged as a unique and direct mechanism through which to relay positional information and drive developmental patterning^{13–17}. The specification of adaxial-abaxial polarity in developing leaves relies on two opposing small RNAs, *tasiARF* and *miR166*, that generate sharp ‘on-off’ gene expression boundaries of their respective targets via an intrinsic and direct threshold-based readout of their mobility gradients^{13,17,18}. *miR166* also serves as a short-range positional signal in the root, where its movement from the endodermis leads to the specification of discrete cell fates in the central stele^{14,15}. Further, the movement of *miR394* from the epidermis of the shoot stem cell niche into the underlying two cell layers enables these cells to retain stem cell competency via down-regulation of the F-box target, *LEAF CURLING RESPONSIVENESS (LCR)*¹⁶.

Small RNAs have properties that set them apart from other developmental signals, such as hormones, peptide ligands, and mobile transcription factors; namely, a high degree of specificity and a direct mode of action that allows for precise and rapid cell fate transitions. Small RNA regulation also confers sensitivity and robustness onto gene regulatory networks^{19,20}, and the morphogen-like readout of small RNA mobility gradients yields sharply delineated domains of target gene expression¹⁷. These properties make mobile small RNAs particularly well suited to drive developmental change, providing a mechanism to solve the mechanistically challenging problem of generating robust and uniform developmental boundaries even under fluctuating environmental conditions.

A further conceivable advantage of employing mobile small RNAs in development may be that they represent yet another class of signals, whose movement could occur through distinct paths and be regulated by independent mechanisms. However, despite its central importance, remarkably little is known regarding the local cell to cell movement of small RNAs, except that this occurs via plasmodesmata¹. The emphasis has been on understanding the vascular transport and reiterative spread of highly abundant and transitive siRNAs (see refs. 6,8,9,21–23). While these studies have been informative with respect to the propagation of RNA silencing at the whole organ or plant level, the insights gained are not informative in relation to the role of small RNAs as positional signals, whose movement occurs within defined spatial and/or temporal contexts.

Here, we show that miRNA mobility is a precisely regulated process. The directional movement of these central signalling molecules across specific cell–cell interfaces indicates the competence to move is determined at the cellular level via polarly localised determinants. These limit long-distance miRNA-mediated signalling, and the movement of miRNAs between functional domains within stem cell niches. Furthermore, we show that the mechanism regulating miRNA mobility acts independent of those controlling protein movement, identifying the small RNA as the mobile unit. Our findings reveal a gate-keeping mechanism in cell-to-cell miRNA mobility that generates selectivity in long-distance trafficking, and that helps safeguard functional domains within dynamic stem cell niches while mitigating a ‘signalling

gridlock’ in contexts where developmental patterning events occur in close spatial and temporal vicinity.

Results

Cell-to-cell movement of miRNAs is developmentally regulated. The shape of miRNA gradients generated by movement from a defined epidermal source is consistent with the passive diffusion of small RNAs between cells¹⁷. This, however, does not preclude the possibility that small RNA mobility is developmentally regulated. The passive diffusion of small proteins, such as free GFP, is observed only in select developmental contexts, reflecting a spatial and temporal regulation of plasmodesmata aperture and structure (see refs. 24,25). Therefore, the first questions we addressed were whether miRNA mobility is developmentally regulated, and if so whether the pattern of regulation parallels that of small diffusible proteins. To this end, we took advantage of the previously described miRGFP sensor system¹⁷, in which the artificial miRNA miRGFP silences a ubiquitously expressed, cell autonomous, nuclear-localised GFP reporter (*p35S:3xNLS-GFP*) without triggering systemic silencing via biogenesis of secondary siRNAs (Supplementary Fig. 1a–i and Supplementary Table 1). Importantly, earlier findings indicate that inheritance of miRGFP through cell division is limited, and that the behaviour of this artificial miRNA reflects that of endogenous small RNAs, such as *miR166* and the trans-acting siRNA *tasiARF*¹⁷.

To determine whether the movement of miRNAs and small diffusible proteins follows the same developmental regulation, we compared the pattern of miRGFP-directed GFP silencing to that of free GFP movement from the *ATML1*, *RbcS*, and *SUC2* promoters. These are active in the epidermis, mesophyll, and phloem companion cells, respectively (Supplementary Fig. 2a), and have been used extensively to study protein mobility (see refs. 24,25). When expressed from the *RbcS* promoter, free GFP and miRGFP show comparable non-cell autonomous effects, and are detectable in both the leaf epidermis and vasculature (Supplementary Figs. 3a–h and 4a, b). Likewise, both free GFP and miRGFP show non-cell autonomous patterns of activity when expressed in the epidermis (Supplementary Fig. 3i–p), although GFP fluorescence persists in the primary vasculature of *pATML1:miRGFP* leaves (Supplementary Fig. 3i–l). This, however, reflects an effective range rather than a movement barrier, as GFP silencing extends into the vasculature when levels of miRGFP in the epidermal source layer are inducibly increased (Supplementary Fig. 5¹⁷).

Small proteins move freely out of phloem companion cells as well, but only in sink tissues, such as young leaves (Fig. 1a, c). In source tissues, plasmodesmatal properties change and consequently *pSUC2:GFP* lines show a cell autonomous pattern of fluorescence (Fig. 1a, b, d; see also refs. 24,25). Unlike free GFP, expression of miRGFP in phloem companion cells (*pSUC2:miRGFP*) results in a non-cell autonomous pattern of GFP silencing in both sink and source leaves (Fig. 1i–l). Evidence that miRGFP acts as the mobile signal comes from co-expression of the viral-suppressor protein P19. P19 sequesters 21-nt small RNA duplexes into a cell autonomous complex^{9,21} and its co-expression in phloem companion or epidermal cells eliminates the non-cell autonomous silencing effects of miRGFP (Supplementary Fig. 4c–l).

The differences in free GFP versus miRGFP mobility in source leaves are unlikely explained by differences in their molecular weight or stokes radius, even if we consider that small RNAs move in a free rather than a protein-bound form. For example, in root meristems, free GFP shows a less restrictive pattern of mobility compared to miRGFP (Supplementary Fig. 6).

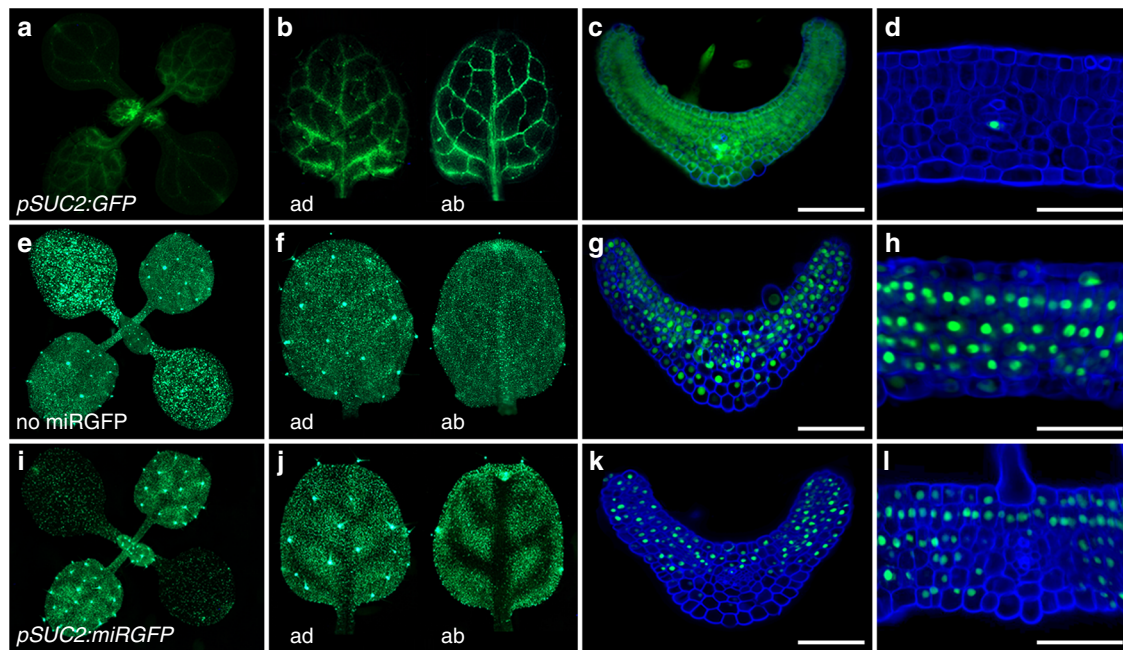


Fig. 1 miRNA mobility is regulated independently from small protein movement. **a–d** Free GFP expressed in phloem companion cells (*pSUC2:GFP*) diffuses throughout **a, c** young sink leaves, but behaves cell autonomously in **b, d** mature source leaves. **e–h** In *p35S:3xNLS-GFP* seedlings not expressing miRGFP (no miRGFP), GFP is ubiquitously expressed. **i–l** miRGFP expressed in phloem companion cells (*pSUC2:miRGFP*) results in a non-cell autonomous pattern of GFP silencing that extends over 4–6 cells and appears more extensive on the abaxial (ab) side of **k** young as well as **j, l** mature leaves. ad, adaxial; ab, abaxial. Scale bars, 50 μ m

Fluorescence in *pSUC2:GFP* lines is phloem-restricted in the differentiation zone of the root, but GFP is efficiently off-loaded from the phloem into primary and lateral root meristems (Supplementary Fig. 6a, d, g). Conversely, in *pSUC2:miRGFP* lines, a non-cell autonomous GFP silencing pattern is only detectable in the differentiation zone (Supplementary Fig. 6). These data indicate that miRNA mobility is developmentally regulated via mechanisms distinct from those modulating basic plasmodesmatal properties, such as aperture and density, which govern the regulated symplastic diffusion of small proteins.

miRNAs show directional mobility. Further evidence indicating that the movement of miRNAs is developmentally regulated comes from observations in the hypocotyl. Here, miRGFP expressed in the ground tissue (*pRbcS:miRGFP*) silences GFP in the epidermis and central stele, with the notable exception of the phloem poles (Fig. 2c and Supplementary Fig. 2a). Conversely, when expressed in the phloem companion cells (*pSUC2:miRGFP*), miRGFP silences GFP in the ground tissue and epidermis (Fig. 2d and Supplementary Fig. 2a). The conceivable caveat that miRGFP levels in *pRbcS:miRGFP* lines are below a threshold needed to clear GFP expression in cells adjacent to the source¹⁷, cannot explain these disparate behaviours. Small RNA deep-sequencing shows miRGFP accumulates to comparable levels in *pRbcS:miRGFP* vs. *pSUC2:miRGFP* seedlings (Supplementary Table 1), in which miRGFP levels are sufficiently high to clear GFP expression across a range of at least four cells (Fig. 2d). Also, miRGFP levels in *pRbcS:miRGFP* lines are sufficient to silence GFP in the hypocotyl procambium (Fig. 2c). Thus, whereas miRGFP is able to move out of the phloem companion cells to silence GFP in the hypocotyl ground tissue, miRGFP expressed from the *RbcS* promoter does not silence GFP in the phloem poles, indicating that miRGFP movement between endodermis and phloem is unidirectional (Fig. 2c, d).

miRNA mobility between the endodermis and vascular procambium is also unidirectional. When expressed in the procambium (*pATHB8:miRGFP*), miRGFP acts cell autonomously (Fig. 2e and Supplementary Fig. 2a). Again, levels of miRGFP cannot explain this pattern of GFP silencing. miRGFP accumulates to substantially higher levels in *pATHB8:miRGFP* than *pATML1:miRGFP* hypocotyls, which show a non-cell autonomous pattern of GFP silencing that extends across at least three cells (Fig. 2e–g and Supplementary Fig. 2a). Movement of miRGFP out of the procambium should, therefore, result in a detectable silencing effect, at least in cells immediately adjacent. Thus, the movement of miRGFP in and out of the procambium also shows directionality in a manner that is not explained by the presence of plasmodesmata or miRGFP levels at the source. Taken together, these observations reveal that miRNA mobility between neighbouring cells is regulated by a mechanism that can confer directionality across a given cell–cell interface.

Long-distance movement of miRNAs is highly restrictive. The finding that entry into the hypocotyl phloem is restricted (Fig. 2c), has important implications for long-distance communication via miRNAs. It implies that only those miRNAs expressed in phloem companion cells are able to efficiently move long-distance from the shoot into the root. Indeed, small RNA deep-sequencing revealed that miRGFP accumulates in *pRbcS:miRGFP* seedling roots at levels three orders of magnitude below that observed in shoots (Fig. 3e). In fact, the limited loading of miRNAs into the hypocotyl phloem is likely even more extreme if we consider that miRGFP can move into the phloem in developing leaves (Supplementary Fig. 3c, d).

The minimal levels of miRGFP moving into the root are insufficient to noticeably repress GFP expression (Fig. 3a–c). Moreover, the pattern of GFP fluorescence in *pSUC2:miRGFP* roots indicates that in the absence of transitivity, miRNAs transported through the phloem fail to repress their targets in

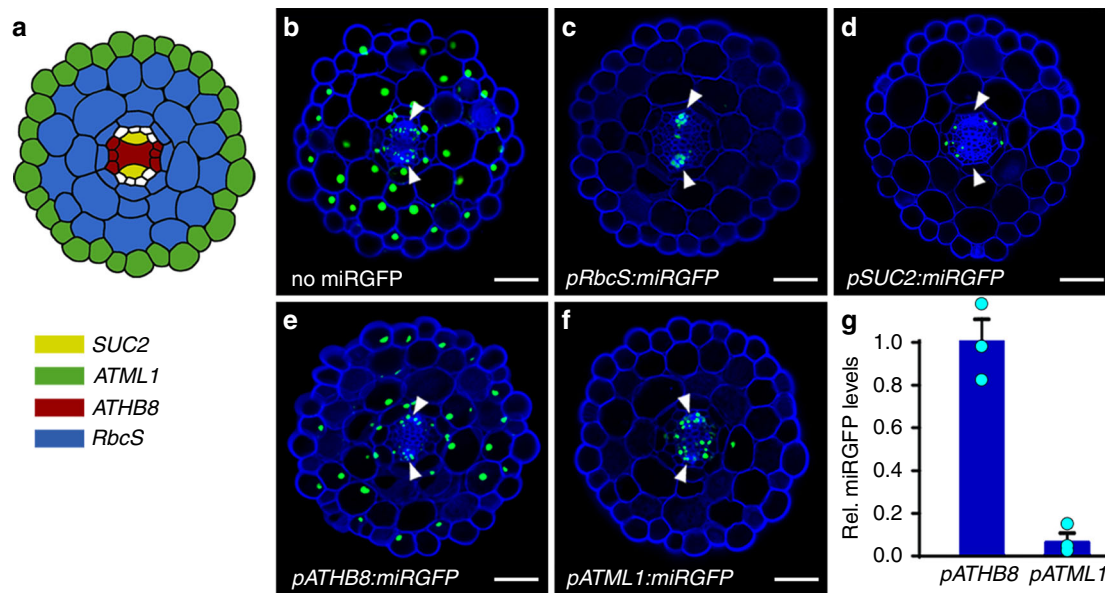


Fig. 2 miRNAs show directional mobility. **a** Diagram illustrating the expression domains of the *SUC2* (yellow), *ATML1* (green), *ATHB8* (red), and *RbcS* (blue) promoters, as verified in Supplementary Fig. 2a. **b** Transverse section of a *p35S:3xNLS-GFP* (no miRGFP) hypocotyl shows ubiquitous GFP expression. **c–f** The patterns of GFP silencing in lines expressing miRGFP in **c** mesophyll (*pRbcS:miRGFP*), **d** phloem companion (*pSUC2:miRGFP*), **e** procambial (*pATHB8:miRGFP*), and **f** epidermal (*pATML1:miRGFP*) cells reveal directionality in miRGFP mobility, with miRGFP moving out but not into the phloem pole. Note, *pATHB8:miRGFP* lines show a cell autonomous pattern of GFP silencing. **g** Small RNA qRT-PCR shows that miRGFP levels are significantly ($p < 0.001$, two-sided Student's *t*-test) higher in *pATHB8:miRGFP* vs. *pATML1:miRGFP* hypocotyls. Relative miRGFP levels (means ± SE; $n = 3$) normalised to U6 are shown. Scale bars, 50 μ m. White arrowheads, phloem poles

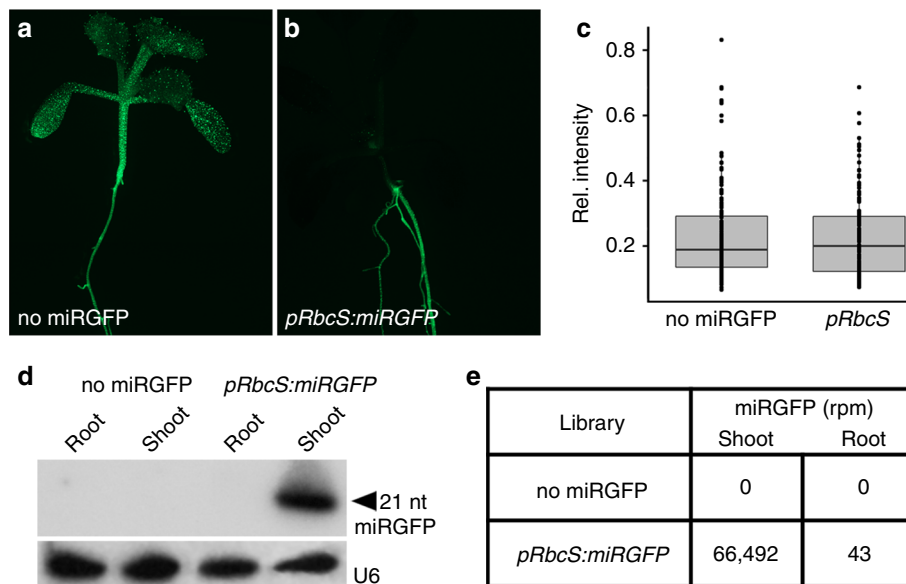


Fig. 3 Long-distance shoot-to-root trafficking of miRNAs is limited by entry into the phloem. **a, b** Compared to **a** *p35S:3xNLS-GFP* (no miRGFP) seedlings, GFP silencing is apparent in the shoot but not the root of **b** *pRbcS:miRGFP* lines. **c** Quantification of the mean GFP fluorescence intensity in endodermal cells ($n \geq 130$) normalised to fluorescence intensity in cells of the lateral root cap reveals this to not deviate significantly ($p > 0.05$, two-sided Student's *t*-test) between *p35S:3xNLS-GFP* (no miRGFP) and *pRbcS:miRGFP* root meristems. Horizontal line, median; box, 1st to 3rd quartiles. **d** Small RNA gel blot shows miRGFP accumulates in shoots of *pRbcS:miRGFP* seedlings but is undetectable in roots. **e** Read counts for miRGFP in reads per million (rpm) normalised to the total number of mapped 19–25 nt small RNA reads in libraries constructed from shoot and root samples of *p35S:3xNLS-GFP* (no miRGFP) and *pRbcS:miRGFP* seedlings. The substantially lower levels of miRGFP in *pRbcS:miRGFP* roots indicate limited miRNA trafficking from shoot to root

primary and lateral root meristems (Supplementary Fig. 6c, i, k). Nonetheless, a number of miRNAs are proposed to function as long-distance mobile signals to coordinate physiological responses between the shoot and root^{2,3,11,12,26}. Our findings indicate that for such miRNAs to function effectively they should

be produced in the phloem companion cells and trigger transitivity to propagate the silencing signal into the growing root tips. Indeed, those miRNAs reported to relay stress responses from the shoot to the root, such as miR399 in the case of phosphate deficiency, have been found to trigger transitivity²⁷.

Selective miRNA mobility in the shoot stem cell niche. As in the root, the movement of miRGFP from the central vasculature into the stem cell niche at the shoot apex is restricted. GFP fluorescence persists in the shoot apical meristem, at least prior to the floral transition, even in lines expressing miRGFP from the *ATHB8* or *RbcS* promoters, which show silencing in the vasculature and ground tissue below (Supplementary Fig. 7). Systemic transitive siRNA signals are also excluded from the shoot apex prior to flowering (see refs. 8,9,22,28,29). Although counterintuitive with respect to the spread of anti-viral siRNAs, a barrier at the base of the shoot apical meristem might be relevant to environmental plasticity, preventing small RNAs from establishing irreversible epigenetic change in response to transient cues^{6,9,21,22}.

Nonetheless, expression of important cell fate determinants within the shoot apical meristem is regulated by miRNAs³⁰, and the movement of small RNAs such as miR394 and miR166 is a key feature of their role in development^{16–18}. Given the dynamic nature of the stem cell niche and the fact that cell fates are continuously defined in close spatial and temporal vicinity, miRNA mobility may need to be precisely regulated, leading us to investigate the behaviour of miRNA mobility within the shoot apical meristem.

In line with the role of miR166 in specifying adaxial-abaxial polarity^{17,31}, expression of miRGFP in the abaxial epidermis of incipient and developing leaf primordia (*pMIR166A:miRGFP*) results in a non-cell autonomous pattern of GFP silencing (Fig. 4a–c and Supplementary Fig. 2b). However, loss of GFP fluorescence is seen only in primordia, not elsewhere in the shoot apical meristem (Fig. 4c). Similarly, when expressed in the tunica (*pSCR:miRGFP*), miRGFP-directed silencing extends one cell layer, from the tunica into the third layer of the meristem, but GFP expression persists in the underlying organising centre and rib meristem (Fig. 4d and Supplementary Fig. 2b). These observations imply that miRNAs are able to move between cells within a given functional domain of the meristem but not between such domains.

Consistent with this idea, expression of miRGFP in the central zone (*pCLV3:miRGFP*) or organising centre (*pWUS:miRGFP*) reveals domain-autonomous patterns of GFP silencing (Fig. 4e, f and Supplementary Fig. 2b). As in the hypocotyl, these data cannot be explained by relative miRNA-to-target levels along a mobility gradient being insufficient to clear GFP expression. Deep sequencing demonstrates that miRGFP levels in *pCLV3:miRGFP* lines are almost half that of *pSUC2:miRGFP* lines, even though the *SUC2* promoter is active in many more cells throughout the seedling (Supplementary Table 1). In addition, the restrictive cell-to-cell movement of miRGFP in the shoot apical meristem is not linked to the distribution of plasmodesmata (see ref. 29), or the presence of pre-existing symplastic fields^{32,33}, as free GFP expressed from the *WUS* promoter (*pWUS:GFP*) is able to move out of the organising centre and diffuse throughout the meristem (Fig. 4g). Instead, these data reveal the existence of additional regulatory mechanisms that spatially limit the movement of miRNAs between functional domains of the shoot stem cell niche. Importantly, given that the plasmodesmata-facilitated movement of *WUS* protein out of the organising centre is critical for meristem function^{34,35}, the mechanism underlying the dynamic regulation of miRNA mobility in the shoot stem cell niche must also act independently of any controlling facilitated protein trafficking.

Selective miRNA mobility is a property of stem cell niches. miRGFP when expressed in the hypocotyl procambium (*pATHB8:miRGFP*; Supplementary Fig. 2a), acts cell autonomously (Fig. 2e). The procambium comprises the vascular stem cells responsible for

the continuous formation of phloem and xylem tissues. Considering the above, this observation presents the intriguing possibility that a dynamic regulation of miRNA mobility might be a general feature of stem cell niches. To address this, we analysed the pattern of miRGFP-mediated GFP silencing within the root meristem. Here, the quiescent centre is surrounded by a single layer of tissue-specific stem cells (initials) that divide asymmetrically to generate the concentrically arranged tissue files of the root, comprising the stele, cortex, endodermis, and epidermis, as well as the lateral root cap and columella³⁶ (Fig. 5a).

Distinct from the binary readout of mobility-derived small RNA gradients in developing leaf primordia¹⁷, the movement of miR165/166 in the root generates an inversely graded pattern of HD-ZIPIII activity across the stele to pattern meta vs. protoxylem^{14,15}. The pattern of GFP silencing resulting from miRGFP expression in the root endodermis, whether from the *SCR* or *MIR166A* promoter (Supplementary Fig. 2c), is consistent with the silencing gradient of endogenous miR165/166 and extends from the endodermis into the stele and cortex (Fig. 5a–d). However, predictive of higher miRGFP source levels, a more extensive pattern of GFP silencing is seen in *pSCR:miRGFP* lines. Here, GFP silencing extends into the epidermis as well as into the columella. Importantly, the *MIR166A* promoter is not active in the stem cell niche itself (Supplementary Fig. 2c), and whereas miRGFP moves across multiple cell layers in the stele, GFP fluorescence persists in niche cells directly adjacent to the endodermis (Fig. 5d). Given that cells within the root stem cell niche are symplastically connected^{37,38}, this finding implies that, as in the shoot meristem, miRGFP is unable to move from more determined cells *into* underlying stem cell initials and the quiescent centre.

Moreover, the GFP silencing pattern observed in *pATHB8:miRGFP* lines, where miRGFP is generated in the central vasculature, quiescent centre, and columella (Supplementary Fig. 2c), predicts that miRNAs are unable to move between stem cell initials or *out* of the quiescent centre. In these lines, miRGFP generates a non-cell autonomous pattern of GFP silencing in the stele, even though the *ATHB8* promoter shows a relatively low level of activity here (Fig. 5e and Supplementary Fig. 2c). In contrast, GFP fluorescence persists in the cortex/endodermis and epidermis/lateral root cap initials adjacent to the quiescent centre (Fig. 5e) where expression from the *ATHB8* promoter is comparatively strong (Supplementary Fig. 2c). Also miRGFP from the columella initials does not silence GFP in neighbouring stem cells (Fig. 5e). Mobility of miRGFP in the stele, despite limited *ATHB8* promoter activity (Supplementary Fig. 2c), argues against source levels underlying the cell autonomous behaviour of miRGFP in the niche. Instead, the GFP silencing patterns observed in the *pATHB8:miRGFP* and *pMIR166A:miRGFP* lines imply a level of regulation that permits the movement of miRNAs between more determined cells of the root meristem while limiting mobility between stem cells, and in and out of the quiescent centre. In addition, the columella presents an additional example of directional miRNA mobility, as miRGFP moves in (*pSCR:miRGFP*) but not out of the columella (*pATHB8:miRGFP*) (Fig. 5c, e).

Substantiating the finding that miRNA mobility from the quiescent centre is restricted, expression of miRGFP specifically in these cells (*pWOX5:miRGFP*) results in a domain-autonomous pattern of GFP silencing (Supplementary Fig. 2c and Fig. 5f). This restrictive miRNA activity pattern contrasts to the diffusion of small proteins, as free GFP can move both into (*pSUC2:GFP*; Supplementary Fig. 6g) and out of the quiescent centre (*pWOX5:GFP*; Fig. 5g). Furthermore, as for *WUS* in the SAM, symplastic movement of *WOX5* protein out of the quiescent centre is essential for maintaining meristematic activity in the root tip³⁹.

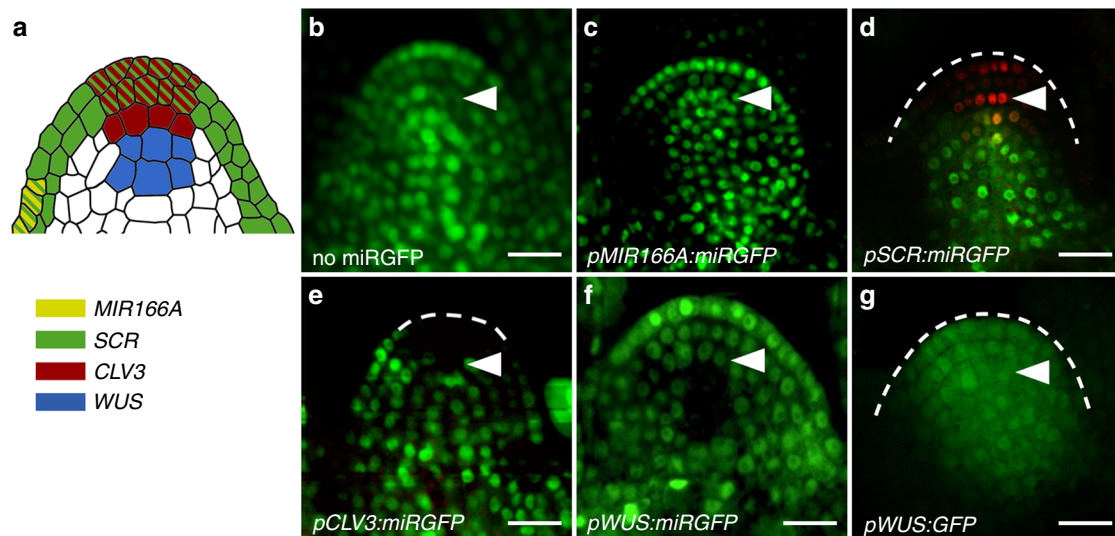


Fig. 4 miRNAs act domain-autonomously within the shoot stem cell niche. **a** Diagram illustrating the expression domains of the *MIR166A* (yellow), *SCR* (green), *CLV3* (red), and *WUS* (blue) promoters, as verified in Supplementary Fig. 2. **b–g** Longitudinal sections through the shoot apical meristem of **b** a *p35S:3xNLS-GFP* (no miRGFP) seedling, and lines expressing miRGFP in the **c** abaxial epidermis (*pMIR166A:miRGFP*), **d** meristem tunica (*pSCR:miRGFP*), **e** stem cells of the central zone (*pCLV3:miRGFP*), and **f** organising centre (*pWUS:miRGFP*), and **g** free GFP expressed in the organising centre (*pWUS:GFP*) show domain-autonomous patterns of miRGFP-directed GFP silencing. Cells in the central zone in **d** are marked using a *pCLV3:dsRED* reporter line. In contrast to **f** miRGFP, **g** free GFP expressed in the organising centre (*pWUS:GFP*) moves freely throughout the shoot stem cell niche. Arrowheads, third layer of the central zone. Scale bars, 10 μ m

Thus, despite their distinct organisations, miRNA mobility within the shoot, root, and vascular stem cell niches is highly regulated. Movement between the organising centre, stem cells, and more determined daughter cells within the niche is restricted, and this regulation occurs via mechanisms independent of those regulating protein trafficking, whether the diffusion of small proteins or the facilitated transport of larger transcription factors.

miRGFP mobility reflects general behaviours of miRNAs. The pattern of miRGFP-directed GFP silencing in leaf primordia was shown to recapitulate the patterning properties of the endogenous small RNAs, miR166 and tasiARF¹⁷. Additionally, the highly restrictive shoot-to-root movement of miRGFP explains previously noted inefficiencies in the long-distance movement of siRNAs across graft junctions^{5,26}. To further substantiate that our findings regarding miRGFP mobility reflect general behaviours of miRNAs, we developed a second synthetic sensor system based on an artificial miRNA targeting the cell autonomous GUS reporter (miRGUS). Whereas miRGFP is generated from the *MIR390A* backbone, the miRGUS design is based on the backbone of *MIR319A* (Supplementary Fig. 8a and Supplementary Table 2), which differs in its pre-miRNA structure and is processed via a different mechanism⁴⁰.

The miRGUS system is less efficient than the miRGFP system, with miRGUS accumulating at levels sixfold lower than miRGFP expressed from the same 35S promoter (62 rpm; Supplementary Fig. 8b vs. 391 rpm¹⁷). Furthermore, unlike miRGFP¹⁷, miRGUS biogenesis produces 20- as well as 21-nt miRNA species, thus rendering the effective levels even lower (Supplementary Fig. 8c). Nonetheless, the patterns of miRGUS-directed gene silencing observed in *pATML1:miRGUS* and *pRbcS:miRGUS* lines are comparable to those of their miRGFP counterparts (Supplementary Fig. 8d–i). Notably while GUS silencing is observed in *pRbcS:miRGUS* shoots, reporter activity persists throughout the root (Supplementary Fig. 8g). Furthermore, expression of miRGUS in the meristem tunica (*pSCR:miRGUS*) silences GUS activity in the third cell layer, but not in the underlying organising centre (Supplementary Fig. 8i), confirming the domain-autonomous

behaviour of miRNAs in the shoot apical meristem (Fig. 4). Thus, mobility parameters of miRGUS mirror those of miRGFP, which in turn recapitulates the behaviour of endogenous small RNAs, including miR166 and tasiARF^{14,15,17}.

Taken together, these data show that miRNA mobility is a highly regulated process that allows for directional movement in more developed tissue contexts, and domain-autonomous behaviours within stem-cell niches. The capacity for a small RNA to move is not dictated by small RNA sequence or even the pathway via which it is generated, but rather movement is spatiotemporally regulated at the cell level. This occurs independently of mechanisms governing protein movement through plasmodesmata.

Discussion

The movement of small RNAs is fundamental to plant development, growth, and survival. Mobile small RNAs are critical for protection against the damaging effects of transposons, and in coordinating abiotic and biotic stress responses across the plant (see refs. 9,10,13). In addition, mobile small RNAs serve as short-range positional signals with morphogen-like activities in developmental patterning¹⁷. Our results show that the movement of miRNAs is a carefully regulated process, adding another level by which key responses can be controlled.

The mechanisms underlying the regulated mobility of miRNAs are distinct from those controlling the facilitated transport of transcription factors such as *WUS* and *WOX5*^{34,35,39}. In addition, the basic mechanisms that modulate plasmodesmata to govern the sink-source relationship and the passive diffusion of small proteins during development or in the case of stress (see refs. 24,25,41), cannot explain the specific instances of selective mobility described here for miRNAs. This, however, does not preclude the importance of plasmodesmata in the regulation of small RNA mobility. Instances where miRNAs are able to move from a given cell into one neighbour but not another, indicate that mobility can be regulated asymmetrically within a given cell. Examples of this include the movement of miRNAs from the ground tissue into all neighbouring cells except those of the phloem pole, and

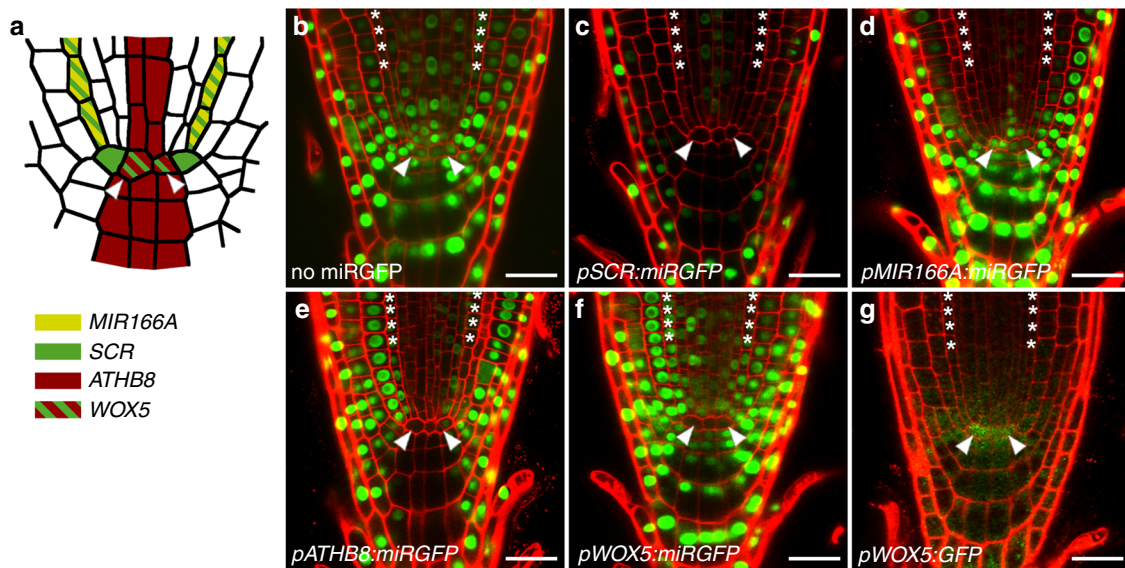


Fig. 5 Regulated miRNA mobility within the root stem cell niche. **a** Diagram illustrating the expression domains of the *MIR166A* (yellow), *SCR* (green), *ATHB8* (red), and *WOX5* (red-green) promoters, as verified in Supplementary Fig. 2c. **b–g** Optical longitudinal sections through the root meristem of **b** a *p35S:3xNLS-GFP* (no miRGFP) seedling, and lines expressing miRGFP in the **c** endodermis and quiescent centre (*pSCR:miRGFP*), **d** endodermis (*pMIR166A:miRGFP*), **e** stele, QC and columella (*pATHB8:miRGFP*), and **f** QC (*pWOX5:miRGFP*), show that miRGFP acts domain-autonomously within the niche but moves between determined daughter cells of the root meristem. Note: persistence of GFP fluorescence in cells of the lateral root cap is likely explained by a low density of plasmodesmatal connections to these cells^{37,38}. In contrast to **f** miRGFP, **g** free GFP expressed in the QC (*pWOX5:GFP*) moves freely throughout the root apex. Asterisks, endodermal cells; arrowheads, QC. Scale bars, 20 µm

the domain-autonomous miRNA mobility observed in the stem cell niches. These reveal the presence of mobility factors that are able to polarise at defined cell–cell interfaces and function as ‘gate-keepers’ regulating the passage of miRNAs locally (Fig. 6). In this regard, it is interesting to note that many proteins, including receptors-like kinases, are preferentially located at plasmodesmata^{42,43}, providing lots of scope to polarise the movement of small RNAs independently of other molecules⁴⁴.

Regulation of miRNA mobility via polarised ‘gate-keepers’ can be envisioned irrespective of whether mobility occurs via diffusion or active transport. However, the shape of small RNA gradients observed in the leaf¹⁷, and their dose-dependence, favour the simple diffusion of small RNAs. In line with this notion, prior screens for factors facilitating the movement of small RNAs identified a substantial number of the known regulators of small RNA biogenesis (see refs. 8,9,23), but left open the question whether small RNA mobility is a regulated process. The passive diffusion of small RNAs implies that regulation occurs via ‘mobility restrictors’ preventing movement through plasmodesmata at specific cellular interfaces. Thus, perhaps analogous to the regulated movement of *SHORT-ROOT* and *CAPRICE*^{45–47}, miRNA mobility is spatiotemporally regulated by mechanisms that restrict rather than facilitate movement.

Given that miRNA mobility is gated at individual cell–cell interfaces, regulated mobility cannot reflect any general sequestration mechanism. Thus, although AGO proteins act cell autonomously^{9,21}, our data cannot be explained by AGO1-loading as the underpinning mechanism. Similarly, the capacity to move is not explained by miRNA overabundance, with only small RNAs exceeding the loading capacity of cell autonomous proteins, such as AGO1, moving into neighbouring cells. Levels do affect the range of mobility, but not the actual capacity to move. For example, highly expressed miRNAs in the central zone of the shoot apical meristem are domain-autonomous, whereas lowly expressed miRNAs in the epidermis silence targets across several cell layers. Considering this, and the fact that the

movement of miRNAs is regulated independently from that of proteins, it is compelling to conclude that mobile small RNAs carry distinguishing marks and are themselves the mobile unit recognised by polarly localised ‘gate-keepers’.

The gating of miRNA mobility allows for selectivity in long-distance signalling. The polarised regulation of miRNA mobility at the phloem of the central vasculature generates directional cell-to-cell movement, with miRNAs moving out but not into the phloem poles (Fig. 6a). Consequently, miRNAs not produced or amplified in phloem tissues of the shoot are restricted from moving long distance into the root. Thus, the gate-keeping mechanism regulating miRNA mobility at the central vasculature creates a movement barrier that ensures some small RNA-mediated signalling responses are contained while permitting others to be propagated systemically.

Moreover, in the absence of transitivity, the root apical meristem appears protected from the activity of mobile miRNAs, as their effects are limited to the root differentiation zone. This finding is in sharp contrast to the behaviour of mobile 24-nt siRNA signals. When transported from the shoot to the root, these siRNAs, even when present at reduced levels, can direct epigenetic change in cells of the root meristem, giving rise to clonal sectors in which target genes are repressed^{5,7,26}. However, while providing greater signal sensitivity, the stable epigenetic repression triggered by 24-nt siRNAs is ineffective in mediating plastic adaptive responses. Instead, miRNAs that trigger transitivity, enabling the amplification and progressive spread of silencing from a phloem source, may be particularly advantageous as long-distance messengers of environmental change. Indeed, the phloem-loaded miRNAs involved in coordinating stress responses across the plant, such as miR399 in phosphate deprivation, trigger transitivity^{27,48}. This identifies miRNA precursor features and protein components required to trigger miRNA-directed transitivity as a source for selection to act upon during plant evolution.

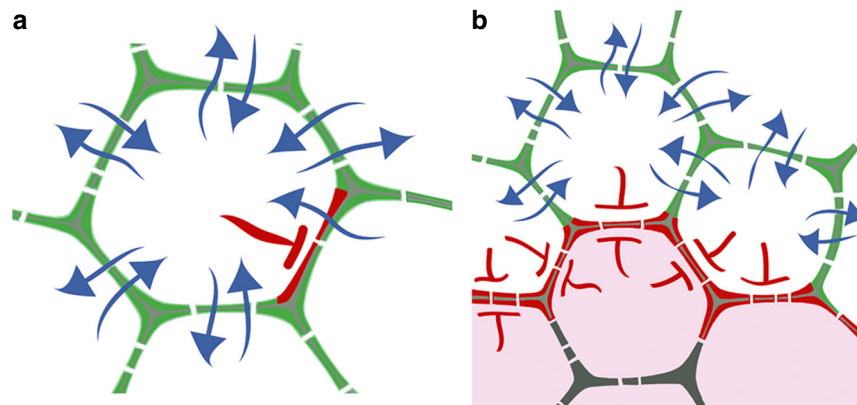


Fig. 6 Schematic representation of polarised gate-keepers regulating the cell-to-cell movement of miRNAs. **a** Polarisation of factors that block miRNA mobility to defined cell–cell interfaces can establish unidirectional movement between neighbouring cells, or **b** when polarised to both sides of select interphases between multiple adjacent cells create domains with confined miRNA mobility. Blue arrows, miRNA movement; red line, polarised inhibition of miRNA movement; pink shading, miRNA mobility domain

The polarised gating mechanism also underpins a domain-autonomous behaviour of small RNAs within stem cell niches (Fig. 6b). The regulated movement of miRNAs between domains of a meristem is understandable when we consider that cell fates within stem cell niches are dynamically specified. Expression of multiple important cell fate determinants within meristems is under miRNA control (see refs. 30,49), but that miRNA mobility between functional domains needs stringent control is particularly well illustrated by the action of miR394. This miRNA moves from the shoot apical meristem epidermis into underlying cells where it promotes stem cell activity by repressing LCR¹⁶. Mechanisms that prevent the movement of miRNAs from the central zone into the organising centre below can thus help safeguard organisation in the dynamic shoot stem cell niche. Likewise, by repressing GRF transcription factor activity, miR396 ensures the properly timed transition between stem cells and transit-amplifying cells in the root stem cell niche⁵⁰. Also, movement of miR166, while essential for the specification of adaxial-abaxial polarity in the incipient primordium^{17,31}, cannot extend into the central zone where its HD-ZIPIII targets are required for stem cell activity. Mechanisms that restrict the cell-to-cell movement of miRNAs can thus help safeguard organisation in structures such as meristems (Fig. 6b), where cells in each of the domains are continuously dividing, or where miRNA levels fluctuate due to inherent noisiness in gene expression.

Still, recruiting small RNAs as a class of patterning molecules may be particularly relevant to plant stem cell niches where multiple patterning processes are occurring in close spatial and temporal vicinity. For example, within the shoot apical meristem, organ polarity is established in close proximity to signals that maintain the stem cell niche, instruct the positioning and outgrowth of the primordium, or trigger vascularisation. Careful coordination between events is thus required. The mobile signals that operate within plant stem cell niches belong to different classes of molecules, including secreted peptide ligands (e.g., CLEs), actively transported plant hormones (e.g., auxin), mobile transcription factors (e.g., WUS, WOX5), as well as mobile small RNAs (see refs. 36,51). The movement of these signals occurs through separate paths or, as our data indicates for plasmodesmata trafficking, is controlled by independent regulatory mechanisms. Thus, in addition to their high specificity, favourable network properties and unique patterning outputs, an advantage of employing mobile small RNAs in development is that they represent yet another class of signalling molecules whose independent movement mitigates a ‘signalling gridlock’.

Thus, small RNAs are not simply repressors of gene expression. They are important signalling molecules whose movement is precisely regulated independently from other signals via a gating mechanism polarised at defined cell–cell interfaces. This creates selectivity in shoot-to-root phloem transport to control systemic responses at the whole plant level, and defines the scope of small RNAs as local positional cues to precisely pattern the highly dynamic plant stem cell niches.

Methods

Plant materials and growth conditions. All analyses were performed in the Col-0 ecotype, either wild type or *rdm6-15* (SAIL_617). The *pCLV3:dsRED* line⁵² was provided by H. Jönsson, Sainsbury Laboratory, University of Cambridge. Plants were grown at 22 °C under long-day conditions in soil or on 1% agar plates containing 1x Murashige and Skoog (MS) medium (Sigma-Aldrich) supplemented with 0 or 1% sucrose and appropriate antibiotics. β -Estradiol inductions were performed by germinating seedlings on the above media then transferring daily to 0.7% agar MS plates supplemented with fresh 20 μ M β -estradiol for the indicated incubation times. Analyses on roots were performed 7–8 days after germination, and all other analyses were performed on 10–12 day-old seedlings.

Generation of constructs and transgenic plants. The following promoter fragments were used in this study: 0.7 kb *2x35S*, 2.2 kb *ATML1*, 1.8 kb *RbcS*, 2.5 kb *MIR166A*, 2.3 kb *SUC2*, 2.2 kb *ATHB8*, 2.5 kb *SCR*, 2.2 kb *WUS*, 4.2 kb *CLV3* and 4.2 kb *WOX5*. Promoter fragments were amplified using PCR primers with appropriate attB1–attB2 sites (Supplementary Table 3) and introduced into pDONR207 (Invitrogen). Transcriptional GUS reporter fusions were generated by cloning these promoters upstream of the *uidA* gene in the pGreen II 0029 binary vector using Gateway technology. Transcriptional GFP reporter constructs were generated similarly by introducing the *ATML1*, *RbcS*, *SUC2*, and *WUS* promoter fragments upstream of *GFP6-6xHIS* in pMDC107. The *pWOX5:GFP* construct was generated by Gibson assembly (NEB) introducing the mGFP6 coding sequence downstream of the *WOX5* promoter in the pK7WG plasmid backbone.

The *p35S:3xNLS-GFP* reporter line and the *miRGFP* precursor have been described previously¹⁷. The β -estradiol inducible *pATML1:miRGFP* construct was created by inserting the miRGFP precursor into pMDC7 using Gateway technology. The G10-90 promoter of this vector was subsequently replaced by a Gateway cassette via Gibson assembly (NEB). To create the final *pATML1:miRGFP* construct, the 2.1 kb *ATML1* promoter was introduced upstream of the miRGFP precursor using Gateway technology. The miRGUS sequence was introduced into a 404 bp *MIR319A* precursor fragment using overlapping PCR⁵³. This *MIR319A*-based *miRGUS* precursor fused to the NOS terminator was custom synthesised and cloned downstream of the Gateway cassette in the pGreen II 0029 binary vector using *SpeI/SacI* restriction sites. Using Gateway technology, the *2x35S*, *ATML1*, *RbcS*, and *SCR* promoter fragments were introduced upstream of *miRGUS* to create *p35S:miRGUS*, *pATML1:miRGUS*, *pRbcS:miRGUS*, and *pSCR:miRGUS*, respectively. A Gateway-based p19 expression vector, with the 578 bp coding sequence of the viral-suppressor protein p19 fused to HA inserted downstream of the Gateway cassette in pGreen II 0029, was assembled by Gibson assembly (NEB). Using Gateway technology, the *ATML1* and *SUC2* promoter fragments were subsequently introduced upstream of *p19-HA* to create *pATML1:p19-HA* and *pSUC2:p19-HA*, respectively.

The *p35S:3xNLS-GFP* and *p35S:GUS* reporter lines were generated in the *rd6-15* background and subsequently transformed with *miRGFP* and *miRGUS* precursor constructs, respectively. Multiple independent transformants per construct (*n* of between 10 and 20) were observed, of which at least four independent lines with representative behaviour were analysed in greater detail. Select *pATML1-*, *pRbcS-*, *pSUC2-*, *pSCR-*, and *pWOX5-miRGFP* lines were crossed onto Col-0 to confirm the silencing patterns also in this wild-type background. P19 constructs were initially transformed into Col-0 and subsequently introduced into *pSUC2:miRGFP* and *pATML1:miRGFP* lines via crossing. The GUS and GFP promoter fusions were also generated in the *rd6-15* background. Artificial miRNA sequences are listed in Supplementary Table 2, and cloning primers are listed in Supplementary Table 3.

Confocal microscopy. Ten-day-old seedlings were fixed in 4% paraformaldehyde (PFA) dissolved in 1x PBS supplemented with 0.01% Tween 20 (Sigma-Aldrich) under vacuum (33 mBar) for 45 min. Fixed tissues were washed 3 times (10 min per wash) in 1x PBS and embedded in 8% Low Melting Agarose (Invitrogen)¹⁷. Sections were obtained using a VT1000S vibratome (Leica). For imaging of leaf primordia and hypocotyls, 100 µm sections were acquired while, for shoot apices, the thickness was set to 50 µm. Tissue sections were stained with 0.01% Fluorescent Brightener 28 (FB) in 1x PBS (Sigma-Aldrich) for 20 min, then washed three times (10 min per wash) in 1x PBS. Imaging of tissue sections was performed using an inverted laser-scanning confocal microscope (Zeiss LSM 780). Excitation for FB, GFP and Chlorophyll was at 405, 488, and 633 nm, respectively, using 2% laser power. Image acquisition was at 410–475 nm, 491–597 nm, and 638–721 nm, respectively. For root imaging, 7-day-old roots were incubated in 10 µg/mL Propidium Iodide (PI) (Sigma-Aldrich) in water for 20 min at room temperature, and washed three times in water before imaging. Excitation of PI was at 561 nm and images were collected at 566–719 nm. Root imaging was performed using a Leica (SP8) laser-scanning confocal microscope.

For quantification of nuclear-localised GFP signal, 28.5 µm z-stacks were imaged in 0.45 µm intervals with an effective pixel dwell time of 1 µs at 1044 × 1044-pixel frame resolution. All images were collected using a bit depth of 16 bits. Nuclear-localised GFP signal in the endodermal layer of root meristems was quantified using the surfaces module of Imapris v. 8.0.2 (Bitplane). The stacks were processed using a 3 µm diameter background subtraction, with a minimum absolute intensity threshold of 75.3, and a seed detection diameter of 2–3 µm in the x-level. Z-stacks were manually processed and mean GFP intensities measured from the first eight endodermal nuclei on either side of the quiescent centre in 8–12 roots per line. GFP intensities were normalised to the mean signal intensity in lateral root cap nuclei. Values (means ± SE) were plotted and statistical significance calculated using Student's *t*-test.

Histology and microscopy. For GUS analyses, seedlings were harvested into ice-cold acetone and prefixed for 20 min at room temperature. Seedlings were washed with 100 mM sodium phosphate (pH 7.0), 10 mM EDTA, 0.1% Triton-X buffer with the indicated concentrations of ferrocyanide and ferricyanide, and allowed to sit on ice for 5 min. The same buffer supplemented with 0.05% X-Gluc was then added and the seedlings vacuum-infiltrated for 30 min at 600 mm Hg. The following concentrations of supplemented ferro/ferricyanide were used: 2 mM for *pATML1:GUS*, *pSUC2:GUS*, *pATHB8:GUS*, and *pWUS:GUS*, 6 mM for *pRbcS:GUS*, *pSCR:GUS*, and *pMIR166A:GUS*, and 10 mM for *pCLV3:GUS*. For GUS staining in roots, 10 mM supplemented ferro/ferricyanide was used for *pSCR:GUS* and *pWOX5:GUS* and 4 mM for *pATHB8:GUS* and *pMIR166A:GUS*. Seedlings were incubated at 37 °C as needed, and subsequently dehydrated to 50% ethanol, fixed in FAA (50% ethanol, 5% formaldehyde, 10% acetic acid), and embedded and sectioned¹³. Clearing of stained roots was performed overnight using 15 M chloral hydrate in 30% glycerol. Imaging of tissue sections and whole-mount GUS-stained seedlings was performed using DIC on a Zeiss Axiophot. Whole-mount fluorescence imaging was performed on a SMZ1500 dissecting microscope (Nikon), equipped with a P-FLA2 epi-fluorescence attachment.

Small RNA in situ hybridisations⁵⁴ were performed on 10-day-old seedlings. Tissue sections from seedlings fixed in 4% PFA in 1x PBS, were treated with 0.125 mg/mL Protease for 30 min at 37 °C prior to hybridisation. Treated sections were hybridised overnight at 50 °C with double-digoxigenin labelled *asmiRGFP* LNA probe (Exiqon) at a concentration of 50 nM. Slides were washed twice in 0.2x SSC for 1 h each at 50 °C. Hybridisation signal was detected by immunohistochemistry using anti-DIG-AP Fab fragments from sheep (Roche) at 0.6 U/mL in 1x TBS with 1% BSA and 0.3% Triton-X-100 at room temperature for 2–4 h and visualised using NBT/BCIP mix (Roche). The *asmiRGFP* probe sequence is listed in Supplementary Table 2.

Small RNA analysis. Total RNA was isolated from 10-day-old seedlings using TRIzol reagent (Invitrogen). For analysis of small RNA levels by northern blotting, 20 µg total RNA was resolved on a 17% polyacrylamide gel containing 7 M urea. Samples were transferred to Hybond N+ membrane (Sigma-Aldrich), crosslinked using a Stratilinker UV crosslinker model 1800 (Stratagene), and hybridised using ³²P end-labelled *asmiRGFP* probe⁵⁵. U6 was used as loading control. Original gel images are provided in the Supplementary Information (Supplementary Fig. 9). For small RNA quantitative reverse transcription PCR (qRT-PCR) analysis, RNA was isolated from a pool of dissected 10-day-old hypocotyls using the ISOLATE II Plant

miRNA Kit (Bioline) and 350 ng used for cDNA synthesis using the iScript™ cDNA Synthesis Kit. qRT-PCR was performed using multiplex primers for *miRGFP* and U6. Small RNA levels normalised to U6 were calculated based on three technical and three biological replicates using the $\Delta\Delta CT$ method and significance was tested using the two-sided Student's *t*-test.

Small RNA libraries were constructed from 10-day-old seedlings, or when indicated from separate shoot and root samples, using the TruSeq Small RNA sample preparation kit (Illumina). Libraries were quantified with the KAPA Illumina Library Quantification Kit (Kapabiosystems), and sequenced on the Illumina HiSeq 2000 platform. Reads were trimmed using the FASTX-Toolkit (http://hannonlab.cshl.edu/fastx_toolkit/), and trimmed reads 19- to 25-nt in length aligned to the *Arabidopsis* reference genome (TAIR10) with GFP and GUS target sequences added using the Burrows-Wheeler Aligner⁵⁶. For analysis of *miRGFP* levels, a single mismatch was allowed in the alignments to accommodate for the mismatch at position 20 of *miRGFP* relative to GFP. Similarly, for *miRGUS*, three mismatches were allowed in the alignments. Reads matching known structural RNAs (rRNAs, tRNAs, sn-RNAs, and sno-RNAs) from Rfam 10.0 were removed from further analysis. For comparison of small RNA levels across samples, read counts were normalised per million mapped reads (reads per million) using SAM Tools⁵⁶.

Data availability. All high-throughput sequencing data, both raw and processed files, are available through NCBI's Gene Expression Omnibus under accession number [GSE102236](https://www.ncbi.nlm.nih.gov/geo/query/acc.cgi?acc=GSE102236). The authors declare that all other data supporting the findings of this study are available within the manuscript and its supplementary files or are available from the corresponding author upon request.

Received: 20 March 2018 Accepted: 13 July 2018

Published online: 06 August 2018

References

- Vatén, A. et al. Callose biosynthesis regulates symplastic trafficking during root development. *Dev. Cell* **21**, 1144–1155 (2011).
- Buhtz, A., Springer, F., Chappell, L., Baulcombe, D. C. & Kehr, J. Identification and characterization of small RNAs from the phloem of *Brassica napus*. *Plant J.* **53**, 739–749 (2008).
- Lin, S. I. et al. Regulatory network of microRNA399 and PHO2 by systemic signaling. *Plant Physiol.* **147**, 732–746 (2008).
- Ruiz-Ferrer, V. & Voinnet, O. Roles of plant small RNAs in biotic stress responses. *Annu. Rev. Plant Biol.* **60**, 485–510 (2009).
- Molnar, A. et al. Small silencing RNAs in plants are mobile and direct epigenetic modification in recipient cells. *Science* **328**, 872–875 (2010).
- Zhang, W. et al. Graft-transmissible movement of inverted-repeat-induced siRNA signals into flowers. *Plant J.* **80**, 106–121 (2014).
- Lewsey, M. G. et al. Mobile small RNAs regulate genome-wide DNA methylation. *Proc. Natl Acad. Sci. USA* **113**, 801–810 (2016).
- Brosnan, C. A. & Voinnet, O. Cell-to-cell and long-distance siRNA movement in plants: mechanisms and biological implications. *Curr. Opin. Plant Biol.* **14**, 580–587 (2011).
- Melnyk, C. W., Molnar, A. & Baulcombe, D. C. Intercellular and systemic movement of RNA silencing signals. *EMBO J.* **30**, 3553–3563 (2011).
- Borges, F. & Martienssen, R. A. The expanding world of small RNAs in plants. *Nat. Rev. Mol. Cell Biol.* **16**, 727–741 (2015).
- Yoo, B. -C. et al. A systemic small RNA signaling system in plants. *Plant Cell* **16**, 1979–2000 (2004).
- Pant, B. D., Buhtz, A., Kehr, J. & Scheible, W. R. MicroRNA399 is a long-distance signal for the regulation of plant phosphate homeostasis. *Plant J.* **53**, 731–738 (2008).
- Chitwood, D. H. et al. Pattern formation via small RNA mobility. *Genes Dev.* **23**, 549–554 (2009).
- Carlsbecker, A. et al. Cell signalling by microRNA165/6 directs gene dose-dependent root cell fate. *Nature* **465**, 316–321 (2010).
- Miyashima, S., Koi, S., Hashimoto, T. & Nakajima, K. Non-cell-autonomous microRNA165 acts in a dose-dependent manner to regulate multiple differentiation status in the *Arabidopsis* root. *Development* **138**, 2303–2313 (2011).
- Knauer, S. et al. A protodermal miR394 signal defines a region of stem cell competence in the *Arabidopsis* shoot meristem. *Dev. Cell* **24**, 125–132 (2013).
- Skopelitis, D. S., Benkovics, A. H., Husbands, A. Y. & Timmermans, M. C. P. Boundary formation through a direct threshold-based readout of mobile small RNA gradients. *Dev. Cell* **43**, 265–273 (2017).
- Juarez, M. T., Kui, J. S., Thomas, J., Heller, B. A. & Timmermans, M. C. P. microRNA-mediated repression of *rolled leaf1* specifies maize leaf polarity. *Nature* **428**, 84–88 (2004).

19. Schmiedel, J. M. et al. MicroRNA control of protein expression noise. *Science* **348**, 128–132 (2015).
20. Plavskin, Y. et al. Ancient trans-acting siRNAs confer robustness and sensitivity onto the auxin response. *Dev. Cell* **36**, 276–289 (2016).
21. Chitwood, D. H. & Timmermans, M. C. Small RNAs are on the move. *Nature* **467**, 415–419 (2010).
22. Liang, D., White, R. G. & Waterhouse, P. M. Gene silencing in Arabidopsis spreads from the root to the shoot, through a gating barrier, by template-dependent, nonvascular, cell-to-cell movement. *Plant Physiol.* **159**, 984–1000 (2012).
23. Taochy, C. et al. A genetic screen for impaired systemic RNAi highlights the crucial role of DICER-LIKE 2. *Plant Physiol.* **175**, 1424–1437 (2017).
24. Burch-Smith, T. M. & Zambryski, P. C. Plasmodesmata paradigm shift: regulation from without versus within. *Annu. Rev. Plant Biol.* **63**, 239–260 (2012).
25. Tilsner, J., Nicolas, W., Rosado, A. & Bayer, E. M. Staying tight: Plasmodesmal membrane contact sites and the control of cell-to-cell connectivity in plants. *Annu. Rev. Plant Biol.* **67**, 337–364 (2016).
26. Melnyk, C. W., Molnar, A., Bassett, A. & Baulcombe, D. C. Mobile 24 nt small RNAs direct transcriptional gene silencing in the root meristems of *Arabidopsis thaliana*. *Curr. Biol.* **21**, 1678–1683 (2011).
27. Manavella, P. A., Koenig, D. & Weigel, D. Plant secondary siRNA production determined by microRNA-duplex structure. *Proc. Natl Acad. Sci. USA* **109**, 2461–2466 (2012).
28. Schwach, F., Vaistij, F. E., Jones, L. & Baulcombe, D. C. An RNA-dependent RNA polymerase prevents meristem invasion by Potato Virus X and is required for the activity but not the production of a systemic silencing signal. *Plant Physiol.* **138**, 1842–1852 (2005).
29. Kitagawa, M. & Jackson, D. Plasmodesmata-mediated cell-to-cell communication in the shoot apical meristem: How stem cells talk. *Plants* **6**, 12–26 (2017).
30. Fouracre, J. P. & Poethig, R. S. The role of small RNAs in vegetative shoot development. *Curr. Opin. Plant Biol.* **29**, 64–72 (2016).
31. Husbands, A. Y., Benkovics, A. H., Nogueira, F. T., Lodha, M. & Timmermans, M. C. P. The ASYMMETRIC LEAVES complex employs multiple modes of regulation to affect adaxial-abaxial patterning and leaf complexity. *Plant Cell* **27**, 3321–3335 (2015).
32. Rinne, P. L. & van der Schoot, C. Symplasmic fields in the tunica of the shoot apical meristem coordinate morphogenetic events. *Development* **125**, 1477–1485 (1998).
33. Gisel, A., Barella, S., Hempel, F. D. & Zambryski, P. C. Temporal and spatial regulation of symplastic trafficking during development in *Arabidopsis thaliana* apices. *Development* **126**, 1879–1889 (1999).
34. Yadav, R. K. et al. WUSCHEL protein movement mediates stem cell homeostasis in the *Arabidopsis* shoot apex. *Genes Dev.* **25**, 2025–2030 (2011).
35. Daum, G., Medzihradsky, A., Suzuki, T. & Lohmann, J. U. A mechanistic framework for noncell autonomous stem cell induction in *Arabidopsis*. *Proc. Natl Acad. Sci. USA* **111**, 14619–14624 (2014).
36. Sparks, E., Wachsman, G. & Benfey, P. N. Spatiotemporal signalling in plant development. *Nat. Rev. Genet.* **14**, 631–644 (2013).
37. Zhu, T., Lucas, W. J. & Rost, T. L. Directional cell-to-cell communication in the *Arabidopsis* root apical meristem I. An ultrastructural and functional analysis. *Protoplasma* **203**, 35–47 (1998).
38. Zhu, T., O'Quinn, R. L., Lucas, W. J. & Rost, T. L. Directional cell-to-cell communication in the *Arabidopsis* root apical meristem II. Dynamics of plasmodesmata formation. *Protoplasma* **204**, 84–93 (1998).
39. Pi, L. et al. Organizer-derived WOX5 signal maintains root columella stem cells through chromatin-mediated repression of CDF4 expression. *Dev. Cell* **33**, 576–588 (2015).
40. Bologna, N. G., Mateos, J. L., Bresso, E. G. & Palatnik, J. F. A loop-to-base processing mechanism underlies the biogenesis of plant microRNAs miR319 and miR159. *EMBO J.* **28**, 3646–3656 (2009).
41. Han, X. & Kim, J. Y. Integrating hormone- and micromolecule-mediated signaling with plasmodesmal communication. *Mol. Plant* **9**, 46–56 (2016).
42. Fernandez-Calvino, L. et al. *Arabidopsis* plasmodesmal proteome. *PLoS ONE* **6**, e18880 (2011).
43. Stahl, Y. & Faulkner, C. Receptor complex mediated regulation of symplastic traffic. *Trends Plant Sci.* **21**, 450–459 (2016).
44. Rosas-Diaz, T. et al. A virus-targeted plant receptor-like kinase promotes cell-to-cell spread of RNAi. *Proc. Natl Acad. Sci. USA* **115**, 1388–1393 (2018).
45. Sena, G., Jung, J. W. & Benfey, P. N. A broad competence to respond to SHORT ROOT revealed by tissue-specific ectopic expression. *Development* **131**, 2817–2826 (2004).
46. Kurata, T. et al. Cell-to-cell movement of the CAPRICE protein in *Arabidopsis* root epidermal cell differentiation. *Development* **132**, 5387–5398 (2005).
47. Wu, S. & Gallagher, K. L. The movement of the non-cell-autonomous transcription factor, SHORT-ROOT relies on the endomembrane system. *Plant J.* **80**, 396–409 (2014).
48. Chen, H. M. et al. 22-Nucleotide RNAs trigger secondary siRNA biogenesis in plants. *Proc. Natl Acad. Sci. USA* **107**, 15269–15274 (2010).
49. Couzigou, J. M. & Combier, J. P. Plant microRNAs: key regulators of root architecture and biotic interactions. *New Phytol.* **212**, 22–35 (2016).
50. Rodriguez, R. E. et al. MicroRNA miR396 regulates the switch between stem cells and transit-amplifying cells in *Arabidopsis* roots. *Plant Cell* **27**, 3354–3366 (2015).
51. Benkovics, A. H. & Timmermans, M. C. Developmental patterning by gradients of mobile small RNAs. *Curr. Opin. Genet. Dev.* **27**, 83–91 (2014).
52. Willis, L. et al. Cell size and growth regulation in the *Arabidopsis thaliana* apical stem cell niche. *Proc. Natl Acad. Sci. USA* **113**, 8238–8246 (2016).
53. Schwab, R., Ossowski, S., Riester, M., Warthmann, N. & Weigel, D. Highly specific gene silencing by artificial microRNAs in *Arabidopsis*. *Plant Cell* **18**, 1121–1133 (2006).
54. Javelle, M. & Timmermans, M. C. In situ localization of small RNAs in plants by using LNA probes. *Nat. Prot.* **7**, 533–541 (2012).
55. Petsch, K. et al. Novel DICER-LIKE1 siRNAs bypass the requirement for DICER-LIKE4 in Maize development. *Plant Cell* **27**, 2163–2177 (2015).
56. Li, H. & Durbin, R. Fast and accurate short read alignment with Burrows-Wheeler transform. *Bioinformatics* **25**, 1754–1760 (2009).

Acknowledgements

We thank members of the Timmermans lab for their insightful feedback, Anna Benkovics for technical assistance, and Tim Mulligan for plant care. Damianos Skopelitis was supported by an HFSP long-term postdoctoral fellowship (LT000257/2009), and Kristine Hill is supported by a Marie Skłodowska-Curie Individual Fellowship (GAP-709293). Work on small RNA regulation and leaf polarity in the Timmermans lab is supported by grants from the National Science Foundation (IOS-1355018), The Deutsche Forschungsgemeinschaft (SFB 1101 project C06), and an Alexander von Humboldt Professorship.

Author contributions

D.S., K.H., S.K., and M.T. designed the project and experiments. D.S., K.H., S.K., C.M., P.B., and D.C. performed the experiments. K.H. and M.T. wrote the manuscript.

Additional information

Supplementary Information accompanies this paper at <https://doi.org/10.1038/s41467-018-05571-0>.

Competing interests: The authors declare no competing interests.

Reprints and permission information is available online at <http://npg.nature.com/reprintsandpermissions/>

Publisher's note: Springer Nature remains neutral with regard to jurisdictional claims in published maps and institutional affiliations.

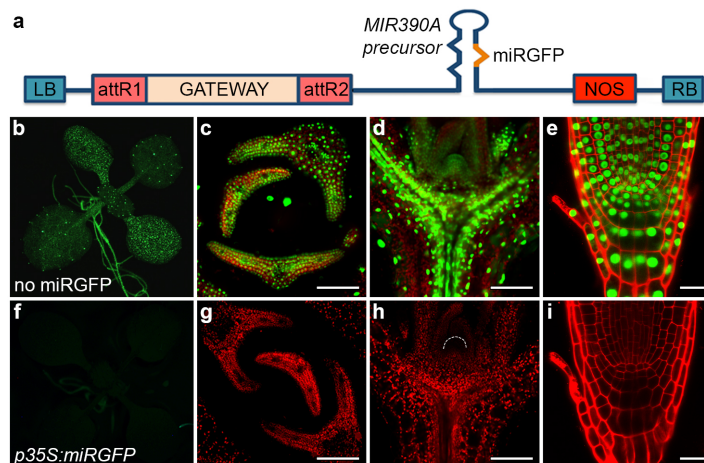


Open Access This article is licensed under a Creative Commons Attribution 4.0 International License, which permits use, sharing, adaptation, distribution and reproduction in any medium or format, as long as you give appropriate credit to the original author(s) and the source, provide a link to the Creative Commons license, and indicate if changes were made. The images or other third party material in this article are included in the article's Creative Commons license, unless indicated otherwise in a credit line to the material. If material is not included in the article's Creative Commons license and your intended use is not permitted by statutory regulation or exceeds the permitted use, you will need to obtain permission directly from the copyright holder. To view a copy of this license, visit <http://creativecommons.org/licenses/by/4.0/>.

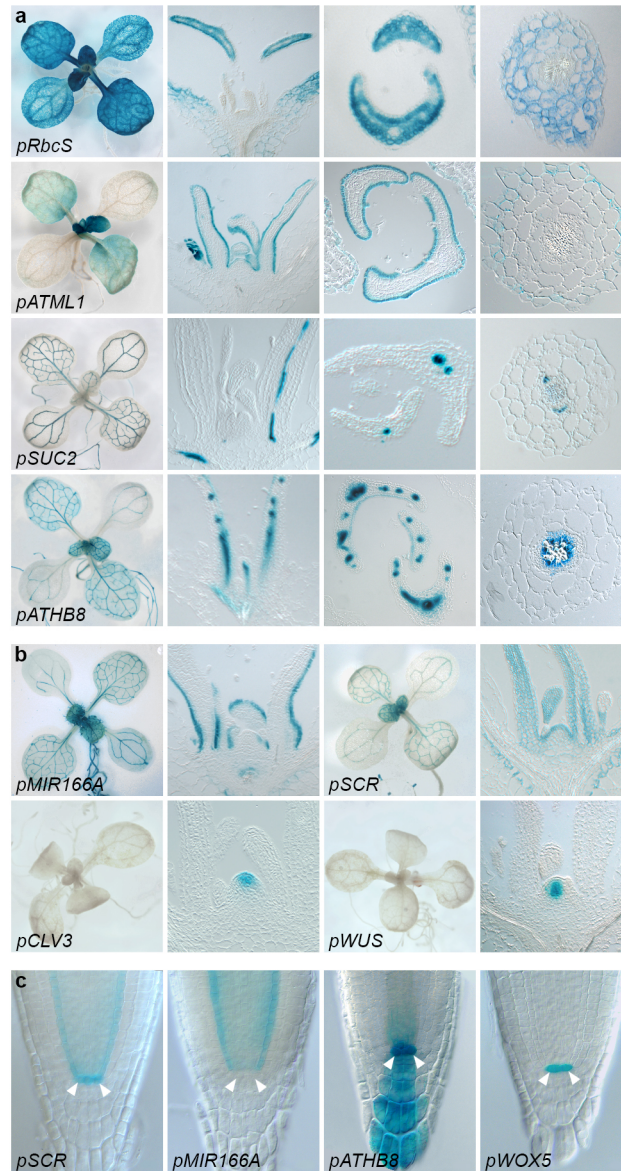
© The Author(s) 2018

**Gating of miRNA Movement at Defined Cell-Cell Interfaces Governs Their
Impact as Positional Signals**

Skopelitis, Hill et al.

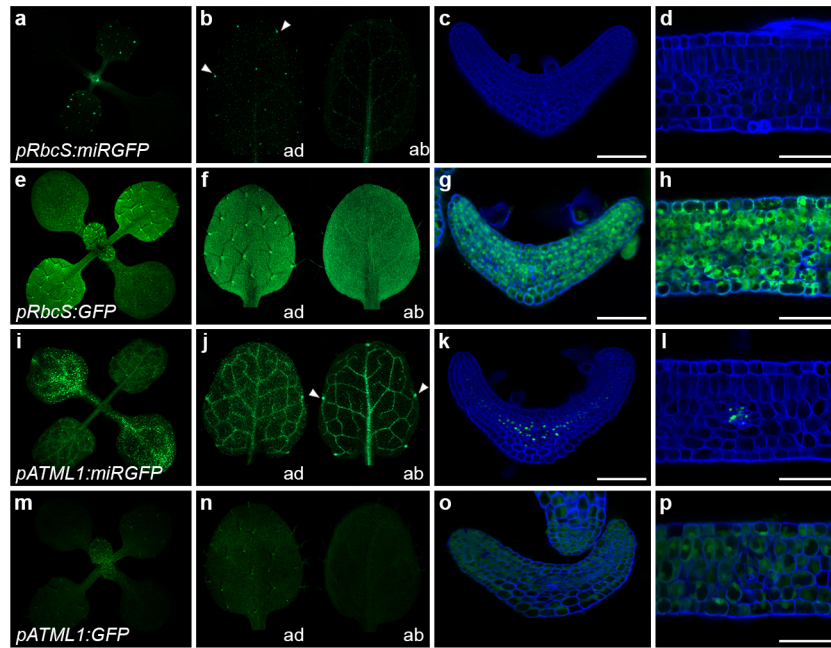


Supplementary Figure 1. miRGFP efficiently silences GFP expression. **(a)** Schematic of the Gateway-based miRGFP precursor construct. **(b-i)** GFP fluorescence in **(b-e)** *p35S:3xNLS-GFP* (no miRGFP) seedlings is completely eliminated in **(f-i)** such seedlings ubiquitously expressing miRGFP (*p35S:miRGFP*). **(b, f)** 10-day old seedlings, **(c-e, g-i)** confocal images of tissue sections from **(c, g)** young leaf primordia, **(d, h)** shoot apices and **(e, i)** root tips. Scale bars, **(c, d, g, h)** 100 μm and **(e, i)** 20 μm .

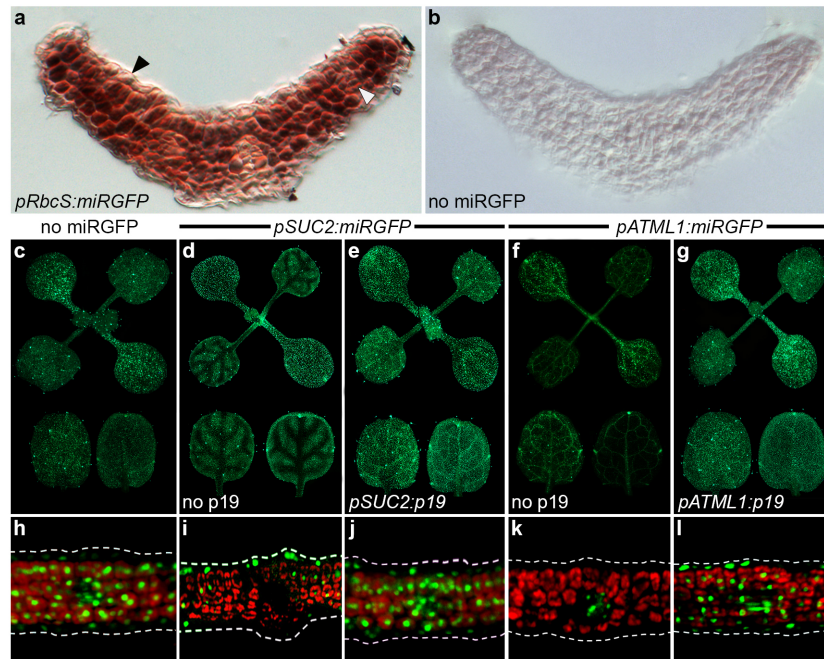


Supplementary Figure 2. All promoter fragments used in this study yield the expected spatiotemporal patterns of expression. **(a)** Transcriptional GUS reporter fusions reveal the established tissue specific patterns of activity (left to right) in 10-day old seedlings, longitudinal apex sections, transverse leaf primordia sections, and transverse hypocotyl sections for the selected *RbcS*, *ATML1*, *SUC2*, and *ATHB8* promoter fragments. GUS reporter activity in *pRbcS*:GUS, *pATML1*:GUS, *pSUC2*:GUS and *pATHB8*:GUS seedlings is limited to the ground tissue, epidermis, phloem companion cells and procambium, respectively. **(b)** Patterns of GUS reporter activity in *pMIR166A*:GUS, *pSCR*:GUS, *pCLV3*:GUS and *pWUS*:GUS 10-day old seedlings (left) and longitudinal apex sections (right) confirms these promoters are active in the SAM in the abaxial epidermis of the incipient leaf, the tunica (L1 and L2), central zone and organizing centre, respectively. **(c)** Whole mount images of the of the root apical meristem of *pSCR*:GUS, *pMIR166A*:GUS, *pATHB8*:GUS and *pWOX5*:GUS seedlings reveal the expected patterns of GUS reporter

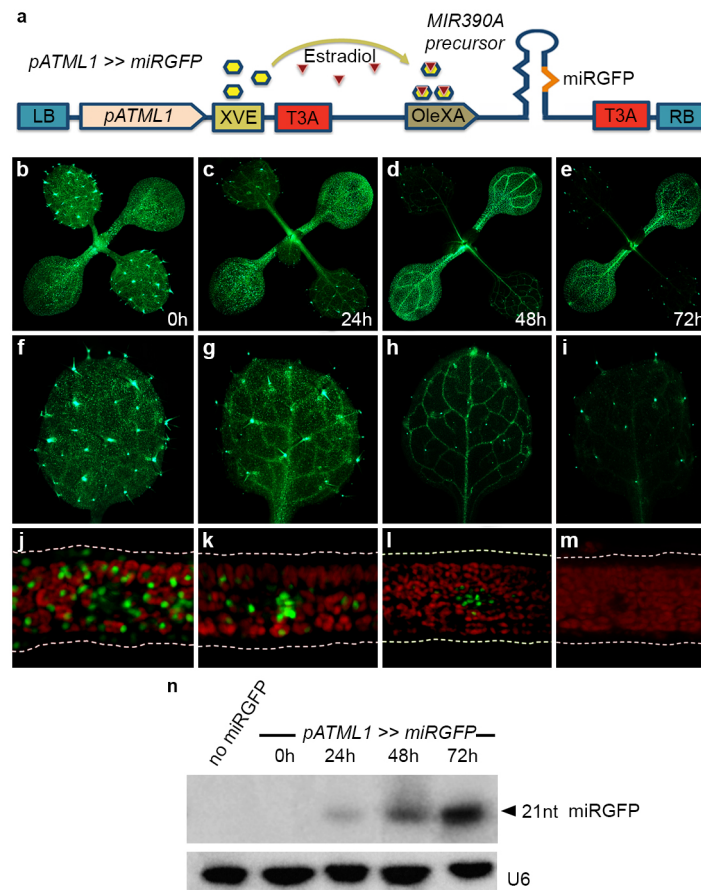
activity in the endodermis and QC (*SCR*), the endodermis (*MIR166A*), the vasculature, QC and columella (*ATHB8*), and the QC (*WOX5*).



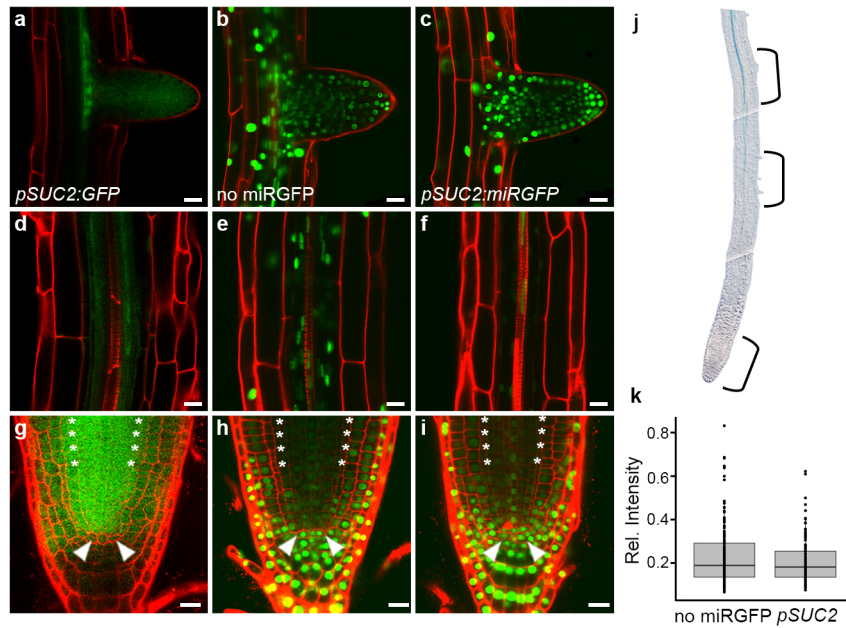
Supplementary Figure 3. miRNA mobility is regulated independently from small protein movement. **(a-h)** Imaging of **(a, e)** whole seedlings, **(b, f)** individual leaves, **(c, g)** sections of leaf primordia and **(d, h)** sections of expanded leaves reveals that miRGFP and free GFP show comparable non-cell autonomous effects when expressed in mesophyll, with **(a-d)** miRGFP-mediated GFP silencing and **(e-h)** free GFP diffusion detectable in both the epidermis and vasculature in *pRbcS:miRGFP* and *pRbcS:GFP* lines, respectively. **(i-p)** Likewise, imaging of **(i, m)** whole seedlings, **(j, n)** individual leaves, **(k, o)** sections of leaf primordia and **(l, p)** sections of expanded leaves shows the non-cell autonomous spread of **(i-l)** miRGFP-directed GFP silencing and **(m-p)** free GFP diffusion from the epidermis in *pATML1:miRGFP* and *pATML1:GFP* lines, respectively. Note, GFP fluorescence persists in the symplastically isolated trichomes and hydathodes (arrow heads), consistent with miRGFP moving through plasmodesmata. Scale bars, 50 μm .



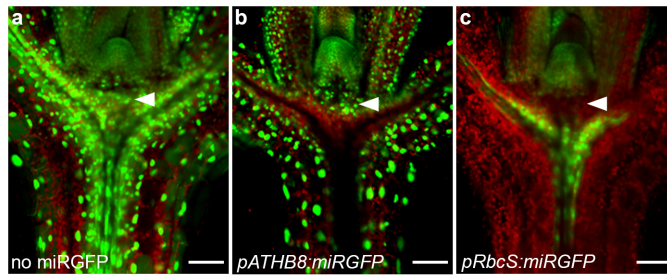
Supplementary Figure 4. miRGP is the mobile silencing signal. **(a, b)** Small RNA *in situ* hybridization shows that **(a)** miRGP produced in the mesophyll accumulates in the epidermis and vasculature (arrowheads) of *pRbcS:miRGP* leaf primordia, and is **(b)** undetected in *p35S:3xNLS-GFP* primordia not expressing miRGP (no miRGP). **(c-i)** Compared to the uniform pattern of GFP fluorescence in **(c, h)** leaves of *p35S:3xNLS-GFP* (no miRGP) seedlings, **(d, i)** *pSUC2:miRGP* lines expressing miRGP in the phloem companion cells show a non-cell autonomous pattern of GFP silencing around major veins that is **(e, j)** suppressed upon co-expression of the viral suppressor protein p19. Likewise, the non-cell autonomous pattern of GFP silencing seen in **(f, k)** *pATML1:miRGP* lines expressing miRGP in the epidermis is **(g, l)** suppressed upon co-expression of p19. **(c-g)** Fluorescence images of whole seedlings (top) and individual leaves (bottom); adaxial side, left; abaxial side, right. **(h-l)** Confocal microscopy images of transverse leaf sections.



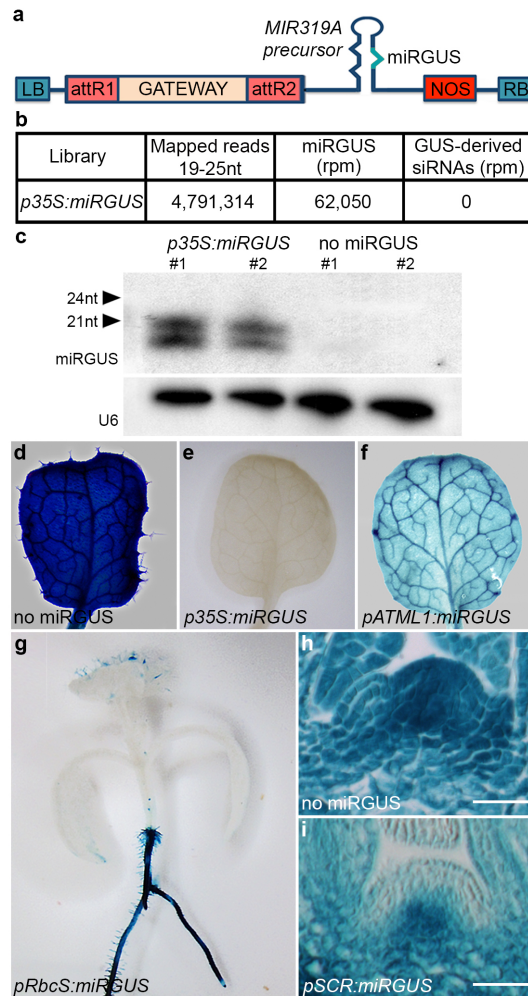
Supplementary Figure 5 The extent of miRGFP-directed GFP silencing correlates with miRNA levels at the source. **(a)** Schematic of the epidermal-specific, estradiol-inducible *pATML1 >> miRGFP* construct. **(b-m)** Imaging of **(b-e)** whole seedlings, **(f-i)** mature leaves, and **(j-m)** transverse leaf sections shows that the miRGFP-directed silencing of GFP extends progressively from the epidermis into the mesophyll and vasculature of *pATML1 >> miRGFP* seedlings upon induction with 20 μ M estradiol for **(b, f, j)** 0, **(c, g, k)** 24, **(d, h, l)** 48, and **(e, i, m)** 72 hours. **(n)** Small RNA gel blot showing a time-dependent increase in miRGFP levels in *pATML1 >> miRGFP* seedlings upon induction with 20 μ M estradiol.



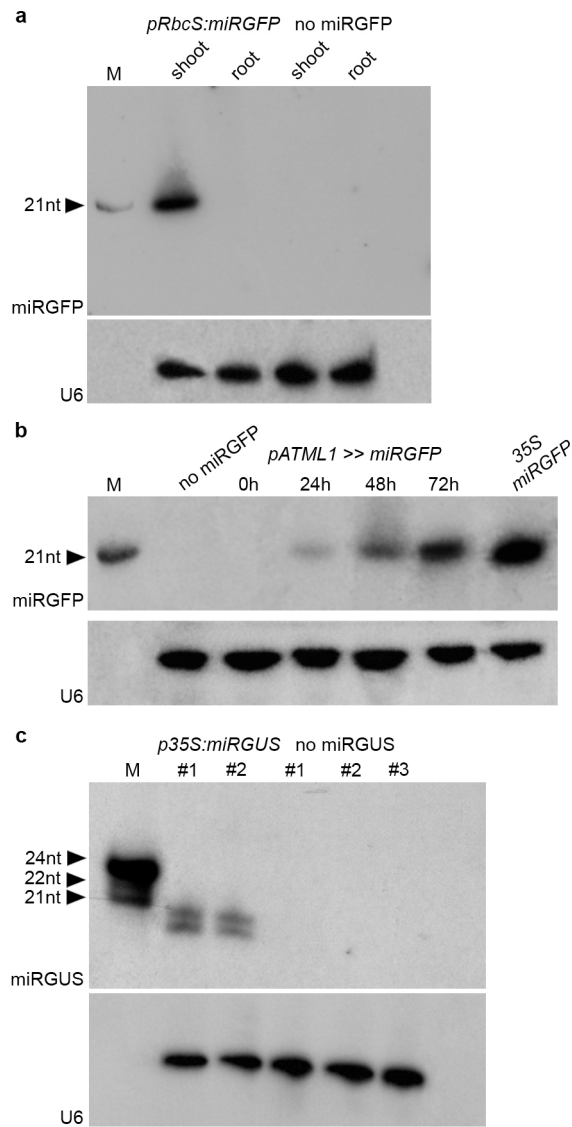
Supplementary Figure 6. miRNA mobility is regulated independently from small protein movement. **(a-i)** Optical confocal sections through **(a-c)** a lateral root meristem, **(d-f)** the root differentiation zone, and **(g-i)** the root apical meristem reveal opposite patterns of mobility for miRGFP and free GFP from phloem companion cells. **(a, d, g)** Free-GFP behaves **(d)** cell autonomously in the differentiation zone of *pSUC2:GFP* lines, but diffuses throughout the **(a)** lateral and **(g)** primary root meristem. Conversely, compared to the **(b, e, h)** ubiquitous pattern of GFP fluorescence in *p35S:3xNLS-GFP* (no miRGFP) roots, **(c, f, i)** *pSUC2:miRGFP* lines show a non-cell autonomous pattern of miRGFP-directed GFP silencing in **(f)** the root differentiation zone, and no silencing in **(c)** lateral or **(i)** primary root meristems. **(j)** GUS reporter activity shows the spatiotemporal pattern of *SUC2* promoter activity in root phloem companion cells. Box areas, regions imaged for the lateral root, differentiation zone, and root apical meristem. **(k)** Quantification of the mean GFP fluorescence intensity in endodermal cells ($n \geq 125$) normalised to fluorescence intensity in cells of the lateral root cap reveals this to not deviate significantly ($p > 0.05$, two-sided Student's t test) in *p35S:3xNLS-GFP* (no miRGFP) versus *pSUC2:miRGFP* root meristems. Horizontal line, median; boxes, 1st and 3rd quartiles. Note, the same no miRGFP data is shown here and in Fig. 3c, as the *pSUC2:miRGFP* and *pRbcS:miRGFP* lines were analysed concurrently. Scale bars, 20 μm .



Supplementary Figure 7. miRNA mobility into the shoot stem cell niche is restricted. **(a-c)** Longitudinal sections through the shoot apex of **(a)** a *p35S:3xNLS-GFP* (no miRGFP) seedling and seedlings expressing miRGFP in **(b)** the procambium (*pATHB8:miRGFP*) and **(c)** the mesophyll (*pRbcS:miRGFP*) reveal a lack of miRGFP-directed GFP silencing in the shoot meristem of these lines. White arrowhead, pith region below the shoot apical meristem. Scale bars, 50 μ m.



Supplementary Figure 8. miRGUS recapitulates the patterns of regulated miRGFP mobility. **(a)** Schematic of the Gateway-based miRGUS precursor construct. **(b)** Read counts for miRGUS and *GUS*-derived secondary siRNAs in reads per million (rpm) normalised to the total number of mapped 19-25 nt small RNA reads in libraries constructed from *p35S:miRGUS* seedlings. The absence of *GUS*-derived secondary siRNAs confirms the lack of transitivity in these lines. **(c)** Small RNA gel blot shows the miRGUS precursor in *p35S:miRGUS* lines generates both 20- and 21-nt miRNA species. U6 hybridization confirms near even loading of RNA samples. **(d, e)** GUS activity in **(d)** *p35S:GUS* (no miRGUS) seedlings is completely silenced in **(e)** lines ubiquitously expressing miRGUS (*p35S:miRGUS*). **(f)** A non-cell autonomous pattern of GUS silencing is detected in *pATML1:GUS* lines expressing miRGUS in the leaf epidermis. **(g)** miRGUS-directed GUS silencing in *pRbcS:miRGUS* seedlings is apparent in the hypocotyl and leaves but not in the root. **(h, i)** Longitudinal sections show GUS activity is detectable throughout **(h)** the *p35S:GUS* shoot apical meristem (no miRGUS), whereas a non-cell autonomous pattern of GUS silencing extends into the third meristem layer in **(i)** *pSCR:miRGUS* apices expressing miRGUS in the meristem tunica.



Supplementary Figure 9. Original small RNA northern blots. **(a)** Original images for the small RNA northern blots shown in Fig. 3d. **(b)** Original images for the small RNA northern blots shown in Supplementary Fig. 5n. **(c)** Original images for the small RNA northern blots shown in Supplementary Fig. 8b.

Supplementary Table 1. miRGFP read counts in libraries constructed from *pRbcS:miRGFP*, *pCLV3:miRGFP*, and *pSUC2:miRGFP* seedlings.

Library	Mapped reads 19-25 nt	miRGFP (rpm)	GFP-derived siRNAs (rpm)
<i>pRbcS:miRGFP</i>	14,985,989	42,250	0
<i>pCLV3:miRGFP</i>	27,294,977	14,808	0
<i>pSUC2:miRGFP</i>	15,817,134	30,117	0

Supplementary Table 2. Artificial small RNA and *in situ* LNA probe sequences

Artificial Small RNA	Sequence
miRGFP	TTGAAGTTCACCTTGATGCGG
miRGUS	TAATGAGTGACCGCATCGACC

Artificial Small RNA Precursor	Sequence*
<i>MIR390A</i> -based miRGFP precursor	GTAGAGAAGAATCTGTATGTAT TTGAAGTTCACCTT GATGCGG ATGATGATCACATTCGTTATCTATTTTT TCCGCATCAAGATGAACTTCAACATTGGCTCTTCT TACTAC
<i>MIR319A</i> -based miRGUS precursor	AGGGCCGATGCGGTCTCTCATTTCACAGGTCGT GATATGATTCAATTAGCTTCCGACTCATTATCCA AATACCGAGTCGCCAAAATTCAAAGTAGACTCGTT AAATGAATGAATGATGCGGTAGACAAATTGGATC ATTGATTCTCTTTGAT TAATGAGTGACCGCATCGA CCCT

LNA Probe	Sequence
asmiRGFP	CCGCATCAAGGTGAACTTCAA

* Mutated nucleotides are italicised and the mature miRNA is marked in bold

Supplementary Table 3. Cloning and qRT-PCR primers

Primers	Sequence
p2X35S-F	GGTACCGGTCTCAGAAGACCAGAGGGCTATTG
p2X35S-R	GAATTCGGTCCTCTCCAAATGAAATGAACTTCCTTATATAGAG G
pATML1-F	GAACTTACGTAGTTTACATGCATCTCATCCC
pATML1-R	AAACTCTATAGAACAGATCTCTTTTTTTTTTTGAAG
pRbcS-F	TTTACCCTAACTACTCCTTTCTCAGTTGG
pRbcS-R	TATATAGTGGGAACCGCTAGAGGCAACTAGCCC
pMIR166A-F	TCGAGAATTACTATATCATAC
pMIR166A-R	TAGGGTTTCTGAATATATATC
pSUC2-F	AGTCATTATCAACTAGGGGTG
pSUC2-R	AAAGAAATTTCTTTGAGAGGG
pATHB8-F	AGTGTGCCTTATCACAGGGG
pATHB8-R	CTCTCTATTTAATTTTGTTC
pSCR-F	GTAGGTACCACCACCACCGTCAACAATTTTGAATCC
pSCR-R	AGCTCGAGGGGGTTGGTCGTGAGATTGCATGG
pWUS-F	GTACTIONTAGGAGTTTATAAATCAAAGGG
pWUS-R	TGTGTTTGATTTCGACTTTTGTTCACAAAG
pCLV3-F	CGCGGTTTGTGTAATGGTATTATTATC
pCLV3-R	CTACATGAACATAACACATGAATATTGAG
pWOX5-F	AGAACCTCGGGGATGAAGAC
pWOX5-R	AAACAGTTGAGGACTTTACATCTGAAC
P19-HA-F	AAACTAGTATGGAACGAGCTATACAAGG
P19-HA-R	AAGCGGCCGCGGTGATTTGCGGACTCTAGATTAAGCGTAGTC TGGG
pFK390-miRGFP-F	TTATAGGGGGGAAAAAAGGTAG
pFK390-miRGFP-R	GAGACTAAAGATGAGATCTAATC
WOX5:GFP Gibson-1	GTCTTCATCCCCGAGGTTCTGCGGCCGCCTGCAGGTGAC
WOX5:GFP Gibson-2	GCATGGTAGAACTATACAAATGATATCCCGCGGCCATGCTAG AGT
WOX5:GFP Gibson-3	AGCATGGCCGCGGGATATCATTGTATAGTTCTACCATGCCA
WOX5:GFP Gibson-4	GTCGACCTGCAGGCGGCCGCAGAACCTCGGGGATGAAGAC
miRGFP stemloop	GTCGTATCCAGTGCAGGGTCCGAGGTATTCGCACTGGATACG ACCGGCAT
miRGFP-F qRT-PCR	CCGCGTGGCTTGAAGTTCACCTTG
miRGFP-R qRT-PCR	CCAGTGCAGGGTCCGAGGTA
U6 stemloop	GTGCAGGGTCCGAGGTTTTGGACCATTTCTCGAT
U6-F	GGAACGATACAGAGAGAAGATTAGCA
U6-R	GTGCAGGGTCCGAGGT

Appendix III

Table of candidate genes

	ID	Name	Homologues	Known function/GO-term	Progress
single mutants	AT1G49340	ATPI4K ALPHA	none	1-phosphatidylinositol 4-kinase activity	mutant obtained
	AT1G79280	NUCLEAR PORE ANCHOR	none	Sumoylation and mRNA export	mutant obtained
	AT2G17930	TRA1A	none	Component of the SPT module of the SAGA complex.	mutant obtained
	AT2G37050	unknown	none	Kinase activity	mutant obtained
	AT3G24660	TRANSMEMBRANE KINASE-LIKE 1	none	ATP binding, kinase activity	mutant obtained
	AT3G51740	INFLORESCENCE MERISTEM RECEPTOR-LIKE KINASE 2	none	Protein kinase activity, ATP binding	mutant obtained
	AT5G30510	PLASTID RIBOSOMAL PROTEIN S1	none	RNA binding	mutant obtained
	AT1G35720	ANNEXIN 1	none	Peroxidase activity	mutant obtained
	AT4G09320	NUCLEOSIDE DIPHOSPHATE KINASE 1	none	Kinase activity	mutant obtained
double mutants	AT1G27170	unknown	AT1G27180	Transmembrane receptors / ATP binding protein	screening T1 mutant seed
	AT1G52540	unknown	AT3G15890	Protein kinase superfamily protein	screening T1 mutant seed
	AT1G70520	ALTERED SEED GERMINATION 6	AT5G40380	Regulating microbe-associated molecular pattern-triggered ROS production.	screening T1 mutant seed
	AT1G73080	PEP1 RECEPTOR 1	AT1G17750	Receptor for AtPep1 to amplify innate immunity	screening T1 mutant seed
	AT2G16250	unknown	AT4G39270	Leucine-rich repeat protein kinase family protein	screening T1 mutant seed
	AT4G08850	MDIS1-INTERACTING RECEPTOR LIKE KINASE2	AT1G35710	Forms a complex with MDIS1/MIK2 and binds LURE1.	screening T1 mutant seed
	AT3G20820	unknown	AT5G12940	Leucine-rich repeat (LRR) family protein	screening T1 mutant seed
	AT3G09820	ADENOSINE KINASE 1	AT5G03300	Involved in the salvage synthesis of adenylates and methyl recycling.	screening T1 mutant seed
	AT5G07350	ARABIDOPSIS THALIANA TUDOR-SN PROTEIN 1	AT5G61780	RNA binding protein with nuclease activity essential for stress response. Involved in mechanisms acting on mRNAs entering the secretory pathway. Functionally redundant with TSN2.	screening T1 mutant seed
triple mutants	AT1G06700	unknown	At2g43230; AT2G30740	Protein kinase superfamily protein	T1 mutant seed obtained
	AT1G11130	SCRAMBLED, STRUBBELIG	AT2G20850; AT4G03390	Expressed in developing root, kinase activity is not essential for its function in vivo.	T1 mutant seed obtained
	AT1G48480	RECEPTOR-LIKE KINASE 1	AT3G17840; AT5G16590	Arabidopsis thaliana receptor-like protein kinase (RLK1) gene	T1 mutant seed obtained
	AT1G63500	BRASSINOSTEROID-SIGNALING KINASE 7	AT5G41260; AT5G59010	Kinase with tetratricopeptide repeat domain-containing protein	T1 mutant seed obtained
	AT2G20850	STRUBBELIG-RECEPTOR FAMILY 1	AT4G03390; AT1G11130	Kinase activity	T1 mutant seed obtained
	AT2G30740	unknown	At2g30730; AT1G06700	Protein kinase superfamily protein	T1 mutant seed obtained
	AT3G02880	KINASE 7	AT5G16590; AT3G17840	Leucine-rich repeat protein kinase family protein	T1 mutant seed obtained
	AT3G08680	unknown	AT5G58300; AT4G23740	Leucine-rich repeat protein kinase family protein	T1 mutant seed obtained
	AT3G14840	LYSM RLK1-INTERACTING KINASE 1	AT1G07650; AT1G53430	Regulation of plant innate immunity to microbes. LIK1 is phosphorylated by CERK1, a kinase involved in chitin perception. The mRNA is cell-to-cell mobile.	T1 mutant seed obtained
	AT3G23750	BAK1-ASSOCIATING RECEPTOR-LIKE KINASE 1	AT2G01820; AT1G66150	Leucine-rich repeat protein kinase family protein	T1 mutant seed obtained
	AT3G24550	PROLINE-RICH EXTENSIN-LIKE RECEPTOR KINASE 1	AT4G32710; AT2G18470	Proline-rich extensin-like receptor kinase (PERK) family	T1 mutant seed obtained
	AT3G46290	HERCULES RECEPTOR KINASE 1	AT5G59700; AT2G39360	Receptor kinase regulated by Brassinosteroids and required for cell elongation during vegetative growth.	T1 mutant seed obtained
	AT3G51550	FERONIA	AT5G28680; AT5G61350	Mediates male-female gametophyte interactions during pollen tube reception. Involved in powdery mildew infection.	T1 mutant seed obtained
	AT3G57530	CALCIUM-DEPENDENT PROTEIN KINASE 32, CPK32	AT2G41860; AT5G12480	Calcium-dependent Protein Kinase. ABA signaling component that regulates the ABA-responsive gene expression via ABF4	T1 mutant seed obtained
	AT3G59110	unknown	AT2G42960; AT1G56720	Protein kinase superfamily protein	T1 mutant seed obtained
	AT4G00710	BRASSINOSTEROID-SIGNALING KINASE 3, BSK3	AT1G01740; AT3G54030	Mediates signal transduction from receptor kinase BRI1 by functioning as the substrate of BRI1.	T1 mutant seed obtained

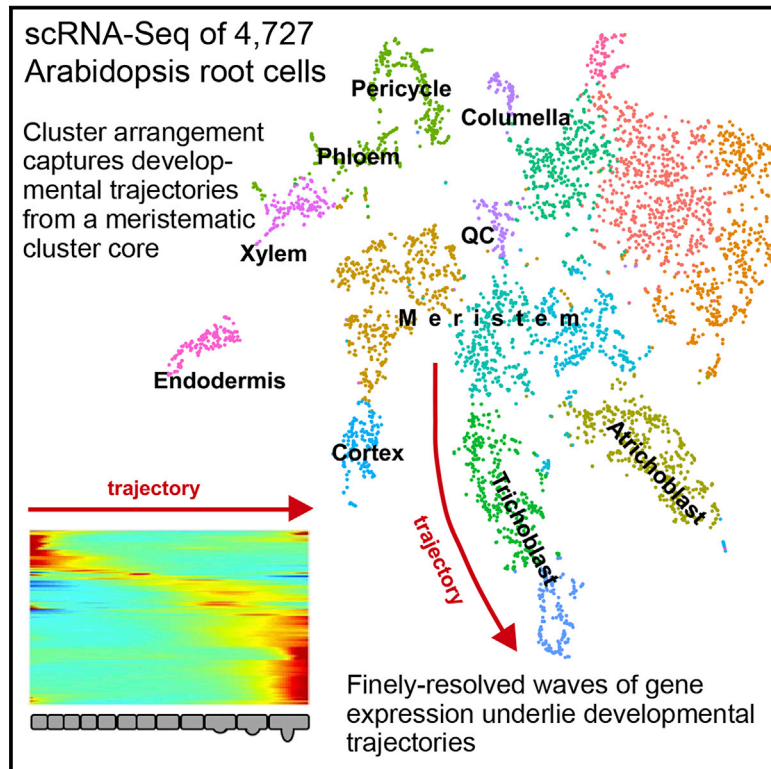
	AT4G02630	unknown	AT4G34500; AT1G01540	Protein kinase superfamily protein	T1 mutant seed obtained
	AT4G04710	CALCIUM-DEPENDENT PROTEIN KINASE 22, CPK22	AT4G04695; AT4G04700	Member of Calcium Dependent Protein Kinase family	T1 mutant seed obtained
	AT4G04720	CALCIUM-DEPENDENT PROTEIN KINASE 21, CPK21	AT4G04740; AT1G76040	Member of Calcium Dependent Protein Kinase family	T1 mutant seed obtained
	AT4G11010	NUCLEOSIDE DIPHOSPHATE KINASE 3, NDPK3	AT4G23895; AT4G23900	Nucleoside diphosphate kinase 3 (ndpk3), located to the inter-membrane space in mitochondria.	T1 mutant seed obtained
	AT4G21380	ARK3, RECEPTOR KINASE 3, RK3	AT4G21230; AT1G65790	Putative receptor-like serine/threonine protein kinase	T1 mutant seed obtained
	AT4G27300	unknown	AT4G27290; AT4G03230	S-locus lectin protein kinase family protein	T1 mutant seed obtained
	AT4G35230	BRASSINOSTEROID-SIGNALING KINASE 1, BSK1	AT1G50990; AT5G46570	Mediates signal transduction from receptor kinase BRI1 by functioning as the substrate of BRI1.	T1 mutant seed obtained
	AT5G01820	CBL-INTERACTING PROTEIN KINASE 14, CIPK14	AT2G30360; AT4G18700	Encodes a CBL-interacting serine/threonine protein kinase.	T1 mutant seed obtained
	AT5G16590	LEUCINE RICH REPEAT PROTEIN 1	AT3G02880; AT3G17840	Leucine-rich repeat protein kinase family protein	T1 mutant seed obtained
	AT5G24010	unknown	AT5G54380; AT1G30570	Protein kinase superfamily protein	T1 mutant seed obtained
triple mutants	AT5G35980	YAK1, YEAST YAK1-RELATED GENE 1	AT2G40120; AT3G17750	Protein kinase which phosphorylates substrate proteins on Ser/Thr and Tyr residues. Some substrates include annexin family proteins. YAK1 mutations suppress TOR deficiency in Arabidopsis and consequences of Ist8 mutations.	T1 mutant seed obtained
	AT5G48380	BAK1-INTERACTING RECEPTOR-LIKE KINASE 1, BIR1	AT3G28450; AT1G27190	Negatively regulates multiple plant resistance signaling pathways.	T1 mutant seed obtained
	AT5G56460	PBL16, PBS1-LIKE16	AT5G01020; AT2G07180	Protein kinase superfamily protein	T1 mutant seed obtained
	AT5G60320	L-TYPE LECTIN RECEPTOR KINASE I.11, LECRK-I.11	AT3G45420; AT3G45440	Concanavalin A-like lectin protein kinase family protein	T1 mutant seed obtained
	AT4G33430	BAK1, BRI1-ASSOCIATED RECEPTOR KINASE	AT1G71830; AT1G34210	Component of BR signaling that interacts with BRI1 in vitro and in vivo to form a heterodimer. Brassinolide-dependent association of BRI1 and BAK1 in vivo.	T1 mutant seed obtained
	AT2G39660	BIK1, BOTRYTIS-INDUCED KINASE1	AT3G55450; AT5G02290	Crucial component of host response signaling required to activate the resistance responses to Botrytis and A. brassicicola infection.	T1 mutant seed obtained
	AT1G22300	14-3-3 PROTEIN G-BOX FACTOR14 EPSILON	AT1G34760; AT1G78220	Interacts with the BZR1 transcription factor involved in brassinosteroid signaling. Might act as a stabilization factor to mediate the oligomerization of REM on the plasma membrane.	T1 mutant seed obtained
	AT1G79550	PGK3, PHOSPHOGLYCERATE KINASE 3	AT3G12780; AT1G56190	Encodes cytosolic phosphoglycerate kinase (PGK3).	T1 mutant seed obtained
	AT3G12780	PGK1, PGKP1, PHOSPHOGLYCERATE KINASE 1	AT1G56190; AT1G79550	Encodes a chloroplast phosphoglycerate kinase.	T1 mutant seed obtained
	AT5G63710	APEX	AT5G10290; AT5G65240	Leucine-rich repeat protein kinase family protein	T1 mutant seed obtained
	AT5G38480	GENERAL REGULATORY FACTOR 3, GRF3	AT5G16050; AT3G02520	General regulatory factor, a 14-3-3 gene	T1 mutant seed obtained

Appendix IV

Developmental Cell

Spatiotemporal Developmental Trajectories in the *Arabidopsis* Root Revealed Using High-Throughput Single-Cell RNA Sequencing

Graphical Abstract



Authors

Tom Denyer, Xiaoli Ma, Simon Klesen, Emanuele Scacchi, Kay Nieselt, Marja C.P. Timmermans

Correspondence

marja.timmermans@zmbp.uni-tuebingen.de

In Brief

Denyer and Ma et al. generate a single-cell RNA expression atlas of the *Arabidopsis* root that captures spatiotemporal information for all major cell types and uncovers new regulators. Pseudotime-analysis-derived developmental trajectories depict a cascade of developmental progressions between stem cell and final differentiation mirrored by waves of transcription factor expression.

Highlights

- scRNA-seq of *Arabidopsis* root cells captures precise spatiotemporal information
- Defining expression features for cell types identify new developmental regulators
- Cluster arrangement reflects developmental time with a centrally localized niche
- Intricate waves of gene expression finely resolve developmental trajectories



Spatiotemporal Developmental Trajectories in the *Arabidopsis* Root Revealed Using High-Throughput Single-Cell RNA Sequencing

Tom Denyer,^{1,3} Xiaoli Ma,^{1,3} Simon Klesen,¹ Emanuele Scacchi,¹ Kay Nieselt,² and Marja C.P. Timmermans^{1,4,*}

¹Center for Plant Molecular Biology, University of Tübingen, Auf der Morgenstelle 32, Tübingen 72076, Germany

²Center for Bioinformatics, University of Tübingen, Sand 14, Tübingen 72076, Germany

³These authors contributed equally

⁴Lead Contact

*Correspondence: marja.timmermans@zmbp.uni-tuebingen.de

<https://doi.org/10.1016/j.devcel.2019.02.022>

SUMMARY

High-throughput single-cell RNA sequencing (scRNA-seq) is becoming a cornerstone of developmental research, providing unprecedented power in understanding dynamic processes. Here, we present a high-resolution scRNA-seq expression atlas of the *Arabidopsis* root composed of thousands of independently profiled cells. This atlas provides detailed spatiotemporal information, identifying defining expression features for all major cell types, including the scarce cells of the quiescent center. These reveal key developmental regulators and downstream genes that translate cell fate into distinctive cell shapes and functions. Developmental trajectories derived from pseudotime analysis depict a finely resolved cascade of cell progressions from the niche through differentiation that are supported by mirroring expression waves of highly interconnected transcription factors. This study demonstrates the power of applying scRNA-seq to plants and provides an unparalleled spatiotemporal perspective of root cell differentiation.

INTRODUCTION

In recent years, high-throughput single-cell transcriptomics has developed to a point of becoming a fundamental, widely used method in mammalian research (Potter, 2018). Thousands of cells can be profiled simultaneously and analyzed accurately, revealing unique insights into developmental progressions, transcriptional pathways, and the molecular heterogeneity of tissues. The increasingly high-throughput nature of single-cell RNA sequencing (scRNA-seq) has been facilitated by the development of droplet technology (Macosko et al., 2015; Klein et al., 2015) and increased automation (Zheng et al., 2017). In brief, a cell is encapsulated within an oil droplet and lysed, and its transcripts reverse transcribed on barcoded beads. Following library production and sequencing, transcripts from individual cells can be identified from the bead-derived barcode and individual transcripts accounted for using unique molecular identifiers (UMIs)

(Prakadan et al., 2017). However, while commonly used in animal systems, additional technical demands such as the necessity to break down cell walls (with subsequent transcriptional effects), high osmotic pressure sensitivities, and high cell size variability present potential challenges when applying this technology to plants.

The *Arabidopsis* root provides an ideal tissue for analyzing the promise of scRNA-seq. The transcriptomes of key cell types have been well profiled, and the root shows a strict spatiotemporal organization. Radially, the root is organized in concentric rings of endodermis, cortex, and epidermis that surround a central stele, comprising the pericycle, phloem, and xylem (Figure S1A). These cell types originate from a specialized stem cell niche in which initials, surrounding the quiescent center (QC), divide in a predictable manner, giving rise to long cell files that capture their developmental trajectory along the length of the root (Figure S1B). Several gene expression atlases of the *Arabidopsis* root have been produced (Birbaum et al., 2003; Brady et al., 2007a; Li et al., 2016). These, however, have focused primarily on describing either radial or temporal expression profiles and typically relied on reporter lines to assess select cell types. scRNA-seq, on the other hand, allows the simultaneous, unbiased sampling of every type of cell at every developmental stage in one experiment.

Here, we present a high-resolution scRNA-seq expression atlas of the *Arabidopsis* root that captures its precise spatiotemporal information, revealing key regulators and defining features for all major cell types. We show how QC cells and meristematic cells are distinguished and resolve intricate developmental trajectories that cells undergo during their transition from stem cell through differentiation. The precise waves of gene expression characterizing this process are mirrored by similar expression changes of highly interconnected transcription factors (TFs). Our atlas offers an unparalleled spatiotemporal perspective of root cell-type differentiation at a resolution not previously achievable.

RESULTS

Single-Cell RNA Sequencing Is Highly Sensitive and Highly Reproducible

4,727 *Arabidopsis* root cells from two biological replicates were isolated and profiled using droplet-based scRNA-seq. At



~87,000 reads per cell, the median number of genes and transcripts detected per cell was 4,276 and 14,758, respectively (Figure S1C; Table S1). In total, transcripts for 16,975 genes were detected (RPM \geq 1), which, after correction for read depth, represents ~90% of genes detected by bulk RNA sequencing (RNA-seq) of protoplasted root tissue. Further, the global gene expression profiles of pooled scRNA-seq and bulk RNA-seq are highly correlated ($r = 0.9$; Figure S1D), indicating that plant scRNA-seq is highly sensitive. This methodology is also highly reproducible, as demonstrated by the facts that ~96% of genes expressed (RPM \geq 1) in one scRNA-seq replicate are detectable in the second and that expression across the two replicates is highly correlated ($r = 0.99$; Figure S1E).

Clusters Comprise the Major Cell Types in the Root

To identify distinct cell populations based on gene expression profiles, an unbiased, graph-based clustering was performed on the 4,727 single-cell transcriptomes using the Seurat software package (Satija et al., 2015; Butler et al., 2018) (Figure 1A). Genes induced by protoplasting (≥ 2 -fold; $q < 0.05$) were identified by standard RNA-seq and dismissed prior to analysis (Figure S1F; Table S1). 15 distinct clusters were identified, each containing between 81 and 596 cells. These clusters harbored similar numbers of cells from each replicate, and their gene expression profiles were highly correlated across the replicates (r between 0.95 and 1; Table S2), highlighting again the impressive reproducibility of this technique.

In order to attribute cell identities to these clusters, expression of cell-type-specific marker genes, either well established or identified from a curated collection of root transcriptomic datasets (Table S2; Efroni et al., 2015), was compared across clusters. This allowed cell identities to be confidently assigned to 8 of the 15 clusters in the cluster cloud (Figure 1B; Table S2). Expression of key root development genes among these markers, such as *PLT1*, *SCR*, *SHR*, *APL*, *COBL9*, and *GL2*, shows high specificity to particular clusters (Figure S2). Cluster identities were confirmed with a complementary approach, whereby transcription profiles of differentially expressed (DE) genes governing the clusters were harvested from microarray datasets (Brady et al., 2007a) and analyzed for tissue specificity (Figure S1G). Together, these approaches revealed that, with the exception of lateral root cap cells (for which limited marker data are available), all known major tissue types in the root were captured and are represented by identifiable clusters.

Clusters 9 and 13 comprise cortex and endodermal cells, respectively (Figures 1B and S1G; Table S2). The identity of the endodermal cluster was further validated by the localized accumulation of *GFP* transcripts in one of the replicates generated from the *pMIR166A:erGFP* reporter line (see STAR Methods; Figures 2A and S3A). In addition, when cells were re-clustered incorporating scRNA-seq data of *shortroot* mutants (*shr-3*), which lack a defined endodermis (Helariutta et al., 2000; Figure S3A), otherwise well-dispersed *shr-3* cells were absent from a cluster comprising endodermal cells of both wild-type replicates (Figures 2B and S3). This cluster analysis also shows that *shr* cells, while present in all other clusters, localize on the outskirts of some (Figure 2B). This points to subtler effects of *SHR* on cell types other than the endodermis;

although some of this phenomenon may also be attributable to the fact that *shr-3* is in the Ler background. Irrespective, this observation nicely highlights the potential of applying scRNA-seq to identify hidden phenotypic changes, whether stemming from natural variation or mutations.

Clusters 10 and 3 comprise trichoblast and atrichoblast cells, respectively (Figures 1B and S1G; Table S2). Cluster 5 also contains trichoblast cells (Figure S1G). Although cells in this cluster show low expression of a number of atrichoblast marker genes, crucially, the trichoblast marker *COBL9* is expressed in this cluster, whereas the atrichoblast marker, *GL2*, is not (Figures 1B and S2). The co-expression of atrichoblast marker genes hints at a degree of commonality between this subset of trichoblasts and its epidermal counterparts, perhaps reflecting a distinction in developmental stage to the trichoblast cells contained in cluster 10.

Cluster 4 comprises stele cells while a neighboring cluster (12) comprises maturing xylem cells (Figures 1B and S1G; Table S2). Consistent with the tissue complexity of the stele, subclustering reveals cell heterogeneity within cluster 4. Particularly, phloem and pericycle cells are separated into two discrete subclusters (Figure S4), as highlighted by the highly subcluster-specific expression of genes such as *APL* (4.2), *LBD29*, and *TIP2-3* (4.1) (Figure 2D; Bonke et al., 2003; Porco et al., 2016; Gattolin et al., 2009).

Finally, cluster 11 comprises both columella and QC cells (Figures 1B and S1G; Table S2), which can be separated into two subclusters. Subcluster 11.2 contains columella cells that express marker genes such as *COBL2*, *NCED2*, and *ATL63* (Figure 2E; Brady et al., 2007b; Efroni et al., 2015). In contrast, transcripts for the QC-expressed genes *AGL42*, *BBM*, and *TEL1* are largely limited to cells in subcluster 11.1 (Figure 2E; Navy et al., 2005; Efroni et al., 2015). Given the small number of QC cells per root, this cluster may well contain other transcriptionally similar cells, perhaps the adjacent initials in the niche. However, importantly, the fact that QC cells are captured illustrates well the possibilities of this methodology for studying rare cell types or elucidating transcriptional subtleties affecting small numbers of cells within a tissue.

Meristematic Cells Cluster Independently of Tissue Identity

The identity of cells in the remaining clusters is less obvious. Overall gene expression in cells within clusters 0, 1, and 14 is comparatively low (Figure S5A), likely masking their identity at this level of sequencing resolution. However, expression values extracted from a longitudinal microarray dataset (Brady et al., 2007a) for the top DE genes defining these clusters suggest that they comprise mature cells of mixed identity (Figure S5B). In contrast, cells in the final four clusters (2, 6, 7, and 8) show markedly meristematic-based expression profiles (Figure S5B). Notable histone and cytokinesis-linked genes, such as *KNOLLE*, *ENODL14*, and *ENODL15*, are among the most prominently DE genes for these clusters (Figure S2; Table S2; Lauber et al., 1997; Adrian et al., 2015). Subclustering revealed some cell-type identities, albeit that they are generally less distinct than those of the clusters described above. For example, subcluster 2.4 shows a distinct cortex identity (Figure S4). Curiously, this subcluster is positioned adjacent to the main cortex cell cluster.

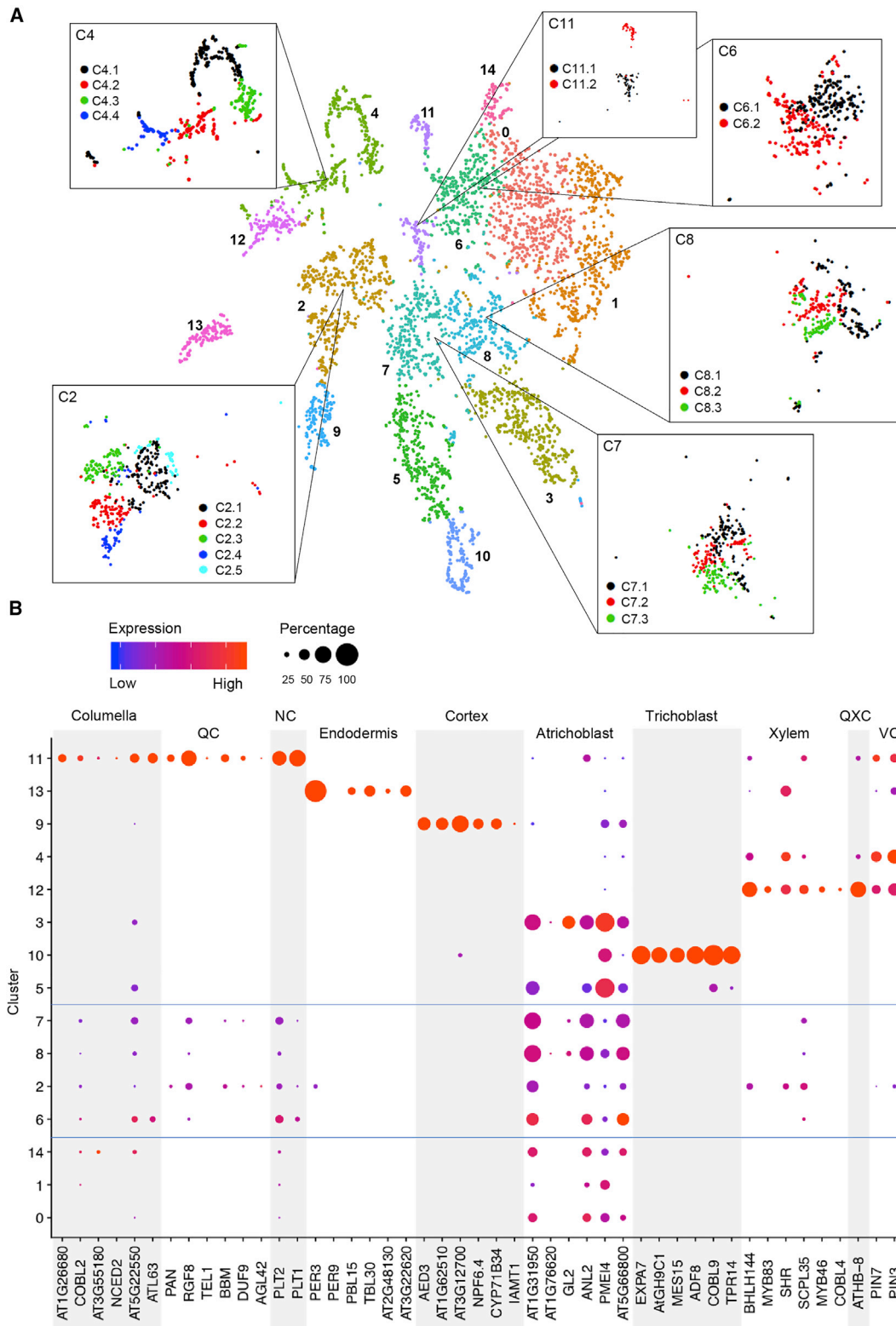
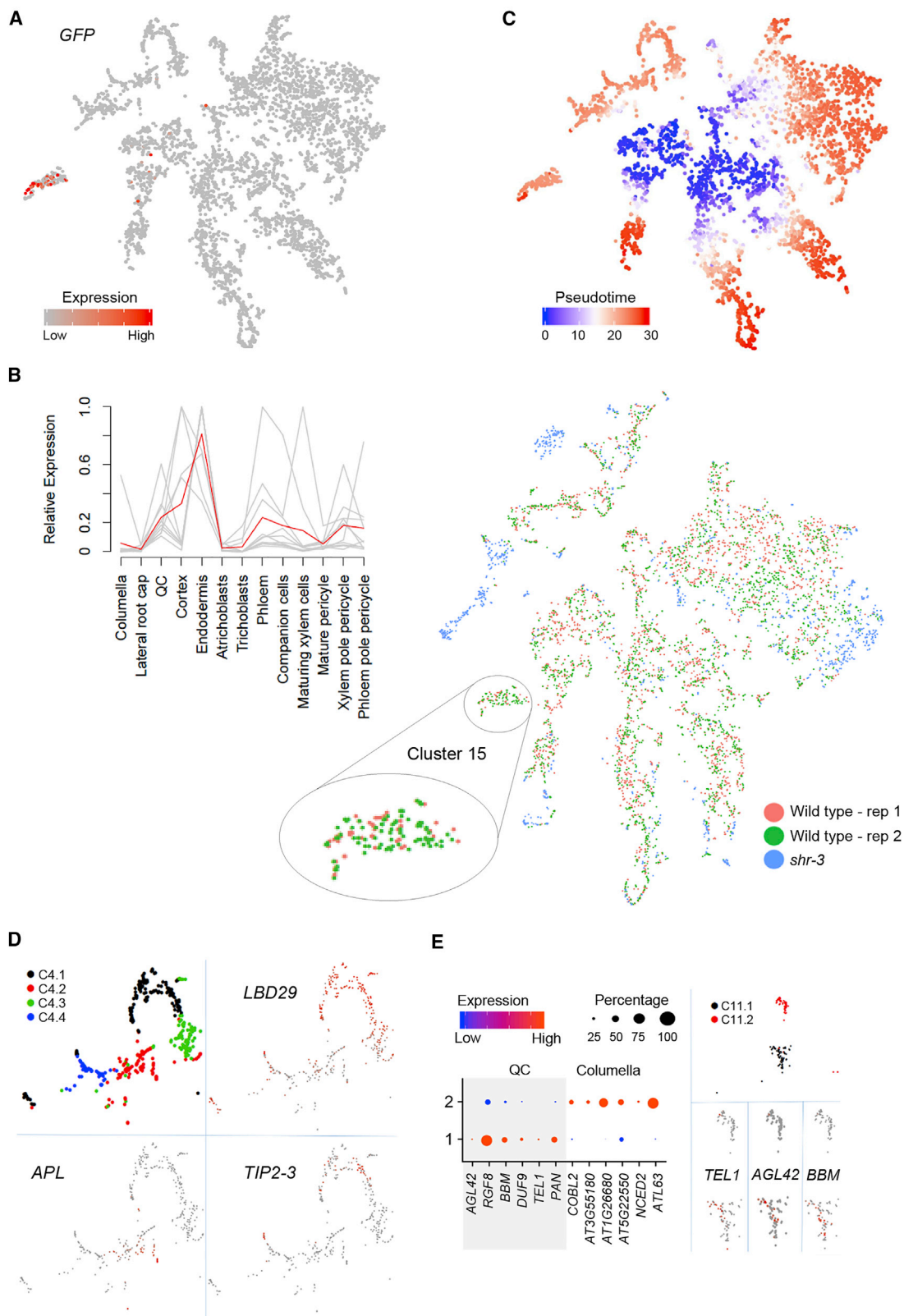


Figure 1. Sequenced Single Cells Cluster by Identity

(A) t-SNE (t-distributed stochastic neighbour embedding) plot of 4,727 *Arabidopsis* root cells shows these group into 15 clusters with additional subclusters. (B) Expression of known cell-type marker genes across cells reveals the identity of clusters. Dot diameter, proportion of cluster cells expressing a given gene; color, mean expression across cells in that cluster. NC, niche and columella; QXC, QC, xylem, and columella; VC, vasculature and columella. See [Table S2](#) for details of all marker genes assessed.



(legend on next page)

A comparable pattern is seen in clusters 7 and 8 with trichoblast cell identity apparent in those subclusters (7.3 and 8.3) closest to the adjacent defined trichoblast clusters (Figure S4).

It is interesting to note that when comprehending all the clusters together, the meristematic clusters are closely localized in the center of the cluster cloud with the subcluster containing QC cells (11.1) at the heart of this. Meanwhile, those clusters with distinct, mature cell identities span out from the meristematic clusters (Figure 1A; Video S1), suggesting an overall cluster arrangement that reflects developmental time. Subclustering of the meristematic clusters refines this idea, showing a degree of closeness of mature and developing cells of the same eventual fate. This notion is further supported by pseudotime analysis across all cells, which reveals that genes DE in cells of the central clusters describe the beginning of cell fate progressions (Figure 2C).

Likewise, the cluster cloud reveals an organization that captures the “lineage” relationships between cell and tissue types. For instance, the trichoblast and atrichoblast clusters, as well as the xylem, vasculature, and the cortex and endodermis clusters, are positioned next to each other within the cluster cloud. The position of the columella in a cluster with QC cells indicates a higher degree of transcriptional accord between these cell types than between these cell types individually and others. This is reflected in the fact that key developmental regulators, such as *PLT2*, *PLT3*, and *PIN4* are co-expressed in the columella and QC (Galinha et al., 2007; Feraru and Friml, 2008). This way of contemplating clusters, along with pseudotime visualization, thus offers a valuable director for early comprehension of developmental trajectories, particularly in the absence of *a priori* knowledge, such as a reference atlas.

Unique Marker Genes Define Cluster Identity in an Unbiased Manner

Given that detailed reference datasets are available only for select tissue and organ types in very few plant species, we developed an unbiased approach to assign cell type identities to scRNA-seq-generated cell clusters. Genes DE in a given cluster compared to all other clusters ($q < 0.01$; average log fold change [FC] ≥ 0.25) were identified using “biomod” on Seurat (McDavid et al., 2013). DE genes were further narrowed down by applying the criteria that cluster-specific marker genes must be expressed in $\geq 10\%$ of cells within the cluster (PCT1), and $\leq 10\%$ of cells across all other clusters (PCT2). Applying these criteria, we uncovered expected marker genes alongside hundreds of additional genes diagnostic for a given developmental stage or cell type that encompass every cluster (Table S3).

The top two cluster-specific genes (based on average log FC) for each cluster are expressed across a substantial proportion of cells specifically within one cluster, with the exception of genes

for clusters 0 and 1, which show substantial co-expression in cluster 14 (Figure 3A). In addition, Gene Ontology (GO) overrepresentation analysis on cluster-specific gene sets reveal GO terms appropriate to their biology (Table S3). For example, the meristematic clusters 2 and 8 show an abundance of marker genes implicated in processes related to cell proliferation and DNA replication, respectively. Further, markers for the root-hair-cell cluster 10 are enriched in trichoblast differentiation and maturation terms; for the QC- and columella-containing cluster 11, in root development and starch biosynthesis; and for cluster 12, in xylem development and secondary cell wall biogenesis. Finally, genes required for the formation and suberization of the Casparian strip are among the markers for cluster 13, which comprises endodermal cells. However, a notable outcome of this analysis is the number of marker genes for which a root function has yet to be assigned. This illustrates the potential of scRNA-seq for identifying new developmental regulators.

To further validate this strategy for marker gene calling and for assigning cell identity to clusters without other references, we assessed the spatiotemporal patterns of expression for select genes using transcriptional *promoter:3xVenus-NLS* reporter lines. Prioritizing by a balance of high log-fold change, high PCT1, low PCT2, and a lack of prior biological information relating to cell-type specificity and root development, we selected ten genes from across clusters. Expression for eight of the ten genes tested localized to specific cell types and/or root zones in line with predictions. Specific expression in the cortex (*AT1G62510*) and maturing trichoblasts (*MES15*) was observed for marker genes for clusters 9 and 10, respectively (Figures 3B and 3C), while genes selected from cluster 4 revealed highly specific phloem (*PME32*) and pericycle (*ATL75*) expression (Figures 3D and 3E). *MLP34* is expressed in the atrichoblasts, as expected for a marker for cluster 3 (Figure 3F). However, expression is also seen in cells of the lateral root cap (Figure 3F), a cell type to which a cluster could not be assigned. *MLP34* shows expression in some cells in cluster 1 (Figure S2), indicating that this cluster may in fact contain cells of the lateral root cap, although further analysis is needed to confirm this. Finally, expression of genes selected from the meristematic cluster 2 was found to localize to the meristematic cortex and endodermis (*AT3G22120*), the meristematic cortex (*AT1G62500*), or the meristematic vasculature (*PIP2-8*) (Figures 3G–3I).

Given the common occurrence of *cis*-regulatory motifs in the introns of genes, the fact that promoter fusions for eight out of the ten marker genes tested confirm predictions is notable. This unbiased approach for assigning identities to cell clusters could prove invaluable when no reference data are available. Moreover, our results reveal a level of sensitivity beyond that of assigning whole cluster identity. This is typified by *PME32* and

Figure 2. Cell Identity and Developmental Stage Are Reflected in the (Sub)clustering

- (A) t-SNE visualization of the cluster cloud (both replicates) shows *GFP* transcripts localize specifically to *pMIR166:erGFP* cells in the endodermal cluster.
- (B) Wild-type and *shr-3* cells were combined and clustered. (Left) The expression profiles for the top 10 DE genes from cluster 15, taken from a microarray root atlas (Brady et al., 2007a), reveal an endodermal identity. Red line, mean expression profile; gray lines, individual expression profiles. (right) t-SNE visualization of the wild-type and *shr-3* cell cluster cloud shows endodermal cluster 15 lacks *shr-3* cells.
- (C) Pseudotime analysis of all wild-type cells reveals cells in the central clusters are earlier in the pseudotime trajectory, consistent with their meristematic identity.
- (D) t-SNE visualization of cluster 4 subclusters. Expression profiles of selected genes reveal pericycle and phloem identities for subclusters 4.1 and 4.2, respectively.
- (E) Expression of known cell-type marker genes across cells of cluster 11 reveals the identity of subclusters. Dot diameter, proportion of cluster cells expressing a given gene; color, mean expression across cells in that cluster. t-SNE visualization of expression profiles of selected QC marker genes.

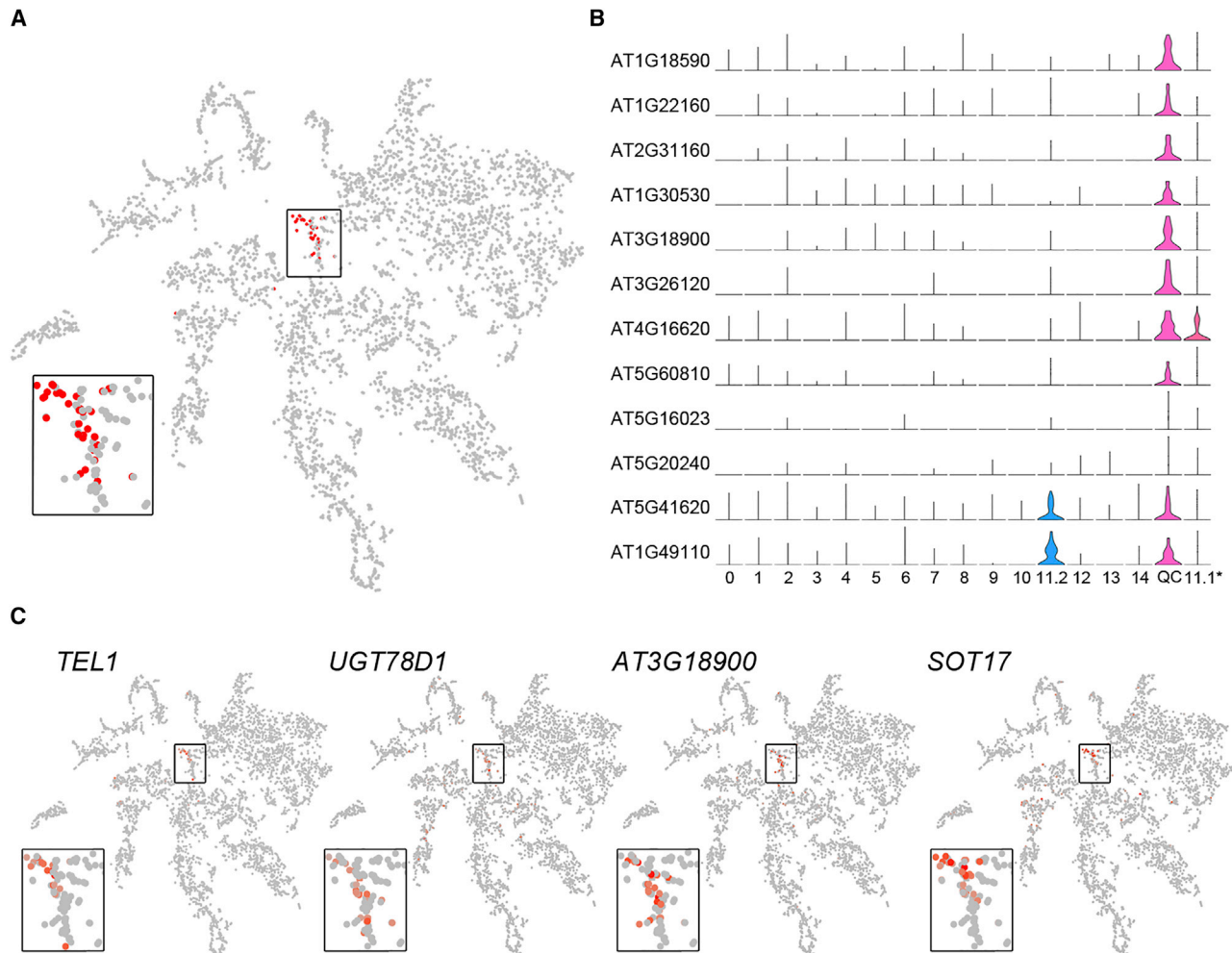


Figure 4. scRNA-Seq Data of QC Cells Identify Unique QC Marker Genes

(A) t-SNE visualization indicating the position of 36 QC cells at the center of the cluster cloud.

(B) QC cell specificity revealed by violin plots depicting expression level (length) and proportion of cells expressing (width) for 10 QC cell marker genes (y axis) across each cluster (x axis). Violin plots for two genes showing expression in the QC cells and the columella cluster (11.2) are also shown. *11.1, subcluster 11.1 with QC cells removed.

(C) t-SNE visualization of expression profiles of selected QC marker genes. Subcluster 11.1 is magnified in each case.

expression in the QC cells. Additionally, cells expressing such genes cluster away from the QC, in localized regions of meristematic cluster 2, adjacent to their mature-cell counterparts (Figure S2).

Transcriptomic comparison between the QC cells and undifferentiated cells of the meristem (cells in clusters 2, 6, 7, and 8), identified 254 genes preferentially expressed in the QC (Table S3). While meristematic cells are distinguished by expression of genes involved in cell division and DNA replication, cells of the QC are not. Instead, transcription is an enriched GO term, as is auxin biosynthesis, which is fitting given the role of auxin in QC specification (Sabatini et al., 1999; Galinha et al., 2007). Further, unexpectedly, genes with functions in glucosinolate biogenesis and callose deposition are overrepresented among those genes DE in the QC (Table S3). This finding, in particular, is intriguing. Both processes are characteristic of a defense response, which seems curious given the QC's internal location,

insulated from external stimuli. Their prominence instead points toward a biology of QC cells not previously appreciated. The recent finding that 3-hydroxypropylglucosinolate acts as a reversible inhibitor of root growth (Malinovsky et al., 2017) is, in this regard, intriguing. Likewise, that small RNAs are prevented from moving in and out of the QC (Skopelitis et al., 2018) points to a unique regulation of cell-cell communication via plasmodesmata in the QC.

Among the genes DE between the QC and meristematic cells of the root, 47 show a particularly strong expression bias to the QC cells ($\log FC \geq 0.25$; $PCT1 \geq 10$; $PCT2 \leq 10$) (Table S3). Many of these genes are also expressed in mature cell types, predominantly columella cells, further reinforcing a certain shared biology not present in the apical root meristem. However, ten genes clearly mark the QC cells (Figures 4B and 4C). Reporter lines for one of them (*TEL1*) revealed high expression in the QC cells and minimal expression elsewhere (Figure 3J).

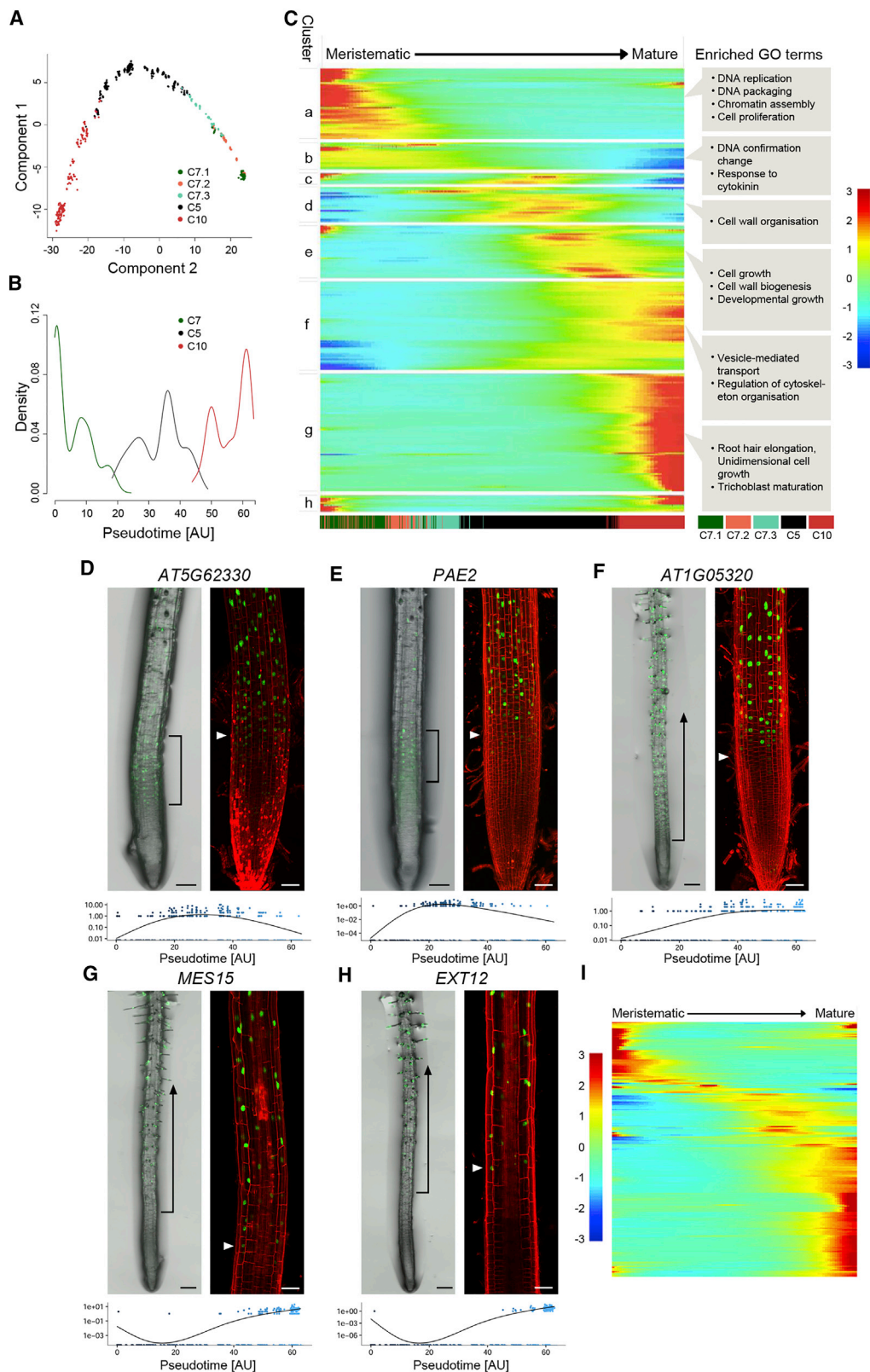


Figure 5. Trichoblast Development Is Guided by Progressive Waves of Gene Expression

(A) Pseudotime reconstruction of trichoblast development reveals a linear ordering of cells, reflecting cluster and subcluster arrangement.

(B) Density distribution of cells across pseudotime.

(legend continued on next page)

This expression contrasts strongly with that of genes marking various cell-type initials (Figures 3G–3I). Among the eleven QC markers are several genes not previously described in connection to the QC, including *AT3G18900* and *SOT17* (Figure 4C; Table S3). Intriguingly, the latter functions in the glucosinolate pathway (Klein et al., 2006). This reinforces the prospect of there being another layer to QC function and highlights the potential for this technology in identifying developmental regulators and the downstream genes that translate cell fate into distinctive cell shapes and functions.

The limited number of QC-specific genes, in comparison to the number of specific markers identified for cell types such as the endodermis, xylem, and trichoblasts, would indicate that QC identity reflects the integrative outcome of multiple overlapping expression signatures. This idea is supported by the position of the QC at the intersection of an auxin maximum and SCARECROW activity (Shimotohno et al., 2018). However, an alternative, non-mutually exclusive interpretation of this finding is that QC identity reflects a “subtractive” expression signature. In this scenario, the absence of expression of drivers of tissue identity and differentiation forms a key feature of QC identity. The facts that *WOX5* acts as a transcriptional repressor (Forzani et al., 2014; Pi et al., 2015) and that genes, such as *AT3G22120*, *AT1G62500*, and *PIP2-8* are mostly undetectable in the QC, support this idea.

Cell Differentiation Reflects Finely Resolved Waves of Gene Expression

One of the most exciting benefits of scRNA-seq is that it allows for the simultaneous, unbiased analysis of every type of cell at every developmental stage in one experiment. This is broadly illustrated by pseudotime analysis across all cells, which shows how central clusters are defined by expression of genes at the beginning of cell fate progressions, whereas mature cell types are peripheral in the cluster cloud (Figure 2C). However, although the cluster cloud represents a coarse landscape of developmental cell states, it does not reveal how individual cells traverse these states. To resolve the progressions that cells undergo during their transition from stem cell to mature trichoblast, we performed pseudotime analysis on cells of clusters 7, 5, and 10. This revealed a linear ordering of cells that reflects the cluster and sub-cluster arrangement (Figures 5A and 5B). In addition, we identified 3,657 highly dispersed, DE genes that fall into 8 distinct gene clusters (*a–h*) and depict successive waves of gene expression across pseudotime (Figures 5C and S6A; Table S4).

Reporter lines generated for representative genes of select clusters precisely reflect their pseudotime profiles (Figures 5D–5H). *AT5G62330* and *PAE2* (cluster *d*) show a distinct peak of expression near the center of the pseudotime trajectory. Reporter lines for both genes capture this expression dynamic. *pAT5G62330:3xVenus-NLS* expression initiates in the distal meristem and persists into the elongation zone, whereas *PAE2* is expressed slightly later and shows strong expression, particu-

larly in the early elongation zone (Figures 5D and 5E). Expression of *AT1G05320* (cluster *f*) overlaps with that of *AT5G62330* and *PAE2* in elongating cells, but expression persists into the maturation zone and differentiated trichoblasts (Figure 5F). Finally, reporter activity for *MES15* and *EXT12* (cluster *g*), whose expression initiates late in the pseudotime trajectory, is first detected in cells exiting the elongation zone, with *MES15* expression starting slightly earlier with respect to the first visible protrusion of the emerging hair (Figures 5G and 5H), in accordance with its slightly earlier pseudotime projection.

The pseudotime trajectory thus reflects with great precision the temporal expression changes of individual genes along the length of the root (Figure 5C), providing a refined view of the changes a cell undergoes during its transition from stem cell through to full differentiation. Genes predominantly expressed at the beginning of the developmental trajectory show an overrepresentation of DNA replication, cell proliferation, and ribosomal functions, as is expected for meristematic cells (clusters *a* and *b*; Table S4). At the other end of the trajectory, cluster *g* captures expression of genes involved in unidimensional growth and root hair elongation and maturation. A previous gene regulatory network (GRN) for epidermal cell differentiation had identified 154 core root hair genes from which a temporal progression could be deduced (Bruex et al., 2012). scRNA-seq provides another dimension of temporal resolution. Of the subset (98) of core root hair genes that show a dynamic pattern of expression across the pseudotime, the vast majority (84) are expressed late in the trajectory (cluster *g*; Table S4). In contrast, early cell fate determinants, including *GL2*, *TRY*, and *WER*, are expressed in cluster *a* (meristem). Our analysis thus reveals stepwise temporal progressions more dynamic than previously appreciated that connect early cell-fate decisions to morphological and cellular changes.

These stepwise progressions are primarily captured by the central gene expression clusters. Clusters *d* and *e* reveal cell growth and cell wall biogenesis among their enriched GO terms, while those of cluster *f* indicate a burst of cell morphogenesis activity with an overrepresentation of genes involved in cytoskeleton reorganization, vesicle trafficking, and a plethora of transport processes. Cell expansion and cell reorganization are processes known to occur during root hair development (Balcerowicz et al., 2015), and the pseudotime analysis identifies specific genes that could drive processes such as these during root hair differentiation (Table S4). Also found in cluster *d* is an abundance of flavonoid-associated genes, suggesting that this signaling is occurring during cell elongation, downstream of *GL2* and *WER* but upstream of many auxin or ethylene-responsive genes that are overwhelmingly found in the later gene clusters (*f* and *g*).

A Highly Interconnected TF Gene Regulatory Network Coordinates Cell Differentiation

Expression profiles of the 239 TFs among the dynamically expressed genes mirror their waves of expression (Figure 5I;

(C) Expression heatmap of 3,657 highly dynamically expressed genes ordered across pseudotime reveals trichoblast differentiation reflected in multiple progressive waves of gene expression. Significantly enriched GO terms for clusters are labeled. Lower bar, cell density distribution across clusters.

(D–H) Spatiotemporal expression patterns for promoter fusions for the following genes reveals the pseudotime-predicted temporal localization: (D) *AT5G62330*, (E) *PAE2*, (F) *AT1G05320*, (G) *MES15*, and (H) *EXT12*. White arrowheads indicate the start of expression. Expression dynamics for single genes plotted across trichoblast pseudotime are under the corresponding root images.

(I) Expression heatmap of 230 transcription factors (TFs) extracted from Figure 4C shows similar waves of TF expression. See Table S4 for full data.

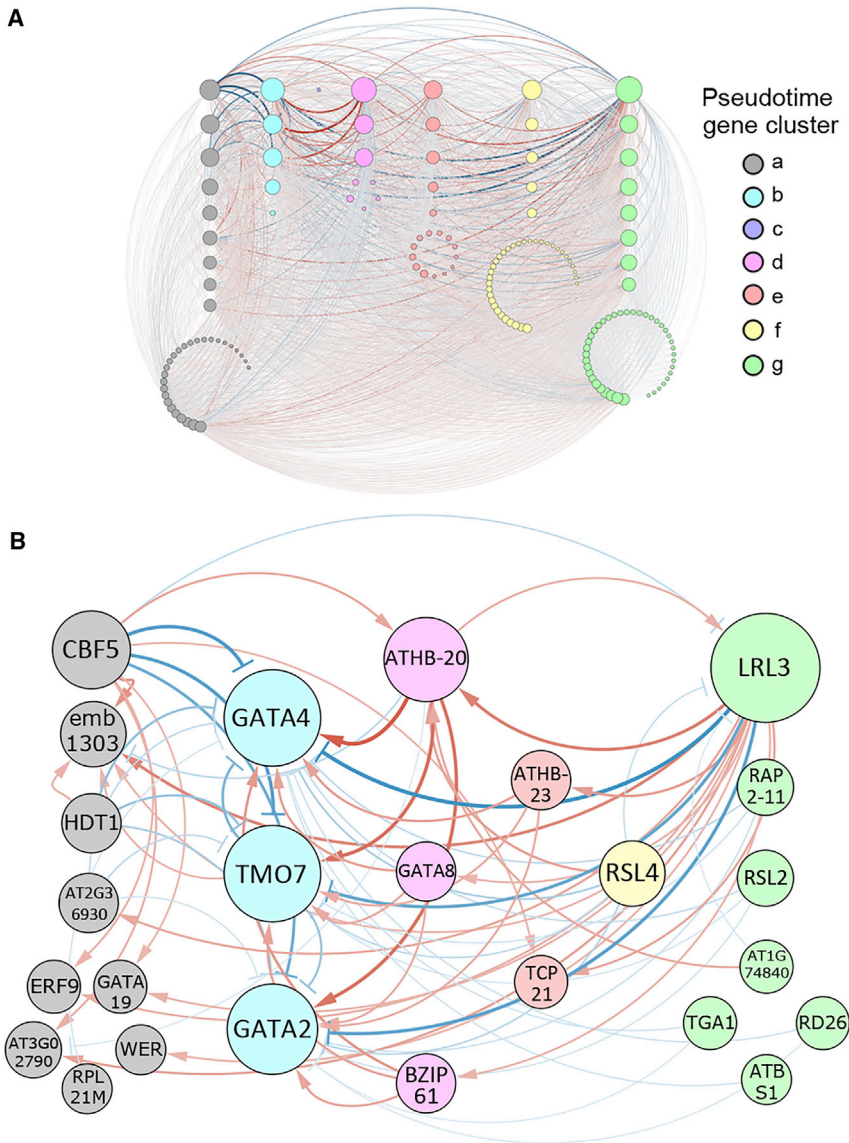


Figure 6. A Gene Regulatory Network (GRN) Predicts Key Regulators during Trichoblast Cell Differentiation

(A) A GRN built of 229 TFs expressed dynamically across trichoblast pseudotime with a parameter cutoff of 0.1 (Table S4).

(B) The same network with a parameter cutoff of 1.5. Node size is equivalent to the number of predicted connections. Edge color represents activation (red) or repression (blue). Edge width represents the strength of the predicted connection.

dynamics across pseudotime, the resultant network reveals key players in this process and their regulatory interactions. What is immediately clear from the network is the presence of major, highly connected central regulators along the whole trajectory (Figure 6A), the majority of which have not previously been implicated in root development. Filtering the network down to its 25 core components (see STAR Methods), we see several distinct passages of feedback regulation along each step of the trichoblast differentiation trajectory (Figure 6B). Notable among these is considerable negative feedback from TFs at the end of the trajectory back to major nodes in the meristem, especially LRL3 (Figure 6B). This suggests that while positive and negative feedback loops in the meristem (also distinct) might maintain meristematic identity, the progression to differentiation gives rise to dominant components that influence the meristematic master players.

ATHB-20 and, to a lesser extent, ATHB-23 stand out as positive regulators of the core network components in the neighboring, upstream, meristematic cluster, including the aforementioned TMO7.

Table S4), pointing toward a causative relationship and an intricate regulation of cell fate progressions. Several of these are known to regulate specific stages of root hair development, including TRY, WER, and many basic-helix-loop-helix (bHLH) TFs (notably, RSL2, RSL4, and LRL1). The expression clusters in which they reside accurately reflect their biological roles (Schellmann et al., 2002; Diet et al., 2006; Bruex et al., 2012; Balcerowicz et al., 2015). Likewise, TMO7, previously reported as a central cell-to-cell communicator and regulator of root meristem activity (Lu et al., 2018), is found early on in the trajectory, while the central clusters contain TCP TFs connected to the exit of cell proliferation (Nicolas and Cubas, 2016) and ARR1, which regulates root meristem size (Dello Iorio et al., 2008).

To elucidate further the genetic coordination along the trichoblast differentiation process, we inferred a GRN using a pipeline integrating the transformation of linear ordinary differential equations (ODEs) and linear regression (SCODE) (Matsumoto et al., 2017; Table S4; see STAR Methods). Incorporating TF expression

While it has been linked to ABA sensitivity in the root (Barrero et al., 2010), no defined role has yet been assigned to ATHB-20 in root development; yet, a connection to a major player such as TMO7 suggests this to be the case. Pertinent to this, it is important to note that, with the exception of those in the late developmental cluster, the 25 core genes displayed in the network are not specific to trichoblast cell development (Figure S2; Table S4). This would indicate that they fulfill a similar role in other tissue layers, possibly coordinating growth and differentiation across the root. This notion is supported by pseudotime analysis of the cortex, which reveals an equally dynamic gene expression cascade mirrored by waves of TF expression (Figures S6B and S6C; Table S4). With the notable exception of TMO7, many of the core nodes identified in the trichoblast network, including ATHB-20, ATHB-23, CBF5, GATA4, and GATA2, are also present in equivalent positions along cortex pseudotime.

While negative feedback from differentiating root hair cells toward the meristem is notable in the simplified network, forward

regulation of cell differentiation can be found as a culmination of many, weaker interactions from the meristematic and central nodes in the extended network (Figure 6A; Table S4). The well-established regulators of trichoblast maturation, expressed at the end of the trajectory, are regulated by a combination of additive and opposing effects of broadly expressed (for example, ATHB-20 and ATHB-23) and locally restricted (such as GL2 and WER) TFs. Network configurations in which tissue-specific expression reflects the combinatorial output of many broadly expressed and locally restricted TFs are emerging as a general feature underlying development (Sparks et al., 2016; Reiter et al., 2017; Niwa, 2018; Barolo and Posakony, 2002), buffering the system and providing robustness.

Our network serves to particularly highlight the complex wiring between components mediating the transition of cells from the stem cell niche to the root maturation zone. Altogether, the pseudotime analysis of scRNA-seq data indicates that these transitions are more gradual than previous data suggested. We see evidence of intricate dynamic transcriptional regulation, particularly across cells of the elongation zone. Termination of meristem activity and the initiation of the differentiation process appear coordinated across tissues, while the trichoblast maturation process relies on tissue-specific TFs whose activity comes about from the combinatorial regulation of dozens of temporally upstream players.

DISCUSSION

While scRNA-seq in plants has previously been limited to analysis of cells in their hundreds, the data presented here show that profiling of developmentally complex tissues using high-throughput scRNA-seq of thousands of cells offers an unparalleled view of the spatiotemporal expression dynamics cells undergo between exiting the niche and their final differentiation.

scRNA-seq of the *Arabidopsis* root proved to be sensitive and highly reproducible. Select genes induced by protoplasting, as well as other plant physiology-based challenges, are not prohibitive but must be considered. For instance, the technology has an inherent bias toward smaller cells, such as those from meristems. Mature cells, while captured in sufficient numbers for analysis, are underrepresented in the atlas as their identities appear to become partially clouded during the protoplasting and cell capture processes. Likewise, epidermal cells are captured more readily than cells of the central stele. These trends, however, do not affect the types of analyses presented here.

The nearly five thousand root cells profiled form a high-resolution atlas that captures all major cell types and developmental stages, including the scarce cells of the QC and niche. With this atlas, we can predict with precision the spatiotemporal patterns of gene expression within the root, as demonstrated by our reporter lines. Further, the atlas offers valuable insights into cellular processes characterizing distinct cell and tissue types. An unbiased approach to marker gene calling identified expression features defining each cluster and subcluster. These negate the need for *a priori* knowledge in assigning cluster identities and identify unique developmental regulators and downstream genes that give cells their distinctive forms and functions. As an example, *SOT17* shows a QC-specific pattern of expres-

sion, and genes implicated in glucosinolate biosynthesis and callose deposition more generally show preferential expression in QC cells. Although a connection to cell-specific defense responses cannot formally be excluded, the latter finding more likely relates to plasmodesmata-mediated signaling, given the recent finding that small RNAs are blocked from moving in and out of the QC (Skopelitis et al., 2018).

It is remarkable just how well the arrangement of cell clusters and subclusters described in our atlas reflects developmental time. In the very center are QC cells with a transcriptome distinctive from that of the surrounding initials and meristematic cells. Differentiating cells are on the periphery of the cluster cloud, adjacent to relevant meristematic subclusters. This cluster arrangement is likely a general feature of tissues that capture developmental trajectories, as a similarly developmentally informed cluster orientation has been recorded in a study of mouse spermatogenesis (Lukassen et al., 2018). In the case of the *Arabidopsis* root, it indicates that expression signatures linked to cell fate are not as strong as those defining stem cell or meristem identity.

The progressions that cells undergo during differentiation are, however, far more dynamic than captured in just the cluster arrangement. As illustrated by the successive waves of gene expression revealed by pseudotime analysis, cells transitioning from the niche through differentiation follow finely resolved developmental trajectories, with progression steps beyond the commonly described meristematic, elongation, and maturation zones. Our scRNA-seq data offer the required resolution to distinguish the stepwise temporal progressions connecting early cell-fate decisions to morphological and cellular changes. While the beginning and end of the trichoblast developmental trajectory have been described (Bruex et al., 2012; Balcerowicz et al., 2015), our data not only add to this but reveal additional gene expression dynamics occurring particularly in cells in the elongation zone. The number of progression steps observed, compared to the number of cells along the root, from the meristem to maturation, implies that the distinct progressions are characteristic of few, perhaps even individual, cells along the root elongation zone.

Recent studies elaborate the idea that cell fate reflects the output of intricate GRNs in which numerous TFs control gene expression in a combinatorial manner (Sparks et al., 2016; Reiter et al., 2017; Niwa, 2018; Barolo and Posakony, 2018). This notion is reinforced by the pseudotime-derived trichoblast GRN, which shows that expression of major regulators of trichoblast maturation is linked to many weak interactions from meristematic and central nodes. Interestingly, the network also implies a high degree of feedback regulation toward the meristem, not only from the elongation zone but also from genes in the maturation zone, such as *LRL3*. Normal root development requires that growth and differentiation be coordinated across tissue layers. In line with this, the central highly integrated nodes predicted to coordinate the transitions between zones show similar pseudotime profiles in both the cortex and trichoblast lineages.

An additional key application for the scRNA-seq technology will be the profiling of mutants to more precisely define the cellular processes, cell types, or developmental stage affected. Cluster analysis of *shr* and wild-type scRNA-seq data revealed an expected absence of endodermal cells in the mutant

(Helariutta et al., 2000) but also points to more extensive SHR-dependent cell-fate changes. The *shr* scRNA-seq data thus nicely exemplify the enticing prospect this technology offers to discern phenotypes not easily recognized by standard RNA-seq, physiological, or even reporter-based approaches, whether stemming from natural variation, mutations, localized stress responses, or plant-microbe interactions.

In summary, the atlas of the *Arabidopsis* root described here provides a unique spatiotemporal perspective of root cell-type differentiation, increasing the number of discernible developmental domains along the length of the root and pointing to countless candidate developmental regulators that orchestrate this process. scRNA-seq will rapidly become a central technique in the plant sciences as it already is in mammalian studies, providing previously unobservable developmental insights.

STAR★METHODS

Detailed methods are provided in the online version of this paper and include the following:

- KEY RESOURCES TABLE
- CONTACT FOR REAGENT AND RESOURCE SHARING
- EXPERIMENTAL MODEL AND SUBJECT DETAILS
- METHOD DETAILS
 - Protoplast Isolation
 - Bulk RNA-seq Library Preparation and Sequencing
 - Single Cell RNA-seq Library Preparation and Sequencing
 - Generation and Confocal Imaging of Reporter Lines
- QUANTIFICATION AND STATISTICAL ANALYSIS
 - Bulk RNA-seq Analysis
 - Generation of Single Cell Expression Matrices
 - Dimensionality Reduction, t-SNE Visualization, and Cell Clustering Analysis
 - Identification of Differentially Expressed Genes and Cluster-Specific Marker Genes
 - Identification of Cluster Identities
 - Correlation Analysis
 - Single Cell Developmental Trajectory Analysis
 - GO Enrichment Analysis
 - Gene Regulatory Network Analysis
- DATA AND SOFTWARE AVAILABILITY
- ADDITIONAL RESOURCES

SUPPLEMENTAL INFORMATION

Supplemental Information can be found with this article online at <https://doi.org/10.1016/j.devcel.2019.02.022>.

ACKNOWLEDGMENTS

We thank members of the Timmermans lab for their insightful feedback, Chong Lu for input into computational analyses, George Janes for providing *shr-3* seed, and Felicity Jones for access to the 10x chromium single-cell controller. This work was supported by an Alexander von Humboldt Professorship to M.C.P.T.

AUTHOR CONTRIBUTIONS

T.D., X.M., and M.C.P.T. designed the project and experiments. T.D. generated the scRNA-seq and bulk RNA-seq libraries and, together with S.K.,

generated and analyzed reporter lines. X.M. performed bioinformatics analyses. X.M. and E.S. carried out the GRN analysis. K.N. provided statistical and bioinformatic support. T.D. and M.C.P.T. wrote the manuscript.

DECLARATION OF INTERESTS

The authors declare no competing interests.

Received: November 30, 2018

Revised: January 30, 2019

Accepted: February 22, 2019

Published: March 25, 2019

REFERENCES

- Adrian, J., Chang, J., Ballenger, C.E., Bargmann, B.O., Alassimone, J., Davies, K.A., Lau, O.S., Matos, J.L., Hachez, C., Lanctot, A., et al. (2015). Transcriptome dynamics of the stomatal lineage: birth, amplification, and termination of a self-renewing population. *Dev. Cell* 33, 107–118.
- Anders, S., Pyl, P.T., and Huber, W. (2015). HTSeq—a Python framework to work with high-throughput sequencing data. *Bioinformatics* 31, 166–169.
- Assenov, Y., Ramírez, F., Schelhorn, S.E., Lengauer, T., and Albrecht, M. (2008). Computing topological parameters of biological networks. *Bioinformatics* 24, 282–284.
- Balcerowicz, D., Schoenaers, S., and Vissenberg, K. (2015). Cell fate determination and the switch from diffuse growth to planar polarity in *Arabidopsis* root epidermal cells. *Front. Plant Sci.* 6, 1163.
- Barolo, S., and Posakony, J.W. (2002). Three habits of highly effective signaling pathways: principles of transcriptional control by developmental cell signaling. *Genes Dev.* 16, 1167–1181.
- Barrera, J.M., Millar, A.A., Griffiths, J., Czechowski, T., Scheible, W.R., Udvardi, M., Reid, J.B., Ross, J.J., Jacobsen, J.V., and Gubler, F. (2010). Gene expression profiling identifies two regulatory genes controlling dormancy and ABA sensitivity in *Arabidopsis* seeds. *Plant J.* 61, 611–622.
- Birnbaum, K., Shasha, D.E., Wang, J.Y., Jung, J.W., Lambert, G.M., Galbraith, D.W., and Benfey, P.N. (2003). A gene expression map of the *Arabidopsis* root. *Science* 302, 1956–1960.
- Bolger, A.M., Lohse, M., and Usadel, B. (2014). Trimmomatic: a flexible trimmer for Illumina sequence data. *Bioinformatics* 30, 2114–2120.
- Bonke, M., Thitamadee, S., Mähönen, A.P., Hauser, M.T., and Helariutta, Y. (2003). APL regulates vascular tissue identity in *Arabidopsis*. *Nature* 426, 181–186.
- Brady, S.M., Orlando, D.A., Lee, J.-Y., Wang, J.Y., Koch, J., Dinneny, J.R., Mace, D., Ohler, U., and Benfey, P.N. (2007a). A high-resolution root spatiotemporal map reveals dominant expression patterns. *Science* 318, 801–806.
- Brady, S., Song, S., Dhugga, K., Rafalski, A., and Benfey, P. (2007b). Combining expression and comparative evolutionary analysis. The COBRA gene family. *Plant Phys.* 143, 172–187.
- Breiman, L. (2001). Random forests. *Machine Learning* 45, 5–32.
- Bruex, A., Kainkaryam, R.M., Wiecekowsky, Y., Kang, Y.H., Bernhardt, C., Xia, Y., Zheng, X., Wang, J.Y., Lee, M.M., Benfey, P., et al. (2012). A gene regulatory network for root epidermis cell differentiation in *Arabidopsis*. *PLoS Genet.* 8, e1002446.
- Butler, A., Hoffman, P., Smibert, P., Papalex, E., and Satija, R. (2018). Integrating single-cell transcriptomic data across different conditions, technologies, and species. *Nat. Biotechnol.* 36, 411–420.
- Dello Ioio, R., Nakamura, K., Moubayidin, L., Perilli, S., Taniguchi, M., Morita, M.T., Aoyama, T., Costantino, P., and Sabatini, S. (2008). A genetic framework for the control of cell division and differentiation in the root meristem. *Science* 322, 1380–1384.
- Diet, A., Link, B., Seifert, G.J., Schellenberg, B., Wagner, U., Pauly, M., Reiter, W.D., and Ringli, C. (2006). The *Arabidopsis* root hair cell wall formation mutant *lrx1* is suppressed by mutations in the *RHM1* gene encoding a UDP-L-rhamnose synthase. *Plant Cell* 18, 1630–1641.

- Dobin, A., Davis, C.A., Schlesinger, F., Drenkow, J., Zaleski, C., Jha, S., Batut, P., Chaisson, M., and Gingeras, T.R. (2013). STAR: ultrafast universal RNA-seq aligner. *Bioinformatics* 29, 15–21.
- Efroni, I., Ip, P.L., Nawy, T., Mello, A., and Birnbaum, K.D. (2015). Quantification of cell identity from single-cell gene expression profiles. *Genome Biol.* 16, 9.
- Feraru, E., and Friml, J. (2008). PIN polar targeting. *Plant Physiol.* 147, 1553–1559.
- Forzani, C., Aichinger, E., Sornay, E., Willemsen, V., Laux, T., Dewitte, W., and Murray, J.A. (2014). WOX5 suppresses *cyclin D* activity to establish quiescence at the center of the root stem cell niche. *Curr. Biol.* 24, 1939–1944.
- Galinha, C., Hofhuis, H., Luijten, M., Willemsen, V., Bllou, I., Heidstra, R., and Scheres, B. (2007). PLETHORA proteins as dose-dependent master regulators of *Arabidopsis* root development. *Nature* 449, 1053–1057.
- Gattolin, S., Sorieul, M., Hunter, P.R., Khonsari, R.H., and Frigerio, L. (2009). In vivo imaging of the tonoplast intrinsic protein family in *Arabidopsis* roots. *BMC Plant Biol.* 9, 133.
- Helariutta, Y., Fukaki, H., Wysocka-Diller, J., Nakajima, K., Jung, J., Sena, G., Hauser, M.T., and Benfey, P.N. (2000). The SHORT-ROOT gene controls radial patterning of the *Arabidopsis* root through radial signaling. *Cell* 101, 555–567.
- Klein, M., Reichelt, M., Gershenzon, J., and Papenbrock, J. (2006). The three desulfoglucosinolate sulfotransferase proteins in *Arabidopsis* have different substrate specificities and are differentially expressed. *FEBS J.* 273, 122–136.
- Klein, A.M., Mazutis, L., Akartuna, I., Tallapragada, N., Veres, A., Li, V., Peshkin, L., Weitz, D.A., and Kirschner, M.W. (2015). Droplet barcoding for single-cell transcriptomics applied to embryonic stem cells. *Cell* 161, 1187–1201.
- Laubert, M.H., Waizenegger, I., Steinmann, T., Schwarz, H., Mayer, U., Hwang, I., Lukowitz, W., and Jürgens, G. (1997). The *Arabidopsis* KNOLLE protein is a cytokinesis-specific syntaxin. *J. Cell Biol.* 139, 1485–1493.
- Li, S., Yamada, M., Han, X., Ohler, U., and Benfey, P.N. (2016). High-resolution expression map of the *Arabidopsis* root reveals alternative splicing and lincRNA regulation. *Dev. Cell* 39, 508–522.
- Love, M.I., Huber, W., and Anders, S. (2014). Moderated estimation of fold change and dispersion for RNA-seq data with DESeq2. *Genome Biol.* 15, 550.
- Lu, K.J., De Rybel, B., van Mourik, H., and Weijers, D. (2018). Regulation of intercellular TARGET of MONOPTEROS 7 protein transport in the *Arabidopsis* root. *Development* 145.
- Lukassen, S., Bosch, E., Ekici, A.B., and Winterpacht, A. (2018). Characterization of germ cell differentiation in the male mouse through single-cell RNA sequencing. *Sci. Rep.* 8, 6521.
- van der Maaten, L., and Hinton, G. (2008). Visualizing data using t-SNE. *Mach. Learn. Res.* 9, 2579–2605.
- Macosko, E.Z., Basu, A., Satija, R., Nemes, J., Shekhar, K., Goldman, M., Tirosh, I., Bialas, A.R., Kamitaki, N., Martersteck, E.M., et al. (2015). Highly parallel genome-wide expression profiling of individual cells using nanoliter droplets. *Cell* 161, 1202–1214.
- Malinovsky, F.G., Thomsen, M.F., Nintemann, S.J., Jagd, L.M., Bourguin, B., Burrow, M., and Kliebenstein, D.J. (2017). An evolutionarily young defense metabolite influences the root growth of plants via the ancient TOR signaling pathway. *Elife* 6, e29353.
- Mathieu, J., Yant, L.J., Mürdter, F., Küttner, F., and Schmid, M. (2009). Repression of flowering by the miR172 target *SMZ*. *PLoS Biol.* 7, e1000148.
- Matsumoto, H., Kiryu, H., Furusawa, C., Ko, M.S.H., Ko, S.B.H., Gouda, N., Hayashi, T., and Nikaïdo, I. (2017). SCODE: an efficient regulatory network inference algorithm from single-cell RNA-Seq during differentiation. *Bioinformatics* 33, 2314–2321.
- McDavid, A., Finak, G., Chattopadhyay, P.K., Dominguez, M., Lamoreaux, L., Ma, S.S., Roederer, M., and Gottardo, R. (2013). Data exploration, quality control and testing in single-cell qPCR-based gene expression experiments. *Bioinformatics* 29, 461–467.
- Miyashima, S., Koi, S., Hashimoto, T., and Nakajima, K. (2011). Non-cell-autonomous microRNA165 acts in a dose-dependent manner to regulate multiple differentiation status in the *Arabidopsis* root. *Development* 138, 2303–2313.
- Nawy, T., Lee, J.Y., Colinas, J., Wang, J.Y., Thongrod, S.C., Malamy, J.E., Birnbaum, K., and Benfey, P.N. (2005). Transcriptional profile of the *Arabidopsis* root quiescent center. *Plant Cell* 17, 1908–1925.
- Nicolas, M., and Cubas, P. (2016). TCP factors: new kids on the signaling block. *Curr. Opin. Plant Biol.* 33, 33–41.
- Niwa, H. (2018). The principles that govern transcription factor network functions in stem cells. *Development* 145.
- Pi, L., Aichinger, E., van der Graaff, E., Llavata-Peris, C.I., Weijers, D., Hennig, L., Groot, E., and Laux, T. (2015). Organizer-derived WOX5 signal maintains root columella stem cells through chromatin-mediated repression of *CDF4* expression. *Dev. Cell* 33, 576–588.
- Porco, S., Larrieu, A., Du, Y., Gaudinier, A., Goh, T., Swarup, K., Swarup, R., Kuempers, B., Bishopp, A., Lavenus, J., et al. (2016). Lateral root emergence in *Arabidopsis* is dependent on transcription factor LBD29 regulation of auxin influx carrier LAX3. *Development* 143, 3340–3349.
- Potter, S.S. (2018). Single-cell RNA sequencing for the study of development, physiology and disease. *Nat. Rev. Nephrol.* 14, 479–492.
- Prakadan, S.M., Shalek, A.K., and Weitz, D.A. (2017). Scaling by shrinking: empowering single-cell 'omics' with microfluidic devices. *Nat. Rev. Genet.* 18, 345–361.
- Reiter, F., Wienerroither, S., and Stark, A. (2017). Combinatorial function of transcription factors and cofactors. *Curr. Opin. Genet. Dev.* 43, 73–81.
- Sabatini, S., Beis, D., Wolkenfelt, H., Murfett, J., Guilfoyle, T., Malamy, J., Benfey, P., Leyser, O., Bechtold, N., Weisbaeck, P., et al. (1999). An auxin-dependent distal organizer of pattern and polarity in the *Arabidopsis* root. *Cell* 99, 463–472.
- Satija, R., Farrell, J.A., Gennert, D., Schier, A.F., and Regev, A. (2015). Spatial reconstruction of single-cell gene expression data. *Nat. Biotechnol.* 33, 495–502.
- Schellmann, S., Schnittger, A., Kirik, V., Wada, T., Okada, K., Beermann, A., Thumfahrt, J., Jürgens, G., and Hülskamp, M. (2002). TRIPTYCHON and Caprice mediate lateral inhibition during trichome and root hair patterning in *Arabidopsis*. *EMBO J.* 21, 5036–5046.
- Shimotohno, A., Heidstra, R., Bllou, I., and Scheres, B. (2018). Root stem cell niche organizer specification by molecular convergence of PLETHORA and SCARECROW transcription factor modules. *Genes Dev.* 32, 1085–1100.
- Skopelitis, D.S., Hill, K., Klesen, S., Marco, C.F., von Born, P., Chitwood, D.H., and Timmermans, M.C.P. (2018). Gating of miRNA movement at defined cell-cell interfaces governs their impact as positional signals. *Nat. Commun.* 9, 3107.
- Shannon, P., Markiel, A., Ozier, O., Baliga, N.S., Wang, J.T., Ramage, D., Amin, N., Schwikowski, B., and Ideker, T. (2003). Cytoscape: a software environment for integrated models of biomolecular interaction networks. *Genome Res.* 13, 2498–2504.
- Sparks, E.E., Drapek, C., Gaudinier, A., Li, S., Ansariola, M., Shen, N., Hennacy, J.H., Zhang, J., Turco, G., Petricka, J.J., et al. (2016). Establishment of expression in the SHORTROOT-SCARECROW transcriptional cascade through opposing activities of both activators and repressors. *Dev. Cell* 39, 585–596.
- Trapnell, C., Cacchiarelli, D., Grimsby, J., Pokharel, P., Li, S., Morse, M., Lennon, N.J., Livak, K.J., Mikkelsen, T.S., and Rinn, J.L. (2014). The dynamics and regulators of cell fate decisions are revealed by pseudotemporal ordering of single cells. *Nat. Biotechnol.* 32, 381–386.
- Villani, A.C., Satija, R., Reynolds, G., Sarkizova, S., Shekhar, K., Fletcher, J., Griesbeck, M., Butler, A., Zheng, S., Lazo, S., et al. (2017). Single-cell RNA-seq reveals new types of human blood dendritic cells, monocytes, and progenitors. *Science* 356, 4573.
- Zheng, G.X., Terry, J.M., Belgrader, P., Ryvkin, P., Bent, Z.W., Wilson, R., Zivaldo, S.B., Wheeler, T.D., McDermott, G.P., Zhu, J., et al. (2017). Massively parallel digital transcriptional profiling of single cells. *Nat. Commun.* 8, 14049.

STAR★METHODS

KEY RESOURCES TABLE

REAGENT or RESOURCE	SOURCE	IDENTIFIER
Bacterial and Virus Strains		
<i>Agrobacterium tumefaciens</i>	N/A	gv3101
<i>E.coli</i>	N/A	TOP10
Biological Samples		
<i>Arabidopsis thaliana shr-3</i> mutant	Helariutta et al. (2000)	N/A
<i>Arabidopsis thaliana pMIR166A:erGFP</i>	Miyashima et al. (2011)	N/A
<i>Arabidopsis thaliana</i> Columbia ecotype	N/A	N/A
Chemicals, Peptides, and Recombinant Proteins		
Murashige and Skoog basal medium	SERVA	Cat#M0221.0005
Agar	Duchefa Biochem.	11396.03
Cellulase R-10	Duchefa Biochem.	Cat#C8001.0010
Pectolyase Y-23	Duchefa Biochem.	Cat#P8004.0001
Bovine serum albumin	Sigma-Aldrich	Cat#A7907-50G
Mannitol	Duchefa Biochem.	Cat#M0803.1000
Propidium iodide	Sigma-Aldrich	Cat#P4864-10ML
Critical Commercial Assays		
Chromium i7 Multiplex Kit v3	10X Genomics	Cat#PN-120262
Chromium Single Cell 3' Library & Gel Bead Kit v2	10X Genomics	Cat#PN-120237
Chromium Single Cell A Chip Kit v2	10X Genomics	Cat#PN-1000009
DNA High Sensitivity Bioanalyzer kit	Agilent	Cat#5067-4626
DynaBeads® MyOne™ Silane Beads	Thermo Fisher Scientific	Cat#37002D
GeneJET Plasmid Miniprep. Kit	Thermo Fisher Scientific	Cat#K0502
Monarch DNA Gel Extraction Kit	New England Biolabs	Cat#T1020L
Monarch PCR and DNA Cleanup Kit	New England Biolabs	Cat#T1030L
NEBNext Library Quantification Kit	New England Biolabs	Cat#E76305
NEBNext Poly(A) mRNA Magnetic Isolation Module	New England Biolabs	Cat#E74905
NEBNext Ultra II RNA Library Prep Kit	New England Biolabs	Cat#E77605
RNA Bioanalyzer kit	Agilent	Cat#5067-1511
Spectrum Plant Total RNA Extraction Kit	Sigma-Aldrich	Cat#STRN250-1KT
Deposited Data		
Single Cell and mRNA Sequencing data	This Study	GSE123818
Single Cell RNA-Seq wild type Replicate 1 Sequencing data	This Study	GSM3511858
Single Cell RNA-Seq wild type Replicate 2 Sequencing data	This Study	GSM3511859
Single Cell RNA-Seq shr-3 mutant Sequencing data	This Study	GSM3511860
mRNA Unprotoplasted wild type Replicate 1 Sequencing data	This Study	GSM3511861
mRNA Unprotoplasted wild type Replicate 2 Sequencing data	This Study	GSM3511862
mRNA Protoplasted wild type Replicate 1 Sequencing data	This Study	GSM3511863
mRNA Pprotoplasted wild type Replicate 2 Sequencing data	This Study	GSM3511864

(Continued on next page)

Continued

REAGENT or RESOURCE	SOURCE	IDENTIFIER
Experimental Models: Organisms/Strains		
<i>Arabidopsis thaliana</i>		
Oligonucleotides		
AT1G62510 fw	This Study	GCGGTACCCAAGCCATTGGTGTGTTGTT
AT1G62510 rev	This Study	TCCCGGGGTTATAGAGGAGAGGTTTC
MES15 fw	This Study	GCGGTACCTGGAACCGAGGAGAGTACGG
MES15 rev	This Study	TCCCGGGTAAGGTGTAGACACGTTTGTAAAG
PME32 fw	This Study	GCGGTACCTTGCATGGAAGTGTATTGCG
PME32 rev	This Study	TCCCGGGTGCAAAGGTAGTGAAGTTGA
AT3G22120 fw	This Study	GCGGTACCGCCAGGTTACGGTGAGAACA
AT3G22120 rev	This Study	TCCCGGGGAGTGTACGTGTACCTTTTATAG
ATL75 fw	This Study	GCGGTACCTGTACATGACCCATCTCGGTG
ATL75 rev	This Study	TCCCGGGTCTGCTTTGCTTGGCTTTGTT
MLP34 fw	This Study	GCGGTACCGGAGAACAATCGGGCCACA
MLP34 rev	This Study	TCCCGGGTATCTTGGAAACAGTTAGGG
AT1G62500 fw	This Study	GCGGTACCGTTGGTCTAACGTTTGATTA
AT1G62500 rev	This Study	TCCCGGGTATCGTTATTAACAGGGTTC
PIP2-8 fw	This Study	GCGGTACCACGACCCGTCTCTCTTTATCC
PIP2-8 rev	This Study	TCCCGGGTCTTGCATCTTGTGTGTGCT
AT3G53980 fw	This Study	GCGGTACCACTCTACCACTCTCTGGCGA
AT3G53980 rev	This Study	TCCCGGGTGTGTGGAATTTGAGGCACTG
AT3G15357 fw	This Study	GCGGTACCGATGTGTGATTGGGGTCTTTGTTTT
AT3G15357 rev	This Study	TCCCGGGACTGATAAAGAGTTTAGGACGGC
TEL1 fw	This Study	GCGGTACCCATGTGGAGGTTGTCAAAGTGC
TEL1 rev	This Study	TCCCGGGTAATACCAGAGTTGATATTTCCG
JM164 fw	This Study	ACGCTTACAATTTCCATTCC
Recombinant DNA		
JM164 binary vector	Mathieu et al. (2009)	N/A
Software and Algorithms		
Trimmomatic - version 0.36	Bolger et al. (2014)	http://www.usadellab.org/cms/?page=trimmomatic
STAR	Dobin et al. (2013)	https://github.com/alexdobin/STAR/wiki
HTSeq - version 0.7.2	Anders et al. (2015)	https://htseq.readthedocs.io/en/release_0.11.1/
DESeq2	Love et al. (2014)	https://bioconductor.org/packages/release/bioc/html/DESeq2.html
Cell Ranger 2.0.2	10X Genomics	https://support.10xgenomics.com/single-cell-gene-expression/software/release-notes/2-0
Seurat - version 2.3.4	Satija et al., 2015	https://satijalab.org/seurat/
Monocle2 - version 2.8.0	Trapnell et al. (2014)	http://cole-trapnell-lab.github.io/monocle-release/docs/
SCODE	Matsumoto et al. (2017)	https://github.com/hmatsu1226/SCODE
Cytoscape	Shannon et al. (2003)	https://cytoscape.org/
NetworkAnalyzer	Assenov et al. (2008)	http://apps.cytoscape.org/apps/networkanalyzer

CONTACT FOR REAGENT AND RESOURCE SHARING

Further information and requests for resources and reagents should be directed to and will be fulfilled by the Lead Contact, Marja C.P. Timmermans (marja.timmermans@zmbp.uni-tuebingen.de).

EXPERIMENTAL MODEL AND SUBJECT DETAILS

All analyses were performed in the *Arabidopsis* Columbia (Col-0) ecotype with the exception of the *shr-3* mutant line, which is in the Ler. ecotype. The *pMIR166A:erGFP* reporter and *shr-3* mutant have been described previously ([Miyashima et al., 2011](#); [Helariutta](#)

et al., 2000, respectively). Plants were grown at 22°C on 1% agar plates containing 0.5x Murashige and Skoog (MS) medium (Duchefa Biochem.).

METHOD DETAILS

Protoplast Isolation

Seedlings were grown vertically on nylon mesh on agar plates. Roots of 6-day-old seedlings were cut approximately one centimetre from their tip, broadly diced with a scalpel blade, and treated with 7 ml protoplasting solution optimised for scRNA-seq from a protocol in Birnbaum et al. (2003). Immediately before use, 1.5% Cellulase R-10 and 0.1% Pectolyase (Duchefa Biochem.) were added to fresh protoplast buffer (0.1 M KCl, 0.02 M MgCl₂, 0.02 M CaCl₂, 0.1% BSA (Sigma Aldrich), 0.08 M MES, and 0.6 M Mannitol, adjusted to pH 5.5 with 0.1M Tris HCl), and mixed thoroughly. Root tissues were protoplasted for 2 hours at 20°C on an orbital shaker set at 200 revolutions/minute. The mixture was subsequently filtered through a 100 µm nylon filter and rinsed with 1-5 ml of root protoplast buffer. Protoplasts were then centrifuged for 10 minutes (500 g – 4°C), the supernatant gently removed, and the pellet resuspended in 10 ml root protoplast buffer containing 0.4 M Mannitol and no CaCl₂. This wash procedure was repeated once more, the protoplasts centrifuged as before, and resuspended in ~500 µl or less protoplast buffer without CaCl₂ and with 0.4 M Mannitol. Protoplasts were validated under a light microscope, and if necessary any excess debris or un-protoplasted tissues removed with an additional washing step. Cells were filtered through a 40 µm cell strainer (Flowmi Bel Art SP Scienceware), quantified using a haemocytometer, and adjusted to a density of approximately 800-900 cells per µl.

Bulk RNA-seq Library Preparation and Sequencing

RNA was extracted using the Spectrum Plant RNA Extraction Kit (Sigma) from protoplasted and equivalent un-protoplasted root tissue collected at completion of the protoplasting procedure. RNA samples were quantified by Nanodrop, and quality assured based on Agilent RNA Bioanalyzer chip traces. mRNA was enriched by oligo-dT pull-down using the NEBNext Poly(A) mRNA Magnetic Isolation Module, and RNA libraries constructed using the NEBNext Ultra II Directional RNA Library Prep Kit for Illumina with NEB Multiplex oligos. Final library size and quality was checked on a DNA High Sensitivity Bioanalyzer chip (Agilent), and libraries were quantified using the NEBNext Library Quantification Kit for Illumina.

Single Cell RNA-seq Library Preparation and Sequencing

Single cell RNA-seq libraries were prepared from fresh protoplasts according to the 10x Genomics Single Cell 3' Reagent Kit v2 protocol. For each replicate, 12,200 cells were loaded in the 10x Genomics Chromium single cell microfluidics device with the aim of capturing 7,000 cells. 11 cycles were used for cDNA amplification, as well as for final PCR amplification of the adapter-ligated libraries. Final library size and quality was checked on a DNA High Sensitivity Bioanalyzer chip (Agilent), and libraries were quantified using the NEBNext Library Quantification Kit for Illumina. ScRNA-seq library sequencing was performed on the NextSeq (Illumina) platform, using the sequencing parameters 26,8,0,98.

Generation and Confocal Imaging of Reporter Lines

To verify select marker genes in vivo, *promoter:3xYFP-NLS* reporter lines were generated for the following genes: *AT1G62510*, *MES15*, *PME32*, *TEL1*, *AT3G22120*, *ATL75*, *MLP34*, *AT1G62500*, *PIP2-8*, *AT6G53980*, *AT3G15357*, *AT5G62330*, *AT1G57590*, *AT1G05320* and *EXT12*. Full names for all genes referenced in this paper can be found in Table S5. Promoter fragments between approx. 1.2 - 3.5 kb were amplified using PCR primers containing *KpnI* and *XmaI* restriction sites, and introduced by classical cloning into binary vector JM164 (Mathieu et al., 2009) to generate transcriptional fusions to a nuclear-localised triple Venus tag. All reporter constructs were transformed into the Col-0 background, and multiple independent events per construct ($n \geq 3$) analysed. Roots of 7-day-old seedlings were mounted in 10 µg/mL Propidium Iodide (PI) (Sigma-Aldrich) and imaged using a Zeiss LSM880 laser-scanning confocal microscope. Excitation for YFP was at 514 nm and images were acquired at 517 - 571 nm. For PI, the excitation wavelength was 561nm, and images were collected at 589 - 718nm.

QUANTIFICATION AND STATISTICAL ANALYSIS

Bulk RNA-seq Analysis

Sequence reads (pair-end, 75 bp) were trimmed using Trimmomatic (version 0.36; Bolger et al., 2014), and aligned to the *Arabidopsis* TAIR10 reference genome with STAR (Dobin et al., 2013). Gene expression values were calculated on uniquely mapped reads using HTSeq (version 0.7.2; Anders et al., 2015), and DESeq2 (Love et al., 2014) was used to calculate differential expression (absolute log₂FC ≥ 1 and $q < 0.05$) on genes with expression levels ≥ 1 RPM in either replicate. For correlation analysis of gene expression between protoplasted and un-protoplasted root tissues, the Log₂ (mean RPM+1) expression values were calculated for each gene and the Pearson-correlation coefficient determined in R.

Generation of Single Cell Expression Matrices

Cell Ranger 2.0.2 (10X Genomics) was used to process scRNA-seq data. Cell Ranger Count aligned the sequencing reads to the *Arabidopsis* TAIR10 reference genome using STAR (Dobin et al., 2013). For the mapping of *GFP*-derived transcripts, the sequence

and gene structure for GFP were added to the reference fastq and gtf files, respectively. Aligned sequence reads with a valid cell barcode and UMI that mapped to exons (Ensembl GTFs TAIR10.37) were used to generate gene expression matrices from which PCR duplicates were removed. Valid cell barcodes were defined based on UMI distribution with the cutoff: cell read count > 5% of 99th percentile of 7000 cells (Zheng et al., 2017). The output files for the two replicates were aggregated into one gene-cell expression matrix using Cell Ranger aggr with the mapped read depth normalization option.

Dimensionality Reduction, t-SNE Visualization, and Cell Clustering Analysis

The Seurat R package (version 2.3.4) (Satija et al., 2015; Butler et al., 2018) was used for dimensionality reduction analysis. Highly variable genes were identified across the single cells, after controlling for the relationship between average expression and dispersion. Genes were placed into 20 bins based on their average expression, and genes with an average expression value <0.011 removed. Within each bin, a z-score of log transformed dispersion measure (variance/mean) was calculated. A z-score cut-off of 1 was applied to identify the highly variable genes. PCA was then performed using the variable genes as input. 50 PCs were selected as input for a graph-based approach to cluster cells by cell type (Villani et al., 2017) and used as input for t-distributed stochastic neighbour embedding (t-SNE; van der Maaten and Hinton, 2008) for reduction to two- or three-dimensional visualization. A resolution value of 0.8 was used in all clustering analyses. Additionally, we used a random forest classifier (Breiman, 2001; Butler et al., 2018) to examine cluster distinctness and merged any clusters where the out-of-bag error (OOBE) of the classifier was >10%.

Identification of Differentially Expressed Genes and Cluster-Specific Marker Genes

Genes differentially expressed across clusters or subclusters were identified by comparing average expression values in cells of a given cluster to that of cells in all other clusters using the Seurat package likelihood ratio test (Bimod). The following cutoffs were applied: average expression difference ≥ 0.25 natural Log and $q < 0.01$. Cluster-specific marker genes were selected from among the differentially expressed genes based on the criteria that marker genes must be expressed in $\geq 10\%$ of cells within the cluster (PCT1), and $\leq 10\%$ of cells across all other clusters (PCT2).

Identification of Cluster Identities

The top 10 DE genes ($q < 0.01$) by fold change were identified for each cluster and expression profiles harvested from a cell-type specific and longitudinal microarray dataset (Brady et al., 2007a). In the case that microarray data was not available, the next best DE gene was selected. Average normalised expression for 10 DE genes across cell types and developmental stages was calculated and visualised in R. In a complementary approach, marker genes for key cell types were identified from Efroni et al. (2015), which integrates root expression data from multiple independent studies. Genes with high normalised expression in a particular cell type (spec. score ≥ 0.6 as detailed in Efroni et al., 2015) were filtered for specificity by applying a <0.2 spec. score cutoff for all other cell types. This latter criterion was not applied to phloem/phloem companion cells, and phloem/protophloem comparisons, as these cell types show considerable co-expression of most genes. See Table S2 for the list of marker genes. Expression of these genes was extracted from the combined single cell expression matrix and visualised using Seurat's SplitDotPlot GG function. Genes with well-defined expression patterns were considered similarly.

Correlation Analysis

For correlation analysis of merged single cell and bulk RNA sequence data, Log_2 (mean RPM+1) expression values for each gene from two replicates of pooled single cell and bulk RNA sequencing were quantile normalized and the Pearson-correlation coefficient calculated in R. For correlation analysis between single cell RNA-seq replicates, the single cell data replicates were simulated as bulk RNA sequencing data, the Log_2 (mean RPM+1) expression values calculated for each gene, and the Pearson-correlation coefficient between replicates calculated in R. For correlation analysis between the single cell replicates across individual clusters, the average expression of cells within a cluster was calculated for each replicate using the Seurat command `AverageExpression(object, use.raw=T)`. The Pearson-correlation coefficient between the replicates was then determined for each cluster using Seurat CellPlot.

Single Cell Developmental Trajectory Analysis

Pseudotime trajectory analysis was performed using the Monocle2 R package (version 2.8.0) algorithm (Trapnell et al., 2014) on genes with a mean expression value ≥ 0.011 , and dispersion empirical value larger than the dispersion fit value. Cells were ordered along the trajectory and visualized in a reduced dimensional space. Significantly changed genes along the pseudotime were identified using the differential GeneTest function of Monocle2 with q -value < 0.01. Genes dynamically expressed along the pseudotime were clustered using the 'plot_pseudotime_heatmap' function with the default parameters. Transcript factors were annotated based on information from AtTFDB (<https://agris-knowledgebase.org/AtTFDB/>). Gene description information was downloaded from (<https://www.arabidopsis.org>).

GO Enrichment Analysis

Gene ontology (GO) biological process enrichment analyses (<http://pantherdb.org>) were performed on cluster-grouped differently expressed genes along the pseudotime (average expression ≥ 0.011) via fisher exact test ($q < 0.01$, Fold enrichment >1).

Gene Regulatory Network Analysis

The gene expression levels of transcription factors (Table S4) without genes with dual-polar expression (cluster h) were normalized using the Monocle2 R package (version 2.8.0) genesmoothcurve function (Trapnell et al., 2014). The pseudotime of each cell assigned by Monocle2 was normalized from 0 to 1. Gene regulatory network inference was calculated on dynamic TFs using SCODE (Matsumoto et al., 2017) with parameter z setting as 4, averaging 50x results to obtain reliable relationships. Gene regulatory inference was filtered using various cutoffs on parameter value, the results visualized using Cytoscape (Shannon et al., 2003), and the network topological parameters obtained with NetworkAnalyzer (Assenov et al., 2008).

DATA AND SOFTWARE AVAILABILITY

All high-throughput sequencing data, both raw and processed files, have been deposited in NCBI's Gene Expression Omnibus and are accessible under accession number GEO: GSE123818.

ADDITIONAL RESOURCES

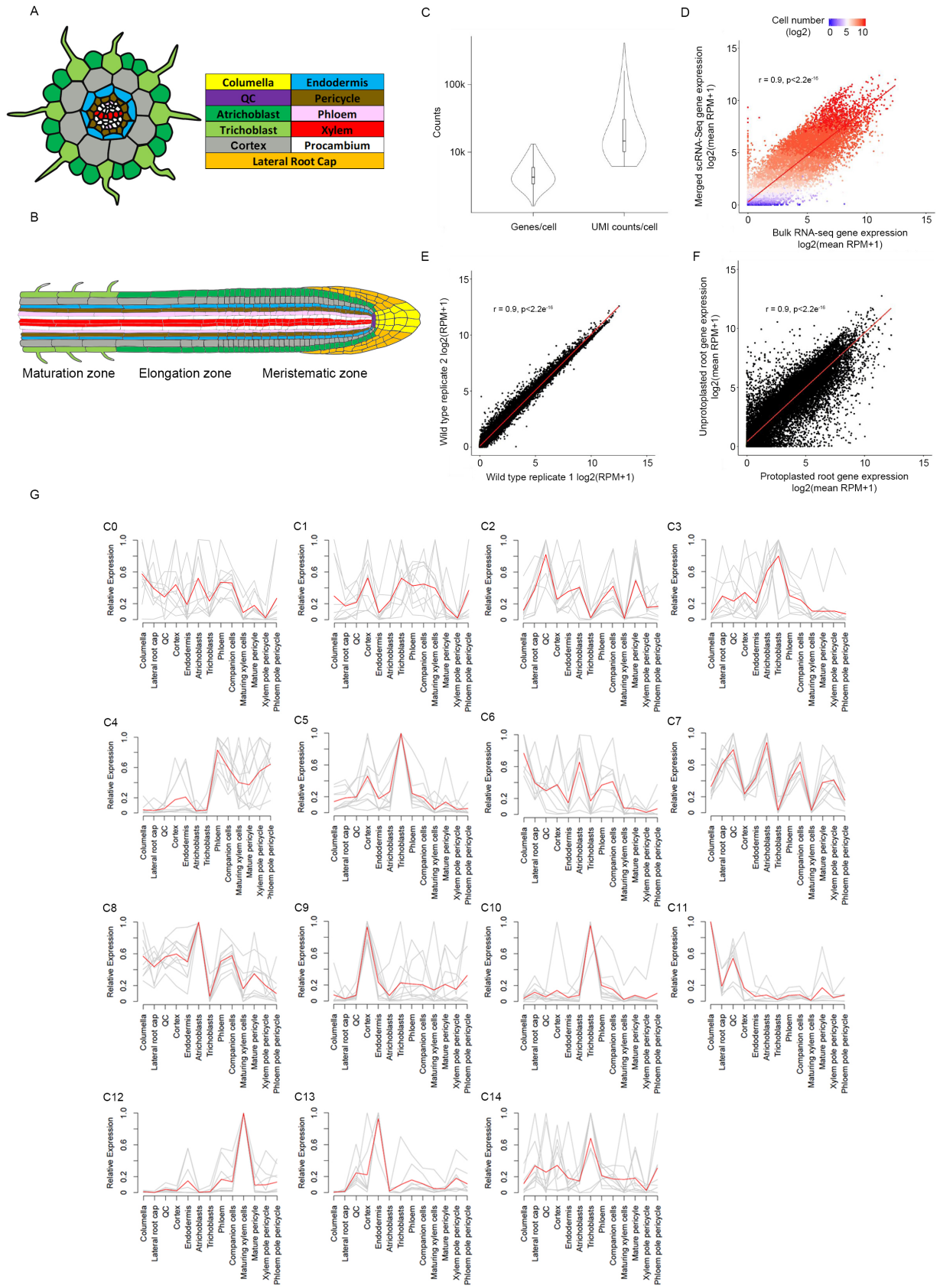
Data deposition: <https://www.ncbi.nlm.nih.gov/geo/>

Developmental Cell, Volume 48

Supplemental Information

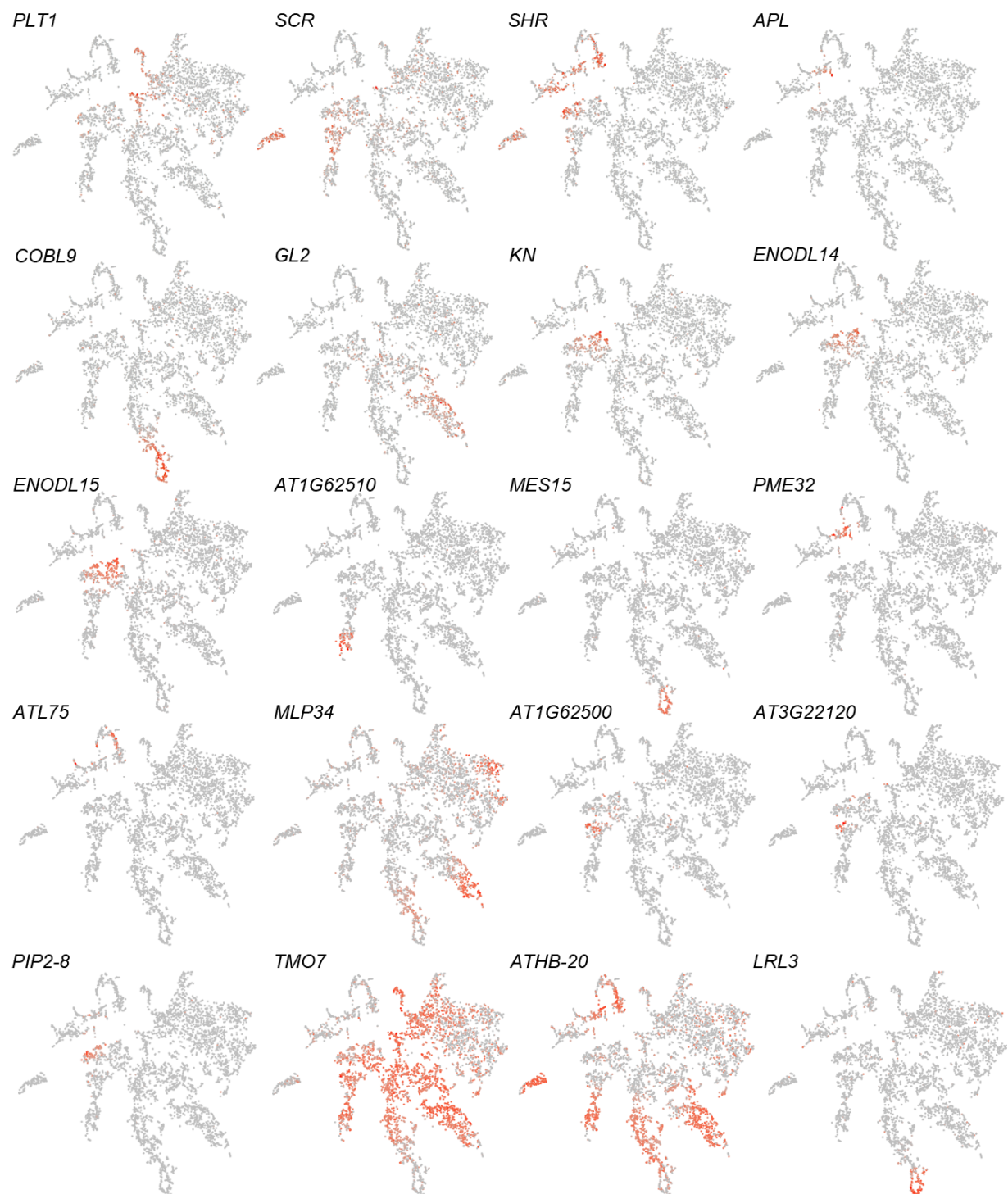
**Spatiotemporal Developmental Trajectories
in the *Arabidopsis* Root Revealed Using
High-Throughput Single-Cell RNA Sequencing**

Tom Denyer, Xiaoli Ma, Simon Klesen, Emanuele Scacchi, Kay Nieselt, and Marja C.P. Timmermans

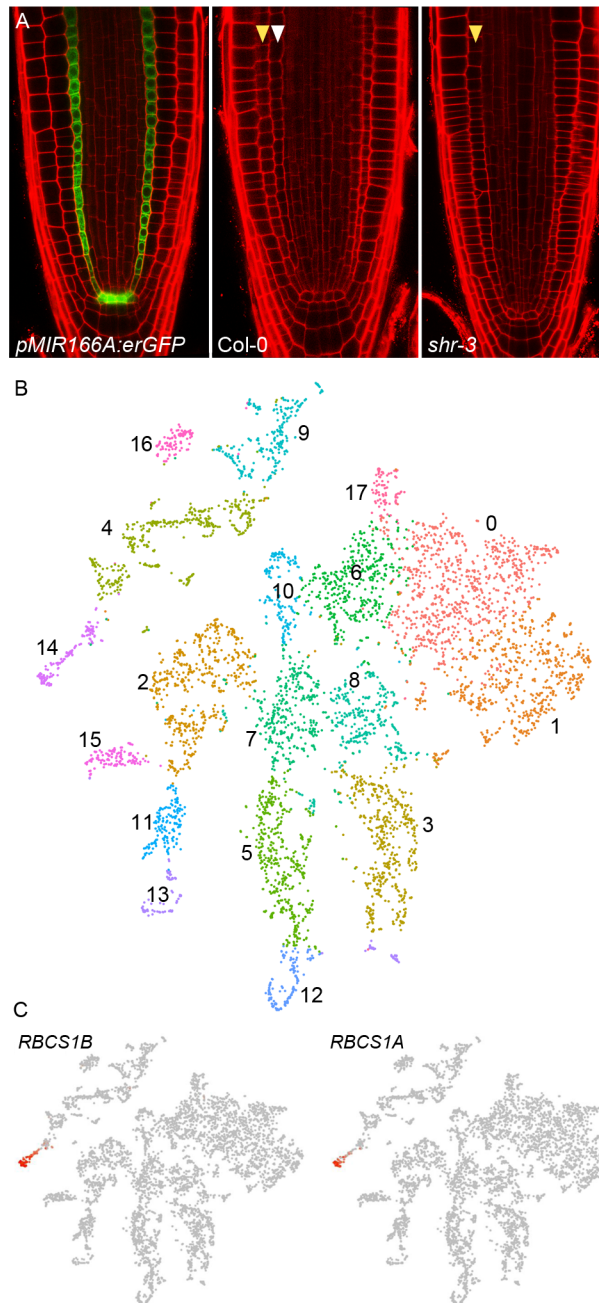


Supplemental Figure 1. scRNA-seq of the *Arabidopsis* root reveals distinct cell-type specific clusters; Related to Figure 1. (A) Transverse section of a mature root illustrating its radial

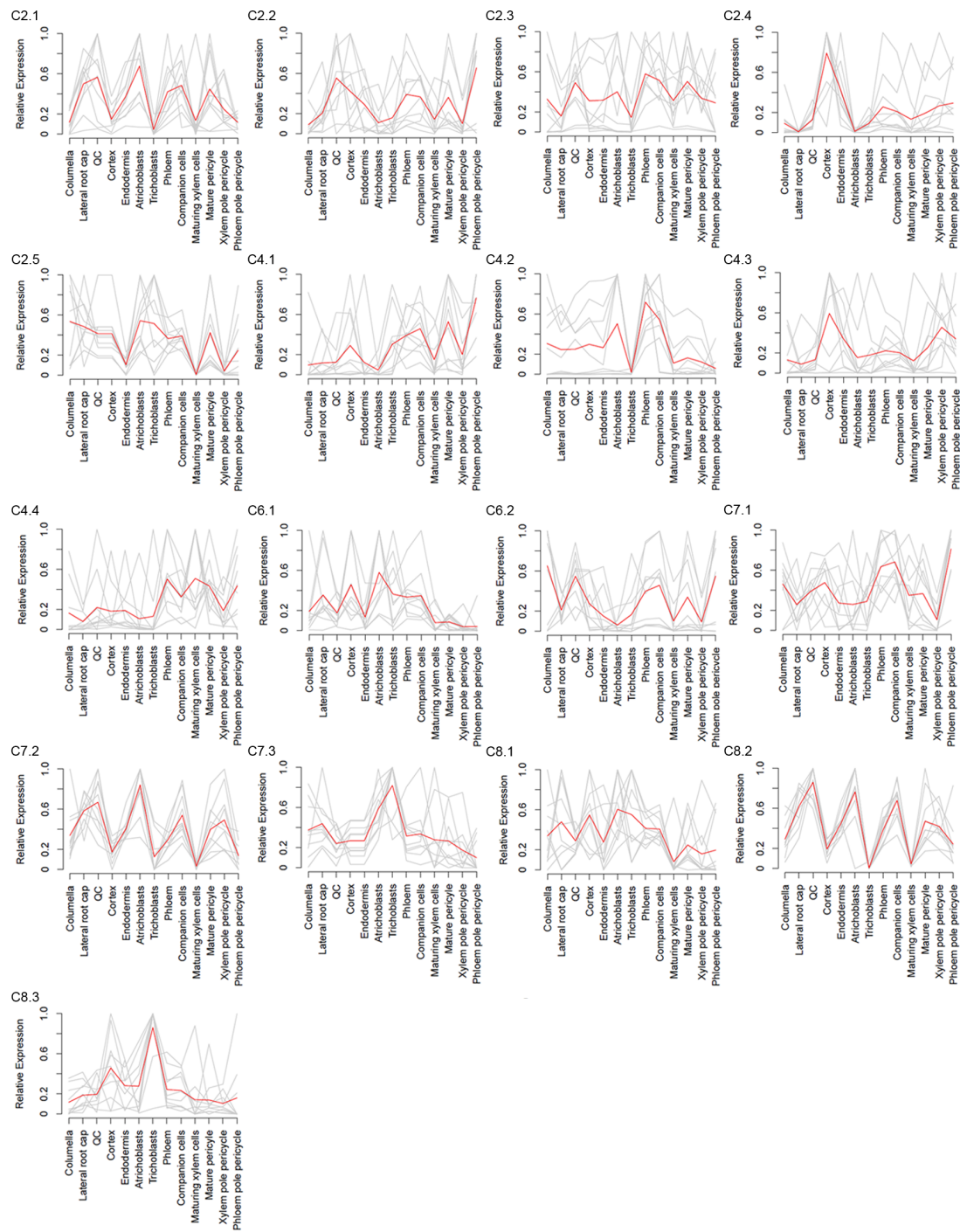
organisation. (B) Longitudinal cross-section of a mature root illustrating an organisation in three distinct developmental zones. Figures adapted from Root illustrations – figshare collection (2018). (C) Violin plots showing the distribution of genes and transcripts (UMIs) detected per cell. (D) Correlation between merged single cell and bulk-tissue RNA-seq measurement of gene expression from *Arabidopsis* root protoplasts. For each gene, the quartile normalisation of the log₂-transformed mean RPM + 1 values from the merged scRNA-seq and bulk RNA-seq are plotted against each other. Colour represents cell numbers (log₂, +1) from the scRNA-seq data. (E) Correlation between single cell RNA-seq replicates of *Arabidopsis* Col-0 (Rep. 1) and *pMIR166A:erGFP* (Rep 2) root protoplasts. For each gene, log₂-transformed RPM +1 values are plotted against each other. (F) Correlation between bulk RNA-seq measurements of gene expression from protoplasted and un-protoplasted *Arabidopsis* root tissue. r = Pearson's correlation coefficient. 3,545 genes were induced upon protoplasting (see Table S1). (G) The expression profiles for the top 10 DE genes defining clusters, taken from a microarray root atlas (Brady *et al.*, 2007a), reveal discreet cell identities. Red line, mean expression profile; grey lines, individual expression profiles.



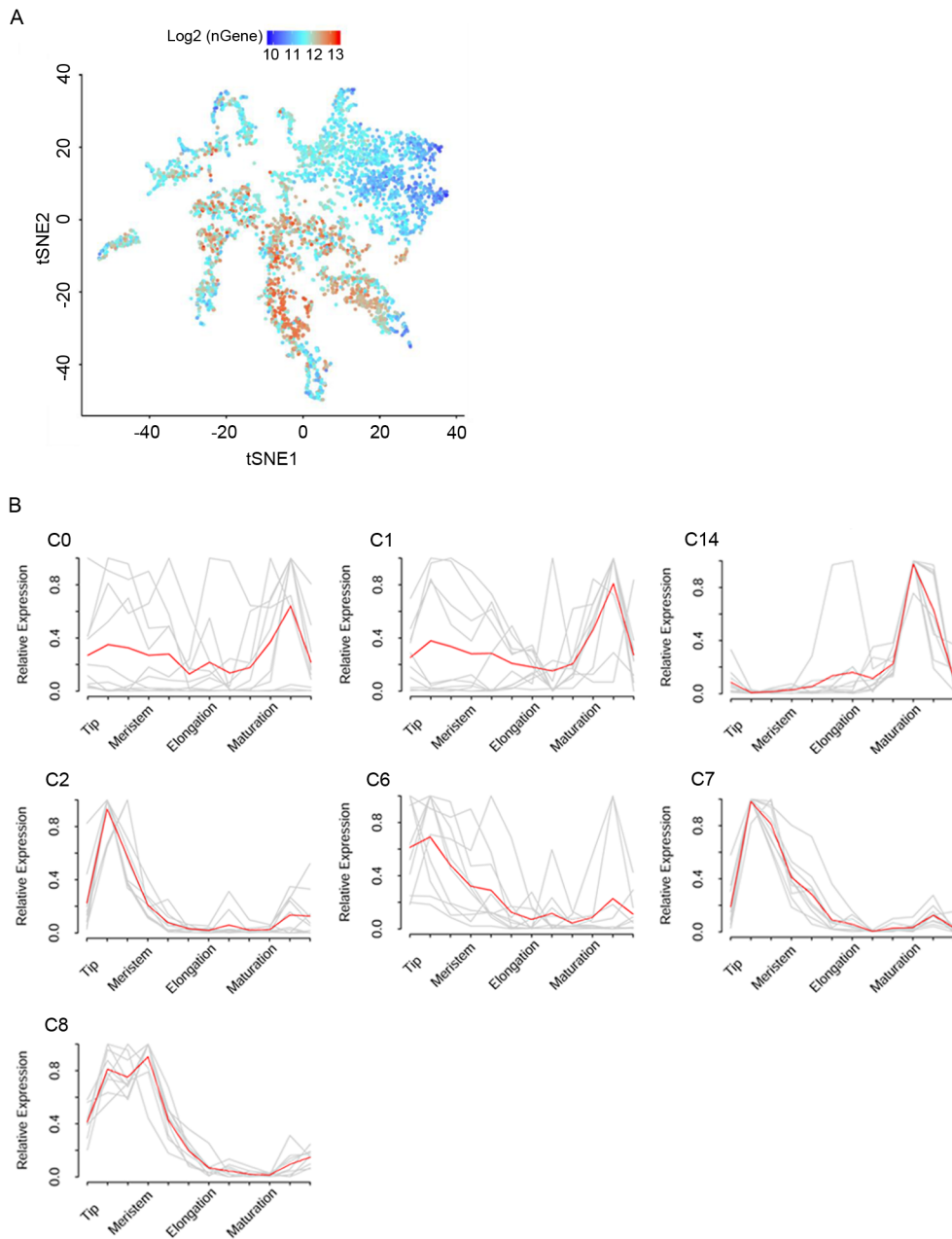
Supplemental Figure 2. Key *Arabidopsis* genes reveal distinct expression profiles across clusters.
Related to Figure 1. t-SNE visualisations of cell clusters revealing defined expression profiles of key *Arabidopsis* development genes.



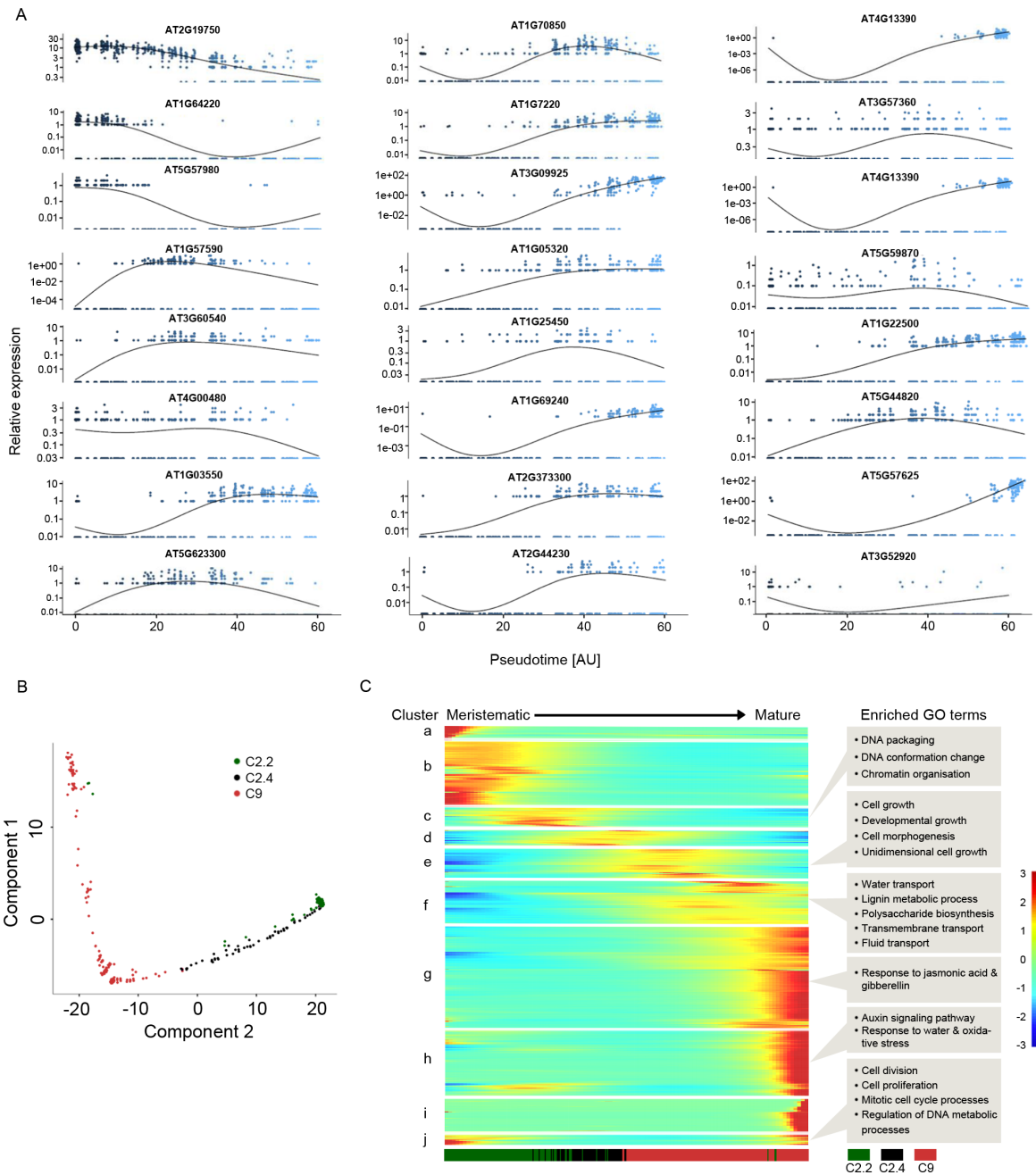
Supplemental Figure 3. A localised GFP marker and mutant line validate cluster calling; Related to Figure 2. (A) Left - *pMIR166A:erGFP* expression is limited to the endodermal cell layer and the QC cells. Centre and right - wild-type (Col-0) and *SHR* mutant (*shr-3*). Yellow arrowheads indicate cortex cell-layers, white arrowhead indicates endodermal cell layer in Col-0, missing in *shr-3*. 6-day old root tips. (B) t-SNE visualisation (right) of wild-type and *shr-3* cells combined reveals 18 distinct clusters. (C) t-SNE visualisation of the cluster cloud (wild-type replicates) reveals expression of select rubisco subunit genes localised to a cluster of spiked in leaf cells.



Supplemental Figure 4. Discreet cell identities can be found within select subclusters; Related to Figure 1. The expression profiles for the top ten DE genes defining subclusters, taken from a microarray root atlas (Brady *et al.*, 2007a), reveal discreet cell identities. Red line, mean expression profile; grey lines, individual expression profiles.



Supplemental Figure 5. Developmental stage-specific clusters can be identified. Related to Figure 1. (A) t-SNE visualisation of UMI counts across all clusters. (B) The expression profiles for the top 10 DE genes defining subclusters, taken from a longitudinal microarray root atlas (Brady *et al.*, 2007a), reveal meristematic- and differentiated-cell identities. Red line, mean expression profile; grey lines, individual expression profiles.



Supplemental Figure 6. Cortex development is guided by distinct waves of gene expression; Related to Figure 5. (A) Expression dynamics for select single genes across pseudotime. Blue-scale, pseudotime value. (B) Pseudotime reconstruction of cortex development reveals a linear ordering of cells, reflecting cluster and subcluster arrangement. (C). Expression heatmap of highly dynamic genes ordered across pseudotime reveals cortex differentiation reflected in multiple distinct waves of gene expression. Significantly enriched GO terms for clusters are labelled. Lower bar, cell density distribution across clusters. See Table S4 for full data.

Curriculum vitae

Personal Information

Name: Simon Christoph Klesen
Date of birth: 13.09.1991
Place of birth: Lebach

Education:

2016 – now Ph.D. in Biology
 University of Tübingen
 Centre for Plant Molecular Biology (ZMBP)
 Department of Developmental Genetics

2014 – 2016 M.Sc. Biology
 University of Tübingen
 Master thesis in molecular plant biology:
 “miRNAs six feet under: How miRNAs move within the root tip of
 Arabidopsis thaliana”

2010 – 2014 B.Sc. Biology
 University of Tübingen
 Bachelor thesis in cognitive neuroscience:
 “Ereignis-korrelierte Potentiale bei der Wiedererkennung von
 verhaltensrelevanten Szenen”

Publications and Manuscripts:

Klesen S., Symeonidi E., Bayer M., Timmermans M.C.P. (2020) Regulation of miRNA mobility by receptor-like kinases localised at plasmodesmata.

Klesen S., Amorim M., Timmermans M.C.P. (2020) A high-throughput forward genetic screen for gatekeepers limiting miRNA mobility.

Klesen S., Hill K., Timmermans M. C. P. (2020) Small RNAs as plant morphogens. *Current Topics in Developmental Biology*, 137, 455-480.

Skopelitis D.S., Hill K., **Klesen S.**, Marco C.F., von Born P., Chitwood D.H., Timmermans M.C.P. (2018) Gating of miRNA movement at defined cell-cell interfaces governs their impact as positional signals. *Nature Communications*, 9, 3107.

Denyer T., Ma X., **Klesen S.**, Scacchi E., Nieselt K., Timmermans M.C.P. (2019) Spatiotemporal Developmental Trajectories in the *Arabidopsis* Root Revealed Using High-Throughput Single-Cell RNA Sequencing. *Developmental Cell*, 48, 840-852.

Acknowledgement

First, I would like to thank my supervisor Prof. Dr. Marja Timmermans for the opportunity to pursue my PhD research and for being a great mentor. I am grateful for everything I could learn and the opportunities to participate in courses and conferences during this time. I also want to thank Prof. Dr. Gerd Jürgens for being my second supervisor as well as reviewer on this thesis.

I want to thank my committee members Dr. Laura Ragni and Dr. Martin Bayer for great input in our meetings.

I want to thank all my former and current colleagues for the nice atmosphere and discussions in the lab. Especially Dr. Ethymia Symeonidi for help with setting up experiments in chapter three and Dr. Marcella Amorim for help with amiR testing. Many thanks to Dr. Thomas Denyer for a critical opinion on this thesis. Special thanks go to Marika Kientz who accelerated this research with her technical expertise.

Last, I would like to thank my family and Lisa for the great support during this time.